

**Study of the Possible Pharmacological Mechanisms of Curcumin in
the Treatment of Alzheimer's Disease**

CHEUNG, Kwok Kuen

**A Thesis Submitted in Partial Fulfillment
of the Requirement for the Degree of
Doctor of Philosophy**

in

Medical Sciences

**The Chinese University of Hong Kong
September 2011**

UMI Number: 3514560

All rights reserved

INFORMATION TO ALL USERS

The quality of this reproduction is dependent on the quality of the copy submitted.

In the unlikely event that the author did not send a complete manuscript and there are missing pages, these will be noted. Also, if material had to be removed, a note will indicate the deletion.



UMI 3514560

Copyright 2012 by ProQuest LLC.

All rights reserved. This edition of the work is protected against unauthorized copying under Title 17, United States Code.



ProQuest LLC.
789 East Eisenhower Parkway
P.O. Box 1346
Ann Arbor, MI 48106 - 1346

ABSTRACT

Introduction: Alzheimer's disease (AD) is the most common form of dementia. It is characterized by the progressive loss of cognitive and intellectual functions and inevitably complete loss of the capability to take care of normal daily activities at the later stages of the disease. It is estimated that the prevalence will exceed 80 million worldwide by 2040, which will impose enormous economic pressure on any country. The cause of the disease remains incompletely elucidated. Based on histopathological and biochemical studies, it is manifested by neuroinflammation, with increasing levels of amyloid plaques and neurofibrillary tangles, loss of acetylcholine (ACh) and loss of neurons. Curcumin is a polyphenolic compound which possesses antioxidative and anti-inflammatory properties. Other studies demonstrated its abilities to reduce amyloid plaque burden and oxidative damage and to improve cognitive function of rodent models of AD. However, the physiological mechanisms by which curcumin achieved these functions are still poorly known, which hinders its development and use to treat AD.

Objective and methods: The main objective of this study was to determine the possible functions of curcumin in the hypothesized pathways of AD development. Cell free models of metal ion induced A β aggregation and hydrogen peroxide (H₂O₂) generation were used to determine the effectiveness of curcumin in reducing A β aggregates and H₂O₂, respectively, at physiologically attainable concentrations. An in vitro model was used to determine the effect of curcumin on the secretion of ApoE protein from the mouse microglial BV2 cell line. Transgenic mouse models, Tg2576, JNPL3 and JNPL3xTg2576, were used to determine the efficacies of curcumin on modulating the activities of α -, β - and γ -secretases; on the expression of genes

regulating $A\beta$ metabolism, protecting against $A\beta$ toxicity and regulating Ach homeostasis; and to determine if curcumin can be used to treat tauopathy.

Results: Our data showed that curcumin at concentrations achievable in vivo was effective at disrupting $A\beta$ aggregates ($IC_{50} < 0.9 \mu M$), but it was ineffective at blocking H_2O_2 production ($IC_{50} = 5.2 \mu M$). In vitro study showed that curcumin was able to increase ApoE protein secretion from a mouse microglial cell line at physiologically attainable concentrations (0.064 to 1 μM , $p < 0.001$). An animal study demonstrated that curcumin was incapable of modulating α -, β - or γ -secretase activity. Gene expression in animal models showed that curcumin was incapable of modulating genes regulating APP cleavage, but it was able to increase the expression of some substrates of secretases: Btc (+26%, $p < 0.005$) and Kl (+96%, $p < 0.05$). Among genes regulating $A\beta$ degradation, curcumin was able to increase Ide (+23%, $p < 0.05$), Mmp2 (+77%, $p < 0.05$) and Mmp14 (+46%, $p < 0.005$). Of genes acting as $A\beta$ chaperones, curcumin was unable to cause any change. Among genes acting as $A\beta$ receptors, curcumin was able to increase the expression of ApoE2 (+37%, $p < 0.05$), Lrp1 (+30%, $p < 0.05$) and Msr1 (+46%, $p < 0.05$). Of genes regulating Ach homeostasis, curcumin did not show any effect. Among genes providing protection against $A\beta$ toxicity, curcumin was capable of increasing Igf2 (+130%, $p < 0.01$) and Irs1 (+30%, $p < 0.01$). Of genes relating to antioxidative defences, curcumin was able to increase Nos2 (+25%, $p < 0.05$), Sod3 (+60%, $p < 0.05$) and Bmp6 (+46%, $p < 0.01$) and suppress Nox1 (-43%, $p < 0.01$). For treating tauopathy, curcumin was able to reduce NFT as measured by AT8-immunopositive area (-75%, $p = 0.02$) in the medulla, but not in the entorhinal cortex or amygdala ($p = 0.89$). The effect was only observed in 18 month old JNPL3 mice administered curcumin in

peanut butter but not in 14 month old JNPL3 mice administered curcumin in chow. A rotarod study of 18 month old JNPL3 mice showed that curcumin was unable to improve motor function ($p=0.67$). Finally, on other phenotypic changes, curcumin was able to reduce both mortality ($p=0.009$) of all male mice and weight loss ($p=0.007$) of all mice.

Conclusion: Our data suggest that curcumin may reduce amyloid burden by increasing $A\beta$ solubilization, degradation and efflux; it may provide protection against $A\beta$ toxicity; and it may also increase antioxidative defences. For tauopathy, curcumin may reduce tangle formation, but more work is needed to confirm this function. Taken together, all the data in this study showed the physiologically relevant functions of curcumin, which favour its beneficial use for AD treatment.

摘要

引言: 阿爾茲海默症 (AD) 是痴呆的最常見形式。它的特徵是認知和智力功能逐漸喪失及在晚期不可避免地完全失去日常活動能力。據估計, 在 2040 年前全球患病率將超越八千萬, 這將對任何國家都造成巨大的經濟壓力。它的病因仍然未完全闡明。基於病理組織學和生物化學的研究, 它表現為神經性炎症, 澱粉樣斑塊及神經元纖維纏結(NFT)的水平不斷提高, 乙酰膽鹼及神經元的損失。薑黃素是一種多酚類化合物, 具有抗氧化和抗炎症特性。研究顯示, 它能減少啮齒類動物 AD 模型的澱粉樣斑塊負荷和氧化損傷, 及改善其認知功能。然而, 薑黃素實現這些功能的生理機制仍知之甚少, 這阻礙了其治療 AD 的發展和使用。

目的及方法: 本研究的主要目標是要確定薑黃素在 AD 發展中可能的作用。採用金屬離子誘導的澱粉樣蛋白聚合及過氧化氫生成的無細胞模型來確定薑黃素在生理濃度下, 減少澱粉樣蛋白聚集物和過氧化氫的有效性。體外模型被用來確定薑黃素對小鼠小膠質細胞 BV2 分泌載脂蛋白 E (ApoE) 的作用。採用轉基因小鼠模型, Tg2576, JNPL3 及 JNPL3xTg2576, 來確定薑黃素對調節 α -、 β - 及 γ - 分泌酶活動; 澱粉樣蛋白代謝, 澱粉樣蛋白毒性保護和調節乙酰膽鹼體內平衡的基因表達; 以及確定薑黃素是否可用於治療 tau 蛋白病變。

結果: 我們的結果顯示, 薑黃素在體內可達到的濃度有效地破壞澱粉樣蛋白聚合 ($IC_{50} < 0.9 \mu M$), 但不能阻止過氧化氫生產 ($IC_{50} = 5.2 \mu M$)。體外研究顯示, 薑黃素在體內可達濃度能夠增加小鼠小膠質細胞分泌 ApoE 蛋白 (0.064 to 1 μM , $p < 0.001$)。動物研究顯示, 薑黃素不能調節 α -、 β - 及 γ - 分泌酶活動。在動物模

型中基因表達研究顯示，薑黃素不能調節澱粉樣前體蛋白裂解的基因表達，但能夠提高分泌酶底物的表達：Btc (+26%, $p < 0.005$) 及 Kl (+96%, $p < 0.05$)。對降解澱粉樣蛋白的基因，薑黃素能夠增加 Idc (+23%, $p < 0.05$)，Mmp2 (+77%, $p < 0.05$) 及 Mmp14 (+46%, $p < 0.005$) 等。對充當澱粉樣蛋白伴侶分子的基因，薑黃素是無法造成任何改變。對於充當澱粉樣蛋白受體的基因，薑黃素能提高 ApoE2 (+37%, $p < 0.05$)，Lrp1 (+30%, $p < 0.05$) 及 Msr1 (+46%, $p < 0.05$) 的表達。對調節乙酰膽鹼體內平衡的基因，薑黃素沒有表現出任何效果。對於提供防止澱粉樣蛋白毒性保護的基因，薑黃素是有能力增加 Igf2 (+130%, $p < 0.01$) 及 Irs1 (+30%, $p < 0.01$)。對於與抗氧化防禦有關的基因，薑黃素能夠增加 Nos2 (+25%, $p < 0.05$)，Sod3 (+60%, $p < 0.05$) 和 Bmp6 (+46%, $p < 0.01$) 及抑制 Nox1 (-43%, $p < 0.01$)。在治療 tau 蛋白病變方面，薑黃素能降低在髓質中(-75%, $p = 0.02$)作為衡量 NFT 的 AT8-免疫陽性面積，但卻不是在內嗅皮質或杏仁核($p = 0.89$)。其效果是只在 18 個月大施用花生醬混合餵食薑黃素的 JNPL3 小鼠觀察到，但不在 14 個月齡以食糧混合餵食薑黃素的 JNPL3 小鼠。旋轉棒試驗研究 18 個月大的 JNPL3 小鼠顯示，薑黃素是無法改善其運動功能($p = 0.67$)。最後，在其他表型的變化，薑黃素能夠同時降低所有雄性小鼠的死亡率($p = 0.009$)和所有小鼠的體重減輕($p = 0.007$)。

結論：我們的數據表明，薑黃素可透過增加澱粉樣蛋白溶解，降解和外排，以減少澱粉樣蛋白的負荷；它可以提供防止澱粉樣蛋白毒性的保護；以及它也可增加抗氧化防禦系統。在 tau 蛋白病變方面，薑黃素可以減少 NFT 的形成，但需更多的工作來證實此功能。總的來說，在這項研究中，所有的數據顯示了薑黃素與生理有關的功能，這顯示其在 AD 治療中的有益作用。

ACKNOWLEDGEMENTS

I would like to express my greatest gratitude to my Lord Jesus Christ. Thanks for His grace, guidance and lead. Without Him, I will not be able to have the opportunity to start my PhD degree and I will not be able to finish my thesis without His amazing guidance and arrangement. I would like to present this thesis to Him and may this thesis glorify His name but not mine. Thank God for His strength and mercy and never fail to listen to my prayers.

I also gratefully acknowledge the help of my thesis supervisor, Professor Larry Baum, who had offered me valuable guidance in the design of this project, proofread my thesis and provided me suggestions. I would not be able to complete my work on time without his generous help, and I will not forget the time that I worked with him.

Special thanks go to Professor Ashley Bush and Robert Cherny, Mental Health Research Institute, Melbourne, Australia. They replied to my questions on their experiment patiently and kindly invited me to learn in their laboratory. They also generously offered expensive chemicals from Australia so that I could finish the experiment in Hong Kong. Their invitation and those conversations inspired me to think of every experiment in a more "physiologically relevant" manner.

Last but not least, I would like to express my sincere appreciation to my wife and son for their love, support and encouragement, and to my parents and sisters for their love and concern. Their love supported me to start, persist and finish this work.

TABLE OF CONTENTS

ABSTRACT	I
摘要	IV
ACKNOWLEDGEMENTS	VI
TABLE OF CONTENTS	VII
Abbreviations	XIV
CHAPTER ONE: INTRODUCTION	1
1.1 Dementia and Alzheimer's disease	1
1.2 Alzheimer's disease and aging	5
1.3 Genetics	6
1.3.1 EOAD	6
1.3.2 LOAD	8
1.4 Amyloid- β protein	9
1.4.1 Amyloid plaques	9
1.4.2 Physiology of A β	10
1.4.3 Production of A β (processing of APP)	13
1.4.3.1 α -secretase	15
1.4.3.2 β -secretase	17
1.4.3.3 γ -secretase	18
1.4.3.4 Competitive substrates	20
1.4.4 Toxicity of A β	21
1.4.5 Oligomerization and fibrillization of A β	21
1.4.6 Protection from A β toxicity	23
1.4.7 Transport of A β	24
1.4.8 Degradation of A β	25
1.5 Tau	27
1.5.1 Function of Tau (general function)	28
1.5.2 Regulation of neurofibrillary tangle formation	29
1.6 Disease hypotheses	30
1.6.1 Amyloid hypothesis	30
1.6.2 Criticism of amyloid hypothesis	31

1.6.3 Tau hypothesis	32
1.7 Current treatments	32
1.8 Drug development	34
1.9 Curcumin	37
1.9.1 General functions of curcumin	37
1.9.2 AD related functions of curcumin	38
1.9.3 Unaddressed issues of curcumin in AD treatment	40
1.10 Aims of study	43
CHAPTER TWO: MATERIALS AND METHODS	44
2.1 Cell free assays	44
2.1.1.1 A β aggregation Thioflavin T assay	44
2.1.1.2 Western blotting of monomeric A β	45
2.1.1.3 Statistical analysis	46
2.1.2.1 Hydrogen peroxide scavenging assay	47
2.1.2.2 Statistical analysis	48
2.2 Cell cultures	48
2.2.1 Culture of microglia (BV-2)	48
2.2.2 MTT cell viability assay	49
2.2.3 Dot blotting of ApoE protein	49
2.2.4 Western blotting of ApoE	50
2.2.5 Signal quantification of secreted ApoE	51
2.2.6 Statistical analysis	51
2.3 Animal studies	51
2.3.1.1 Strains	51
2.3.1.2 Breeding	52
2.3.1.3 Genotyping	53
2.3.1.4 DNA extraction	53
2.3.1.5 DNA quantification	54
2.3.1.6 PCR	55
2.3.2.1 Demographic data	56
2.3.2.2 Husbandry	56
2.3.2.3 Diet	57
2.3.2.4 Drug administration	57

2.3.2.5 Statistical analysis (body weight, mortality)	58
2.3.3.1 Rotarod test	58
2.3.3.2 Statistical analysis	59
2.3.4 Dissection	59
2.3.5 Secretase activity assays	60
2.3.5.1 Protein extraction	60
2.3.5.2 Protein quantification	61
2.3.5.3 α -secretase assay	62
2.3.5.4 β -secretase assay	62
2.3.5.5 γ -secretase assay	63
2.3.5.6 Statistical analysis	64
2.3.6 Total tau quantification	64
2.3.6.1 Protein extraction	64
2.3.6.2 Protein quantification	64
2.3.6.3 Western blotting of total tau	65
2.3.6.4 Signal quantification of total tau	66
2.3.6.5 Statistical analysis	66
2.3.7 PHF quantification	66
2.3.7.1 Sample preparation	66
2.3.7.2 PHF isolation	67
2.3.7.3 Western blotting of AT8-immunopositive PHF	68
2.3.7.4 Signal quantification of PHF	69
2.3.7.5 Statistical analysis	69
2.3.8 Histological staining	69
2.3.8.1 Sample preparation	69
2.3.8.1.1 Fixation	69
2.3.8.1.2 Paraffin embedding	69
2.3.8.1.3 Sectioning	70
2.3.8.2.1 Immunohistological staining of amyloid plaques	71
2.3.8.2.2 Quantification of 4G8-immunopositive plaque area	72
2.3.8.2.3 Statistical analysis	72
2.3.8.3.1 Bielschowsky's silver staining	72
2.3.8.3.2 Quantification of silver stained tangles	73

2.3.8.3.2 Statistical analysis	74
2.3.8.4.1 Immunohistological staining of A τ 8-immunopositive tangles	74
2.3.8.4.2 Quantification of A τ 8-immunopositive area	74
2.3.8.4.3 Statistical analysis	75
2.3.9 Microarray	75
2.3.9.1 RNA extraction	75
2.3.9.2 RNA quantification	76
2.3.9.3 RNA quality determination	76
2.3.9.4 Microarray	77
2.3.9.5 Signal processing	77
2.3.9.6 Data analysis	78
2.3.10 Real-time PCR	78
2.3.10.1 Reverse transcription	78
2.3.10.2 Primers for real-time PCR	79
2.3.10.3 Real-time PCR	81
2.3.10.4 Data calculation	82
2.3.10.5 Statistical analysis	83
CHAPTER THREE: RESULTS	85
3.1 Effects of curcumin on phenotypic changes	85
3.1.1 Effect of curcumin treatment on body weight	85
3.1.2 Mortality upon curcumin treatment	88
3.1.3 Rotarod performance upon curcumin treatment	95
3.2 Effects of curcumin on A β generation	97
3.2.1 Microarray of APP cleavage enzyme and competitive substrate genes	97
3.2.2 Real-time PCR of APP cleavage enzyme and competitive substrate genes	100
3.2.2.1 Gene expression of secretases	102
3.2.2.2 Gene expression of competitive substrates	104
3.2.3 Secretase functional assays	111
3.3 Effects of curcumin on A β aggregate formation	111
3.3.1 Anti-A β -metal aggregation-Thioflavin-T assay	111
3.3.2 Western blotting of monomeric A β from anti-A β aggregation assay	113
3.3.3 Immunohistochemical staining of 4G8-immunopositive plaques	115

3.4 Effects of curcumin on A β degradation	118
3.4.1 Microarray of A β degrading enzyme genes	118
3.4.2 Real-time PCR of A β degrading enzymes	119
3.5 Effects of curcumin on A β removal	124
3.5.1 Cell culture study	124
3.5.1.1 MTT assay of tested compound	124
3.5.1.2 ApoE secretion from BV2 microglial cells treated with phenolic compounds	126
3.5.2 Microarray of A β transporter and receptor genes	131
3.5.2.1 A β transporters	131
3.5.2.2 A β receptors	131
3.5.3 Real-time PCR of A β transporter and receptor genes	133
3.5.3.1 Gene expression of A β transporters	133
3.5.3.2 Gene expression of A β receptors	133
3.6 Effects of curcumin on cholinergic function	142
3.6.1 Microarray of cholinergic genes	142
3.6.2 Real-time PCR data on expression of genes regulating acetylcholine homeostasis	142
3.7 Other neuroprotective and harmful effects of curcumin	147
3.7.1 Cell free assay	147
3.7.1.1 Hydrogen peroxide scavenging assay	147
3.7.2 Microarray of neuroprotective and neurotoxic genes	150
3.7.3 Real-time PCR of neuroprotective and neurotoxic genes	153
3.7.3.1 Gene expression of proteins regulating A β level	155
3.7.3.2 Gene expression of proteins reducing A β toxicity	157
3.7.3.3 Gene expression of proteins involving oxidative stress	160
3.8 Effects of Curcumin on Tauopathy	163
3.8.1 Gene expression of endogenous Mapt	166
3.8.1.1 Microarray of Mapt	166
3.8.1.2 Gene expression of endogenous Mapt by real-time PCR	166
3.8.2 Protein expression of transgenic mutant tau	167
3.8.2.1 Total human mutant tau expression	167

3.8.3 Neurofibrillary tangles	168
3.8.3.1 Bielschowsky's silver staining	168
3.8.3.2 Immunohistochemical staining of AT8-immunopositive tangle	170
3.8.4 PHF level	175
CHAPTER FOUR: DISCUSSION	176
4.1 Effects of curcumin on phenotypic changes	176
4.1.1 Effect of curcumin treatment on body weight	176
4.1.2 Mortality upon curcumin treatment	178
4.1.3 Rotarod performance upon curcumin treatment	180
4.2 Effects of curcumin on A β generation	183
4.2.1 Microarray of APP cleavage enzyme and competitive substrate genes	183
4.2.2 Real-time PCR of APP cleavage enzyme and competitive substrate genes	185
4.2.3 Secretase function assays	188
4.3 Effects of curcumin on A β aggregate formation	189
4.3.1 A β aggregation Thioflavin T assay	189
4.3.2 Western blotting of monomeric A β from anti-A β aggregation assay	190
4.3.3 Immunohistochemical staining of 4G8-immunopositive plaques	191
4.4 Effects of curcumin on A β degradation	193
4.4.1 Microarray of A β degrading enzyme genes	193
4.4.2 Real-time PCR on gene expression of A β degrading enzymes	194
4.5 Effects of curcumin on A β removal	198
4.5.1 Cell culture study	198
4.5.2 Microarray of A β transporter and receptor genes	200
4.5.2.1 A β transporters	200
4.5.2.2 A β receptors	200
4.5.3 Real-time PCR of A β transporter and receptor genes	200
4.5.3.1 Gene expression of A β transporters	200
4.5.3.2 Gene expression of A β receptors	201
4.6 Effects of curcumin on cholinergic functions	204
4.6.1 Microarray of cholinergic genes	204
4.6.2 Real-time PCR on expression of genes regulating acetylcholine	205

homeostasis	
4.7 Other neuroprotective and harmful effects of curcumin	207
4.7.1 Cell free assay	207
4.7.1.1 Hydrogen peroxide scavenging assay	207
4.7.2 Microarray of neuroprotective and neurotoxic genes	208
4.7.3 Real-time PCR of neuroprotective and neurotoxic genes	208
4.8 Effects of Curcumin on Tauopathy	215
4.8.1 Gene expression of endogenous Mapt	215
4.8.2 Protein expression of transgenic mutant tau	216
4.8.3 Neurofibrillary tangles	217
4.8.4 PHF level	219
CHAPTER FIVE: CONCLUSIONS AND FUTURE PERSPECTIVE	221
5.1 Conclusions	221
5.2 Future Perspective	224
REFERENCES	226
APPENDICES	264

Abbreviations

A β	Amyloid- β protein
ACh	Acetylcholine
AChE	Acetylcholinesterase
AD	Alzheimer's disease
ADAMs	A member of the disintegrin and metalloproteases
ADDLs	A β -derived diffusible ligands
AICD	APP intracellular domain
AP	Alkaline phosphatase
ApoE	Apolipoprotein E
Apoer2	Apolipoprotein E receptor 2
APP	Amyloid precursor protein
APS	Ammonium persulfate
Bace1	Beta-site APP-cleaving enzyme
Bmp6	Bone morphogenic protein 6
Btc	Betacellulin
Ca(II)	Calcium ion 2+
Cdk5	Cell division protein kinase 5
ChAT	Choline acetyltransferase
Cht1	High-affinity choline transporter
CLU	Clusterin
CNS	Central nervous system
CR1	Complement receptor type 1
CSF	Cerebrospinal fluid
Ct	Threshold cycle
CTF	Carboxy-terminal fragment
Cu(II)	Copper ion 2+
CuCl ₂	Copper chloride
DCF	2',7'-dichlorofluorescein Diacetate
DMEM	Dulbecco's modified eagle's medium
DMSO	Dimethyl sulfoxide
EOAD	Early-onset AD

ER	Endoplasmic reticulum
Gapdh	Glyceraldehyde 3-phosphate dehydrogenase
Glut4	Glucose transporter 4
GPX	Glutathione peroxidase
Gsk3	Glycogen synthase kinase 3
H ₂ O ₂	Hydrogen peroxide
HRP	Hydrogen peroxidase
IC ₅₀	Half maximal inhibitory concentration
Ide	Insulin-degrading enzyme
Igf2	Insulin-like growth factor 2
IgG	Immunoglobulin G
Irs1	Insulin receptor substrate 1
JNK	c-Jun N-terminal kinase
Kl	Klotho
KPI	Kunitz protease inhibitor
LDL	Low density lipoprotein
LOAD	Late-onset AD
Lrp1	Low density lipoprotein receptor-related protein 1
LTP	Long-term potentiation
MAPs	Microtubule-associated proteins
Mg(II)	Magnesium ion 2+
Mmp	Matrix metalloproteinase
MRI	Magnetic resonance imaging
mRNA	Messenger RNA
Msrl	Macrophage scavenger receptor 1
MTT	3-[4,5-dimethylthiazol-2-yl]-2,5-diphenyl tetrazolium bromide
MWCO	Molecular weight cut-off
NaOH	Sodium hydroxide
NBF	Neutral buffered formalin
Nct	Nicastrin
NFT	Neurofibrillary tangle
NMDA	N-methyl-d-aspartate
Nos2	Nitric oxide synthase 2

Nox1	NADPH oxidase 1
NTF	Amino-terminal fragment
<i>O</i> -GlcNAc	<i>B</i> - <i>n</i> -acetylglucosamine
PBS	Phosphate buffered saline
PCR	Polymerase chain reaction
PHF	Paired helical filaments
PICALM	Phosphatidylinositol binding clathrin assembly protein
PKC	Protein kinase c
PPCs	Proprotein convertases
PS1	Presenilin 1
PS2	Presenilin 2
PVDF	Polyvinylidene fluoride
RAGE	Receptor for advanced glycation endproducts
ROS	Reactive oxygen species
SD	Standard deviation
SDS	Sodium dodecyl sulfate
SDS-PAGE	Sodium dodecyl sulfate polyacrylamide gel electrophoresis,
SEM	Standard error of the mean
siRNA	Small interfering RNA
SIRT1	Sirtuin 1
SOD	Superoxide dismutase
SORL1	Sortilin-related receptor 1
TACE	Tumor necrosis factor- α
TBST	Mixture of Tris-buffered saline and Tween 20
VACht	Vesicular acetylcholine transporter
ZnCl ₂	Zinc chloride

CHAPTER ONE: INTRODUCTION

1.1 Dementia and Alzheimer's disease

Dementia is a set of central nervous system (CNS) disorders characterized primarily by progressive worsening of cognitive and intellectual functions with or without mental disorder of consciousness, which also includes some behavioral abnormalities and changes in patients' personality (Ropper and Samuels, 2009). Dementia involves not only memory impairment, but also deterioration of at least one other cognitive ability, such as language (aphasia), reasoning, and executive function, and impairment in social or occupational functioning (Sadock et al., 2009). Eventually, it leads to complete loss of the patient's capabilities to take care of his daily life.

The highest risk factor for dementia is aging. In the world, about 5 percent of the population presumably has dementia at the age of 65. This proportion rises to almost 50 percent among people age over 85. It was estimated that, in 2005, there were about 24.3 million dementia patients worldwide (Ferri et al., 2005) (**Table 1.1**). The number of AD patients is projected to double every 20 years to 81 million by 2040. The increase between 2001 and 2040 is estimated to exceed 100% in developed countries and 300% in developing countries.

A study conducted in Hong Kong in 2006 showed that the prevalence of dementia is around 2.5 percent in the age group of 65 – 69 and exponentially rises to 32.1 percent for ages above 85 (**Figure 1.1**). More women than men have dementia, but this difference disappears at ages over 85 (Lam et al., 2008) (**Figure 1.2**).

	Number of people with dementia, aged 60 years (millions)			Increase in number of people with dementia (%)	
	2001	2020	2040	2001–2020	2001–2040
Western Europe (EURO A)	4.9	6.9	9.9	43	102
Eastern Europe low adult mortality (EURO B)	1.0	1.6	2.8	51	169
Eastern Europe high adult mortality (EURO C)	1.8	2.3	3.2	31	84
North America (AMRO A)	3.4	5.1	9.2	49	172
Latin America (AMRO B/D)	1.8	4.1	9.1	120	393
North Africa and Middle Eastern Crescent (EMRO B/D)	1.0	1.9	4.7	95	385
Developed western Pacific (WPRO A)	1.5	2.9	4.3	99	189
China and developing western Pacific (WPRO B)	6.0	11.7	26.1	96	336
Indonesia, Thailand, and Sri Lanka (SEARO B)	0.6	1.3	2.7	100	325
India and south Asia (SEARO D)	1.8	3.6	7.5	98	314
Africa (AFRO D/E)	0.5	0.9	1.6	82	235
TOTAL	24.3	42.3	81.1	74	234

Table 1.1. Number of demented patients in 2001 and estimation for 2020 and 2040 in developed and developing countries, grouped by WHO region. Adapted and modified from (Ferri et al., 2005).

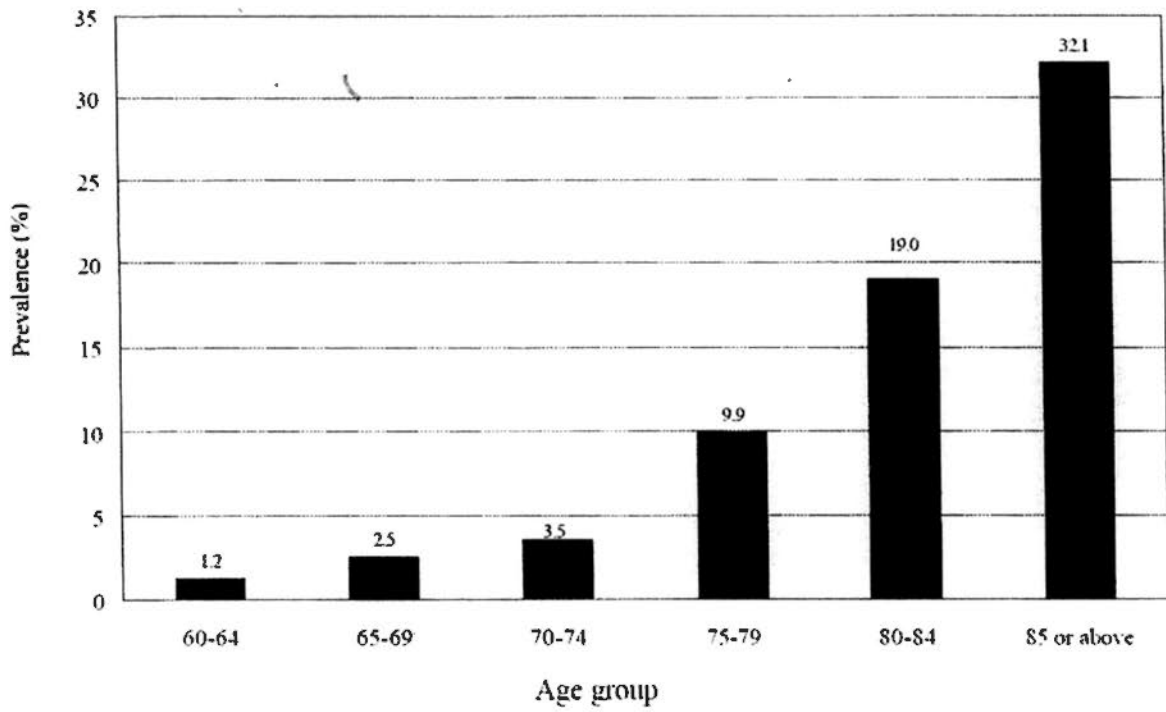


Figure 1.1 Percentage prevalence of dementia in Hong Kong, by age group. Adapted from (Ng and Chan, 2009).

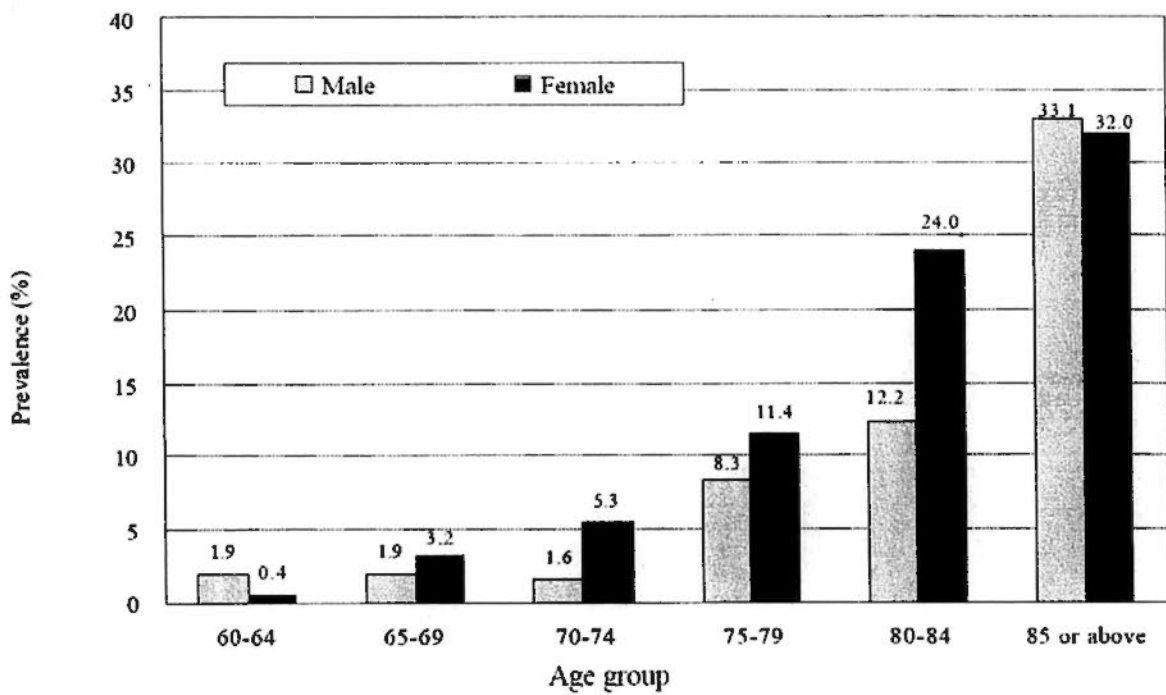


Figure 1.2 Percentage prevalence of dementia in Hong Kong, by age and sex. Adapted from (Ng and Chan, 2009).

With advancing scientific findings and medical technologies, improving living environment and hygiene, increasing education, scientific and medical knowledge of the public, many more people can live longer than ever before. The longevity of people in developed and developing countries is definitely increasing, which inevitably increases the population of dementia patients. Therefore, the demands upon family caregivers, medical and social services impose enormous economic pressure to any society.

Dementia may be reversible or irreversible, depending on the cause, which could be neurodegenerative, vascular, neurological disease, endocrine, nutritional, infectious, metabolic, traumatic, or various environmental exposures (Sadock et al., 2009). Neurodegenerative disorders are the most prevalent cause. The neurodegenerative disease, Alzheimer's disease (AD) accounts for about 50 to 70 percent of all dementia cases (Sadock et al., 2009).

AD is the most common form of dementia for ages over 65. It is manifested firstly and primarily by symptoms of dementia, such as memory impairment and confusion, together with a unique set of histopathological changes including the presence of extracellular amyloid plaques, intracellular neurofibrillary tangles (NFT) and loss of neuronal cells in the regions of cerebral cortex, such as hippocampus, amygdala and entorhinal cortex. These pathological changes are detected by post-mortem analysis. The cholinergic system in the affected areas is severely degenerated. These changes suggest why the patients have memory impairment. Gross neuroanatomical analysis shows severe brain atrophy due to the loss of grey matter which, in turn, causes thinning of the cortical gyri. Therefore, AD brains have enlarged ventricles and widened sulci.

The first case of AD was identified and described by a German psychiatrist and neuropathologist named Alois Alzheimer in 1906. He identified a rapidly deteriorating, demented patient, Frau Auguste D., with loss of memory, depression and hallucinations. She died at age 55. The autopsy done by Dr. Alzheimer showed the presence in the cerebral cortex of shrinkage and lesions, substantial distorted tissue and neuronal cell damage (Turkington and Mitchell, 2011). Histopathological analysis showed the presence of substantial numbers of senile plaques and NFTs. More than 100 years later, however, AD is still incurable, and the etiology is still unclear.

1.2 Alzheimer's disease and aging

The prevalence of AD increases from 5% at age 65 to as much as 30% at age 85 (Sadock et al., 2009). This observation suggests that age is the strongest risk factor for AD development. There is, indeed, considerable overlapping of changes between brains of people undergoing normal aging and brains of people suffering AD. An early study suggested that there is a gradual but very slow decrease of brain weight at about 0.1% per year from young adulthood to the age of 60 (Blinkov and Glezer, 1968). Loss of brain volume is a common sign of aging and AD. Similarly, a study using quantitative volumetric MRI showed that the rate of brain volume loss observed over time is slow and constant amongst healthy younger and oldest-old elderly (Mueller et al., 1998). In contrast, another 6-year longitudinal MR imaging study showed that the atrophy rate of the median temporal lobe amongst the healthy elderly is about 0.2 to 0.3 percent per year, which is considerably slower than that of AD patients, which is over 0.8 percent per year (Rusinek et al., 2003). Amyloid plaques

and neurofibrillary tangles also coexist in nondemented persons. They become more widespread and increase in numbers with aging. However, the number of plaques is much fewer in mentally intact individuals compared with AD patients (Tomlinson et al., 1968, 1970). Therefore, some researchers believe that AD is an exaggerated form of the process of brain aging. Whether the presence of neuritic plaques and tangles causes neurodegeneration and AD is still a controversial issue.

1.3 Genetics

According to the age of onset of AD, it can be classified as early-onset AD (EOAD) or late-onset AD (LOAD) by the cut-off age of 65 years old. Over 95 percent of AD patients develop it after the age of 65 years old. Only 1 to 5 percent of patients are identified between 50 and 65 years old. The pathology of these two types of AD is essentially the same, but EOAD is more severe, with rapid progression.

1.3.1 EOAD

Most EOAD is due to defects in one of three genes: amyloid β precursor protein (APP), presenilin 1 (PS1) or presenilin 2 (PS2). AD caused by mutations in these genes is inherited in an autosomal dominant manner. These mutations either increase secretion of total amyloid- β proteins ($A\beta$) or increase the ratio of longer (42 or 43 amino acid) to shorter (40 amino acid) fragments of $A\beta$.

APP is an integral membrane-associated type-1 transmembrane protein (see Figure 1.3). The gene is located on chromosome 21 (Levy et al., 1990). A variety of

mRNA species can be alternatively transcribed from 18 exons of the APP gene to form different lengths of APP protein (APP695, APP751, APP770). APP is widely expressed in different organs and tissues, with relatively higher expression in brain, heart and kidney. Predominant APP transcripts in neurons, microglia and astrocytes are different. In neurons but not in microglia and astrocytes, APP generally lacks the Kunitz protease inhibitor (KPI) domain. The number of known APP mutations which have been confirmed to cause AD is still increasing (Cruts, 2011). All of them are located within exons 16 and 17, which are around the A β -encoding exons. The known effects of these AD-inherited missense mutations in APP, so far, are on the processing of the encoded APP protein. All APP mutations, however, only account for less than 0.1 percent of all AD cases.

On the other hand, 182 and 14 AD-related mutations have so far been confirmed in PS1 and PS2, respectively (Cruts, 2011). The PS1 and PS2 genes are located on chromosome 14 (Sherrington et al., 1995) and 1 (Levy-Lahad et al., 1995), respectively. They are ubiquitously-expressed, multiple transmembrane domain proteins. These presenilins are involved in the γ -secretase cleavage of APP, and the AD-linked mutations in presenilins affect this cleavage and augment the ratio of A β 1-42(43) to A β 1-40 (see section 1.5).

As a whole, the net effects of AD-related mutations in APP, PS1 and PS2 are an increase in the level of A β 1-40 or in the ratio of A β 1-42(43) to A β 1-40. Ultimately, the normal balance of A β production, accumulation and removal is distorted, which leads to the initiation and progression of AD, according to the amyloid hypothesis.

1.3.2 LOAD

LOAD is not autosomal dominant in nature. The first well established susceptibility gene is apolipoprotein E (ApoE). It is located on chromosome 19 and encodes a protein of 299 amino acids which is responsible for lipid-binding and delivery in the plasma and cerebrospinal fluid (CSF). In humans, it exists in three different alleles, APOE- ϵ 2, APOE- ϵ 3 and APOE- ϵ 4, based on the substitution of amino acids at positions 112 and 158 (Mahley, 1988). APOE- ϵ 2 is the protein with a cysteine at both sites, APOE- ϵ 3 differs by a substitution of arginine at position 158, and APOE- ϵ 4 has an arginine at both sites. Studies showed that the presence of one APOE- ϵ 4 allele instead of two APOE- ϵ 3 alleles (the most common genotype) increases the risk of developing AD by 2 to 5 fold (Corder et al., 1993) and significantly reduces the onset age by 7.7 years (Kurz et al., 1996). In contrast, the APOE- ϵ 2 allele is associated with reduced risk of developing AD (Corder et al., 1994). Functionally, it has been showed that ApoE isoforms have different effects on the level of $A\beta$ 1-42 in brain (ϵ 4 \gg ϵ 3 $>$ ϵ 2) (Bales et al., 2009).

Sortilin-related receptor 1 (SORL1) has been identified with haplotypes associated with LOAD (Rogaeva et al., 2007). The gene is located on chromosome 11 and is highly expressed in the CNS. It assists the retention of APP in compartments where low secretase activity is found, thereby reducing both amyloidogenic and nonamyloidogenic processing of APP.

Recently, two large genome-wide association studies have identified more polymorphisms associated with AD (Harold et al., 2009; Lambert et al., 2009). Though functional roles for these genes in AD are not validated yet, clusterin (CLU)

and complement receptor type 1 (CR1) are suggested to be related to A β clearance (Bertrand et al., 1995; Wyss-Coray et al., 2002), and phosphatidylinositol binding clathrin assembly protein (PICALM) may be involved in neurotransmitter release (Baig et al., 2010).

1.4 Amyloid- β protein

A β is the principle constituent of amyloid plaques found in the brain of AD patients. It is produced by the proteolytic cleavage of APP by β -secretase and γ -secretase. The length varies from 39 to 43 amino acid residues, with A β 1-40 as the most abundant and A β 1-42 as the second most abundant and the most fibrillogenic isoform (Kang et al., 1987). It is continuously produced and partially secreted into extracellular space. The function of this peptide is not clear yet.

1.4.1 Amyloid plaques

Amyloid plaques are extracellular proteinaceous deposits of A β peptides and other components, including A β -associated proteins and metal ions. Plaques exist as three forms in Alzheimer's brains: diffuse plaques, senile plaques and cerebrovascular deposits.

Diffuse plaques are believed to appear earlier than senile plaques and are referred to as pre-amyloid deposits. They are abundant, amorphous, spherical and less dense than senile plaques (Tagliavini et al., 1988). These plaques can be detected with A β antibody, but not by β -pleated-sheet specific dyes such as Congo Red and

thioflavin-S, indicating that the structure of the peptides do not transition to a β -pleated-sheet conformation. They do not have surrounding degenerating neurites, tangle-bearing neurons and congophilic angiopathy.

In contrast, senile plaques form spherical structures of around 50-200 μm diameter, with a central amyloid core enriched in longer $\text{A}\beta$ species (42 or 43 amino acids) (Iwatsubo et al., 1994), surrounded by reactive astrocytes, activated microglia, and infiltrating dystrophic neurites which contain paired helical filaments (PHF) (Mandybur and Chuirazzi, 1990). Due to the transformation of $\text{A}\beta$ aggregates to β -pleated sheets, the cores of senile plaques can be stained with Congo Red, which appears as a green birefringence under polarized light, and thioflavin-S.

Axonal sprouting surrounds senile plaques, suggesting that they are related to synaptic dysfunction (Arendt, 2001; Hu et al., 2003). Moreover, the co-existence of acute phase proteins such as α_1 -antichymotrypsin and α_2 -macroglobulin, and of interleukin-1-positive and interleukin-6-positive activated microglia, suggest that senile plaques are associated with neuroinflammation of the surrounding brain tissue (Eikelenboom and Vecrhuis, 1996; Wegiel and Wisniewski, 1990). However, with the finding that $\text{A}\beta$ oligomers are particularly toxic, attention has shifted from amyloid plaque toxicity towards the oligomers.

1.4.2 Physiology of $\text{A}\beta$

$\text{A}\beta$ peptide was first identified and sequenced as the major constituent of the extracellular plaques of AD brains (Glenner and Wong, 1984; Wong et al., 1985). It was then confirmed that it normally exists in the CSF of non-demented persons and in

the conditioned medium from neuronal cell cultures (Haass et al., 1992; Tamaoka et al., 1997). A β 1-40 and A β 1-42 are the most and second-most abundant forms of A β peptides. The concentration of A β 1-40 in human CSF is about 2-3 ng/mL, which is about 10 times as much as A β 1-42. The level of CSF A β 1-40 does not differ between AD patients and non-demented controls, however, the level of A β 1-42 is around 40 to 70 percent lower in AD patients than in controls (Ida et al., 1996). Therefore, A β peptides might have normal physiological functions in the CNS.

APP and A β maintain synaptic plasticity and therefore memory formation. Knockout studies showed that synapse numbers are decreased, dendritic length projection depth of CA1 neurons is reduced, long-term potentiation is impaired and performance on spatial memory tasks is worse in APP null mice (Dawson et al., 1999; Seabrook et al., 1999). These data suggest that APP and probably A β peptides are involved in the maintenance of synaptic plasticity and synaptic function within the hippocampus.

In contrast, transgenic mice overexpressing APP have impaired memory and reduced long-term potentiation (LTP), which can be reversed by inhibiting A β production through PS1 knockout (Dewachter et al., 2002). However, it should be noted that such APP transgenic mice have APP overexpression and A β production several times higher than normal levels, the APP gene has an AD-linked mutation and the origin of the gene is human. Therefore, the defects in this transgenic strain may be due to the abnormally high level of A β , gain-of-toxic-functions from the mutation or the foreign origin of the transgene.

Evidence for a positive role for A β in synapse function can be strengthened by a study showing that wild type mice with PS1 under-expression, which have reduced A β level, display hippocampal LTP impairment (Morton et al., 2002). Recently, another study further showed that endogenous A β is a prerequisite for normal hippocampal synaptic plasticity and memory function. In that study, A β antibody and siRNA against murine APP impaired LTP and memory of mice, and these impairments were reversed by addition of human A β 1-42 peptide, which may play a role in the regulation of α 7-containing nicotinic acetylcholine receptors (Puzzo et al., 2011).

Neurite outgrowth and survival are promoted by A β . In a primary neuronal culture study, nanomolar concentrations of A β 1-40 increase membrane phospholipid concentrations and the expression of APP holoprotein and secreted APP, tau, and growth associated protein-43, which are involved in neurite outgrowth (Wang et al., 2000). Moreover, it was shown that by suppressing A β production in primary cortical neuronal cultures by β - or γ -secretase inhibition, the viability of these cultures decreased to around 20-50% of control levels within 24 hours (Plant et al., 2003). This effect is neuronal specific because rat astrocytes and non-neuronal cell lines were unaffected. With the co-addition of only picomolar A β 1-40, the neuron cultures were protected from the toxicity of secretase inhibitors.

A β has been shown to offer antioxidant protection at low nanomolar concentrations. At physiologically relevant concentrations of A β 1-40 and A β 1-42, auto-oxidation of CSF lipoproteins and plasma low density lipoprotein (LDL) is greatly suppressed. Interestingly, such antioxidant function disappeared at higher concentrations of the peptide. Such an effect may involve chelating transition metal

ions since copper-catalyzed LDL oxidation is also inhibited (Kontush et al., 2001). The protective effects of metal chelation by A β were further proven in vivo. Co-injection into rat cerebral cortex of human A β 1-42 and iron, zinc and copper at the concentrations found in plaques caused significantly less neuronal loss than injecting metals alone (Bishop and Robinson, 2004) or iron with rat variants of A β 1-42 (Bishop and Robinson, 2003). This may further suggest that the presence of senile plaques is a neuroprotective response to elevated levels of redox-active metal ions. Taking together the above evidence, A β peptides can act as a regulator of redox-active metal ion homeostasis.

1.4.3 Production of A β (processing of APP)

APP is a single transmembrane protein containing a large extracellular amino-terminal and a small intracellular cytoplasmic domain. As mentioned before (in section 1.4.1), the gene is localized on chromosome 21 in humans. It is widely expressed in different organs, tissues and cells. From the 18 exons of the pre-mRNA, three main isoforms are formed by alternative splicing: APP695, APP751 and APP770 (Kitaguchi et al., 1988). APP695 is the only isoform that lacks the KPI domain. It is predominantly expressed in the neurons of the brain in the ratio of about 20:10:1 for APP 695:751:770 (Tanaka et al., 1989).

At its amino-terminal, APP has a 17-amino acid signaling peptide (Weidemann et al., 1989), which guides its transportation. Close to its carboxyl-terminal, APP has a 22-amino acid transmembrane domain, which helps its insertion into the endoplasmic reticulum, Golgi apparatus and cell membrane (Caporaso et al.,

1994; Palacios et al., 1992; Tomimoto et al., 1995). APP is processed by posttranslational modifications such as glycosylation, phosphorylation and sulfation (De Strooper and Annaert, 2000).

Full length APP is also modified by cleavage, performed by at least three enzymes, namely, α -, β - and γ -secretase. A number of fragments can be generated by secretase cleavage. The cleavage of full length APP first happens within the luminal/extracellular domain and is performed by either α -secretase or β -secretase. When it is cleaved by α -secretase, APP will undergo non-amyloidogenic proteolytic processing to produce 2 fragments, APPs α and APP-CTF α (C83), which precludes A β peptide generation. C83 is further cleaved by γ -secretase to generate a 3 kDa peptide (p3). When APP is first cleaved by β -secretase, this amyloidogenic proteolytic processing will produce 2 fragments, APPs β and APP-CTF β (C99). C99 is then cleaved by γ -secretase to generate A β and the APP intracellular domain (AICD) (Haass and Selkoe, 1993) (**Figure 1.4.3**).

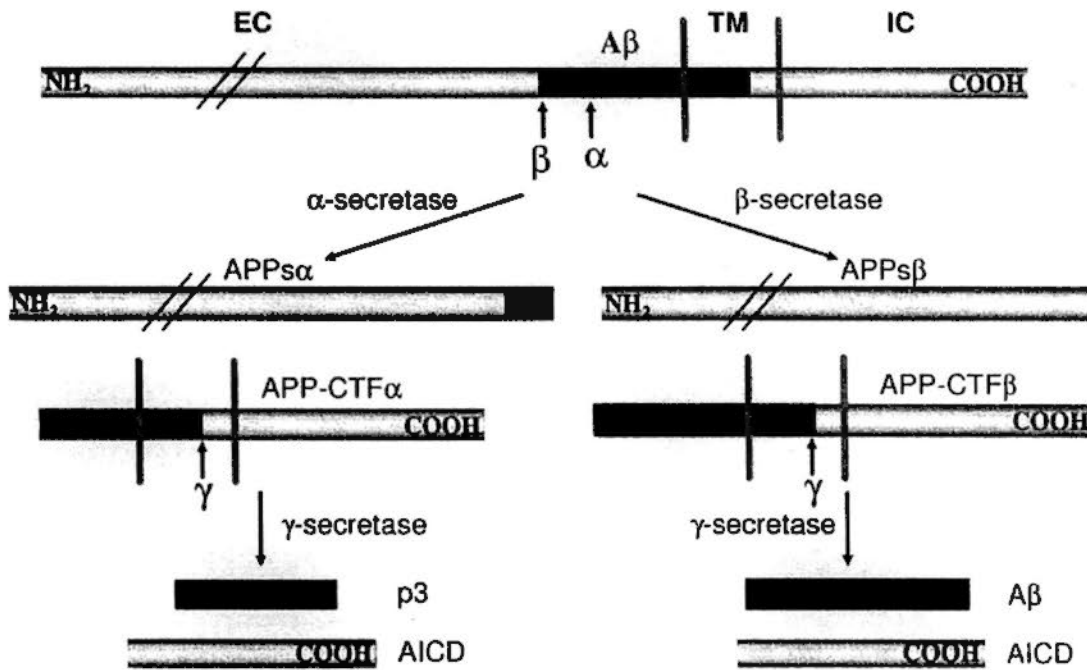


Figure 1.4.3. Schematic diagram of the non-amyloidogenic and amyloidogenic processing of APP.

Only cleavage by α -secretase (non-amyloidogenic), β -secretase (amyloidogenic) and γ -secretase are shown here, where EC, IC, TM are extracellular, intracellular and transmembrane domains, respectively. In non-amyloidogenic processing, APPs α and APP-CTF α are first generated by cleavage by α -secretase, and then p3 and AICD are generated by γ -secretase cleavage. In amyloidogenic processing, APPs β and APP-CTF β are first generated by β -secretase cleavage, followed by γ -secretase cleavage to generate AICD and A β peptides. Adapted from (Zheng and Koo, 2006).

1.4.3.1 α -secretase

The α -secretase cleavage site is between lysine 613 and leucine 614 (of the APP695 isoform), which correspond to amino acids 16 and 17 of A β . Therefore such cleavage precludes the generation of A β peptides and is termed non-amyloidogenic processing. In addition, a soluble and protective fragment called APPs α is generated which can reduce the toxicity of A β .

Three candidate proteins have been so far identified to possess α -secretase activity: ADAM9, ADAM10 and ADAM17. All of them belong to the A member of the Disintegrin And Metalloprotease (ADAMs) family of proteases and are expressed as preproteins which are activated by removal of the prodomain in the late Golgi (Anders et al., 2001; Schlondorff et al., 2000) by proprotein convertases (PPCs) (Seidah and Chretien, 1999). They can be activated by protein kinase C (PKC) stimulation (Buxbaum et al., 1993). ADAM17, also called tumor necrosis factor- α (TACE), can also cleave the TNF- α receptor (Seidah and Chretien, 1999). PKC-stimulated fibroblasts obtained from TACE-knockout mice displayed impaired APP secretion (Buxbaum et al., 1998). An activated ADAM10 located in the plasma membrane has been shown to possess constitutive and regulated α -secretase activity in cell cultures. In HEK 293 cells overexpressing ADAM10, the basal and PKC-stimulated α -secretase cleavage activity was upregulated several fold (Lammich et al., 1999). The endogenous α -secretase activity was suppressed by a point mutation on ADAM10 in the zinc binding region. Moreover, purified ADAM10 cleaved at the correct α -secretase site on A β fragments. In a study using COS cells engineered to co-express ADAM9 and APP, when PKC was activated by phorbol ester, the APP protein was cleaved exclusively at the α -secretase site (Hotoda et al., 2002).

Taken together, the data suggest that ADAM9, ADAM10 and ADAM17 play an important role in α -secretase cleavage of APP. They can be manipulated to increase the non-amyloidogenic processing of APP, such that more APPs α can be produced and, at the same time, less A β generated and the amyloid burden of AD reduced.

1.4.3.2 β -secretase

The β -secretase cleavage site is between residues 596 and 597 of the APP695 isoform, at the amino-terminal of A β . β cleavage is a necessary step for A β peptide generation and is therefore called amyloidogenic processing. The only enzyme so far identified as being responsible for the cleavage at this site is called Bace1 (beta-site APP-cleaving enzyme) (Hussain et al., 1999; Sinha et al., 1999; Vassar et al., 1999; Yan et al., 1999). It is a type I membrane-bound aspartyl protease (Asp2) and is mainly localized to the late Golgi or trans-Golgi network and endosomes (Huse et al., 2000). This localization is consistent with the amyloidogenic processing of APP during endocytic and recycling steps (Koo and Squazzo, 1994). Bace1 can also cleave within the A β region between tyrosine 10 and glutamate 11.

It is known that both concentration and activity of Bace1 are increased in the neocortex with AD (Fukumoto et al., 2002). Solubilized Bace1 protein cleaves synthetic APP peptide at the β -cleavage site correctly. Overexpressing Bace1 in 293 cells stably expressing wild-type APP695 enhanced the β -secretase cleavage products and doubled the amount of A β peptides (Yan et al., 1999). Another similar study also showed that Bace1 over-expression increased A β 1-40/42 and A β 11-40/42 (Vassar et al., 1999). Inhibiting the endogenous Bace1 expression using an antisense oligonucleotide reduced by 30-40% the production of A β from Swedish mutant transfected cells. To further prove the effect in vivo, Bace1 knockout mice were used. As expected, they also showed reduced levels of A β and β -site cleavage products. Interestingly, the knockout of the Bace1 gene did not cause any phenotypical abnormality to the mice (Luo et al., 2001). These results suggest that a very important therapeutic strategy could be to develop Bace1 inhibitors to treat AD (Roberds et al.,

2001) since knockout of *Bace1* does not display any observed abnormality but reduces the production of A β peptides.

1.4.3.3 γ -secretase

The γ -secretase cleavage sites in APP correspond to the carboxyl-terminal of A β peptides. The cleavage is involved in both amyloidogenic and non-amyloidogenic pathways. Two candidate genes, namely presenilin-1 (PS1) and presenilin-2 (PS2), were first identified by genetic linkage analysis of familial early-onset AD (Cruts et al., 1995; Hutton et al., 1996). It is now known that γ -secretase is not a single protein. Instead, it is a complex made of four essential proteins: PS1/PS2, nicastrin (Nct), Aph-1 and Pen-2 (De Strooper, 2003; Selkoe and Wolfe, 2007).

PS1 and PS2 are expressed as precursor proteins. They are intramembrane aspartyl proteases (Wolfe et al., 1999). To mature, they have to be cleaved into 2 subunits, an amino-terminal fragment (NTF) and a carboxy-terminal fragment (CTF), which remain tightly associated as a heterodimer. Each contributes one aspartyl residue to the catalytic site (Thinakaran et al., 1996). The second membrane protein, Nct, was identified by co-immunoprecipitation with PS (Yu et al., 2000). It is a glycosylated, integral single transmembrane protein which binds to the NTF and CTF of PS. The transportation of Nct from the endoplasmic reticulum (ER) to the cell membrane requires PS since Nct precursor accumulates in the ER in PS-deficient cells. On the other hand, Nct suppression also leads to reduced steady-state levels of PS, which suggests that Nct is a stabilizing factor for PS. Later, Aph-1 and Pen-2 were identified in screening studies using *C. elegans*. Aph-1 is a 30 kDa multimembrane

spanning protein (Goutte et al., 2002), and Pen-2 is a 12 kDa hairpin-like membrane protein (Francis et al., 2002). Downregulation of Aph-1 or Pen-2 in *Drosophila* cell culture suppresses the cleavage of APP and Notch at the γ -secretase sites and reduces the level of mature PS (Francis et al., 2002; Lee et al., 2002; Takasugi et al., 2003), resulting in similar effects to the downregulation of Nct and PS (De Strooper et al., 1998; Edbauer et al., 2002).

These data suggest that all these four proteins are required to work together to perform the function of γ -secretase. On the other hand, overexpression of any combination of these four proteins cannot increase the cleavage of APP. However, co-expressing all these four proteins together significantly upregulates the levels of PS heterodimers and glycosylated Ntc and, most importantly, γ -secretase activity (Kimberly et al., 2003).

Though neurons taken from PS1-deficient embryonic mice showed that absence of PS1 displayed inhibited γ -cleavage of the APP transmembrane domain and reduced the production of A β peptides by fivefold, it did not affect the α -secretase and β -secretase processing of APP (De Strooper et al., 1998). Therefore, the author suggested that PS1 inhibition could be a potential way to suppress A β peptide generation and thus treat AD. However, such PS1 knockout mice had severe health problems. The growth of the embryo was retarded, and it died at the embryonic stage (De Strooper et al., 1998) with hemorrhages and impaired neurogenesis in the brain (Shen et al., 1997). Therefore, caution is needed in the development of therapeutic inhibitors of γ -secretase in order to reduce the cleavage of APP to generate A β peptide.

1.4.3.4 Competitive substrates

APP processing can be regulated by altering the levels and activities of α -, β - and γ -secretase such that the processing would favor either amyloidogenic or non-amyloidogenic pathways. Most of the secretases were found to also cleave other proteins. ADAM17 is a converting enzyme which cleaves a number of receptors, such as Tnf receptor (to release Tnf- α) (Black et al., 1997; Moss et al., 1997) and Notch (Brou et al., 2000). Notch is a type I transmembrane receptor which determines cell fate during embryogenesis. It is also cleaved by ADAM10 (Hartmann et al., 2002) and γ -secretase (De Strooper et al., 1999). N-cadherin, ephrinB and p75 neurotrophin receptor can also be cleaved by γ -secretase (Franberg et al., 2010). Klotho (Kl) is an anti-aging protein and a substrate, like APP, for all three types of secretases (Bloch et al., 2009). Overexpressing Kl can extend the life span of transgenic mice (Kurosu et al., 2005). Since there are at least three α -secretases, there are a number of potential α -secretase substrates.

We hypothesize here that APP processing can be regulated by modulating the levels of competitive substrates of these secretases. The activity and specificity of the secretases are not based on the primary sequence of proteins but depend on the local conformation of the targets. Therefore, it is no surprise that proteins sharing very similar secondary structure with that of the cleavage sites of APP could be cleaved by the same secretases. Moreover, the levels of these proteins may affect the processing of APP in that upregulating their levels may downregulate the processing of APP by secretases, and vice versa. Therefore, the substrates of secretases can act as competitive inhibitors to APP processing. Such an approach provides an alternative option to the strategies of designing inhibitors for Bace1 and γ -secretase since direct

inhibitors of these secretases may have toxic effects, as mentioned in the previous section.

1.4.4 Toxicity of A β

Since A β 1-42 is the most aggregation-prone form of A β (Jarrett et al., 1993; Snyder et al., 1994), it has been widely accepted that it is much more toxic than others (Butterfield, 2002). The central themes of the studies of A β toxicity are how A β causes neuronal cell death and how synaptic plasticity and functions are impaired. Early research focused on oxidative stress caused by A β . It was shown that A β induced toxicity to neurons by suppressing oxidative-sensitive glutamine synthetase, generated reactive oxygen species (ROS) in a cell-free system (Hensley et al., 1994), and induced intracellular ROS generation and intracellular calcium ion upregulation (Goodman and Mattson, 1994). Other possible toxicities are more related to higher molecular A β oligomers.

1.4.5 Oligomerization and fibrillization of A β

A β is a small peptide with sizes ranging from 39 to 43 amino acids. Due to the hydrophobic nature of A β , it readily self-aggregates. The core sequence, KLVFFA β E, can form amyloid by itself (Klimov and Thirumalai, 2003). Studies found that the carboxy-terminal residues of A β are a critical determinant of the kinetics of amyloid formation; A β 1-42 fibrillizes much faster than A β 1-40, and the former can act as a “seed” to accelerate the fibrillization of the latter (Jarrett et al., 1993). This finding

agreed with the observation that in familial FOAD brains the ratio of the level of A β 1-42 to A β 1-40 is higher than in non-demented brains, which suggests that A β 1-42 is important in the acceleration of A β fibrillization in vivo (Eckman et al., 1997; Scheuner et al., 1996; Suzuki et al., 1994). Besides the length of the A β peptide itself, the tendency to aggregate is also affected by its concentration, preparation, seeding, environmental pH, presence of metal ions, cholesterol, ApoE, and other factors.

It was generally believed in the last century that the amyloid fibril is the culprit responsible for AD (Lorenzo and Yankner, 1994). Activated microglia were found around the amyloid plaque of AD brains (Griffin et al., 1989) secreting the cytokines interleukin-1 and interleukin-6, which increase cyclooxygenase-2 to produce inflammatory prostaglandins. This finding suggested that the amyloid plaque causes inflammation of the surrounding tissue. Structural studies of amyloid fibrils revealed that A β peptides mainly adopt a β -pleated sheet anti-parallel structure (Roher et al., 2000). It was proposed that monomeric A β adopts an α -helical structure and has to dimerize to associate with other dimers to form larger species, such as A β -derived diffusible ligands (ADDLs) and protofibrils. Eventually, these aggregate into fibrils with a β -pleated sheet anti-parallel structure (Roher et al., 2000).

Recent findings led us to another view of A β toxicity. Dimeric A β was isolated from AD brains and was found to impair the learning and memory of normal rats (Shankar et al., 2008). Dimeric A β aggregated to form larger soluble oligomers, including ADDLs (Lambert et al., 1998) and A β *56 (Lesne et al., 2006). Isolated A β oligomers inhibit hippocampal LTP in rats (Walsh et al., 2002) and impair cognitive function and memory (Cleary et al., 2005; Lesne et al., 2006). The toxicity of oligomers can be neutralized by a monoclonal antibody against A β (Klyubin et al.,

2005). Oligomers were extracted from either cell culture medium or isolated from human AD brains or brains of AD mice. Therefore, these oligomers are formed in physiological conditions. Oligomers showed much more cellular toxicity than did fibrils (Lambert et al., 1998; Takahashi and Mihara, 2008). Furthermore, the severity of cognitive impairment of AD patients and mouse models of AD was found to be better correlated with the level of soluble oligomeric A β in the brain homogenates than with the level of amyloid plaques (Gandy et al., 2010; Tomic et al., 2009). Taken together, the data suggest that oligomeric A β is more important than fibrils for the development of functional impairment in AD brains.

1.4.6 Protection from A β toxicity

Since A β and redox-metal ions are naturally present in the brain in close proximity at physiological concentrations, it is inevitable that they produce ROS. An enormous amount of evidence described the oxidative damage of the human AD brain (Beal, 2000). Lipid peroxidation is one of the most apparent forms of oxidative damage since polyunsaturated fatty acids are abundant in brain tissue (Bassett and Montine, 2003). Protein carbonyl content has been reported to be increased in the hippocampus and inferior parietal lobule of AD brain (Hensley et al., 1995). A study found that, in AD brain mitochondrial DNA, the oxidized nucleoside, 8-hydroxy-2'-deoxyguanosine, was 3-times more abundant than in control brains, which indicated that mitochondria are severely damaged by oxidative stress in the AD brain (Mecocci et al., 1994), especially in the temporal lobe (Wang et al., 2005). Study of animal models of AD showed that lipid peroxidation increased before plaque deposition (Pratico et al., 2001).

Consistent with the increased oxidative damage, activities of the antioxidative enzymes superoxide dismutase and catalase were decreased in the frontal and temporal cortices of AD brain (Marcus et al., 1998). The activity of phospholipase A₂, which is involved in antioxidative defense, was reduced in CSF of AD (Smesny et al., 2008). A similar finding was also confirmed in the serum of AD patients, which showed increased levels of lipid peroxidation markers accompanied by reduced levels of the antioxidative enzymes SOD and GPX (Padurariu et al., 2010).

These evidences suggest that reduced antioxidative enzymes may cause damage from oxidative stress. In view of the above, two studies demonstrated that overexpressing SOD2 in AD mouse models decreased superoxide in hippocampus, decreased oxidized protein, reversed cognitive impairment, decreased plaques and decreased the A β 1-42 to A β 1-40 ratio (Dumont et al., 2009; Massaad et al., 2009). These data suggest that mitochondrial antioxidative enzymes provide strong protection against oxidative stress which enhances memory impairment and plaque formation.

1.4.7 Transport of A β

There are several known pathways by which soluble intact A β peptides are removed from the brain. Some involve receptor-mediated internalization and efflux, and others involve chaperones to transport A β .

A well-characterized receptor mediating the efflux of A β from the brain to the blood is Lrp1 (low density lipoprotein receptor-related protein-1). It interacts with A β directly (Deane et al., 2004) or indirectly through binding chaperone proteins, such as

ApoE (Shibata et al., 2000). Upon interaction, A β is internalized into the cell, transmitted to the neighboring cells and eventually transported into blood by transcytosis (Herz, 2003). By intracerebral injection of 125 I-labeled A β 1-40 peptide to mice whose Lrp1 was inhibited by anti-Lrp1 antibodies, it was shown that Lrp1 is responsible for over 55 percent of A β efflux (Shibata et al., 2000). Two chaperone proteins are believed to play an important role in this process. By inhibiting α 2-macroglobulin using antibodies, clearance of A β was reduced by 30 percent, while ApoE deletion reduced it by 46 percent (Shibata et al., 2000). On the contrary, another study using ApoE knockout and human mutant APP overexpressing mice showed reduced A β deposition and complete lack of A β fibrillogenesis (Bales et al., 1999). Both these studies may suggest that ApoE can act as a chaperone to A β , however, if the complex is not removed immediately or is present in a certain environment, ApoE enhances A β fibrillogenesis (Shibata et al., 2000).

1.4.8 Degradation of A β

A β is continuously produced from cleavage of APP by secretases, and it must be degraded or transported at an equal rate to maintain equilibrium. Besides transport, A β peptides can be degraded by proteases, such as Ide, neprilysin, and a branch of matrix metalloproteinases. Their specificities differ from each other. After A β cleavage, the resulting fragments do not readily aggregate and exert cytotoxicity.

Ide (insulin-degrading enzyme) is a 110 kDa zinc metallo-endopeptidase. It is highly abundant in many organs, such as brain and liver (Kuo et al., 1993) and exists as intracellular (Akiyama et al., 1988) and extracellular forms (Qiu et al., 1998). In

AD brain, histological study showed Ide increased in plaques, however, the mRNA and total protein expression of Ide were decreased (Bernstein et al., 1999).

Neprilysin is a 90-110 kDa neutral zinc metalloendopeptidase plasma membrane glycoprotein (Turner et al., 2000). In the brain, it is located in the pre- and post-synaptic membrane (Barnes et al., 1992). Immunostaining of AD brain tissue showed that the protein level of NEP was reduced in pyramidal neurons of cerebral cortex and hippocampus (Carpentier et al., 2002), and in frontal and temporal neurons (Miners et al., 2006).

Mmp2, 3 and 9 (matrix metalloproteinase-2, -3 and -9) are zinc- and calcium-dependent endopeptidases. They are expressed in neuronal and glial cells in the brain. All of them possess A β -degrading activity in vitro (Backstrom et al., 1996; Roher et al., 1994). In contrast to Ide and Neprilysin, brain homogenate from AD hippocampus has increased Mmp2 and 9 activity (Backstrom et al., 1992).

In fact, in animal studies using models with plaque formation, the protein levels of Ide (Leal et al., 2006), Neprilysin (Apelt et al., 2003), Mmp2 and Mmp9 (Yin et al., 2006) were increased in astrocytes surrounding the plaques. A β levels were increased in Mmp2 and 9 knockout mice (Yin et al., 2006).

These evidences suggest that these enzymes may be involved in A β catabolism. Their localization and expression patterns are changed in response to increased local A β level. Increased A β level may be associated with the malfunctioning of some proteases which may be compensated by upregulating others (Miners et al., 2008).

1.5 Tau

Tau protein is a member of the family of microtubule-associated proteins (MAPs). It is expressed by the gene called *Mapt*, and is highly abundant in neurons of the brain (Goedert et al., 1988). Alternative splicing of the *Mapt* gene leads to the formation of six isoforms of tau (Goedert et al., 1989). Tau isoforms differ from each other in the number of tubulin-binding repeats (3R or 4R) and the absence or presence of one or two inserts of 29-amino-acids at the N-terminal (**Figure 1.5**). The isoforms are functionally similar to each other, though they differ somewhat in microtubule binding ability.

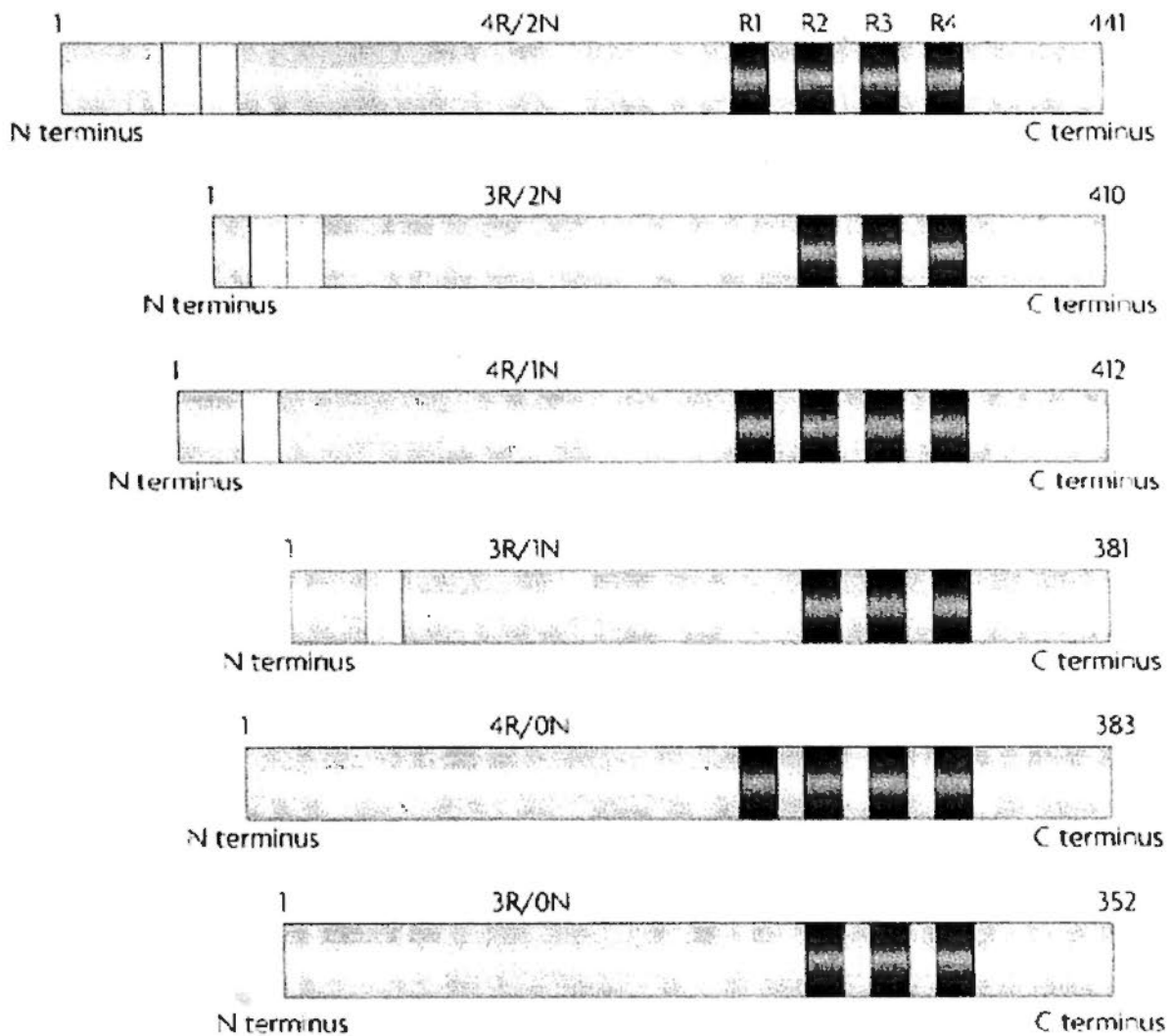


Figure 1.5 Schematic diagram of six isoforms of tau. Diagram adapted from (Ballatore et al., 2007)

1.5.1 Function of Tau (general function)

Under normal conditions, tau interacts with tubulin and stabilizes microtubules in axons (Maccioni and Cambiasso, 1995). Its binding function is regulated by the phosphorylation status of serine and threonine residues (Mazanetz and Fischer, 2007) and by glycosylation (Liu et al., 2004). Other modifications also occur on tau (Gong et al., 2005). Amongst these modifications, phosphorylation is the most often studied.

The phosphorylation level in normal adult brain is lower than in fetal brain. Hyperphosphorylation of tau is highly correlated with different neurodegenerative diseases. Through its ability to bind tubulin and stabilize microtubules, tau can regulate the structure and function of neurons by changing their morphology and axonal transport of materials, such as mitochondria and signaling molecules. Therefore, regulation of tau can lead to change of neuronal connectivity and viability (Roy et al., 2005). The most important implication for AD of these vital roles for tau is that inhibiting tau, by hyperphosphorylation or sequestration in NFT, may lead to serious damage or even death of the neurons.

1.5.2 Regulation of neurofibrillary tangle formation

Unlike APP, no tau mutations are clearly associated with AD. In AD, neurons develop intracellular NFT from non-mutant tau. Mutations in tau, however, cause other neurodegenerative diseases, such as frontotemporal dementia and parkinsonism linked to chromosome 17 (FTDP-17) (von Bergen et al., 2001).

Therefore, tau mutations are not necessary for NFT formation. But hyperphosphorylation of tau is necessary for NFT formation. Tau phosphorylation is a normal regulatory process for controlling the function of tau. Under pathological conditions, some kinases are activated, which can lead to tau hyperphosphorylation (Braak and Braak, 1995). Many kinases were shown to be upregulated or activated in AD brains (Martin et al., 2011). An animal study showed that inhibiting glycogen synthase kinase 3 (Gsk3) by lithium led to a reduced level of tau phosphorylation at sites which can be phosphorylated by Gsk3 and are found in AD brain (Noble et al., 2005). Lithium treatment also reduced the level of aggregated and insoluble tau.

Recently, the NFT level was shown to be related to acetylation of tau. In human AD brain and animal models which develop NFT, it was found that tau was acetylated, which inhibited the degradation of phosphorylated tau (Min et al., 2010). Tau was acetylated by histone acetyltransferase p300 and reversed by protein deacetylase SIRT1. Interestingly, the group also demonstrated that removing SIRT1 increased acetylated tau and pathologically phosphorylated tau, which was totally opposite to the effect of inhibiting p300 (Min et al., 2010).

Another interesting finding showed that *O*-linked glycosylation inhibited tau phosphorylation (Fischer, 2008). This glycosylation requires β -*N*-acetylglucosamine (*O*-GlcNAc) linked to serine or threonine residues on tau. However, an enzyme called *O*-GlcNAcase can cut *O*-GlcNAc from tau (Liu et al., 2004). Data from an animal study showed that inhibiting this enzyme led to reduced tau phosphorylation at ser396, thr231 and ser404, which is probably due to reduced removal of *O*-GlcNAc from tau (Yuzwa et al., 2008).

1.6 Disease hypotheses

1.6.1 Amyloid hypothesis

The amyloid hypothesis of AD summarizes the evidences from years of studies on the cascade of events in the development of AD. It was first proposed in 1991 (Selkoe, 1991). A number of different strategies for intervening in the progression of neurodegeneration are based on this hypothesis. It arises from the observation that extensive senile plaque deposits are found in the brains of Down syndrome and FOAD patients, both of which have increased expression of APP and production of

A β peptides. The hypothesis starts with the overproduction of A β peptide, specifically A β 1-42, which in turn increases A β oligomerization and reduces clearance. Thereby, the concentration of extracellular toxic A β species increases, which activates nearby microglia and astrocytes to secrete pro-inflammatory cytokines. Toxic oligomeric A β together with the inflammatory factors cause progressive synaptic and neuritic injury, altered neuronal ionic homeostasis and oxidative stress and damage. These factors activate kinases which cause hyperphosphorylation of tau and NFT formation along with neuronal dysfunction, cell death and loss of neurotransmitters. Eventually, this cascade results in dementia.

1.6.2 Criticism of amyloid hypothesis

Although the amyloid cascade hypothesis is the most widely accepted model of the development of AD, it is subject to criticism. The severity of cognitive impairment does not correlate with the number of amyloid deposits but does correlate with the concentration of soluble A β , which cannot be detected immunohistologically (Lue et al., 1999). Amyloid plaques can be found in the cortex of normal elderly without symptoms of dementia. On the contrary, the severity of dementia is strongly correlated to the number of NFT, particularly in superior temporal, inferior parietal and midfrontal cortex but not amygdala, hippocampus or entorhinal cortex (Bierer et al., 1995). Transgenic mice overexpressing mutant APP associated with EOAD developed severe amyloid pathology but no observable neuronal loss or NFT (Irizarry et al., 1997).

1.6.3 Tau hypothesis

Due to the criticisms of the amyloid hypothesis, the tau hypothesis (Maccioni et al., 2010) was proposed to complete the mechanism of the development of AD. Hyperphosphorylated tau oligomers, together with A β oligomers, ROS and other stresses, initiate neurotoxic events that lead to pathological change of the neuronal cytoskeleton. These factors stimulate the activation of surrounding microglia and astrocytes to release pro-inflammatory cytokines which lead to neuroinflammation (Orellana et al., 2007). These cytokines eventually leads to tau hyperphosphorylation in the nearby neurons through Cdk5 (Alvarez et al., 2001) and MAPK-p38 (Quintanilla et al., 2004) activation. Hyperphosphorylated tau tends to form oligomeric tau which will be released into the extracellular space when the neurons die and will then stimulate the microglia activation cascade again (Maccioni et al., 2010).

1.7 Current treatments

In AD, loss of choline acetyltransferase (ChAT) and cholinergic functions in the cortex eventually leads to a reduced level of the neurotransmitter acetylcholine (ACh) (Whitehouse et al., 1982). Treatments have been developed to overcome the loss of ACh. Acetylcholinesterase (AChE) is an enzyme secreted into the synaptic cleft to hydrolyse ACh into acetate and choline molecules. This mechanism is used to stop the function of ACh after ACh receptors on the postsynaptic membrane are stimulated. Choline is then recycled by the high-affinity choline transporter (ChT1) (Okuda et al., 2000) to the cytosol of the axon terminal of the presynaptic cell, and new ACh is

synthesized again by ChAT (Bear et al., 2001). New ACh is loaded by the vesicular acetylcholine transporter (VAChT) into secretory organelles in the presynaptic terminal for secretion (Erickson and Varoqui, 2000).

Strategies for increasing the acetylcholine level include by enhancing ChAT, inhibiting acetyl- and butyryl-cholinesterase, supplementing ACh precursors and providing cholinergic receptor agonists. Amongst these strategies, only cholinesterase inhibitors were shown to improve memory as verified by functional magnetic resonance imaging (Bentley et al., 2009). At least three are available as drugs to treat AD.

Donepezil is a reversible acetylcholinesterase inhibitor derived from piperidine (Seltzer, 2007). It is administered orally for treating mild to moderate AD. Many side effects were reported for taking Donepezil, including nausea, vomiting, diarrhea, dizziness and fatigue.

Rivastigmine is an acetyl- and butyryl-cholinesterase inhibitor derived from carbamate. It is approved for treating mild to moderate AD. The reported side effects include nausea and vomiting. It can be administered orally or transdermally, with the latter administrative method producing fewer side effects (Winblad et al., 2007).

Galantamine is a competitive and reversible acetylcholinesterase inhibitor and nicotinic allosteric agonist for treating mild to moderate AD (Robinson and Plosker, 2006). It is a tertiary alkaloid. Side effects reported are similar to other cholinesterase inhibitors.

Only one approved AD medicine is not a cholinesterase inhibitor: Memantine, an N-methyl-D-aspartate (NMDA) non-competitive receptor antagonist. The principle

of this drug is that it can antagonize the excitatory effects of glutamate on NMDA receptors, thus blocking excitotoxic neuronal damage (Sucher et al., 1996). Memantine is approved for treating moderate to severe AD (Mount and Downton, 2006). The efficacy of this medicine for treating mild to moderate AD is still under debate, but it is already available in some countries (Schneider et al., 2011).

Nevertheless, there is no medicine yet approved for AD patients that can slow the progression of AD. All the above available treatments are only considered to relieve symptoms.

1.8 Drug development

With increasing understanding on the molecular pathogenesis of AD, numerous studies on the intervention of the disease progression are being undertaken. These studies mainly focus on how to reduce the histopathological characteristics—amyloid plaques, neurofibrillary tangles and neuronal loss—of the AD brain tissue and the hypothetical toxicities which are thought to be the culprit of the disease (Mangialasche et al., 2010).

The anti-amyloid strategy is the most extensively studied approach. The focus of the toxic species of A β has changed from amyloid fibrils to oligomers with the increased ratio of A β 1-42 to A β 1-40. Therefore, medicines are being developed to reduce the production, to increase the clearance and to prevent the aggregation of A β peptides. In order to reduce the A β production from amyloidogenic cleavage of APP, α -secretase activators and β - and γ - secretase inhibitors and modulators have been investigated. Preclinical studies have shown that inhibitors of β - and γ - secretase can

reduce $A\beta$ production in CNS and plasma and improve cognitive performance of AD animal models (Bateman et al., 2009; Chang et al., 2007; Henley et al., 2009; Hussain et al., 2007; Rakover et al., 2007). However, due to the adverse effects of γ -secretase inhibitors, including haematological and gastrointestinal toxicity (Tomita, 2009), the development direction has changed from γ -secretase inhibitors to modulators which can block APP proteolysis selectively without inducing Notch-signalling and resulting adverse effects. To enhance non-amyloidogenic cleavage of APP, α -secretase activators have been tested. Not only can they reduce $A\beta$ peptide production as hypothesized, but they can also increase the formation of a neuroprotective domain of APP (sAPP α) (Etcheberrigaray et al., 2004; Marcade et al., 2008).

Another approach that has been actively tested in the clinical phase is immunotherapy, which increases the clearance of $A\beta$ peptide. A vaccine against $A\beta$ was tried as a means of active immunotherapy, but adverse effects, such as aseptic meningoenzephalitis and microhaemorrhages, were observed in some patients (Gilman et al., 2005). Although the clinical study of this vaccine was interrupted, research into vaccines against other positions of $A\beta$ with reduced side effects (Wiessner et al., 2011), different adjuvants (Muhs et al., 2007; Wang et al., 2007) and delivery methods are still ongoing. Passive immunotherapy by intravenous infusion of monoclonal antibodies, or immunoglobulins from non-AD patients, which has natural anti- $A\beta$ antibodies, has been performed in clinical studies at different phases. Results suggested that passive immunotherapy enhanced $A\beta$ removal from the CNS through the blood (Dodel et al., 2004; Relkin et al., 2009; Siemers et al., 2010). Other varieties of anti-amyloid therapies focus on inhibition of $A\beta$ aggregation or destabilization of $A\beta$ oligomers by small compounds. Cliquinol and PBT2 work by chelating copper

and zinc ions from A β aggregates (Adlard et al., 2008), and PBT2 was shown to improve executive functions of AD patients in a phase 2 study (Lannfelt et al., 2008).

The presence of neurofibrillary tangles was thought to impair the microtubule-stabilizing and normal functioning of tau. Therefore, medicine has been investigated to inhibit the formation of tangles. The first approach which has been extensively tested is inhibition of the tau-phosphorylating kinases. GSK3, which is one of these kinases, can be inhibited by lithium. However, clinical study showed that lithium did not change the level of phosphorylated and total tau in the CSF, nor did it improve the cognitive function of AD patients (Hampel et al., 2009). Another approach is by inhibiting the tau-aggregate formation through interacting with tau directly. Methylthioninium chloride, which possesses anti-tau-aggregating properties, was tested in a phase 2 study in moderate AD patients. Result showed that it improved cognitive function and slowed disease progression compared with placebo (Gura, 2008).

Mitochondria were thought to be the most importantly defective organelles in the AD brain. Their dysfunction in early AD can induce synaptic and neuronal damage, which eventually leads to apoptosis and neurodegeneration (Reddy and Beal, 2008). Dimebon, which maintains mitochondrial structure and function and protects the mitochondria against A β -induced toxicity and activation of apoptosis-causing permeability transition pores (Bachurin et al., 2003; Moreira et al., 2001; Zhang et al., 2010b), was shown to improve the cognitive performance of AD patients compared with placebo in a phase 2 study (Doody et al., 2008).

Other studies include delivery of nerve growth factor (NGF) to basal forebrain cholinergic neurons, use of omega-3 polyunsaturated fatty acids, antioxidants, anti-

inflammatory compounds and inhibitor of the receptor for advanced glycation endproducts (RAGE) to protect neurons from toxicity. Clinical studies of these targets are ongoing (Mangialasche et al., 2010).

1.9 Curcumin

1.9.1 General functions of curcumin

Curcumin, also called diferuloylmethane, is the principal yellow coloring compound of turmeric, which is derived from the rhizome of the *Curcuma longa* plant. Two other derivatives that naturally exist in turmeric together with curcumin are desmethoxycurcumin and bis-desmethoxycurcumin; they exist in the approximate ratio 75-80% : 15-20% : 3-5% , respectively (Aggarwal et al., 2007). Curcumin is composed of two methoxy-phenolic groups connected by a chain of 7 carbons with two α,β -unsaturated carbonyl functional groups. It has a long history of use as a food additive and Indian Ayurvedic medicine. Since the first published study searchable at Pubmed in 1949 (Schraufstatter and Bernt, 1949), there have been over 4000 publications about the functions of curcumin.

A variety of functions have been claimed for the preventive and therapeutic uses of curcumin by many in vitro and in vivo studies (Strimpakos and Sharma, 2008). Some of the functions appear to contradict others. These include anti-inflammatory, antioxidant, antimicrobial, antiangiogenic, cytotoxic, neuroprotective, cardioprotective, anti-diabetic, wound healing, immunomodulatory, proapoptotic and anti-apoptotic (Strimpakos and Sharma, 2008). Based on these evidences, a number of different preclinical studies on particular disease models have been performed. Due to

its apparently safe use for over a century, it has also been tested in clinical studies of many diseases, such as colon and pancreatic cancer and AD (Hatcher et al., 2008). However, curcumin has still not been confirmed to possess the above properties in humans. The molecular targets which control these functions affected by curcumin in vitro and in vivo are summarized in **Figure 1.9.1**.

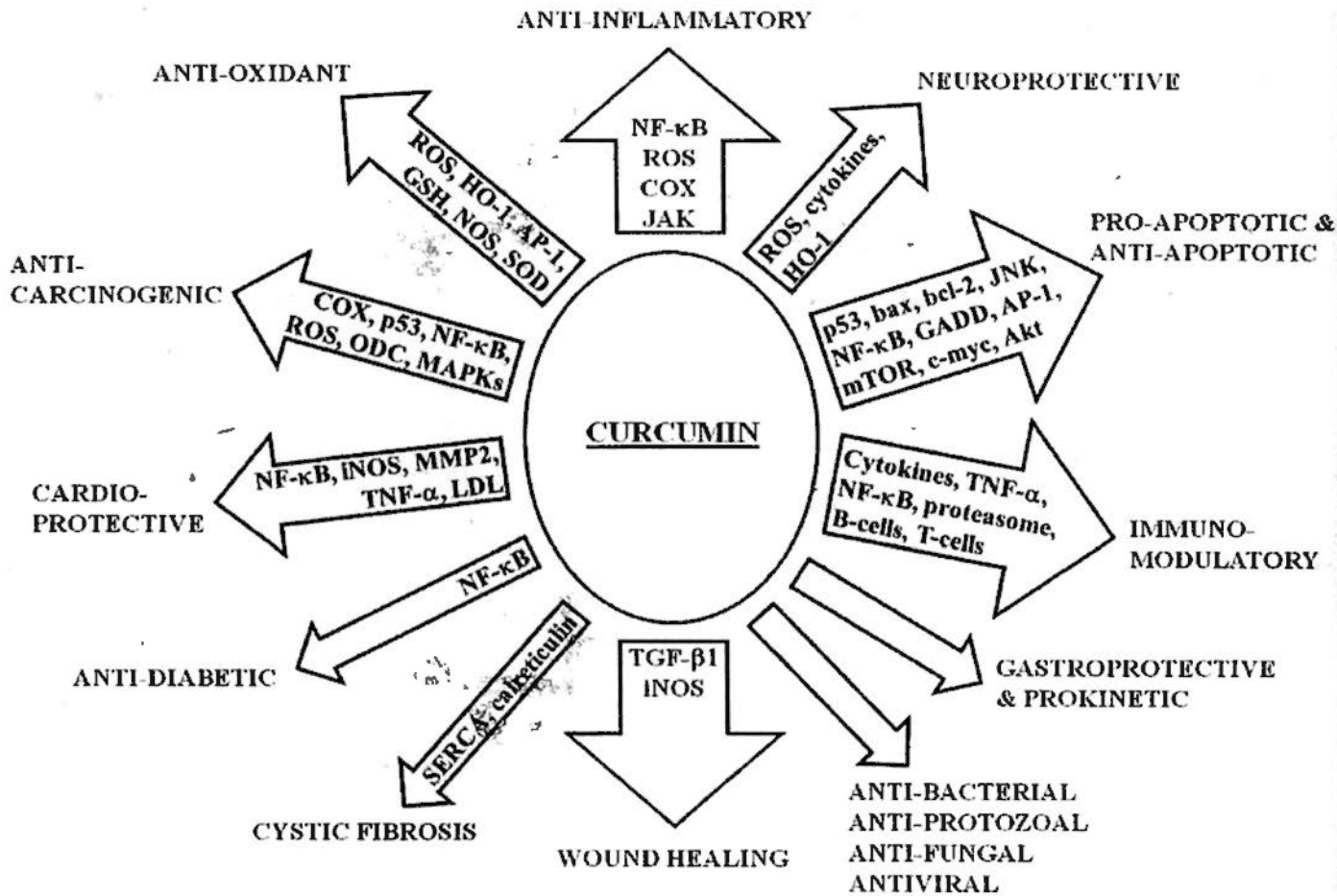


Figure 1.9.1 Summary of the molecular targets via which curcumin exerts its beneficial biological functions. Adapted and modified from (Strimpakos and Sharma, 2008).

1.9.2 AD related functions of curcumin

Amyloid oligomers, oxidative damage and inflammation in brain tissue may be major causes of neurodegeneration in AD. Curcumin has been demonstrated to be an

effective AD treatment by various mechanisms. It has been shown that curcumin can inhibit and reverse amyloid fibril formation (Ono et al., 2004). It can reverse the toxicity of exogenous A β (25-35) peptides applied to PC12 cells by reducing the increased level of DNA fragmentation, intracellular calcium and tau phosphorylation (Park et al., 2008). On the road of A β generation, some cell culture studies showed that curcumin can reduce Bace1 expression (Lin et al., 2008; Liu et al., 2010; Shimmyo et al., 2008), which was shown to be upregulated in brains of AD patients (Coulson et al., 2010). Curcumin may also prevent the maturation of APP in vitro (Zhang et al., 2010a), which may decrease A β production. On the clearance of A β , curcumin was shown to increase the internalization of A β by macrophages isolated from AD patients (Zhang et al., 2006).

In animal studies, curcumin has been shown to reduce soluble and insoluble A β burden (Frautschy et al., 2001; Lim et al., 2001; Yang et al., 2005). Oxidative damage and inflammation were decreased in these models, too. Since it was shown that curcumin cannot affect the levels of APP cleavage products, it was suggested that curcumin has no effect on secretase activity (Cole et al., 2007). Another animal study showed that curcumin can inhibit JNK activation and tau phosphorylation (Ma et al., 2009), which suggests that curcumin may be protective in tauopathy by inhibiting tau phosphorylation by JNK or JNK pathways.

In studies of cholinergic functions, some groups showed that curcumin possesses anti-acetylcholinesterase (Ache) and antioxidant activity (Ahmed and Gilani, 2009) in rodent models which had enhanced Ache activity and oxidative damage (Agrawal et al., 2010). Another study demonstrated that curcumin can enhance choline acetyltransferase (ChAT) activity in dementia models of AD induced

by streptozotocin (Ishrat et al., 2009). In rodent models of AD induced by A β intracerebroventricular injection, curcumin can improve cognitive function in a Morris water maze test (Frautschy et al., 2001).

The above specific and consistent properties of curcumin may be due to its limited bioavailability. By oral administration to mice, curcumin can reach a concentration of approximately 1 μ M in brain (Begum et al., 2008). At this concentration, adverse effects exerted on neurotoxic pathways are physiologically impossible. With such a potentially attractive AD drug candidate, studies of the functions of curcumin on AD treatment are actively ongoing globally. Interestingly, a clinical trial done by our group recently showed that curcumin has no effect on improving memory (Baum et al., 2008).

1.9.3 Unaddressed issues of curcumin in AD treatment

For the studies mentioned above, *in vivo* observations included improvement in cognitive function and reductions in both aggregated and soluble A β . The physiological mechanisms by which curcumin achieved these effects are not entirely known.

For example, an A β fibril disaggregation study was done in a metal-free environment (Ono et al., 2004). A β aggregation was indeed shown to be accelerated by physiological concentrations of metal ions, such as copper and zinc (Bush, 2003). Curcumin is a copper chelator (Baum and Ng, 2004). Therefore, curcumin may reduce amyloid plaque formation by chelating copper ions to prevent and reverse the formation of A β fibrils *in vivo*. However, the currently available data did not prove

this in physiological conditions. Since oxidative stress was suggested to originate partly from the hydrogen peroxide generated from A β peptide facilitated by copper ions (Huang et al., 1999b), curcumin may also reduce the oxidative stress, for example, by taking copper away from A β . Data are not yet available to distinguish which of these potential mechanisms of protection by curcumin—reducing oxidative stress or inhibiting A β aggregation—might be most important in vivo. There are as yet no publications on whether curcumin may affect the expression of genes that could distinguish these alternative pathways.

As another example, the above evidences did not produce a consistent conclusion on the effect of curcumin on A β production and removal in vivo. Whether curcumin affects the expression and activity of secretases has not yet been studied in vivo. For the clearance of A β , the only available data for the effect of curcumin are from a culture study of macrophages isolated from human blood (Zhang et al., 2006). However, these data cannot address the core issue of what really happens in the brain. More studies are necessary to determine the physiologically feasible mechanisms by which curcumin may affect the balance of production and disposal of A β . Whether curcumin may affect the receptors involved in phagocytosis or internalization, whether curcumin may facilitate A β removal through increasing its transporters, or whether curcumin may enhance A β degradation by increasing the A β degrading enzymes are still unknown.

Cholinergic degeneration is known to happen in AD brain, leading to reduced levels of acetylcholine (Whitehouse et al., 1982), but there are still no data available on how curcumin can improve cognitive function in AD rodent models. To study whether curcumin can improve cognitive function in humans, it is necessary to

determine whether curcumin can regulate acetylcholine level by, for instance, inhibiting Ache or enhancing ChAT in vivo.

For the study of tauopathy, published data only suggested that JNK inhibition leads to reduced tau hyperphosphorylation (Ma et al., 2009). However, no report showed that NFT were reduced upon curcumin treatment. Not only kinase activation may lead to increased NFT level, but acetylation may also do so by reducing tau degradation (Min et al., 2010). Coincidentally, curcumin is a well-known inhibitor of histone acetyltransferase P300 (Balasubramanyam et al., 2004), which can acetylate tau (Min et al., 2010). Therefore, it would be interesting to know whether curcumin can reduce NFT level also.

1.10 Aims of study

The main objective of this study is to identify the *in vitro* and *in vivo* mechanisms of curcumin on the treatment of AD in a logical and comprehensive manner. First of all, we will study whether curcumin can affect the activities of the secretases which determine the rate of A β peptide generation. Second, we will determine whether, at physiologically attainable concentrations, curcumin can effectively reverse A β aggregation. Third, we will determine whether curcumin can increase A β degrading enzymes which affect the catabolism of A β . Fourth, we will study whether curcumin can affect the level of A β transporters and receptors which determine the location and fate of A β .

After studying the factors which directly regulate A β metabolism, we will investigate whether curcumin can affect the expression of enzymes controlling acetylcholine homeostasis. Then, we will examine whether curcumin upregulates genes which can provide neuroprotection by reducing A β level, reducing A β toxicity or reducing oxidative stress. Lastly, we will determine whether curcumin can reduce the level of NFTs.

CHAPTER TWO: MATERIALS AND METHODS

2.1 Cell free assays

2.1.1.1 A β aggregation Thioflavin T assay

Lyophilized A β 1-40 and A β 1-42 were gifts generously offered by Professor A.I. Bush, the Mental Health Research Institute (Melbourne). The protocol was adapted from his laboratory and his publication (Adlard et al., 2008).

Before the assay, each A β peptide was dissolved in 0.005 N NaOH in a 1.5 mL microcentrifuge tube by vortexing. The tube was sonicated in a water bath sonicator for 5 minutes, followed by centrifugation at 16,100 x g for 5 minutes. The supernatant was transferred to another 1.5 mL microcentrifuge tube. The protein concentration was measured by diluting 5 μ L of the peptide solution in 495 μ L of MilliQ water and measuring the absorbance at 214 nm using MilliQ water as a blank for autozeroing. The concentration was calculated as follows:

$$\text{Concentration } [\mu\text{g/mL}] = A_{214 \text{ nm}} \times \text{dilution factor} / 0.03 \mu\text{g/mL}.$$

To prepare A β aggregates, 1 mM Thioflavin T solution and 1 mM ZnCl₂ or CuCl₂ were added to a 15-mL centrifuge tube with PBS (Sigma, with Ca(II) and Mg(II)). Then, either A β 1-40 or A β 1-42 solution was transferred to the tube. The final concentrations of A β , Thioflavin T and metal ions were 10 μ M, 20 μ M and 20 μ M, respectively. The tube was covered with aluminium foil and incubated at 37°C for 24 hours on a rotating wheel running at 30 cycles/minute.

For the disaggregation assay, test compounds were prepared and diluted in DMSO. Then they were diluted 100 fold by the aggregate solution in 1.5 mL

microcentrifuge tubes. The tubes were incubated at 37°C for 2 hours on a rotating wheel running at 30 cycles/minute.

After disaggregation, the mixtures were transferred to a Greiner Black Plate. The fluorescence signal, which comes from the β -sheet structure of A β -bound Thioflavin T (LeVine, 1999), was measured by fluorescence plate reader (Spectramax Gemini XS, Molecular Devices) at Ex:432nm/Em:493nm.

2.1.1.2 Western blotting of monomeric A β

To determine changes in the amount of monomeric A β peptide, the solution from the above experiment was centrifuged at 20,000 x g for 15 minutes at room temperature to remove insoluble A β aggregates. The supernatant samples were resolved on a 16.5% Tricine SDS-PAGE gel.

The protocol for Tricine SDS-PAGE analysis was adapted and modified from (Schagger, 2006). 16.5% Separating gel was prepared by mixing 0.61 mL MilliQ water, 3.33 mL 3X Gel buffer (3 M Tris/HCl, 0.3% SDS, pH 8.45), 5 mL 33% acrylamide mix (33% T, 6% C), 1.06 mL 100% glycerol, 34 μ L 10% ammonium persulfate (APS) and 3.4 μ L TEMED. 3.92% stacking gel was prepared by mixing 1.31 mL MilliQ water, 0.50 mL 3X Gel buffer, 196 μ L 40% acrylamide mix (40% T, 3% C), 16 μ L 10% APS and 1.6 μ L TEMED. Samples and standards of known amounts of monomeric A β peptide (1, 5, 10 and 20 ng) were mixed with sample buffer (2% SDS, 40% glycerol, 200 mM Tris, pH 6.8, 0.04% Coomassie blue and 2% β -mercaptoethanol), boiled for 5 minutes and loaded onto the gel with a protein size marker (SeeBlue Plus2, Invitrogen). Electrophoresis was run with cathode buffer (0.1

M Tris, 0.1 M Tricine, 0.1% SDS, pH 8.25) in the upper tank and anode buffer (0.2 M Tris/HCl, pH 8.9) in the lower tank at 100 V for about 2 hours.

Protein was transferred from the gel to nitrocellulose membrane in Transfer buffer (48 mM Tris•Base, 39 mM glycine, 20% methanol, and 0.0375% SDS) with a frozen Bio-Ice cooling unit in the tank at 400 mA for 3 hours. The membrane was taken out and washed in PBS thrice for 5 minutes. Then it was boiled with PBS in a microwave oven for 10 minutes to expose the epitope. It was washed in TBST (25 mM Tris, 192 mM NaCl, pH 7.4 and 0.05% Tween-20), blocked in 10% non-fat milk in TBST and immunoblotted in primary antibody (1:2000 diluted 6E10 in 5% BSA in TBST). After washing, the membrane was blotted with 1:6000 diluted secondary antibody (AP-conjugated goat anti-mouse IgG) in 10% non-fat milk in TBST and then washed with TBST. Excess buffer was removed briefly, and the membrane was put on microwave plastic film. Immun-Star Chemiluminescent Substrate was mixed with Substrate Enhancer and then was added onto the membrane and incubated for 5 minutes. Excess substrate was withdrawn, and the membrane was transferred to another piece of microwave plastic film. The luminescent signal was captured by exposure to Kodak X-ray film in the dark for different lengths of time.

Images of the X-ray film were scanned and saved as Tiff files. Densitometry was performed using ImageJ 1.44i software.

2.1.1.3 Statistical analysis

Data of Thioflavin T assays were normalized. IC₅₀s were calculated by fitting using nonlinear regression by GraphPad Prism. Data of A β western blotting were

statistically compared by one-way ANOVA for multiple comparisons and Tukey HSD as a *post hoc* test. P values of less than 0.05 were considered statistically significant. Signals of bands were calculated by comparing to the standards. Results were plotted using GraphPad Prism and expressed as mean \pm SD from triplicate measurements.

2.1.2.1 Hydrogen peroxide scavenging assay

Lyophilized A β 1-42 was a gift generously offered by Professor A.I. Bush, the Mental Health Research Institute (Melbourne). The protocol was adapted from his laboratory and their published papers (Adlard et al., 2008; Huang et al., 1999b).

A small amount of A β 1-42 peptide was dissolved in Chelex 100 treated MilliQ water, sonicated in a water bath sonicator for 5 minutes and centrifuged at 16,100 x g for 5 minutes. Protein quantification was the same as in section 2.1.1.1. Cu(II)-glycine solution with 1 mM Cu(II) and 6 mM glycine was prepared in MilliQ water and diluted to 100 μ M Cu(II) with PBS. A β 1-42 peptide and Cu(II)-glycine were added to PBS such that their final concentrations were 1 μ M and 2 μ M (A β 42:Cu solution). Dopamine was prepared at 0.5 mM in PBS. Test compounds were dissolved in DMSO and diluted 10-fold in PBS. 2',7'-dichlorofluorescein diacetate (DCF) was dissolved in argon-purged DMSO, then de-acetylated by the same volume of 0.05 M NaOH for 30 minutes. The pH of DCF solution was adjusted by 0.5 M disodium hydrogen phosphate solution to pH 7.4, then diluted 5-fold to PBS at around 1 mM final concentration. Hydrogen peroxidase (HRP) was dissolved in PBS at 100 μ M. Then (1) PBS, (2) Cu(II) or 100:200nM A β 42:Cu, (3) test compound or solvent control, (4) 5 μ M dopamine, (5) 100 μ M DCF solution, and (6) 1 μ M HRP

were added to a 96-well black plate with a transparent bottom. The plate was sealed and shaken in the dark at 37°C for 1 hour. Lastly, the fluorescence signal was measured using an LS55 (PerkinElmer) at Ex: 485 / Em: 535.

2.1.2.2 Statistical analysis

Data were normalized to controls. IC₅₀s were calculated by fitting using nonlinear regression of GraphPad Prism. Results were statistically compared by one-way ANOVA for multiple comparisons and Tukey HSD as a *post hoc* test. P values of less than 0.05 were considered statistically significant. Results were plotted using GraphPad Prism and expressed as mean ± SD from triplicate measurements.

2.2 Cell cultures

The cell line BV-2 was offered by Professor Raymond Chang, Department of Anatomy (HKU).

2.2.1 Culture of microglia (BV-2)

The mouse microglial cell line, BV-2, was maintained in DMEM (Gibco) with high glucose, 4 mM L-glutamate and 20 mM HEPES, and supplemented with 5% fetal bovine serum at 37°C in a humidified incubator with 5% CO₂. It was subcultured every 3 to 4 days at a ratio of 1:5. One day after initial seeding at 2.5 × 10⁵ cells per well in a 24-well plate, cells reached confluence. The medium was then changed to the same medium containing different concentrations of curcumin, ferulic acid and

tannic acid. Each condition was done in triplicate. After 16-24 hours, each well was rinsed twice with serum-free medium. The same concentrations of the above compounds were added to the serum-free medium which was added to the plate. Conditioned medium was collected at 4 and 8 hours of incubation in the humidified incubator, centrifuged at 3000 rpm for 10 minutes and stored at -80°C.

2.2.2 MTT cell viability assay

BV-2 microglial cells were maintained in the same conditions as above. The cells were seeded onto a 96-well plate at the same cell density. After just reaching confluence, the medium was replaced as above and incubated for the same length of time. Then, the medium was removed, and 110 µL of MTT (0.5 mg/mL in DMEM serum-free medium) solution was added. The plate was incubated at 37°C in a humidified incubator with 5% CO₂ for 1 hour and 15 minutes. The medium was removed, and 100 µL of DMSO was added. The plate was then shaken at room temperature for 20 minutes. The absorbance at 570 nm was taken, with 690 nm as the reference wavelength, using a microplate reader (U Quant microplate reader, Bio-Tek Instruments Inc.).

2.2.3 Dot blotting of ApoE protein

100 µL of conditioned medium was transferred onto a nitrocellulose membrane using a dot blot apparatus (Biorad). The membrane was air-dried and blocked in blocking buffer (5% non-fat milk in TBST). After brief washing in TBST, it was blotted in 1:6000 diluted rabbit anti-mouse ApoE antibody (Biodesign International) in 3% BSA

blocking buffer. The membrane was washed thrice in TBST for 5 minutes and blotted in 1:10,000 diluted AP-conjugated goat anti-rabbit IgG antibody. X-ray film was developed as in section 2.1.1.2.

2.2.4 Western blotting of ApoE

Specificities of the antibody and dot blot analysis were confirmed by western blotting. BV-2 microglial cells were maintained in the same conditions as above, except that they were seeded in 6-well plates. The conditions of drug treatment were the same as above. The conditioned medium was concentrated from 4.8 mL to 0.05 mL using a molecular weight cut-off spin concentrator (10k MWCO Amicon Ultra, Millipore). 10 μ L of the concentrated conditioned medium was resolved on a 12% SDS-PAGE gel together with a protein size marker (SeeBlue Plus 2, Invitrogen) according to a published protocol (Sambrook and Russell, 2001). Electrophoresis was run in a Tris-glycine buffer system (25 mM Tris, 0.192 mM glycine, 0.1% SDS, pH 8.3) at 100V until the size marker of 22 kDa approached the end of the gel.

After SDS-PAGE, the gels were taken out and immersed in ice-cold Transfer buffer (48 mM Tris•Base, 39 mM glycine, 20% methanol, 0.038% SDS). PVDF membrane was soaked in 100% methanol. The gel and PVDF membrane were then placed in a gel holder cassette. Protein on the gel was then transferred to PVDF membrane with a frozen Bio-Ice cooling unit in the tank at 400 mA for 2 hours.

After transfer, the procedures of blotting and film development were mostly the same as in section 2.2.3, except that the membrane was not air-dried.

2.2.5 Signal quantification of secreted ApoE

The film was scanned using an Imaging Densitometer (BioRad GS700). Densitometry was performed using Quantity One (Biorad).

2.2.6 Statistical analysis

Data from the dot blot images were compared using SPSS by one-way ANOVA for multiple comparison and Tukey HSD as a *post hoc* test. Results are expressed as mean \pm SD from triplicate measurements. P values of less than 0.05 were considered statistically significant.

2.3 Animal studies

The animal handling and experimental procedures were according to the Animals (Control of Experiments) Ordinance (Cap.340) of Hong Kong. Animal ethics approval was obtained from the Animal Experimentation Ethics Committee of The Chinese University of Hong Kong (Ref. (07-184) in DH/ORHI/8/2/1 pt.9 & Ref. (09-171) in DH/HA&P/8/2/1 pt.7).

2.3.1.1 Strains

Tg2576 is the transgenic mouse generated by (Hsiao et al., 1996). It carries the 695 amino acid isoform of the human β -amyloid precursor protein gene with the Swedish mutation (K670N/M671L) (APP^{swe}) which leads to the mouse expressing five-fold

and 14-fold higher than usual levels of $\text{A}\beta$ 1-40 and $\text{A}\beta$ 1-42, respectively. It is hemizygous for the mutant gene and was bred on F1 progeny of SJL/JcrNTac and C57BL6/NTac strains. Cognitive impairment develops at 9 to 10 months, with the presence of $\text{A}\beta$ plaques in cortical and limbic structures. Taconic Farms, Inc. received it from the Mayo Clinic, and we obtained this strain from Taconic Farms, Inc.

JNPL3 is the transgenic mouse generated by Lewis et al. in the laboratory of Mike Hutton (Lewis et al., 2000). It expresses human 4R0N isoform of Mapt with the P301L mutation. It is homozygous for the mutant gene. Motor function impairment was reported to develop as early as 4.5 months, but we could not observe phenotypic change until age 15 months. Neurofibrillary tangles (NFT) developed extensively in amygdala, thalamus, hypothalamus, midbrain, pons, medulla, cerebellum and spinal cord. The hemizygous mouse was bred on F1 progeny of DBA/2 and C57BL/6 strains, and the homozygous mouse was produced by crossing hemizygous mice and maintained by mating to homozygous mice. We obtained this strain from Taconic Farms, Inc.

JNPL3xTg2576 mice are the F1 progeny of male homozygous JNPL3 and female hemizygous Tg2576 mice. The crossing and phenotypic characterization was first done by (Lewis et al., 2001). Plaques and NFT developed as early as six and three months, respectively.

2.3.1.2 Breeding

Tg2576, JNPL3 and JNPL3xTg2576 were maintained in the Laboratory Animal Services Centre (LASEC) at The Chinese University of Hong Kong. A breeding

agreement was obtained from Taconic Farms, Inc. The breeding scheme is shown below:

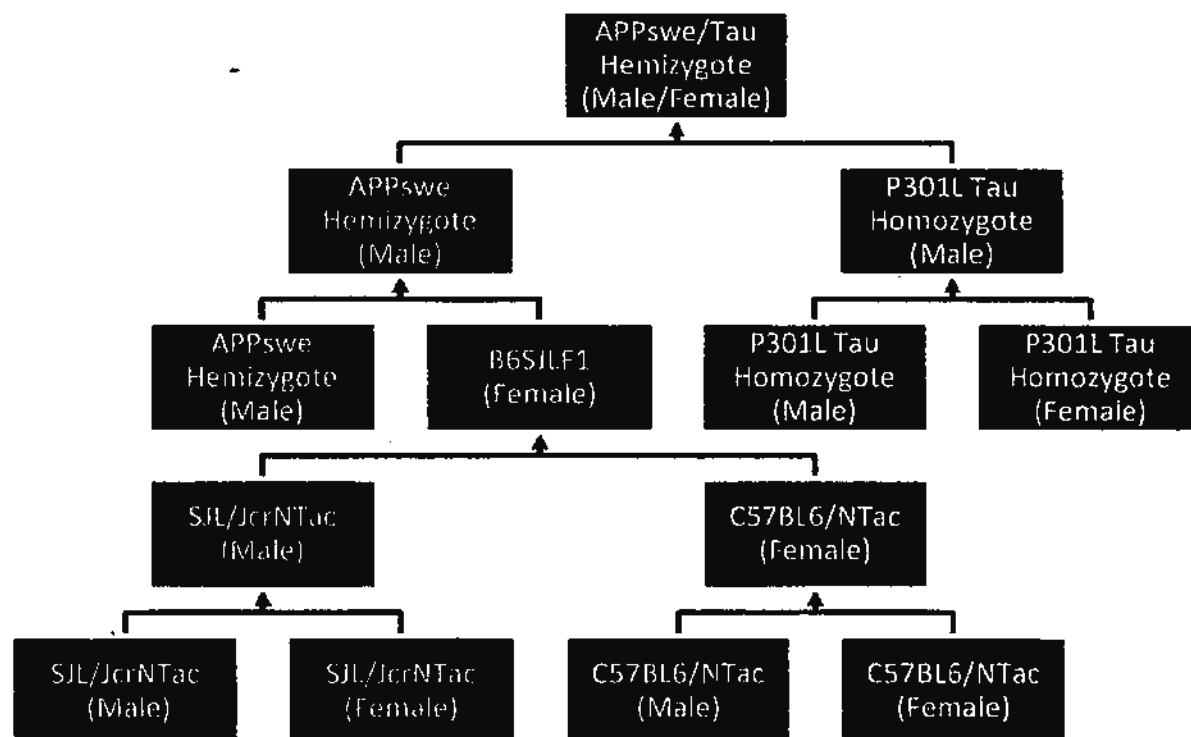


Figure 2.3.1.2 Breeding scheme of Tg2576, JNPL3 and JNPL3xTg2576 strains.

2.3.1.3 Genotyping

Genotyping was carried out on Tg2576 and JNPL3xTg2576 for the presence of the APPswe transgene. A tail biopsy of each mouse was obtained at 2 months old. The samples were stored at -20°C in fresh 1.5 mL microcentrifuge tubes.

2.3.1.4 DNA extraction

Genomic DNA was extracted from mouse tail samples using the High Pure PCR

Template Preparation Kit (Roche). About 0.5-1 cm samples were lysed in 1.5 mL boil-proof microcentrifuge tubes (Axygen) by incubating with 200 μ L of Tissue Lysis Buffer and 35 μ L of Proteinase K solution at 56°C overnight. 200 μ L of Binding Buffer and 100 μ L of isopropanol were added and mixed well. The mixture was centrifuged at 12,000 x g for 5 minutes. Supernatant was transferred into the upper reservoir of a combined High Pure filter tube-collection tube assembly. The tube assembly was centrifuged at 8,000 x g for 1 minute, the flow through was discarded and 500 μ L of Inhibitor Removal Buffer was added to the upper reservoir. The tube assembly was centrifuged at 8,000 x g for 1 minute. The tube was washed twice by adding 500 μ L of Wash Buffer and centrifuged as before. Residual ethanol containing Wash Buffer was removed by centrifugation at 14,000 x g for 10 seconds. Genomic DNA was eluted by adding 200 μ L of prewarmed (70°C) Elution Buffer and centrifuging at 8000 x g for 1 minute. DNA samples were stored at -20°C.

2.3.1.5 DNA quantification

DNA samples were thawed and spun briefly. They were diluted 5-fold in MilliQ water. The quantification was done by measuring the absorbance at 260 nm and 280 nm. The quality was determined by taking the ratio of A_{260} to A_{280} , which should be between 1.5 and 2.0. The DNA concentration was calculated by the following equation:

$$[\text{DNA}] \mu\text{g}/\mu\text{L} = 50 \times \text{dilution factor} \times A_{260} / 1000$$

2.3.1.6 PCR

PCR was performed by using AmpliTaq Gold DNA Polymerase (Applied Biosystems), with β -actin as the internal control, with the following components:

<u>Reaction Mix Component</u>	<u>Final Volume, Concentration</u>
Sterilized MilliQ water	1.89 μ L
10X PCR Buffer	1.25 μ L, 1X
25 mM MgCl ₂	0.75 μ L, 1.5 mM
10 mM dNTP, 2.5 mM each	1 μ L, 0.2 mM each
4 Primers Mix, 2.5 μ M each	2.5 μ L, 0.5 μ M each
<u>5 U/μL AmpliTaq Gold DNA Polymerase</u>	<u>0.13 μL, 0.05 U/μL</u>
Master mix volume	7.5 μ L
<u>25 ng template DNA</u>	<u>5 μL</u>
Total reaction volume	12.5 μ L

Primer (Invitrogen) sequences (5' to 3') are listed as follows:

APPswe forward: CTG ACC ACT CGA CCA GGT TCT GGG T

APPswe reverse: GTG GAT AAC CCC TCC CCC AGC CTA GAC CA

β -actin forward: CGG AAC CGC TCA TTG CC

β -actin reverse: ACC CAC ACT GTG CCC ATC TA

Thermal cycling conditions are as follows:

95°C	15 min - 1 cycle
95°C	45 sec
55°C	1 min
72°C	1 min
	} - 35 cycles
72°C	10 min - 1 cycle
4°C	Forever

The PCR products were mixed with 6x loading buffer. Electrophoresis of the PCR products was run in 2% agarose gels in 1x TAE buffer prestained with 0.5 μ g/ml ethidium bromide at 160 V.

A product size of 300 bp, representing β -actin, indicated that the PCR was successful. A product size of 466 bp was used to indicate the presence of the APPswe

transgene. The picture below shows one of the gels after electrophoresis:



2.3.2.1 Demographic data

Strain	Sex	Group	Starting age	No.	Duration	Mode	Vehicle	Dosage			
JNPL3	Male	Curcumin	8 m	14	6 m	Ad libitum	Chow (5P14)	500 ppm			
		Control		13				0 ppm			
		Curcumin	16 m	8	2 m		Per os	Peanut Butter	100mg/kg		
		Control		9					0mg/kg, 1µL/g		
	Female	Curcumin	8 m	10	6 m	Ad libitum		Chow (5P14)	500 ppm		
		Control		10					0 ppm		
Tg2576	Male	Curcumin	8 m	15	5 m				Ad libitum	Chow (5P14)	500 ppm
		Control		12							0 ppm
	Female	Curcumin		14			500 ppm				
		Control		13			0 ppm				
JNPL3xTg2576	Male	Curcumin	5 m	5	5 m	Ad libitum	Chow (5P14)	500 ppm			
		Control		8				0 ppm			
	Female	Curcumin		7				500 ppm			
		Control		6				0 ppm			
	Male	Curcumin	11 m	5	5 m			Ad libitum	Chow (5P14)	500 ppm	
		Control		5						0 ppm	
	Female	Curcumin		4						500 ppm	
		Control		3						0 ppm	

Table 2.3.2.1 Demographic data showed the ages, numbers, treatment durations, mode of administration, dosages and vehicles of the mice used in this whole study.

2.3.2.2 Husbandry

Mice were raised and kept in LASEC. The environment was maintained at a 12-hour light-and-dark cycle. Sterilized food pellets or chow (LabDiet) and water were

available *ad libitum*. Tg2576 and JNPL3xTg2576 mice were ear-tagged after tail biopsy. After genotyping confirmed the presence of the APP^{swc} transgene, the non-transgenic mice were culled and the transgenic male mice were individually caged.

Mice administered with chow as vehicle were kept in LASEC until the treatment was finished. Their body weights were recorded before and after the treatment regime. Then they were sent to the animal facility at Prince of Wales Hospital (PWH) for rotarod test or dissection. Mice that died during the treatment regime were noted.

Mice administered with peanut butter as vehicle were sent to the animal facility at PWH before the treatment began. Their body weights were recorded daily from Monday to Friday, and deaths were noted.

2.3.2.3 Diet

Since the ingredients of the chow have a significant impact on the pathology of the transgenic mice, all mice were fed chow with the same ingredients (LabDiet, 5P14).

2.3.2.4 Drug administration

For treatment with chow as vehicle, curcumin was sent to LabDiet to be integrated into chow (5P14). The amount of curcumin was about 500 parts per million (ppm). The chow with or without curcumin was available *ad libitum*. Assuming each mouse weighing around 25 grams takes about five grams of chow per day, each mouse would consume about 2.5 mg curcumin per day.

For treatment with peanut butter as vehicle, curcumin was prepared freshly by mixing with peanut butter at 0.1 mg/ μ L. The paste was transferred to a 1 mL syringe without a needle. The mice were fed by injecting onto the mouth at 1 μ L/g of body weight. Therefore, each mouse of 25 grams body weight takes about 25 μ L \times 0.1 mg/ μ L = 2.5 mg curcumin, which is equivalent to the daily consumption of mice administered curcumin in chow. The mice were fed daily from Monday to Friday.

2.3.2.5 Statistical analysis (body weight, mortality)

Comparison of the distributions of mice before treatment among strains was done by Chi-square test, and comparison of the sexual distribution in each strain was done by Fisher's exact test using GraphPad Prism. Comparison of the change of body weight between groups with or without curcumin was performed by Student's t-test using SPSS. Mortality analysis between treatment and control groups was done by Fisher's exact test, and data were plotted using GraphPad Prism. P values less than 0.05 were considered statistically significant.

2.3.3.1 Rotarod test

Motor function performance of mice was assessed by rotarod test. The test was performed based on a published protocol (Rozas et al., 1997). Only JNPL3 mice were used for this test since the motor function is disturbed by the human mutant P301L Mapt transgene. Female mice were excluded due to larger physiological variation. JNPL3 administered curcumin in chow (JNPL3 (chow)) were excluded after preliminary training showing the lack of detectable impairment in motor function.

Rotarod testing was done in the animal facility at PWH.

Mice were placed in the testing room for one hour before commencement of the test to adapt to the testing environment. Then four rounds of trial training and one round of testing were performed with a one hour interval in between. The rotarod apparatus was cleaned with ethanol after every single use. The apparatus was set to accelerate at a rate of about 1 rpm / 9 seconds, beginning from 4 rpm and going up to 40 rpm. Mice were placed onto the rod of the apparatus. Rotation was started at a constant rate of 4 rpm to allow the mice to balance. Then the rotation speed was increased. The time between the beginning of the acceleration of the rod and the falling of each mouse was recorded.

2.3.3.2 Statistical analysis

Statistical analysis of the rotarod performance, assessed by the time each mouse stayed on the rod, was conducted using two-way ANOVA followed by Bonferroni test in SPSS. A time of zero was used for mice that had died or were unable to perform the test. Data were plotted using GraphPad Prism. A p value of less than 0.05 was considered statistically significant.

2.3.4 Dissection

Mice treated with chow as vehicle were dissected after overnight fasting to show the long term effects of curcumin. Mice treated with peanut butter as vehicle were dissected one to 1.5 hours after treatment to determine short term effects of curcumin.

Each mouse was euthanized with isoflurane in a closed glass bottle and was taken out 10 seconds after the final breath. Body weight was recorded. The body was fixed on a dissecting board with the chest facing up. The chest was cut and opened. A needle of a 2 cc syringe was inserted into the apex of the left ventricle to withdraw the blood. The blood was then transferred to a 1.5 mL microcentrifuge tube containing 20 μ L of 0.5 M EDTA and kept on ice. The right atrium was cut open. A needle of a 30 cc syringe with 30 mL of ice-cold PBS was inserted into the apex of the left ventricle. PBS was injected into the heart slowly to let it travel through the body. The head was removed by cutting at the neck. One side of a fine scissors was inserted into the vertebral column to cut up to the skull. After pulling the skull into two halves, the whole brain was taken out. It was washed briefly in ice-cold PBS, then cut into left and right hemispheres. One hemisphere was transferred to 13 mL of 10% neutral buffered formalin (NBF) in a 15 mL centrifuge tube. Another hemisphere was dissected into hippocampus, entorhinal cortex, amygdala, thalamus and hypothalamus, mid-brain, cerebellum, pons and medulla.

Blood was centrifuged at 3000 x g for 15 minutes. Plasma and other brain tissues were snap-frozen in liquid nitrogen and then stored at -80°C. Fixation of the hemisphere continued at 4°C for at least 3 days.

2.3.5 Secretase activity assays

2.3.5.1 Protein extraction

Dissected brain regions, except hippocampus, were thawed from -80°C and transferred into one 1.5 mL microcentrifuge tube. Ice-cold homogenization buffer (20

mM Hepes, pH 7.2, 0.02% NaN₃, 1x complete protease and phosphatase inhibitors) was added. The tissue was lysed by passing through a 23G needle of a 3 mL syringe 20 times. Homogenate was centrifuged at 800 x g for 10 minutes at 4°C. The pellet was homogenized as before for 2 more times. Supernatant was pooled and centrifuged at 100,000 x g for 60 minutes at 4°C (50k rpm using a TLA-100.4 rotor (Beckman Coulter)). Pellet was resuspended, homogenized and ultracentrifuged again. The washed pellet was homogenized in the same buffer with 10% glycerol. The supernatant from the ultracentrifugation and the resuspended pellet were stored as aliquots at -80°C.

2.3.5.2 Protein quantification

Protein quantification was done using the Protein Dc assay (Biorad). BSA standards was prepared in the same buffer as the sample at 3 mg/ml, and then serially diluted to 1.5, 0.75, 0.375, and 0.1875 mg/mL. Frozen protein prepared in the last section was diluted 10 times in the same buffer. Five µL of samples and standards were transferred to a 96-well transparent culture plate. 25 µL of Reagent A of the Biorad Protein Dc Assay was added, followed by 200 µL of Reagent B. After shaking and incubating, the absorption at 750 nm was measured by a microplate reader (U Quant microplate reader, Bio-Tek Instruments Inc.). The protein concentration was calculated by comparing with the linear curve of the BSA standard.

2.3.5.3 α -secretase assay

The α -secretase assay was modified from a published protocol (Moss and Rasmussen, 2007). Information of the substrate: Ac-RE(EDANS)-VHHQKLVF-K(DABCYL)-R-OH (Calbiochem, catalog number 565767). After cleavage, the fluorescence group EDANS was separated from the quencher DABCYL, therefore, upon excitation at 355 nm, emission at 510 nm can be detected.

A protein sample was thawed on ice. Then it was diluted to 5 mg/mL using the same storage buffer, then diluted by α -membrane solubilisation buffer (10 mM Hepes, 0.4% NP-40, 0.01% NaN₃, 1x protease inhibitors) to a final concentration of 2 mg/mL. It was then incubated at 4°C on a rotating wheel for 1 hour. Then the α -secretase cleavage assay was started by adding 5 μ M of fluorogenic substrate in α -secretase reaction buffer (10 mM Hepes, pH 7.5, 0.0006% Brij-35, 0.01% NaN₃, 1x protease inhibitor). Fluorescence signal was read at Ex: 355 nm, Em: 510 nm at time zero, 1, 1.5 and 2 hours.

2.3.5.4 β -secretase assay

The β -secretase assay was modified from a published protocol (Benjannet et al., 2001). Information of the substrate: H-RE(EDANS)EVNLDAEFK(DABCYL)R-OH (Merck, catalog number 565758). The principle is the same as that for the substrate for α -secretase.

A protein sample was thawed on ice. Then it was diluted to 5 mg/mL using the same storage buffer, then diluted by β -membrane solubilisation buffer (0.1 M sodium

acetate, pH 4.5, 1% Triton X-100, 0.01% NaN₃, 1x protease inhibitors) at 0.25 mg/mL final concentration. It was then incubated at 4°C on a rotating wheel for 1 hour. Then the β-secretase cleavage assay was started by adding 5 μM of fluorogenic substrate in β-secretase reaction buffer (0.1 M sodium acetate, pH 4.5, 0.02% NaN₃, 1x protease inhibitors). Fluorescence signal was read at Ex: 355 nm, Em: 510 nm at time zero, 15, 30, 45, 60, 90 and 120 minutes.

2.3.5.5 γ-secretase assay

The γ-secretase assay was modified from a published protocol (Li et al., 2000). Information of the substrate: NMA-GGVVIATVK(DNP)-DRDRDR-NH₂ (Merck, catalog number 565764). Upon cleavage, NMA can be excited at 355 nm and emit at 440 nm.

A protein sample was thawed on ice. Then it was diluted to 5 mg/mL using the same storage buffer, then diluted by γ-membrane solubilisation buffer (20 mM Hepes, pH 7.0, 10 mM MgCl₂, 10 mM CaCl₂, 0.3 M KCl, 2% CHAPSO, 0.02% NaN₃, complete phosphatase inhibitors) at 1 mg/mL final concentration with 1% CHAPSO. It was then incubated at 4°C on a rotating wheel for 1 hour. Then the γ-secretase cleavage assay was started by adding 8 μM of fluorogenic substrate in γ-secretase reaction buffer (50 mM Pipes, pH 7.0, 5 mM MgCl₂, 5 mM CaCl₂, 150 mM KCl, 0.02% NaN₃) with a final concentration of 0.25% CHAPSO. Fluorescence signal was read at Ex: 355 nm, Em: 440 nm at time zero, 18, 24, 36 and 48 hours.

2.3.5.6 Statistical analysis

Data of α -secretase activity assays were calculated by subtracting signals at 0 hours from those at 3 hours. Data of β -secretase activity assays were calculated by subtracting signals at 0 minutes from those at 45 minutes. Data of γ -secretase activity assays were calculated by subtracting signals at 0 hours from those at 18 hours. Statistical comparisons were performed using Student's t-test in SPSS; data were plotted using GraphPad Prism; results were expressed as mean \pm SD.

2.3.6 Total tau quantification

2.3.6.1 Protein extraction

Ultracentrifuged supernatant samples from brain homogenization prepared in section 2.3.5.1 were used in this section. Only JNPL3 (chow) mice were used in this part. Tg2576 mice were excluded due to the lack of human Mapt transgene. JNPL3xTg2576 mice were not used due to small sample size. JNPL3 (PB) mice were not considered because the treatment period was short.

2.3.6.2 Protein quantification

The protein quantification procedure was more or less the same as in section 2.3.5.2, except that the supernatant samples were diluted 5 times for quantification.

2.3.6.3 Western blotting of total tau

After total protein quantification, samples were normalized for equal loading. One normalized sample was loaded on each gel for use in normalizing signal intensities among blots. All samples were mixed with Laemmli sample buffer (final concentration: 62.5 mM Tris-HCl, pH 6.8, 25% glycerol, 2% SDS, 0.01% bromophenol blue and 5% β -mercaptoethanol) and then boiled at 95°C for 3 minutes. 15 μ g total protein of each sample and 7 μ l of SeeBlue Plus2 protein size marker (Invitrogen) were loaded onto a 10% SDS-PAGE gel, which was prepared according to a published protocol (Sambrook and Russell, 2001). Electrophoresis was performed in a Tris-glycine buffer system (25 mM Tris, 0.192 mM glycine, 0.1% SDS, pH 8.3) at 40 V in the beginning. When the dye front approached the revolving gel, the voltage was changed to 110 V until the size marker of 22 kDa approached the end of the gel.

After SDS-PAGE, the gels were taken out and immersed in ice-cold Transfer buffer (25 mM Tris, 192 mM glycine and 20% methanol). PVDF membrane was soaked in 100% methanol. The gel and PVDF membrane were then packed in the Transfer Gel Sandwich. Protein on the gel was then transferred to PVDF membrane with a frozen Bio-Ice cooling unit in the tank at 400 mA for 2 hours.

After transfer, the membrane was washed three times in TBST and then was blocked in 3% BSA-TBST blocking solution for one hour. After blocking, the membrane was immunoblotted by 1:1,000 diluted H17 (Pierce, mouse monoclonal, total human tau specific) in the blocking buffer in the cold room overnight. Then, it was washed 3 times in TBST for 5 minutes. Secondary antibody (Biorad, AP-conjugated goat anti-mouse) diluted at 1:10,000 in 5% non-fat milk was used to probe

HT7. After incubation for 1 hour, the membrane was washed 3 times in TBST for 10 minutes. Excess buffer was withdrawn, and the membrane was put on microwave plastic film. Immun-Star Chemiluminescent Substrate was added onto the membrane and incubated for 5 minutes. Then excess substrate was withdrawn, and the membrane was transferred to another piece of microwave plastic film. Luminescent signal was captured by exposure to Kodak X-ray film in the dark for different lengths of time.

2.3.6.4 Signal quantification of total tau

An image of the X-ray film was scanned and saved as a Tiff file. Densitometry was performed using ImageJ 1.44i software.

2.3.6.5 Statistical analysis

The signals of bands were normalized by dividing by the mean of signals of the normalization samples on the same blot. The data were statistically compared by Student's t-test using SPSS. Results were plotted using GraphPad Prism and expressed as mean \pm SEM.

2.3.7 PHF quantification

2.3.7.1 Sample preparation

Ultracentrifuged pellet samples extracted in section 2.3.5.1 were used in this section. For the same reason as in section 2.3.6.1, only JNPL3 (chow) mice were used in this

part.

2.3.7.2 PHF isolation

PHF were isolated using a published protocol (Lee et al., 1999). Ultracentrifuged pellets were diluted to 6 mg/mL. High salt tissue homogenization buffer (HS-THB) was added to samples with the same amount of total protein to a final concentration of 50 mM Tris-Cl (pH 7.0), 1 mM EGTA, 0.5 mM MgSO₄, 2 mM DTT, 0.75 M NaCl, 0.02% NaN₃, 1x complete protease inhibitors and phosphatase inhibitors. The mixture was vortexed and incubated on ice for 20 minutes to depolymerise any residual microtubules. It was ultracentrifuged at 100,000 x g for 60 minutes at 4°C (50k rpm using a TLA-100.4 rotor (Beckman Coulter)). The pellet was washed the same way again. PHF extraction buffer (10 mM Tris-Cl, 10% sucrose, 0.85 M NaCl, 1 mM EGTA, pH 7.4.) was used to resuspend the pellet. The pellet was homogenized by passing through a 25G needle in a 2 mL syringe 40 times. The homogenate was centrifuged at 15,000 x g for 20 minutes at 4°C. The pellet was extracted the same way again. The supernatants, which were enriched with PHF, of these two centrifugations were pooled and centrifuged at 100,000 x g for 30 minutes at 4°C. The supernatant was transferred to a 1.5 mL microcentrifuge tube. 10% Sarkosyl solution was added to the supernatant to about 1% final concentration. The mixture was incubated on a rotating wheel at 37°C and then centrifugated at 100,000 x g for 120 minutes at 4°C. The pellet was resuspended in Tricine sample buffer (200 mM Tris-HCl, pH 6.8, 40% glycerol, 2% SDS, 0.04% Coomassie Blue G-250 and 5% β-mercaptoethanol), vortexed for 5 minutes and incubated at 95 °C for 4 minutes.

2.3.7.3 Western blotting of AT8-immunopositive PHF

Tricine SDS-PAGE gels were used for protein electrophoresis in this section. 10% SDS-PAGE gels were prepared according to a published protocol (Schagger, 2006). The wells of each gel were rinsed thrice with Cathode buffer (1 M Tris, 1 M Tricine, 1% SDS, pH 8.25). Boiled samples and SeeBlue Plus2 protein size marker (Invitrogen) were loaded onto each gel. Electrophoresis was started at 40 V. When the dye reached the resolving gel, the voltage was increased to 120 V. When the size marker of 24.5 kDa reached the end of the gel, the gel was taken out and immersed in Transfer buffer (25 mM Tris, 192 mM glycine, and 20% methanol). Nitrocellulose membrane was rinsed in Transfer buffer. The Transfer Gel Sandwich was prepared, and the protein on the gel was transferred to the nitrocellulose membrane at 400 mA for 2 hours with a frozen Bio-Ice cooling unit in the tank.

After transfer, the membrane was washed thrice in TBST, each time for 5 minutes. Then it was blocked in Blocking buffer (3% BSA in TBST) for 1 hour, followed by overnight immunoblotting in 1:1000 diluted AT8 antibody (Pierce, mouse monoclonal antibody to tau that was phosphorylated at serine 202 and threonine 205). The membrane was washed thrice in TBST and then blotted in 1:10,000 diluted AP-conjugated goat-anti-mouse secondary antibody. Immun-Star Chemiluminescent substrate was added onto the membrane after the membrane was washed. After incubation for 5 minutes, the signal on the blot was developed onto Kodak X-ray film in the dark for different lengths of time.

2.3.7.4 Signal quantification of PHF

The signal on the film was quantified as in section 2.3.6.4.

2.3.7.5 Statistical analysis

Statistical comparison was done as in section 2.3.6.5. Data are presented as relative PHF level by comparing the signal of PHF from curcumin treated mice to control mice. P values are shown in the figures.

2.3.8 Histological staining

2.3.8.1 Sample preparation

2.3.8.1.1 Fixation

One hemisphere of each brain was immediately immersed after dissection in 13 mL of ice-cold 10% neutral buffered formalin (10% NBF). The fixation was performed for at least 3 days at 4°C. Then the fixative was discarded and the hemisphere was washed five times with PBS for 30 minutes each time. After that, it was washed thrice in 70% ethanol each for 1 hour and stored in 70% ethanol at 4°C until use.

2.3.8.1.2 Paraffin embedding

Paraffin embedding was started with gradient dehydration of the hemisphere in ethanol (70% ethanol, 80% ethanol, 90% ethanol, 100% ethanol thrice). Each cycle

lasted 30 minutes at room temperature. Ethanol was substituted by xylene for a 30 minute incubation. The dehydrated brain tissue was inserted into paraffin wax at 65°C for 45 minutes, and this step was repeated thrice. The brain tissue was transferred to a molten wax tank and embedded at the correct orientation in the centre of the paraffin block holder together with the embedding case. Liquid wax was poured into the holder and the solidification was accelerated by putting the holder onto a cold plate. The block was kept at 4°C until use.

2.3.8.1.3 Sectioning

The block of embedded brain tissue was locked onto the microtome holder. It was trimmed until a section close to the hippocampus was seen. Then it was sliced into sections of 4 and 8 µm thicknesses for Bielschowsky's silver staining and immunohistological staining, respectively. The correct slice was recognized by comparing to a standard atlas (Paxinos and Franklin, 2001). The region for the hippocampus was from bregma -1.70 mm to -2.30 mm, while that of the cerebellum was from -5.60 mm to -6.00 mm. The sections were allowed to stretch on a 37°C water bath, mounted onto Superfrost plus slides and dried at 37°C vertically overnight.

Before immunohistological staining, the slides were briefly heated on a 70°C plate for 10 minutes. The sections were deparaffinised by immersing with shaking into xylene thrice at 2 minutes each. Then the sections were rehydrated in descending concentrations of ethanol (3x 100%, 90%, and 70%) at 2 minutes each. Finally, they were washed in MilliQ water.

2.3.8.2.1 Immunohistological staining of amyloid plaques

Antigen retrieval was done by incubating in 80% formic acid for 20 minutes. The slices were washed in PBS twice for 3 minutes. Endogenous peroxidase activity was blocked in 3% H₂O₂ for 5 minutes. The sections were washed again in PBS as before, followed by blocking in 10% normal goat serum in PBS for 30 minutes. The serum was withdrawn by filter paper. Primary antibody 4G8 (epitope: position 17-24 of A β peptides; Signet), diluted at 1:100 in blocking serum, was added to the sections and incubated overnight at room temperature. A negative control was prepared by adding the same blocking serum instead of the primary antibody.

Sections were washed in PBS twice for 2 minutes. Secondary goat anti-mouse IgG antibody (Dako, HRP labelled polymer) was added and incubated for 45 minutes at room temperature. Secondary antibody was removed by washing in PBS twice for 2 minutes. Then, freshly prepared DAB peroxidase solution was added and incubated for about 3 minutes. Color development was stopped by washing in MilliQ water.

Counterstaining was performed by immersing in Harris Hematoxylin for about 2 minutes. After washing in tap water, the sections were immersed in acid alcohol (70% ethanol, 1% HCl), followed by washing in tap water and immersing in Scott's tap water (3.5 g NaHCO₃, 20 g MgSO₄, 1 L MilliQ water) until they turned blue in about 5 minutes. They were washed again in tap water for 2 minutes.

Dehydration was performed by immersing the slides in ascending concentrations of ethanol (70%, 95% and 100% x 2), for 2 minutes each. Ethanol was removed by xylene incubation for 5 minutes thrice. The slices were mounted with DPX and covered with cover slips.

2.3.8.2.2 Quantification of 4G8-immunopositive plaque area

Procedures to quantify plaques on the immunostained sections were adapted and modified from a published protocol (van Belle et al., 1997). Stained sections were inspected at 5x magnification. Four fields which contained the highest density of plaques were randomly selected from the hippocampus; auditory cortex to entorhinal cortex; and piriform cortex to amygdala and hypothalamus.

Images were captured and analysed using SigmaScan Pro 5.0 to detect pixels of 4G8 immunopositive area within the colour threshold which was selected manually. The percentage of 4G8 immunopositive area was calculated to represent the average density of plaques within the section.

2.3.8.2.3 Statistical analysis

Since the 4G8 immunopositive area of hippocampus, entorhinal cortex to auditory cortex, and amygdala and hypothalamus were very low, they were combined into one value for comparison. Statistical comparison of the percentage of 4G8 immunopositive area of brain regions was performed by Student's t-test using SPSS. Data were normalized relative to the percentage plaque area of the control group. Results were plotted by GraphPad Prism and expressed as mean \pm SEM.

2.3.8.3.1 Bielschowsky's silver staining

Rehydrated slides were immersed into 37°C pre-warmed 20% silver nitrate solution which was prepared freshly. They were incubated at 37°C for 15 minutes in the dark.

followed by washing in MilliQ water for 4 minutes thrice. Ammoniacal silver solution was then prepared by adding concentrated ammonium hydroxide to another fresh 20% silver nitrate solution until the precipitates formed has just disappeared. The slices were then incubated in ammoniacal silver solution at 37°C for 10 minutes in the dark, followed by immersing in ammonia water (2 drops / coplin jar). Developing stock solution was then prepared by adding 0.5 g citric acid and 2 drops of concentrated nitric acid to 100 ml MilliQ water, followed by mixing 1 ml of the mixture with 200 µL of formaldehyde (37 - 40%) freshly. Working developer was then freshly prepared by adding 2 drops of the Developing stock solution to the used ammoniacal silver solution. The slides immersed in ammonia water were then transferred to the Working developer. When slides began to turn brown, they were inspected for tangle development under a light microscope after briefly dipping into another cup of ammonia water. Development was resumed if necessary by further dipping in ammonia water, followed by immersing in the Working developer. The slides were washed in MilliQ water for 5 minutes thrice, then immersed in 5% Hypo (50 g sodium thiosulfate in 1 L MilliQ water) for 5 minutes, followed by rinsing as before. Dehydration was performed as in section 2.3.8.2.1.

2.3.8.3.2 Quantification of silver stained tangles

Stained pons sections were inspected under 40x magnification. The presence of tangles was judged manually by the intracellular deep brown to dark appearance. The numbers of tangles in the pons region were counted thrice, and the average of the two closest counts was used.

2.3.8.3.2 Statistical analysis

Statistical comparison of the number of tangles in pons sections of mice in each group was performed by Student's t-test using SPSS. Data were normalized relative to the average number of tangles in pons of the control group. Results were plotted by GraphPad Prism and expressed as mean \pm SD.

2.3.8.4.1 Immunohistological staining of AT8-immunopositive tangles

Antigen retrieval was done by heating the slides with boiled citrate buffer in a microwave oven for 5 minutes at high power, and then the solution level was refilled with MilliQ water. Lastly, the slices were heated in a microwave oven again at medium power for 10 minutes and cooled to room temperature. Other steps are more or less the same as in section 2.3.8.2.1, except that the primary antibody was AT8 (Pierce) and was diluted 1:50.

2.3.8.4.2 Quantification of AT8-immunopositive area

Procedures to quantify tangles on the immunostained sections were adapted and modified from published protocols (Zehr et al., 2004) and (van Belle et al., 1997). Stained sections were inspected at 40x magnification. Four fields which contained the highest density of tangles were randomly selected in the medulla and entorhinal cortex to amygdala, and images were captured.

The images were analysed using SigmaScan Pro 5.0 to detect pixels of AT8 immunopositive area within the colour threshold which was selected manually. The

percentage of AT8 immunopositive area was calculated to represent the average density of tangles within the section.

2.3.8.4.3 Statistical analysis

Statistical comparison of the percentage of AT8 immunopositive area of brain regions was performed by Student's t-test using SPSS. Data were normalized relative to the percentage of AT8 immunopositive area of the control group. Results were plotted by GraphPad Prism and expressed as mean \pm SEM. P values less than 0.05 were considered statistically significant.

2.3.9 Microarray

In this and the next sections, only male mice were used since female mice have relatively larger physiological variation.

2.3.9.1 RNA extraction

Total RNA extraction was done by using TRIzol (Invitrogen) reagent. Frozen hippocampus tissues were thawed from -80°C . Some tissue samples were weighed. Average weight was about 18 mg. Therefore, 500 μL of TRIzol reagent was used per sample. TRIzol reagent was added before the tissue thawed. Tissue was broken by pipetting up and down at least 10 times with a 1 mL pipette tip. Samples were frozen at -80°C and thawed on ice. The samples were further homogenized by passing

through a 23G needle on a 3 mL syringe until smooth. They were then incubated on ice for 15 minutes and room temperature for 1 minute. Chloroform was then added. The mixture was vigorously shaken for 15 seconds and then incubated on ice for 5 minutes, followed by centrifugation at 12,000 x g for 15 minutes at 4°C. The upper colorless aqueous phase was transferred to a fresh autoclaved 1.5 mL microcentrifuge tube (Axygen). Isopropanol was added to precipitate the total RNA, which was spun down at 12,000 x g for 10 minutes at 4°C. The RNA pellet was washed with 75% ethanol twice and was air-dried until the white pellet just turned colorless. The pellet was dissolved in RNase-free water, incubated in a 60°C water bath, and stored in aliquots at -80°C.

2.3.9.2 RNA quantification

RNA quantification was conducted by using Nanodrop with 1.5 µL samples. Readings of A260/A280 and A260/A230 were taken for determining protein and organic solvent contamination, respectively. Total RNA content was calculated by the formula: [RNA] (µg/mL) = A260 * 40.

2.3.9.3 RNA quality determination

RNA quality was determined using a Bioanalyzer (Agilent) by the values of RIN (RNA integrity number) and rRNA (22S/18S).

2.3.9.4 Microarray

To reduce the cost of the microarray experiment, pooling was adapted as in a previous study (Kendzioriski et al., 2005). RNA samples of mice in each group of the 4 pairs were pooled as one RNA sample. They were JNPL3 (chow), JNPL3 (PB), Tg2576 and JNPL3xTg2576 with or without treatment. Equal amounts (500ng) of samples with rRNA>0.8, RIN>5.4 and 260/230>1.8 were included in the pooling. The number of samples included in the each group is listed below:

Groups	JNPL3(chow)	JNPL3(PB)	Tg2576	JNPL3xTg2576
<i>Treatment</i>				
Curcumin	8	5	8	5
Chow	8	4	4	2

After pooling, the RNA quality of each sample was checked by Bioanalyzer again. Then about 500 ng of RNA sample was used as input for amplification. The dye used for cRNA labelling was Cy3. One-color array type was used.

The procedures of RNA quality determination, RNA amplification, cRNA-Cy3 hybridization and microarray scanning were done in collaboration with Professor Richard Choy of the Department of Obstetrics and Gynaecology (CUHK).

2.3.9.5 Signal processing *

The output files from microarray scanning were used as input for the data analysis software GeneSpring GX11 (Agilent). Signals were normalized by the software to minimize local and chip-to-chip signal variations. The normalized data with differential expression ratio of curcumin:control of each gene in each group were

output.

2.3.9.6 Data analysis

The differential expression data were ranked by the ratio of expression level of curcumin to control according to the JNPL3 (PB) group since the mice in this group had well-controlled drug dosage and time of dissection after treatment, which made it a relatively reliable group for the study of the direct effect of curcumin treatment. A fold change over 2 was used as the cutoff for possible differential expression of a gene due to curcumin treatment.

2.3.10 Real-time PCR

Candidate genes were selected for real-time PCR confirmation based on the fold change ranking of the JNPL3 (PB) group and the relationship of the genes with AD. Therefore, some genes with fold change of less than 2 were selected in this section.

2.3.10.1 Reverse transcription

5 µg of total RNA was used for this and the following experiments. Genomic DNA was removed from the sample by using DNase (Invitrogen) digestion. For each sample, 1 µL of 10X DNase 1 Reaction Buffer, 1 µL of DNase 1 and 0.5 µL of RNaseOUT were added to 5 µg of RNA. The reaction volume was filled to 10 µL. For the control setup, 7.5 µL of nuclease-free water (Invitrogen) was used instead of

an RNA sample. The mixture was incubated at room temperature for 15 minutes. The activity of DNase I was abolished by adding 1 μ L of 25 mM EDTA, heating at 65°C for 10 minutes in a thermal block cycler and cooling on ice.

Reverse transcription of RNA was performed by using Transcriptor First Strand cDNA Synthesis Kit (Roche). To the DNase-treated RNA sample, 2 μ L of random hexamer primer and 1 μ L of anchored-oligo(dT)18 primer were added, followed by heating at 65°C for 10 minutes in a thermal block cycler in order to denature the template-primer mixture, and cooling on ice. Then, a master mixture of 4 μ L of 5x Transcriptor Reverse Transcriptase Reaction Buffer, 0.5 μ L of Protector RNase Inhibitor, 2 μ L of Deoxynucleotide mix (10 mM each) and 0.5 μ L of Transcriptor Reverse Transcriptase was added. After mixing gently with pipetting, it was incubated at 25°C for 10 minutes, followed by 50°C for 60 minutes, in a thermal block cycler. The reaction was finished by heating up the sample to 85°C for 5 minutes in order to inactivate Transcriptor Reverse Transcriptase. The cDNA sample was stored at -20°C.

2.3.10.2 Primers for real-time PCR

Primers of each gene were designed by a Roche online tool called Universal ProbeLibrary Assay Design Center, unless otherwise mentioned. The design was specifically for use with Universal ProbeLibrary (Roche) in real-time PCR reactions. The primer sequences and the probe number of the Universal ProbeLibrary for each gene are listed below according to the functional pathways related to AD:

	Gene	Accession ID	Forward primer	Reverse primer	Probe
Housekeeping					
1	Gapdh	NM_008084	gtgttctaccaccaatgt	tgcatcacttggcaggtttc	80
A β -production					
2	Adam10	AF011379	gtgtgccgacagtgttaattc	tttaaaggattccatactgacctc	55
3	Adam17	NM_009615	ctttgggcctttcgtcct	gagcaaagaatcaagcttctcaa	106
4	Adam9	NM_007404	tccggcagtgagtacaagaa	gcattgaagctttccacaca	48
5	Bace1	NM_011792	cccttctcgtcgtctac	tacacacccttcggaggtc	34
Secretase substrate					
6	Btc	NM_007568	cgggtagcagtgctcagctc	acagtgagagaattgcaagacc	68
7	Ereg	ENSMUST00000031324	accgtgatcccatcatgc	gggatcgtcttccatctgaa	2
8	Fcer2a	NM_013517	atccctgggcttgaatgag	gacatatgttgatgcagttcc	75
9	Kl	ENSMUST00000078856	ccattgacaaccctcactgtg	ttggcatgagccaaaagtag	1
10	Muc1	NM_013605	ctgttcaccaccacatgac	cttgaagggcaagaaaacc	4
11	Sell	NM_011346	ggcatctccagagccaatc	tccatggtaccacactcagg	47
12	APP	NM_007471	cgagagagaatgtcccagggt	agttctggcttgacgtct	103
A β -degradation					
13	Ace	NM_009598	gatggaagggagggtggtgt	caccaagtcctccatgttca	64
14	Bsg	NM_009768	cttctatagagccgcagtg	gggtccttgaggaaaccag	17
15	Ide	NM_031156	agcgtatccaccacagac	ggagggctgacagtgaaact	73
16	Mmp2	ENSMUST00000034187	aactttgagaaggatggcaagt	tgccaccatggtaaacaa	29
17	Mmp3	NM_010809	agctgaggactttcagggtg	tgcaagatccactgaagaa	89
18	Mmp9	NM_013599	acgacatagacggcatcca	gctgtggtcagttgtggtg	19
19	Mmp14	NM_008608	ccaagggcagcaactca	ccctggaggtaggtagccata	71
20	Neprilysin	NM_008604	gggaggctttatgtggaagc	ccggatttgcacatcaagt	67
A β -transporter					
21	A2M	NM_175628	tgaggaggcggtaaaagaag	tggcactctgggttctga	93
22	ApoA1	NM_009692	gcggcagagactatgtgtcc	cagtttccaggagattcagggt	63
23	ApoE	NM_009696	gaccctggaggctaaggact	agagccttcatcttgcacat	12
24	ApoJ	ENSMUST00000022616	tgctgatctgggacaatgg	cctactcccttgagtggacagt	15
25	Ltf	NM_008522	gggcaagtgcggttagtt	ccattgctttggaggattt	53
26	Ttr	NM_013697	cctcgtggactggtatttg	gaccatcagaggacatttga	67
A β -receptor					
27	Ager	NM_007425	ggtcactggataaaggatgg	taggtgccctcatcctcgt	52
28	Apoer2	NM_001080926	ctcccgaagaaccctcttcc	agacttaatgccactcgttg	27
29	Cd36	NM_007643	tggagctgttattggtgcagt	ggttccttctcaaggacaactt	76
30	Colec12	NM_130449	agcgtgtcctcagtcacat	gtaaccgaaggactgcacct	6
31	Ldlr	NM_010700	caagaggcagggtccaga	ccaatctgtccagtacatgaagc	21
32	Lrp1	NM_008512	ggaccaccatcgtggaaa	tcccagccacggtgatag	97
33	Lrp2	ENSMUST00000080953	gatggattagccgtggactg	tccgtgactcttagcatctga	97
34	Msr1	ENSMUST00000110488	ctggacaaactggtccacct	gtccccgatcacctttaaca	1
35	Sort1	ENSMUST00000102632	tgaggacatggtcttcatgc	ggtaaagatggtgccaaacc	80

Cholinergic					
36	Ache	ENSMUST00000085934	ctttctcccaaatgctca	tccagtgcaccatgtaggag	97
37	ChAT	NM_009891	ggttcgggtcgtaacagc	gcgattcttaatccagagtagca	108
38	ChT1	NM_022025	cctgcactgatgggagagat	acatccacatcaatgatcagc	49
39	VAC1t	NM_021712	caagctgtcgggaagcagtg	gcacacgatgaccagcac	45
Regulating A β level					
40	Alox15	ENSMUST00000019068	gaagctgttccgaccctgt	ggccaaggtattctgacac	16
41	Cd74	NM_001042605	caccgaggctccacctaa	gcagggatgtggctgact	72
42	Gpr3	NM_008154	ctgccagaacctgagtgag	tgagaaccaggccatagagc	32
43	Ngfr	NM_033217	actgagcgccagttacgc	cgtagacctgtgatccatcg	26
Reducing A β toxicity					
44	Igf2	NM_010514	cgctcagttgtctgttcg	gcagcactctccacgatg	40
45	Irs1	ENSMUST00000069799	tatgccagcatcagctcc	tgctgaggtcatttaggtctc	106
46	Fas	NM_007987	cagacatgctgtggatctgg	tggagatgctattagtacctgag	100
47	Pla2g4a	NM_008869	agggctccgactgagag	cactcccaggctctctatggt	98
48	Rho	NM_145383	acctggatcatggcgttg	tgccctcagggatgtacc	32
49	Tnf	NM_013693	ctgtagcccacgtcgtagc	ttgagatccatgccgttg	25
Oxidative stress					
50	Duox1	NM_001099297	ctggagctctccgggtct	ttcagccottttagcttgg	109
51	Nos2	NM_010927	gggctgtcacggagatca	ccatgatggtcacattctgc	99
52	Nox1	NM_172203	cctgattctgtgtctgaa	cagtgtagggtgcaaatga	56
53	Nox3	NM_198958	cgggatagctgtcaattcagt	ggcctgaccagggtgata	1
54	Sod3	NM_011435	ggggaggcaactcagagg	tggtgaggttctctgcac	69
55	Bmp6	NM_007556	actgactagcgcgcagga	tggtgggagaactcctgtc	22
Tau-related					
56	Mapt	NM_001038609	ggctctactgagaacctgaagc	tccagctcttattaattatctgcac	10

Gapdh was used as the housekeeping gene based on a study showing the reliability of stable Gapdh expression in brain tissue for the study of neurodegeneration (Calvo et al., 2008). Primers used for Gapdh were from a previous paper (Guibal et al., 2009). Primers for Kl and Irs1 were designed manually due to lack of an amplification plot in preliminary experiments.

2.3.10.3 Real-time PCR

Real-time PCR was performed using FastStart Universal Probe Master and Universal

ProbeLibrary Set (Roche) on an ABI 7900HT Real-time PCR machine. The ingredients of the master mix for the real-time PCR of most genes were as follows, unless otherwise mentioned:

Reagent	Final Concentration
i. FastStart Universal Probe Master (ROX), 2x	1x
ii. UPL probe (10 μ M), 50x	200 nM
iii. Forward primer (18 μ M), 20x	900 nM
iv. Reverse primer (18 μ M), 20x	900 nM
v. Water, RNase-free	
Leave 30% volume for template	

The PCR master mix of Duox1 was optimized to have an additional 0.5 mM MgCl₂, and that of Nos2 was optimized to have an additional 1 mM MgCl₂.

The PCR thermal cycling condition was as follows:

Cycles	Analysis Mode	Temperature	Hold Time	Remarks
1	None	95°C	10 minutes	Activation of FastStart Taq DNA Polymerase
60	None	95°C	15 seconds	Denaturation
	Quantification	60°C	1 minute	Annealing
1	None	40°C	2 minutes	Cooling

The detection channel was set to standard FAM.

2.3.10.4 Data calculation

The Ct (threshold cycle) value and amplification efficiency of each sample were calculated by using the online tool Real-time PCR Miner (Zhao and Fernald, 2005). It was designed by using an objective method to quantify real-time PCR results based on the kinetics of individual raw PCR amplification curves. It uses a four-parameter

logistic model for fitting the raw data of the fluorescence signal of each sample in order to identify the exponential phase of each curve of a reaction and compute the amplification efficiency. The Ct was identified by the first positive second derivative maximum from the logistic model. The advantages of using this method are that it provides an objective calculation instead of subjective judgment, it does not require the setting of a baseline and a threshold, and it calculates the amplification efficiency and Ct based only on the individual PCR amplification curve. It can save time and resources that would otherwise be used to optimize conditions so that the amplification efficiency would be the same as for the housekeeping gene.

Instead of normalizing gene expression using the $2^{-\Delta\Delta Ct}$ method, which requires that the amplification efficiency of the target gene be the same as that of the housekeeping gene of an individual sample, our data were normalized by calculating the starting template concentrations of the target gene (R0 target) and the housekeeping gene (R0 housekeeping) by the amplification efficiency (E) and Ct of that gene of a particular sample obtained by the above described method. The calculation is as follows:

$$R0 = 1 / (1+E)^{Ct}$$

Then, the expression level of the target gene was normalized to that of the housekeeping gene as follows:

$$R0 \text{ (normalized target gene)} = R0 \text{ (target gene)} / R0 \text{ (housekeeping gene)}$$

2.3.10.5 Statistical analysis

Statistical analysis for comparing the mRNA expression of a gene in groups of mice

treated with vs. without curcumin was performed by Mann-Whitney U test using SPSS; data were plotted using GraphPad Prism. Data were shown with a box indicating the median, 25 and 75 percentile, whisker caps indicating 5 and 95 percentile, and filled circles indicating outliers. P values less than 0.05 were considered statistically significant.

CHAPTER THREE: RESULTS

3.1 Effects of curcumin on phenotypic changes

3.1.1 Effect of curcumin treatment on body weight

Body weights of transgenic mice fed with or without curcumin were compared before and after the treatment regime. Data are shown in **Table 3.1.1.1**. Body weight change of each group varied from +4.5% to -24%. The average body weight change amongst all strains differed very significantly between treatments with versus without curcumin.

For males, curcumin generally reduced the loss of body weight in most groups. The difference was significant only in the JNPL3xTg2576 strain. For females, the effect of body weight loss reduction by curcumin treatment was observable in all groups combined and in all individual groups, particularly in JNPL3 mice.

Table 3.1.1.1 Body weights of mice before and after curcumin treatment regime.

Analysis groups	Treatment	Mean pre-treatment weight (gm)	Mean post-treatment weight (gm)	Change of mean weight (%)	P
<i>Both sexes</i>					
JNPL3 (Chow)	Curcumin	40.99	38.63	-5.85	0.151
	Control	42.93	37.72	-12.10	
JNPL3 (PB)	Curcumin	42.50	39.38	-7.21	0.630
	Control	40.43	36.93	-8.56	
Tg2576	Curcumin	28.21	28.71	2.86	0.122
	Control	27.67	26.28	-3.87	
JNPL3 x Tg2576	Curcumin	30.88	31.63	2.60	0.070
	Control	31.25	29.10	-6.45	
All strains	Curcumin	34.95	34.04	-1.50	0.007**
	Control	35.74	32.52	-7.96	
<i>Males</i>					
JNPL3 (Chow)	Curcumin	44.00	41.70	-5.27	0.911
	Control	42.90	40.86	-4.68	
JNPL3 (PB)	Curcumin	42.50	39.38	-7.21	0.630
	Control	40.43	36.93	-8.56	
Tg2576	Curcumin	32.00	31.20	-2.09	0.447
	Control	33.00	30.68	-6.40	
JNPL3 x Tg2576	Curcumin	35.00	36.58	4.49	0.023*
	Control	35.00	31.59	-9.74	
All males	Curcumin	39.15	37.62	-3.45	0.200
	Control	39.54	36.86	-6.73	
<i>Females</i>					
JNPL3	Curcumin	34.96	32.50	-7.01	0.001**
	Control	43.00	32.48	-24.47	

Tg2576	Curcumin	24.80	26.47	7.32	0.098
	Control	25.73	24.68	-2.95	
JNPL3 x Tg2576	Curcumin	26.75	26.68	0.72	0.656
	Control	27.50	26.61	-3.16	
All females	Curcumin	28.17	28.24	1.66	0.014*
	Control	31.18	27.31	-9.44	

Tg2576, strain with APP Swedish mutant transgene; JNPL3, strain with Tau (P301L) mutant transgene; JNPL3xTg2576, strain produced by crossing female JNPL3 with male Tg2576; Chow, curcumin was pre-mixed with the ordinary food pellets; PB, curcumin was mixed in peanut butter and administered orally. Minus sign (-) indicates weight loss after treatment. *, $p < 0.05$; **, $p < 0.01$.

3.1.2 Mortality upon curcumin treatment

Distributions of mice of different strains and genders at the beginning of treatment are listed in **Table 3.1.2.1**. Statistical analysis by Chi-square and Fisher's exact tests of the distribution of mice of different strains was performed in male and female groups separately. There were no significant differences in the distributions of mice of different strains in either males or females at the beginning of the treatment.

After 10 weeks, 5 months or 6 months of curcumin treatment in vehicle of either peanut butter or chow, the numbers of live and dead mice of different strains were recorded. The mortality rates for mice with or without treatment in different combinations of groups or genders were analysed by Fisher's exact test. Gender-independent analysis of the mortality rate of mice amongst different strains and administration vehicles is listed in **Table 3.1.2.2**. The death rate of all curcumin-fed mice was marginally significantly lower than for mice not fed curcumin (**Figure 3.1.2.1**). Breaking down the mice into different strains, each individual strain had a mortality rate that tended to be reduced by treating with curcumin. Amongst strains, only JNPL3xTg2576 showed significant mortality reduction by curcumin treatment (**Figure 3.1.2.4**).

In order to determine the gender effect of curcumin on mortality, analyses were performed on male and female groups separately (**Table 3.1.2.3**). In either males or females, there were no significant differences in the mortality rates of mice with or without curcumin treatment in any strain. But when all male mice were analyzed together (without regard to strain), the effect of curcumin on the mortality rate was very significant (**Figure 3.1.2.2**). When the groups using peanut-butter as vehicle were removed from analysis, the mortality rate of the male mice fed with curcumin in

chow was also significantly different from mice without curcumin (**Figure 3.1.2.3**). Individual strain analysis showed that curcumin tended to reduce mortality of all strains, but only the mortality of JNPL3xTg2576 was significantly reduced (**Figure 3.1.2.5**). **Table 3.1.2.4** illustrates the male specific mortality rate of mice with or without treatment.

Table 3.1.2.1 Distribution of mice strains in treatment and control groups at the beginning of the treatment regime.

	Tg2576	JNPL3 x Tg2576	JNPL3	JNPL3 (PB)	Chi-square test (strains), p value
Male					0.845
Curcumin	15	10	14	8	
Control	12	13	13	9	
Female					0.950
Curcumin	14	11	10		
Control	13	9	10		
Fisher's exact test (sex), p value	1	0.547	1		

Table 3.1.2.2 Gender-independent mortality analysis of mice after curcumin treatment.

Strain	Treatment	Vehicle	Start	Alive	Dead	Death rate (%)	Fisher's exact test
All	Curcumin	Chow+PB	82	59	23	28.0	0.050
	Control	Chow+PB	79	45	34	43.0	
All	Curcumin	Chow	74	51	23	31.1	0.087
	Control	Chow	70	38	32	45.7	
Tg2576	Curcumin	Chow	29	20	9	31.0	0.777
	Control	Chow	25	16	9	36.0	
JNPL3x Tg2576	Curcumin	Chow	21	13	8	38.1	0.033
	Control	Chow	22	6	16	72.7	
JNPL3	Curcumin	Chow+PB	32	26	6	18.8	0.556
	Control	Chow+PB	32	23	9	28.1	
JNPL3	Curcumin	Chow	24	18	6	25.0	0.751
	Control	Chow	23	16	7	30.4	

Group with significant difference of mortality between curcumin and control treatment is shown in **bold**. PB, curcumin was mixed in peanut butter and administered orally; Chow, curcumin was pre-mixed with the ordinary food pellets; Chow+PB, group includes mice treated with curcumin or control in either chow or peanut butter.

Table 3.1.2.3 Mortality analysis of female mice after curcumin treatment.

Strain	Treatment	Vehicle	Start	Alive	Dead	Death rate (%)	Fisher's exact test
All	Curcumin	Chow+PB	35	22	13	37.1	1
	Control	Chow+PB	32	21	11	34.4	
All	Curcumin	Chow	35	22	13	37.1	1
	Control	Chow	32	21	11	34.4	
Tg2576	Curcumin	Chow	14	11	3	21.4	0.596
	Control	Chow	13	12	1	7.7	
JNPL3x Tg2576	Curcumin	Chow	11	5	6	54.5	0.670
	Control	Chow	9	3	6	66.7	
JNPL3	Curcumin	Chow	10	6	4	40.0	1
	Control	Chow	10	6	4	40.0	

Table 3.1.2.4 Mortality analysis of male mice after curcumin treatment.

Strain	Treatment	Vehicle	Start	Alive	Dead	Death rate (%)	Fisher's exact test
All	Curcumin	Chow+PB	47	37	10	21.3	0.009
	Control	Chow+PB	47	24	23	48.9	
All	Curcumin	Chow	39	29	10	25.6	0.011
	Control	Chow	38	17	21	55.3	
Tg2576	Curcumin	Chow	15	9	6	40.0	0.252
	Control	Chow	12	4	8	66.7	
JNPL3x Tg2576	Curcumin	Chow	10	8	2	20.0	0.012
	Control	Chow	13	3	10	76.9	
JNPL3	Curcumin	Chow+PB	22	20	2	9.1	0.412
	Control	Chow+PB	22	17	5	22.7	
JNPL3	Curcumin	Chow	14	12	2	14.3	0.648
	Control	Chow	13	10	3	23.1	
JNPL3	Curcumin	PB	8	8	0	0.0	0.471
	Control	PB	9	7	2	22.2	

Groups with significant difference of mortality between treatment and control are bolded.

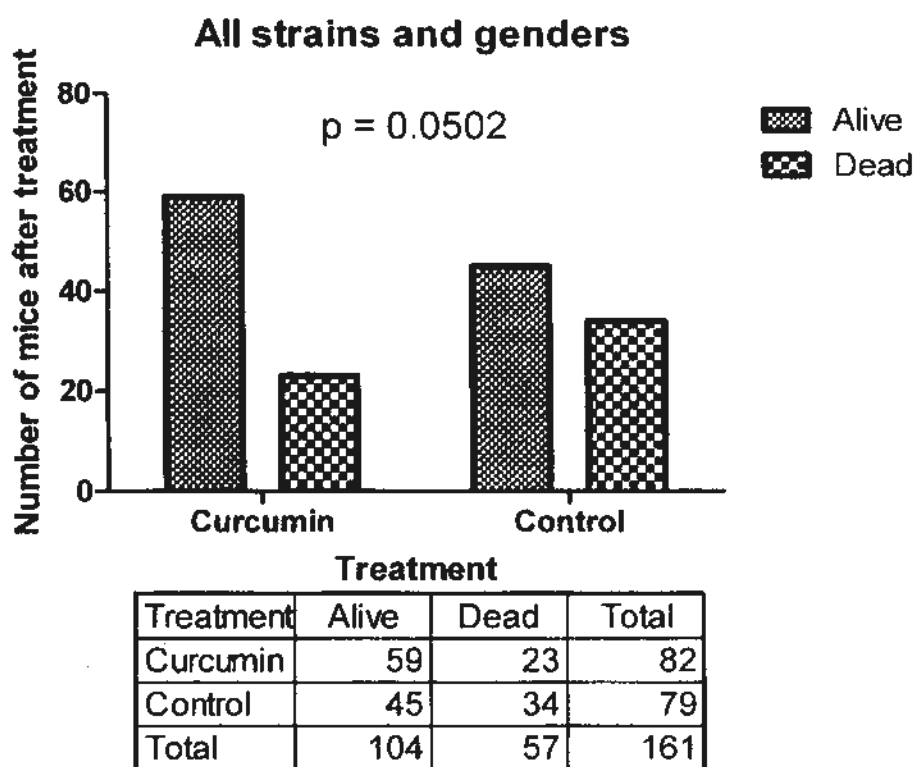


Figure 3.1.2.1 Gender-independent mortality analysis of mice with or without curcumin treatment.

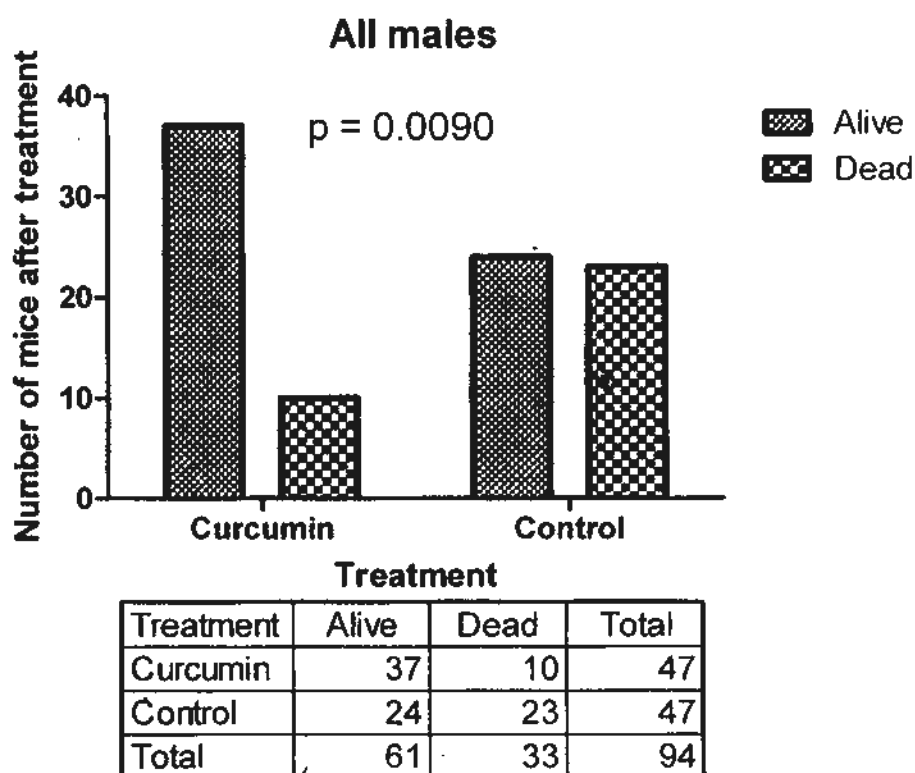


Figure 3.1.2.2 Male specific mortality analysis of mice with or without curcumin treatment.

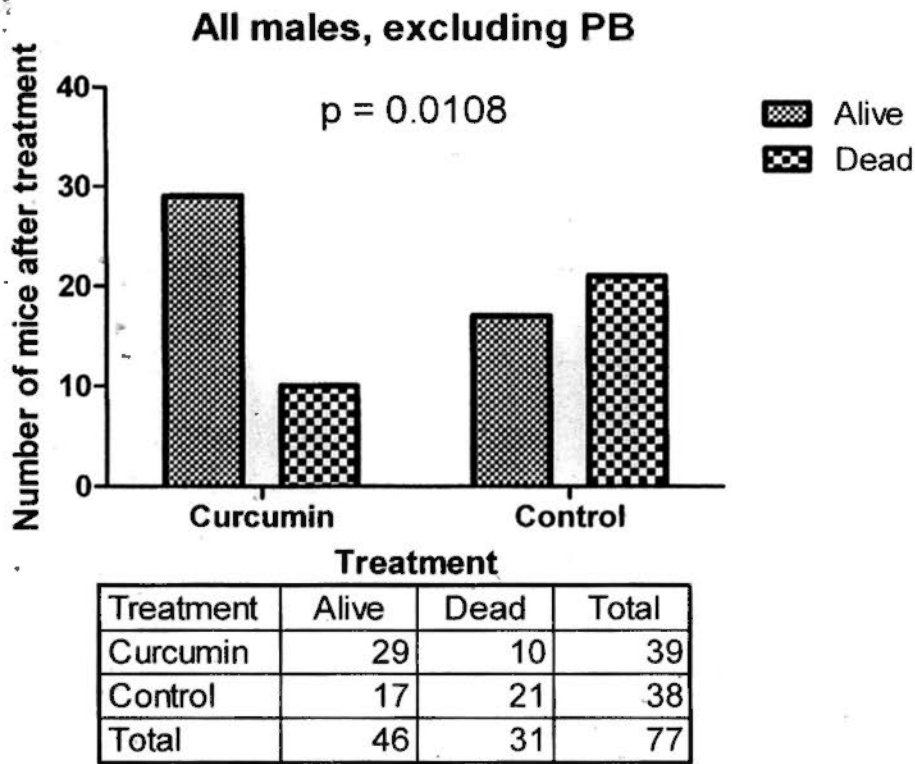


Figure 3.1.2.3 Male specific mortality analysis of mice (except the group using peanut butter as vehicle) with or without curcumin treatment.

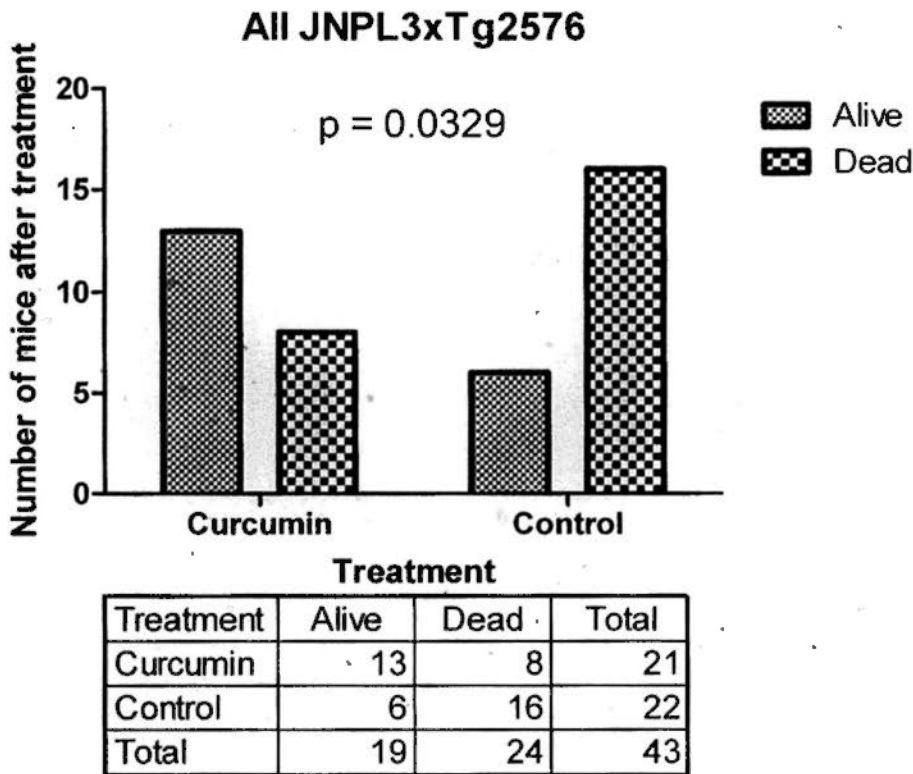
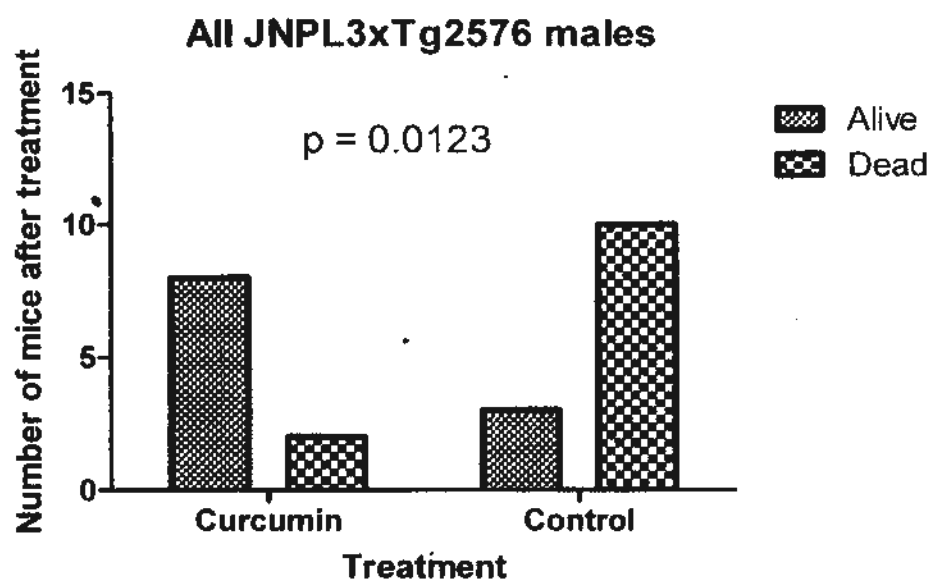


Figure 3.1.2.4 Gender-independent mortality analysis of JNPL3xTg2576 mice with or without curcumin treatment.



Treatment	Alive	Dead	Total
Curcumin	8	2	10
Control	3	10	13
Total	11	12	23

Figure 3.1.2.5 Male specific mortality analysis of JNPL3xTg2576 mice with or without curcumin treatment.

3.1.3 Rotarod performance upon curcumin treatment

The rotarod test was employed to test the motor function of JNPL3 mice, which carry a mutant human *Mapt* transgene, treated with or without curcumin. The mice fed with curcumin (or not curcumin) in chow were excluded from this test due to the observation that their motor impairment was undetectable. Other strains were not tested due to insufficient sample number and lack of information of the loss of motor function. Therefore, only the older JNPL3 mice fed with curcumin in peanut butter were used.

The number of JNPL3 mice capable of performing the rotarod test was recorded before, at the middle and at the end of the treatment period. The data are listed in **Table 3.1.3.1**. The number of mice capable of remaining on the rotarod tended to decrease slower with curcumin treatment.

The performance of JNPL3 mice on the rotarod was quantified by comparing the length of time that each mouse stayed on the rotating rod (**Figure 3.1.3.1**). A time of zero was used for mice that had died or were unable to perform the test. Mice treated with curcumin tended to remain longer on the rotarod than did control mice, though the difference was not significant: $p=0.67$ for interaction of time and treatment on two-way ANOVA.

Table 3.1.3.1 Number of JNPL3 mice capable of performing rotarod test in curcumin and control groups using peanut butter as vehicle.

Treatment Period (weeks)	Before (0 weeks)	Middle (5 weeks)	End (10 weeks)
Curcumin	7	6	5
Control	8	5	3

Performance of JNPL3 mice on rotarod with or without curcumin

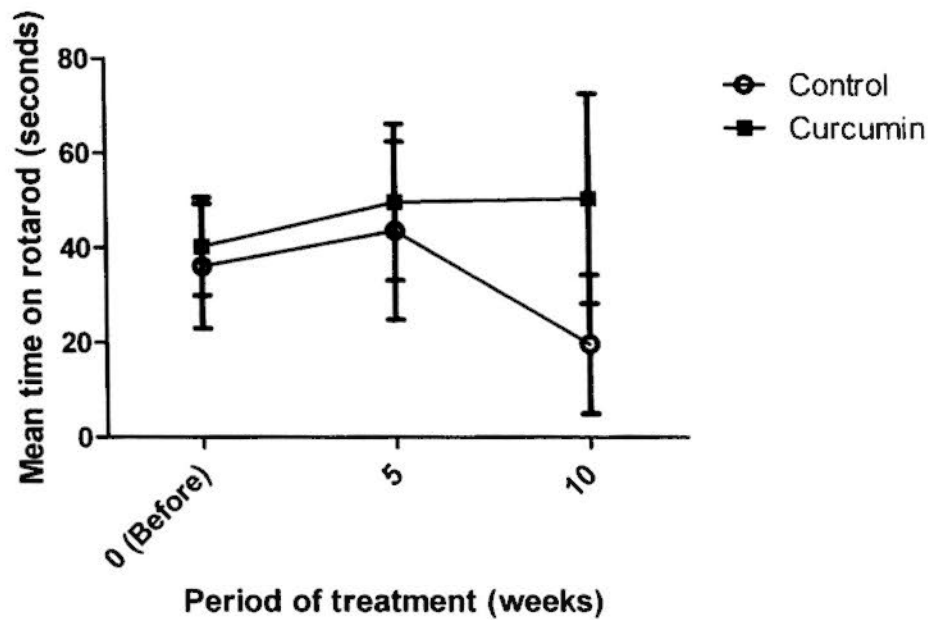


Figure 3.1.3.1 Rotarod performance of JNPL3 mice treated with or without curcumin using peanut butter as vehicle.

3.2 Effects of curcumin on A β generation

3.2.1 Microarray of APP cleavage enzyme and competitive substrate genes

To determine whether curcumin has an effect on A β generation in vivo, we first studied the effect of the change of expression levels of related genes. To limit the cost of doing microarray experiments, all female strains were excluded due to their larger physiological variation. RNA samples were isolated from hippocampus only. The quality of RNA sample from each mouse was checked by Bioanalyser. Samples with RIN over 5.5 and rRNA 22S/18S over 0.8 were pooled into one group for each strain, administration vehicle, and treatment. For each strain and administration vehicle, the group with curcumin was compared with the group without curcumin. Therefore, there were only 4 pairs of results: Tg2576, JNPL3xTg2576, JNPL3 with chow as vehicle and JNPL3 with peanut butter as vehicle. For each gene, the ratio of expression with curcumin to expression without curcumin was calculated.

When the cutoff of fold change was set at 2.0 (or 0.5), there were not any α -, β - or γ -secretase candidate genes with gene expression levels beyond this threshold in any pair of groups of male mice. Data are shown in **Table 3.2.1.1**.

To extend our focus further on genes which may affect the activities of the secretases, we focused on genes encoding proteins which are known to be the substrates of the secretases. Amongst them, Btc, Ereg, Fcer2a, Hs6st3, Muc1 and Sell were found in the microarray to have over 2-fold reduction in JNPL3 (peanut butter) with curcumin treatment compared to the control group. Cd46 was shown to be reduced by over 2-fold in Tg2576 with curcumin treatment. Kl was consistently

upregulated over 2 fold amongst JNPL3 (chow and peanut butter) and JNPL3xTg2576 strains. Details of the fold changes of the selected substrates of secretases are illustrated in **Table 3.2.1.2**.

Table 3.2.1.1 Fold change of RNA levels of genes regulating A β peptide generation in the hippocampus region of selected mice in pooled RNA samples.

Genes	JNPL3 (Chow)	JNPL3 (PB)	Tg2576	JNPL3 x Tg2576
<u>α-secretases</u>				
Adam10	-1.06	1.01	-1.31	-1.57
Adam17	1.13	1.18	1.16	1.11
Adam9	-1.01	-1.09	1.04	-1.02
<u>β-secretase</u>				
Bace1	1.02	-1.11	1.02	-1.05
<u>γ-secretase subunits</u>				
Aph1a	1.38	-1.33	1.06	-1.30
Aph1b	-1.01	1.12	1.03	1.15
GSAP	1.22	1.26	-1.50	-1.20
Nicastrin	1.57	1.66	-1.93	1.52
PEN-2	1.21	-1.08	1.10	-1.10
Psen1	1.16	1.04	-1.06	-1.02
Psen2	-1.07	1.09	1.07	1.02

Table 3.2.1.2 Fold change of RNA levels of genes acting as substrates of secretases in the hippocampus region of selected mice in pooled RNA samples.

Genes	Cleaved by	JNPL3 (Chow)	JNPL3 (PB)	Tg2576	JNPL3 x Tg2576
APP	$\alpha/\beta/\gamma$ -secretases	-1.06	-1.02	-1.04	-1.00
Areg	α -secretase	1.12	-1.55	1.69	-1.40
Btc	α -secretase	-1.07	<u>-2.06</u>	-1.48	1.04
Cd46	α/γ -secretases	-1.38	1.65	<u>-2.10</u>	1.04
Ereg	α -secretase	-1.06	<u>-2.15</u>	1.90	1.01
Fcer2a	α -secretase	1.75	<u>-2.15</u>	-1.97	1.10
Hbegf	α -secretase	1.17	1.05	1.21	1.10
Hs6st3	β -secretase	1.12	<u>2.42</u>	1.10	1.16
Il1r2	α -secretase	-1.03	-1.26	-1.42	1.05
Kl	$\alpha/\beta/\gamma$ -secretases	<u>2.20</u>	<u>7.56</u>	-1.11	<u>2.06</u>
Muc1	α/γ -secretases	1.41	<u>-2.05</u>	-1.60	-1.01
Notch1	α/γ -secretases	-1.13	-1.07	1.01	-1.15
Sell	α -secretase	1.06	<u>-2.21</u>	1.64	1.09

Samples with fold change over two are underlined for easy reference.

3.2.2 Real-time PCR of APP cleavage enzyme and competitive substrate genes

To confirm the findings in the microarray experiment, the candidate genes for α -secretase—Adam9, Adam10 and Adam17—and β -secretase—Bace1—were selected to be examined by real-time PCR. Since γ -secretase is composed of at least four subunits, change in γ -secretase function is not simply explained by change in expression of any one of the subunits. Therefore, candidate genes for γ -secretase were excluded in real-time PCR confirmation. Consistent with the microarray results, none of the candidate genes of α - and β -secretases were shown to have significant differences in expression levels between curcumin and control treatments of any pairs of groups. Data comparing gene expression levels are illustrated in **Figure 3.2.2.1.1**.

For confirmation of microarray results of the differential gene expression of the substrates of secretases, Btc, Ereg, Fcer2a, Kl, Muc1, Sell and APP were selected. Differential gene expression data are shown in **Figure 3.2.2.1 (a-g)**. Amongst them, APP, Ereg, Fcer2a and Muc1 were shown to have no significant differences between curcumin and control treatments for any pairs of groups.

Gene expression of Btc was significantly increased in all mice treated with curcumin. Mean expression was upregulated by around 13 percent. Amongst the groups, gene expression was found to be very significantly different in JNPL3 (chow) mice, with an increase of over 26 percent compared to the control group.

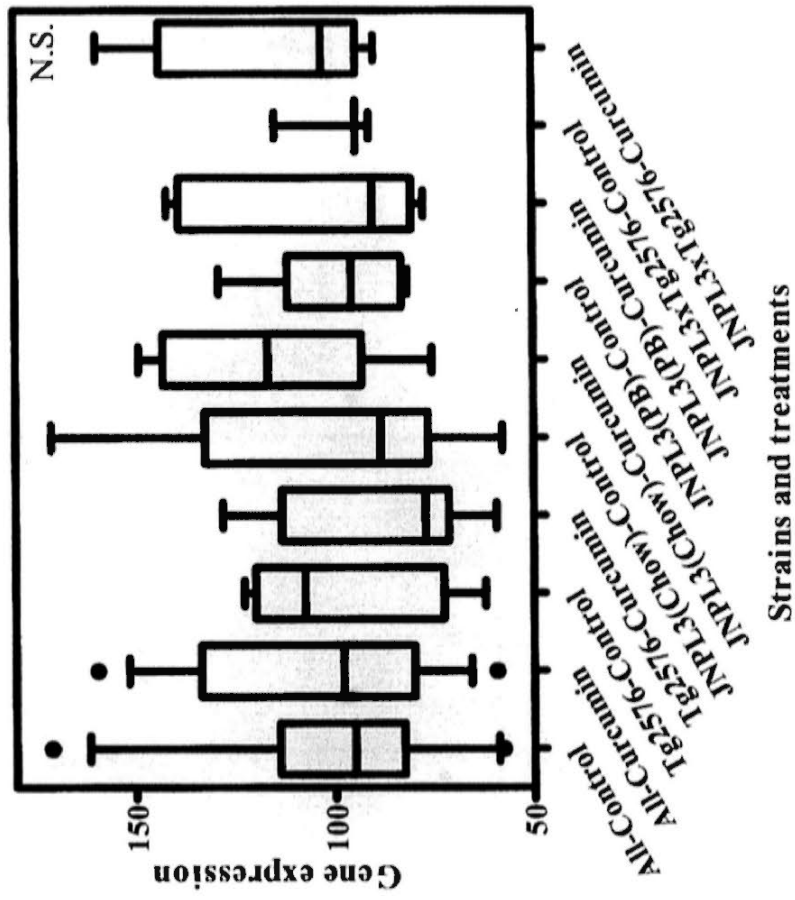
Differential gene expression of Kl was also significant, with mean expression increased by over 47 percent. In JNPL3 (chow) and JNPL3xTg2576, mean

expression of the K1 gene was significantly increased by around 96 and 82 percent, respectively.

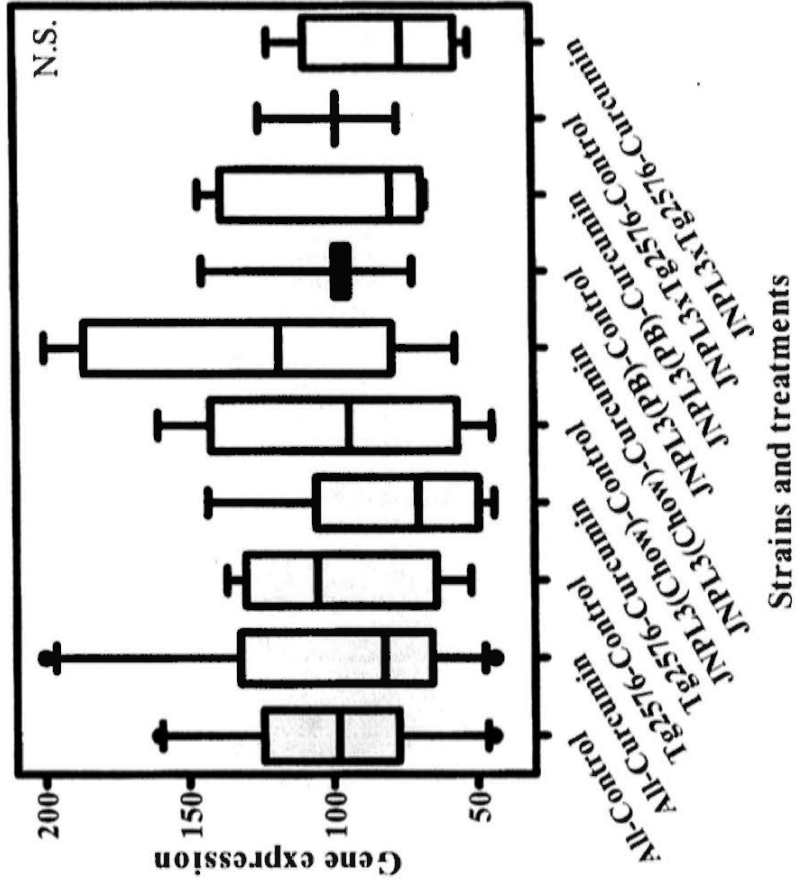
Expression of Sell was significantly increased in the JNPL3xTg2576 strain by curcumin treatment. The increase was 63 percent.

3.2.2.1 Gene expression of secretases

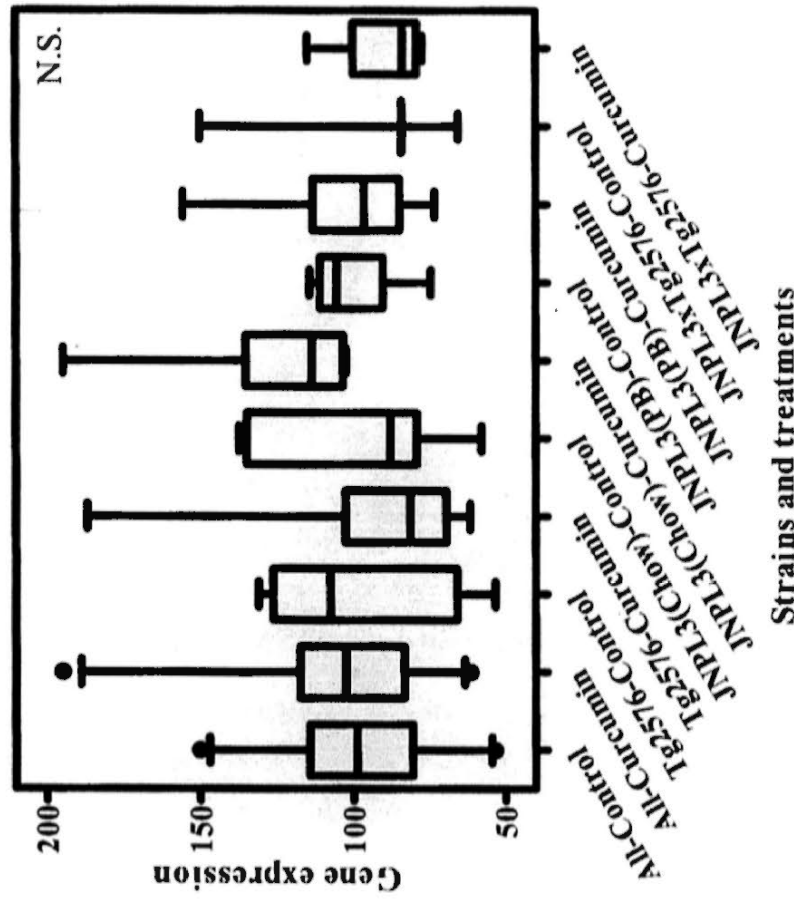
(a) Adam9



(b) Adam10



(c) Adam17



(d) Bace1

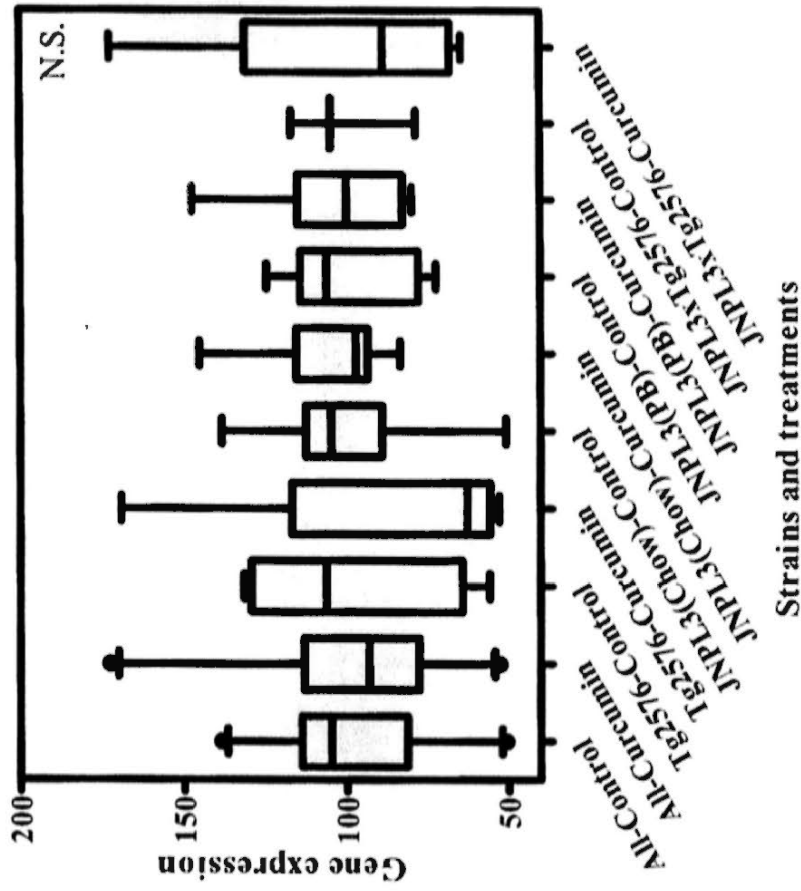
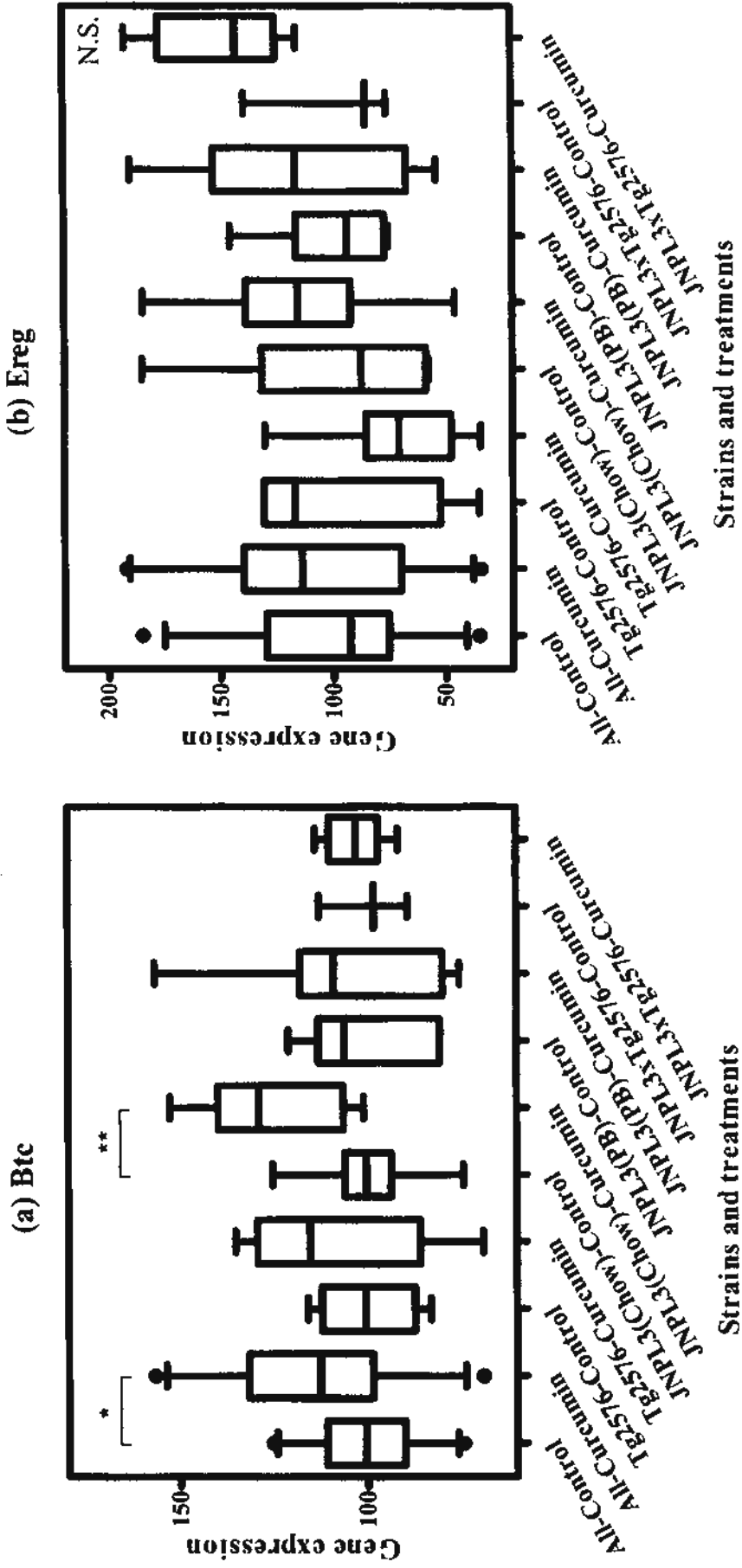
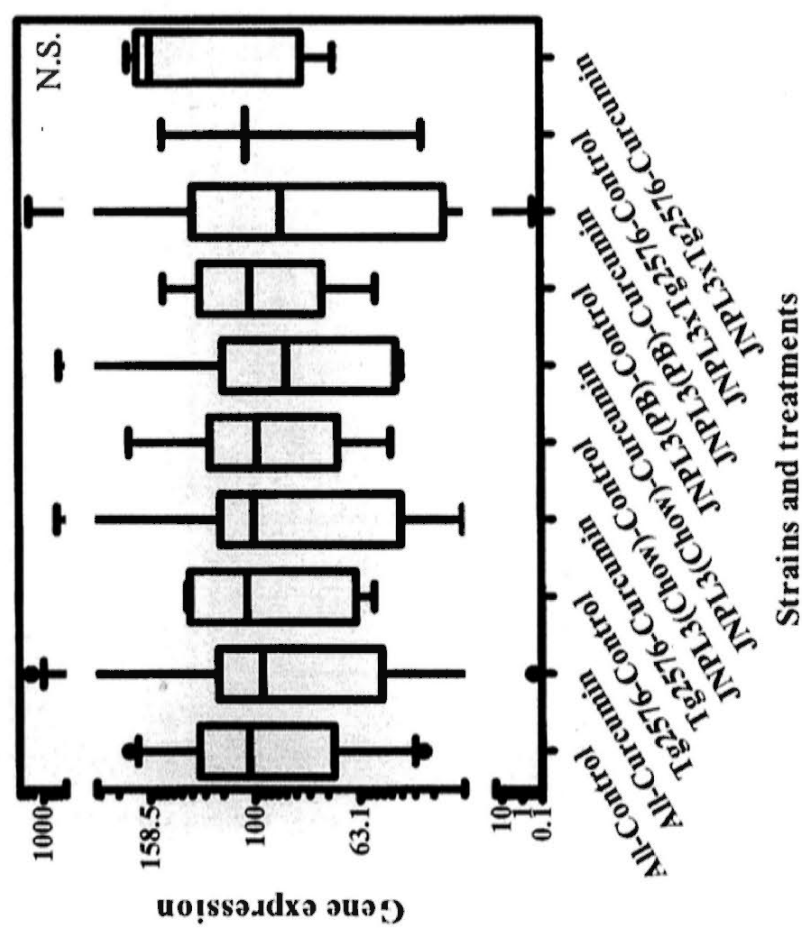


Figure 3.2.2.1.1 Comparison of mRNA expressions of (a) Adam9, (b) Adam17 and (d) Bace1 in hippocampus of different mice strains between curcumin treatment and control groups. The boxes indicate median, 25 and 75 percentile; whisker caps indicate 5 and 95 percentile; filled circles indicate outliers. Data were analyzed by Mann-Whitney U test using SPSS, and were plotted using GraphPad Prism. N.S., no significant difference.

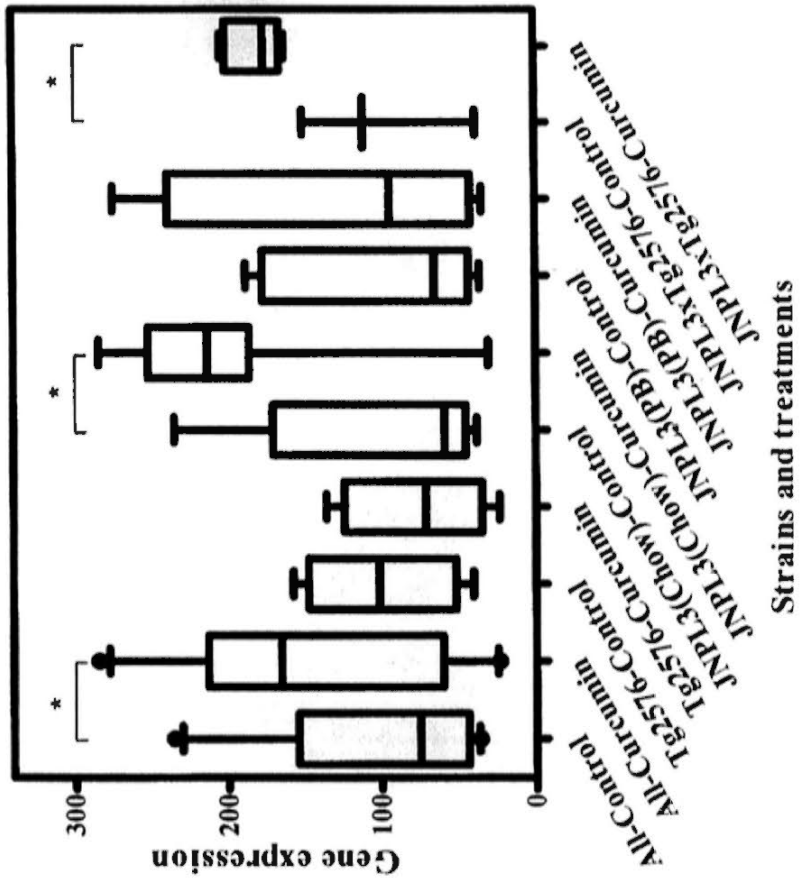
3.2.2.2 Gene expression of competitive substrates



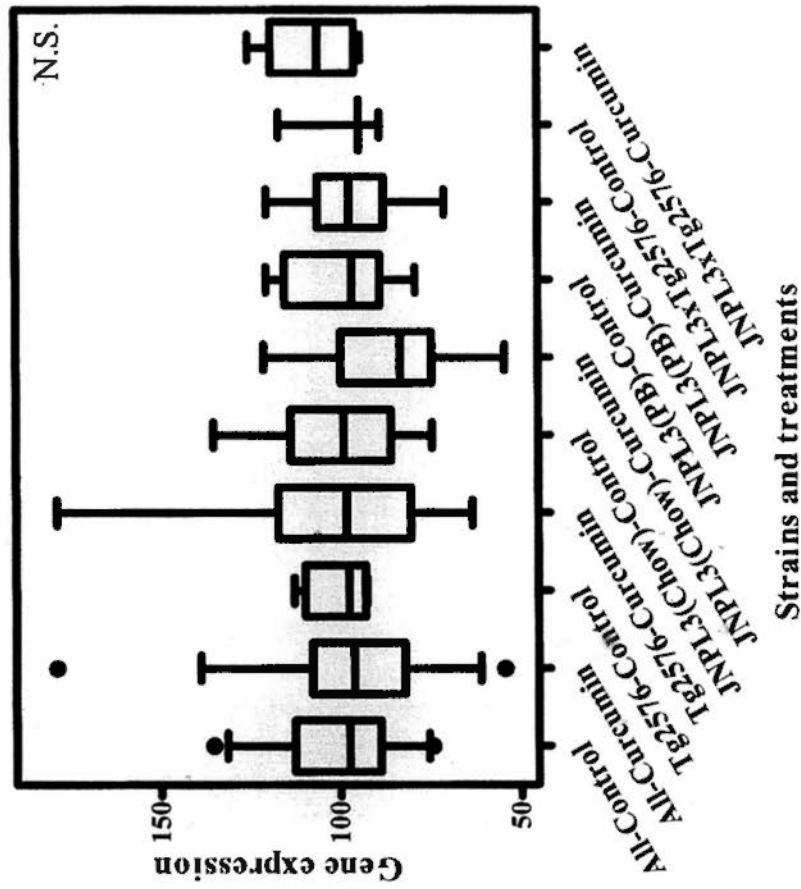
(c) Fcεr2a



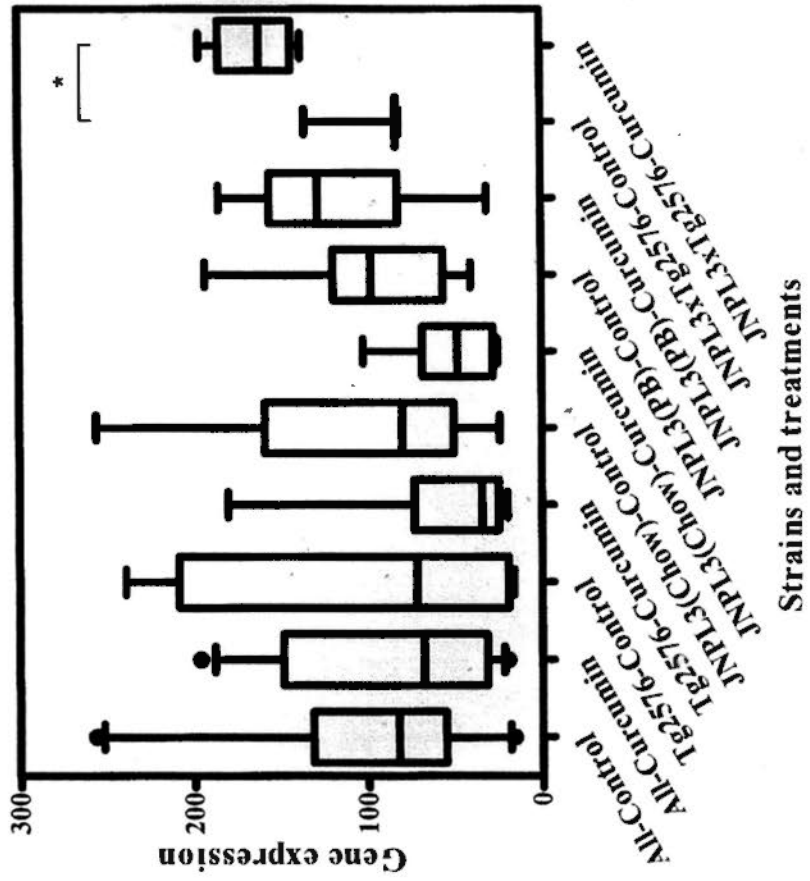
(d) KI



(e) Muc1



(f) Sell



(g) APP

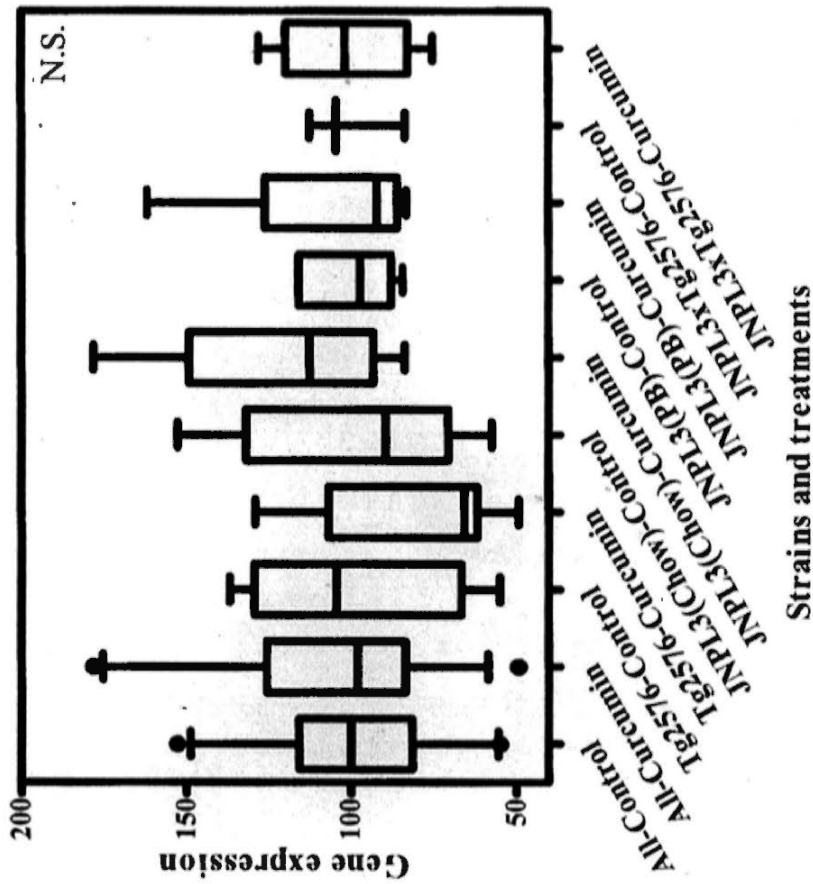
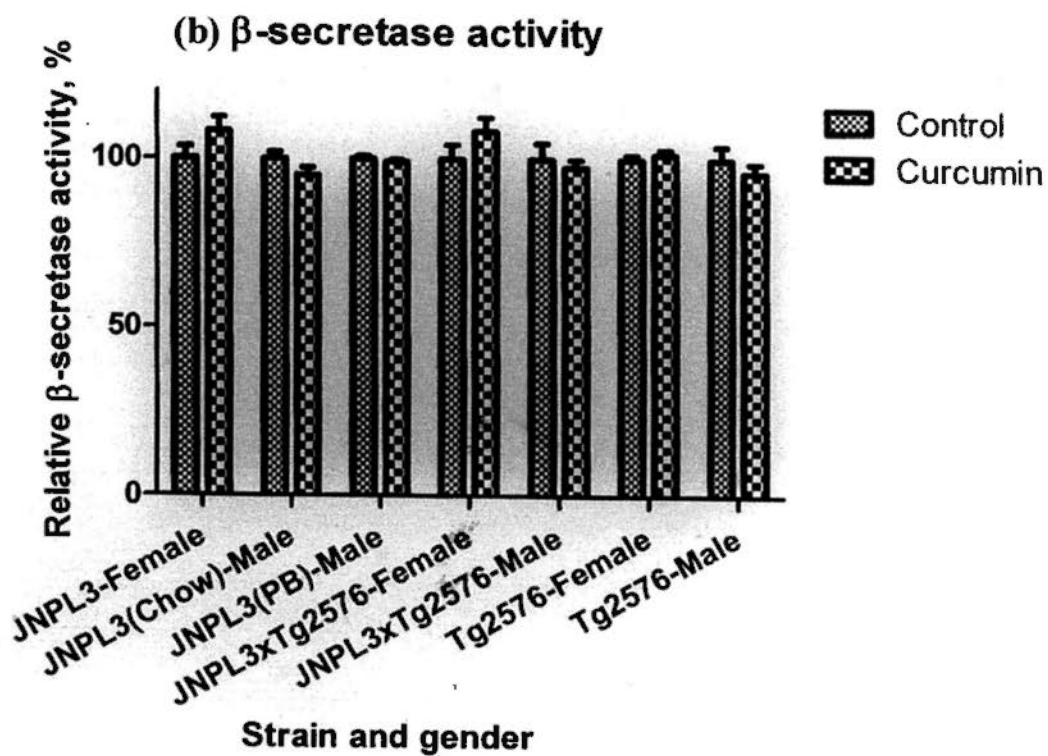
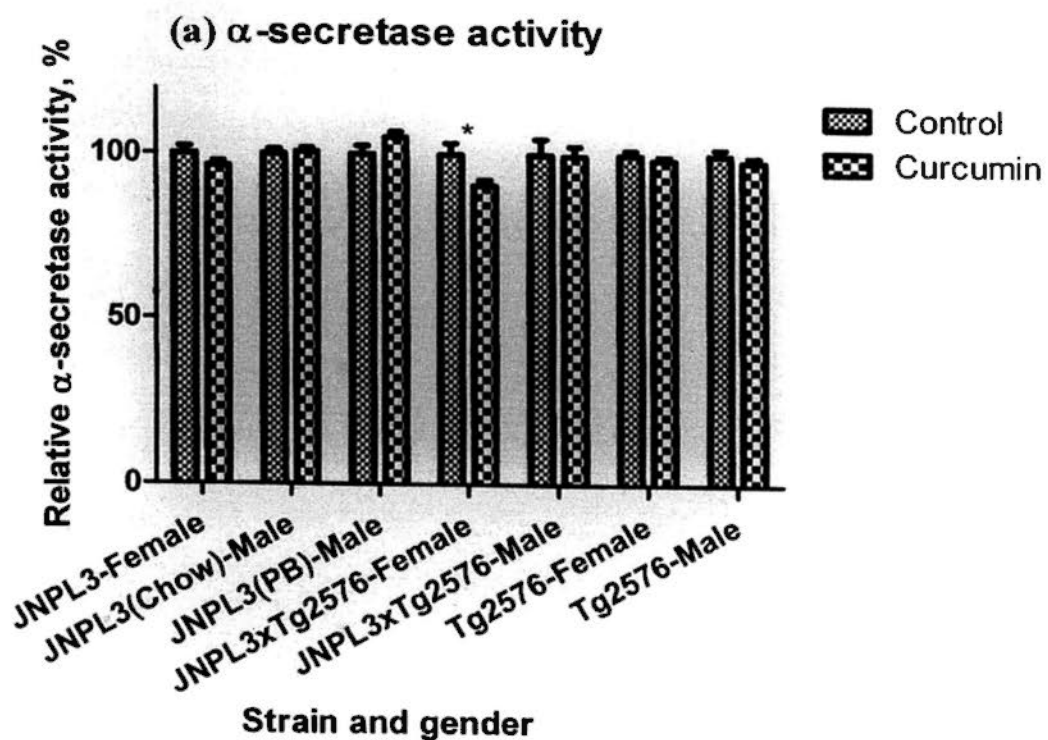


Figure 3.2.2.2.1 Comparison of mRNA expressions of (a) Btc, (b) Ereg, (c) Fcer2a, (d) Kl, (e) Muc1, (f) Sell and (g) App in hippocampus of different mice strains between curcumin treatment and control groups. The boxes indicate median, 25 and 75 percentile; whisker caps indicate 5 and 95 percentile; filled circles indicate outliers. Significant differences between treatment groups of different strains were determined by Mann-Whitney U test using SPSS, and data were plotted using GraphPad Prism. *, $p < 0.05$; **, $p < 0.005$; N.S., no significant difference between treatment and control groups amongst all and individual strains.

3.2.3 Secretase functional assays

To detect differences in functional activity of the secretases of different mouse strains between curcumin and control groups, activity assays using the membrane fraction of cortical regions were performed for α -, β - and γ -secretase separately. α -secretase activity was reduced significantly, by 9.5 percent, in JNPL3xTg2576 female mice with curcumin treatment. Curcumin did not show any significant effect on the function of α -secretase in other strains and sexes. Data are illustrated in **Figure 3.2.3.1(a)**. **Figure 3.2.3.1(b and c)** showed that the activity assays of β - and γ -secretase had no significant differences in any strains between curcumin and control groups.



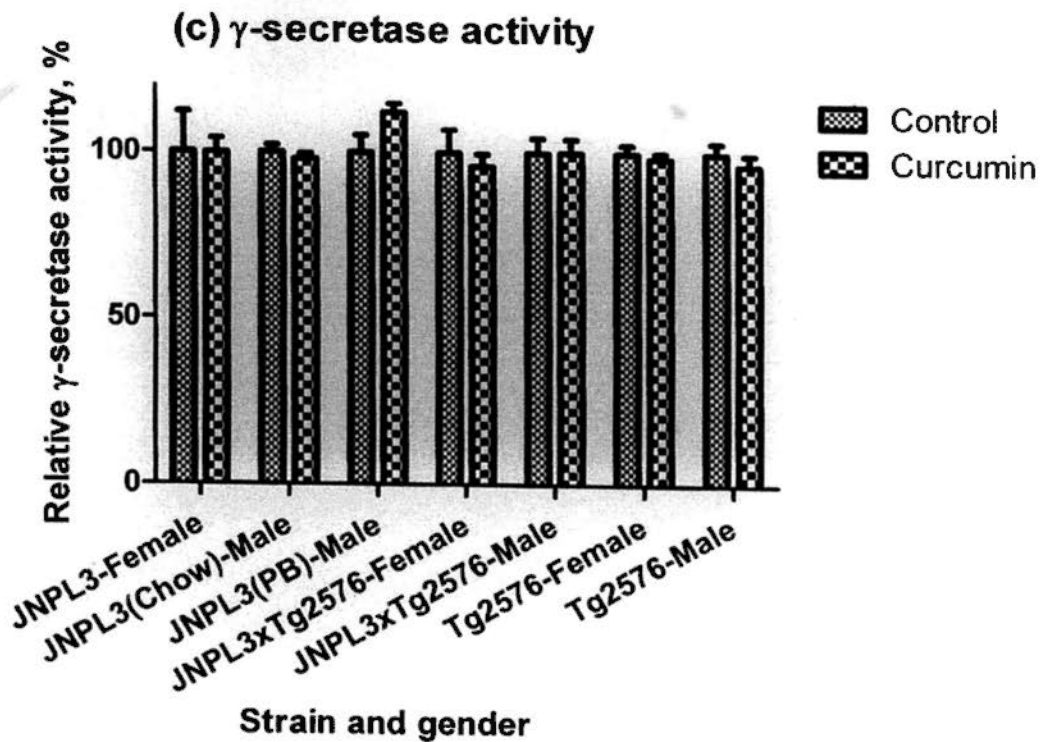


Figure 3.2.3.1 Comparison of activities of (a) α -secretase, (b) β -secretase and (c) γ -secretase of membrane fraction of cortex of different mice strains between curcumin treatment and control groups. Results are expressed as mean \pm SD. Significant difference between treatment groups of different strains was compared by Student's t-test using SPSS; data were plotted using GraphPad Prism. *, $p < 0.05$.

3.3 Effects of curcumin on A β aggregate formation

3.3.1 Anti-A β -metal aggregation-Thioflavin-T assay

Thioflavin-T binds specifically to the β -sheet structure which is adopted by the A β aggregates induced by metal ions. To examine whether curcumin can reduce A β aggregation by disrupting the β -sheet structure of A β , a well-developed disaggregation assay was performed using A β :metal aggregates formed by incubating A β 1-40 or A β 1-42 with either Cu(II) or Zn(II) ions. The amount of β -sheet structure formed by the aggregates was detected by the addition of the fluorescent compound, thioflavin-T. Upon binding to the β -sheet structure, it does not affect the structure of the aggregates, but changes the fluorescent wavelength of excitation and emission of 350 nm and 438 nm to 450 nm and 482 nm, respectively.

The A β -metal disaggregation assay showed that curcumin can reverse aggregate formation by reducing the amount of β -sheet structure with IC₅₀ at sub-micromolar concentrations. The IC₅₀s were calculated by fitting the data using nonlinear regression (**Figure 3.3.1.1**), the dose vs. response curves were obtained for A β 40:Cu, A β 40:Zn, A β 42:Cu and A β 42:Zn aggregates and various concentrations of curcumin. Data of the IC₅₀s with 99% confidence interval are illustrated in **Table 3.3.1.1**. The R² of the goodness of fit of these four curves are in the range between 0.96 and 1.00.

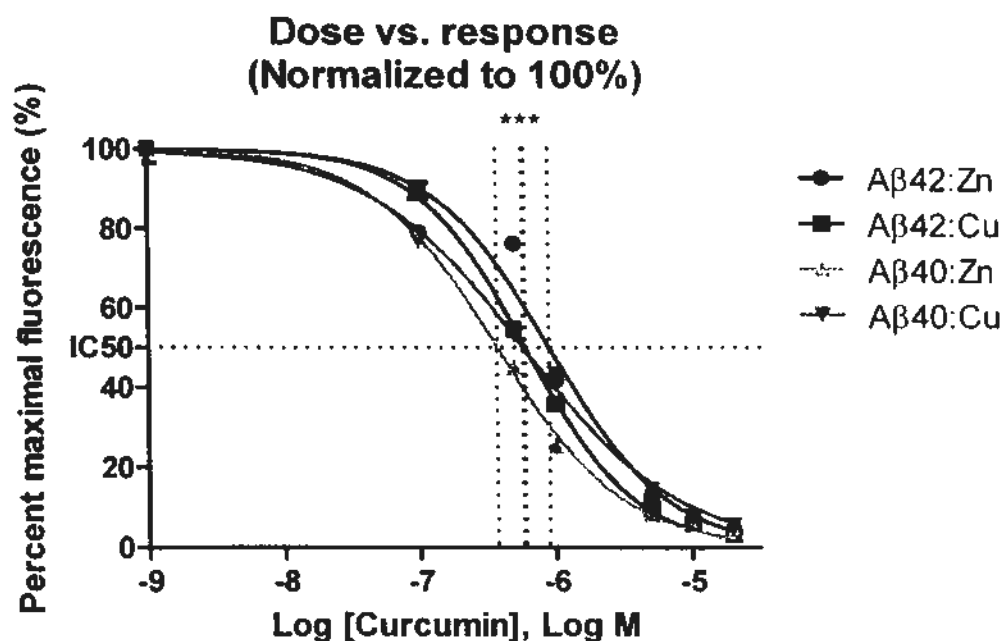


Figure 3.3.1.1 Comparison of dose-response curves of curcumin disaggregation of Zn- or Cu-induced Aβ1-40 or Aβ1-42 peptide aggregates. Normalized data were fitted, relative IC50s were determined and the significance of differences was calculated by nonlinear regression using GraphPad Prism. *, $p < 0.0001$.**

Table 3.3.1.1 Relative IC50 of curcumin disaggregation of Zn- or Cu-induced Aβ1-40 or Aβ1-42 peptide aggregates.

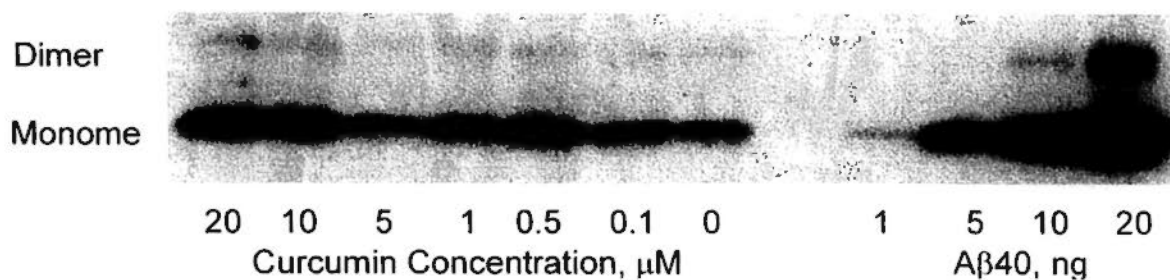
Relative IC50		99% confidence interval		
	Log [Curcumin], M	μM	Upper Limit	Lower Limit
Aβ42:Zn	-6.04	0.90	1.22	0.67
Aβ42:Cu	-6.22	0.61	0.66	0.56
Aβ40:Zn	-6.43	0.38	0.43	0.31
Aβ40:Cu	-6.23	0.59	0.68	0.50

Concentrations of curcumin at IC50 and at upper and lower limits of 99% confidence interval are presented in μM.

3.3.2 Western blotting of monomeric A β from anti-A β aggregation assay

To determine that curcumin not only disaggregates the A β :metal aggregates and reduces the β -sheet structure, but also increases the amount of monomeric A β , western blotting analysis was used. Tricine-SDS PAGE gels were used due to the small molecular weight of A β peptide (4 kDa), which precludes it from being resolved by ordinary Glycine-SDS PAGE gels. The result is shown in **Figure 3.3.2.1(A)**. In order to simplify the figure, the protein size marker is not shown. Aggregates were prepared by incubating A β 40 with Cu(II). After the assay, the supernatant following 14k rpm centrifugation was loaded onto the gel. A β 40 peptide prepared in monomeric form was also run on the gel for quantification and size-checking of the A β aggregates. Quantification of monomeric A β in **Figure 3.3.2.1(B)** shows that the amount of monomeric A β was significantly increased with increasing concentration of curcumin.

A.



B.

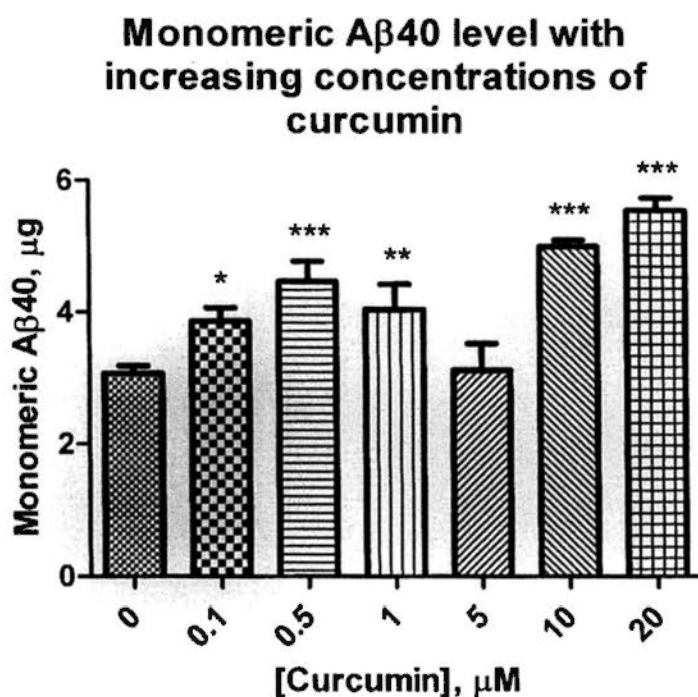


Figure 3.3.2.1 (A) Western blotting analysis of the monomeric A β 1-40 level from the samples after Thioflavin-T disaggregation assay of Cu-induced A β 1-40 aggregates. Known amounts of monomeric A β peptide were loaded in the first four lanes, counting from the left side. Concentrations of curcumin used in the assay are shown on the right side. Image on the film was quantified by ImageJ. Quantification by comparing to the standard curve of known amount of A β 1-40 peptide is illustrated in (B). Results are expressed as mean \pm SD from triplicate measurements. Statistical difference between control and various concentrations of curcumin was determined by one-way ANOVA for multiple comparisons and Tukey HSD as a *post hoc* test. *, $p < 0.05$; **, $p < 0.01$; ***, $p < 0.001$.

3.3.3 Immunohistochemical staining of 4G8-immunopositive plaques

To reproduce the previous findings from other groups that curcumin can reduce the amyloid plaque burden in vivo, immunohistochemical staining using anti-A β antibody 4G8 was performed to detect the presence of amyloid plaques. Selected photomicrographs of 4G8 immunopositive staining are shown in **Figure 3.3.3.1**.

Quantification of the 4G8 positive signal is shown in **Figure 3.3.3.2**. Female groups were excluded due to larger physiological variations. There was no significant difference in male Tg2576 between the groups treated with curcumin (9 mice) and without curcumin (4 mice) in the percentage area occupied by plaques in the brain sections. For each mouse, one view from the hippocampus, entorhinal cortex, auditory cortex, and hypothalamus was quantified and combined since the 4G8-positive area was too little per each view.

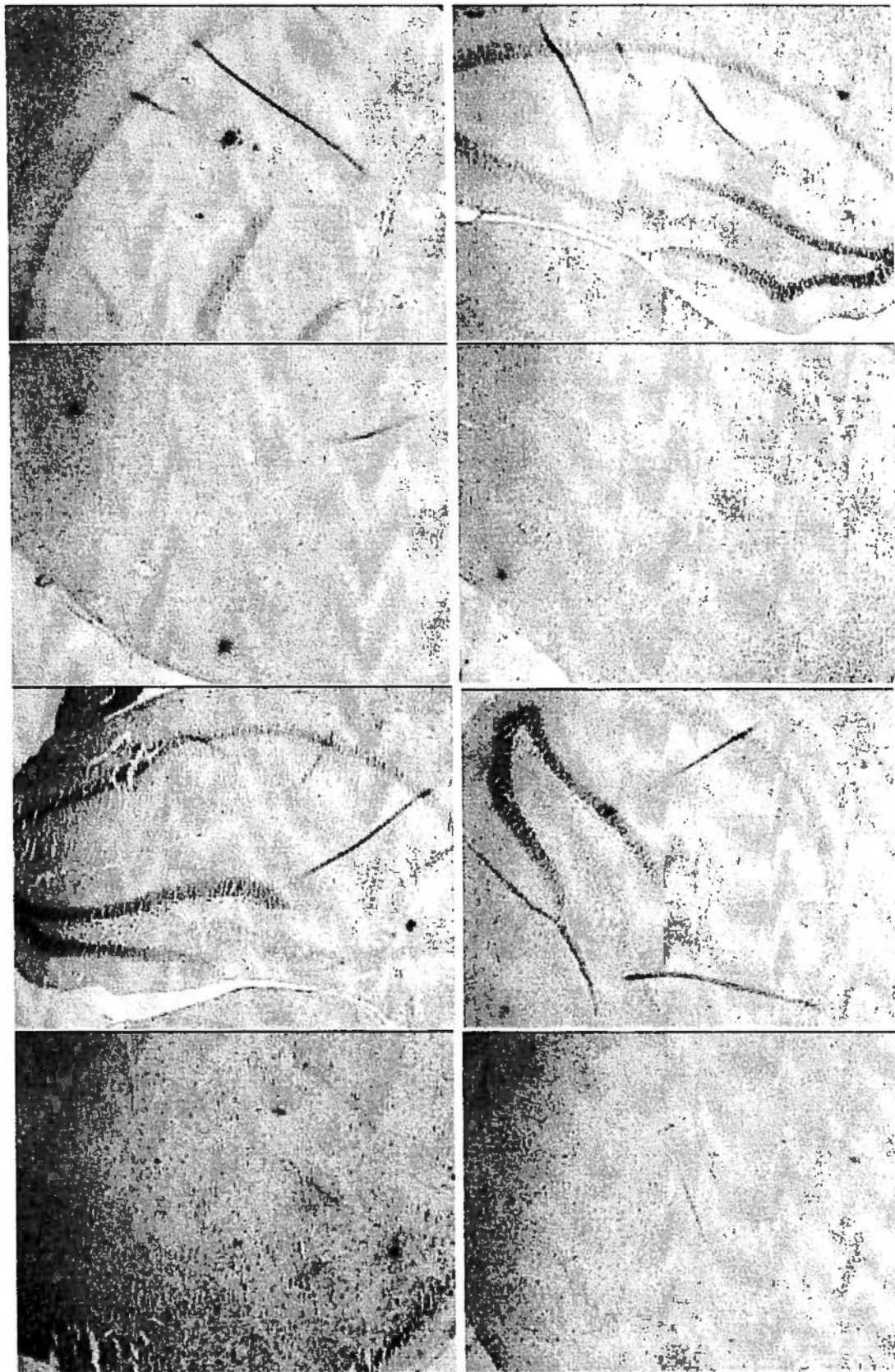


Figure 3.3.3.1 Immunohistochemical staining of amyloid plaques of the brain sections of Tg2576 male mice treated with (right) or without (left) curcumin. Antibody 4G8, which is specific for human A β peptide, was used. Images were captured at 5X magnification.

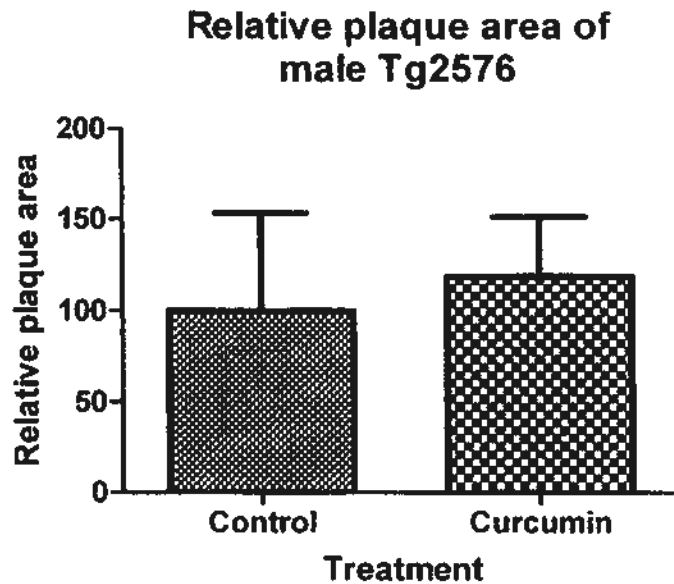


Figure 3.3.3.2 Quantification of percentage plaque (4G8 immunopositive) area of brain regions of hippocampus, entorhinal cortex, auditory cortex and hypothalamus of male Tg2576 mice with or with curcumin treatment. Data are normalized by percentage change of curcumin group compared to control group. Results are expressed as mean \pm SEM. Statistical difference between control and curcumin groups was determined by Student's t-test using SPSS: $p=0.754$. Graph was plotted using GraphPad Prism.

3.4 Effects of curcumin on A β degradation

3.4.1 Microarray of A β degrading enzyme genes

There are many proteins which have been shown to be able to degrade A β peptides in vitro or in vivo. Using microarrays to measure expression of all genes narrows the list of candidate genes which are both responsible for A β degradation and are upregulated by curcumin treatment. (see **Table 3.4.1.1**). Acc was increased by curcumin by over 2 fold in JNPL3 (chow and peanut butter) mice. Bsg and Mmp2 were shown to be increased by curcumin beyond the 2-fold threshold exclusively in JNPL3 (peanut butter) mice. Mmp3 was consistently upregulated over 2 fold by curcumin treatment in JNPL3 (peanut butter) and JNPL3xTg2576 strains but reduced by over 2 fold by curcumin treatment in Tg2576 mice.

Table 3.4.1.1 Fold change of RNA levels of genes involved in A β peptide degradation in the hippocampus region of selected mice in pooled RNA samples.

Genes	JNPL3 (Chow)	JNPL3 (PB)	Tg2576	JNPL3 x Tg2576
Acc	<u>2.26</u>	<u>4.85</u>	-1.34	1.54
Bsg	1.13	<u>2.01</u>	-1.18	1.21
Ece1	-1.07	1.00	1.04	-1.03
Ece2	-1.07	1.09	1.10	-1.03
Ide	1.01	1.20	-1.04	1.01
Mmp14 (MT1-MMP)	1.21	1.38	1.03	1.41
Mmp2	1.80	<u>3.13</u>	-1.16	1.39
Mmp3	-1.09	<u>2.40</u>	<u>-2.60</u>	<u>3.87</u>
Mmp9	1.06	1.23	-1.13	-1.01
Neprilysin (Mme)	1.20	-1.05	-1.23	-1.03

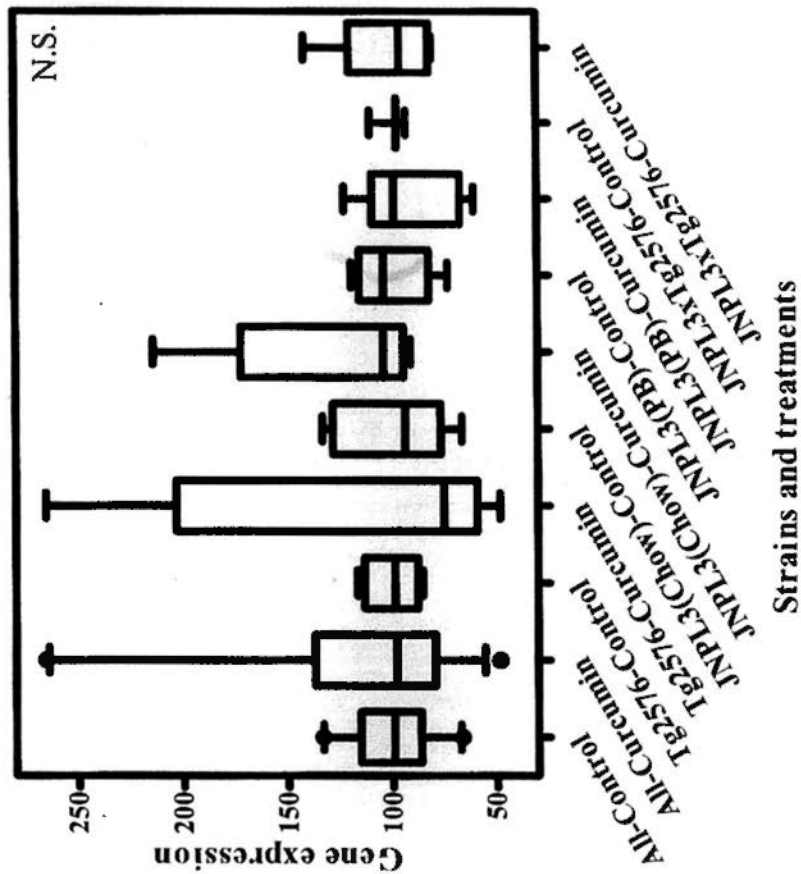
Samples with fold change over two are underlined for easy reference.

3.4.2 Real-time PCR of A β degrading enzymes

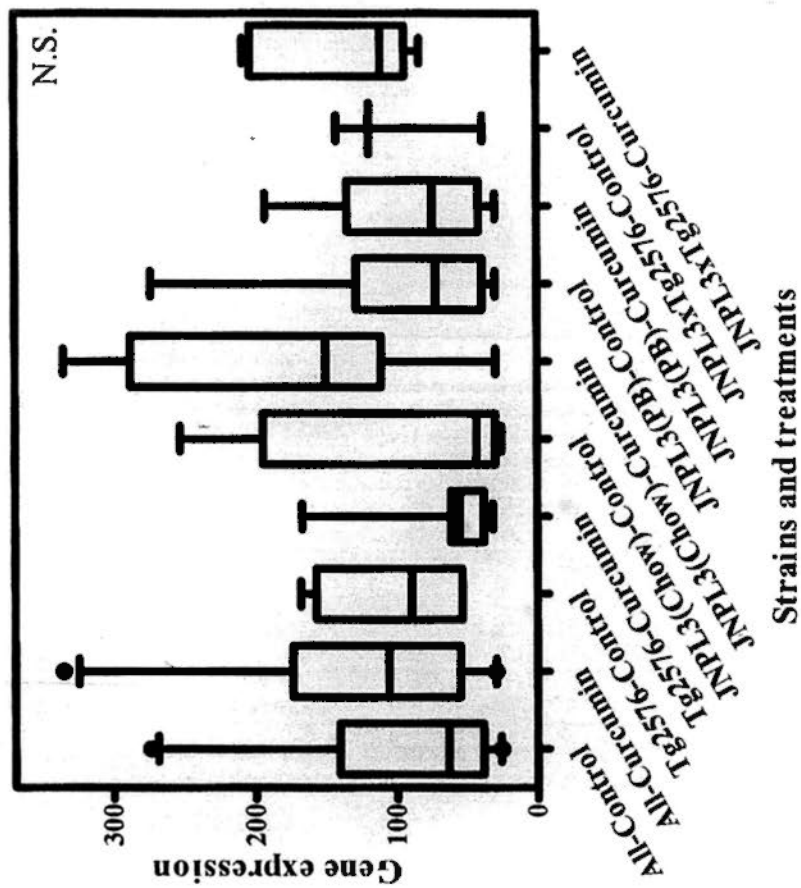
Candidate genes of A β degrading enzymes selected for real-time PCR confirmation were based on microarray data. Some genes were also selected based on our interest in those which have been determined by in vivo study showing the degradation of A β peptides. The selected genes are *Ace*, *Bsg*, *Ide*, *Mmp2*, *Mmp3*, *Mmp9*, *Mmp14* and *Nep*.

Amongst these genes, the expression of *Ide* was found to be significantly upregulated (+23%) by curcumin in JNPL3 (chow) mice. Data of the relative *Ide* gene expression level amongst different groups are illustrated in **Figure 3.4.2.1(c)**. *Mmp2* gene expression levels are shown in **Figure 3.4.2.1(d)**. It was confirmed that *Mmp2* was significantly upregulated with curcumin treatment amongst all strains and particularly in JNPL3 (chow) mice, by 36 percent and 77 percent, respectively. As with *Mmp2*, the gene expression level of *Mmp14*, which is shown in **Figure 3.4.2.1(g)**, was confirmed to be upregulated significantly by curcumin amongst all strains and particularly very significantly in JNPL3 (chow) mice, by 20 percent and 46 percent, respectively.

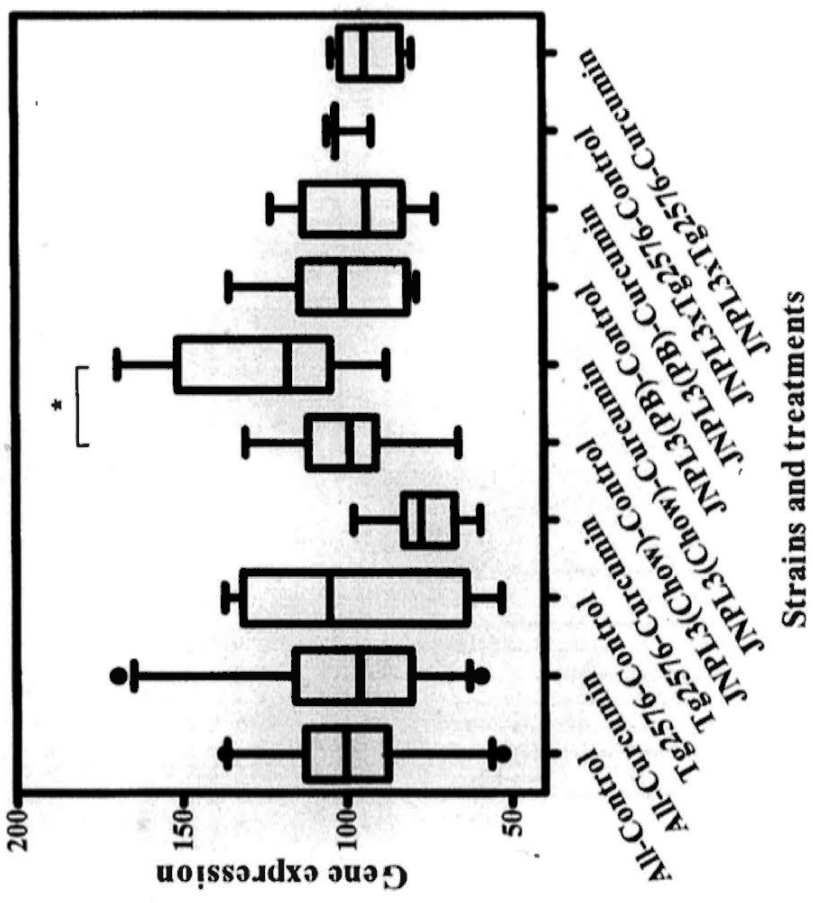
(b) Bsg



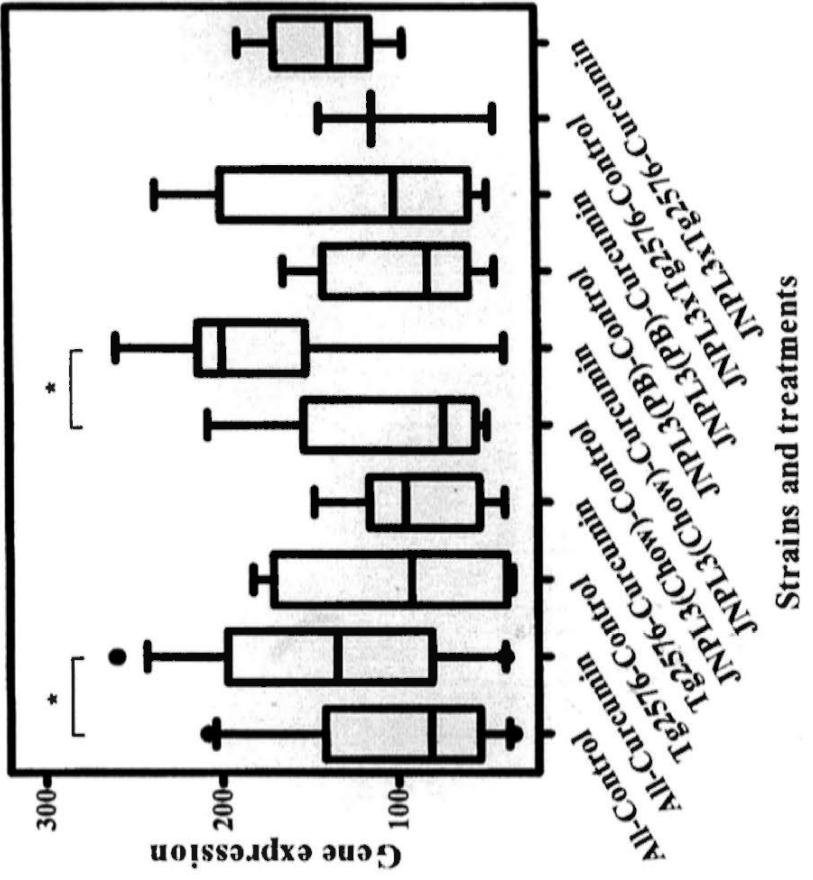
(a) Ace



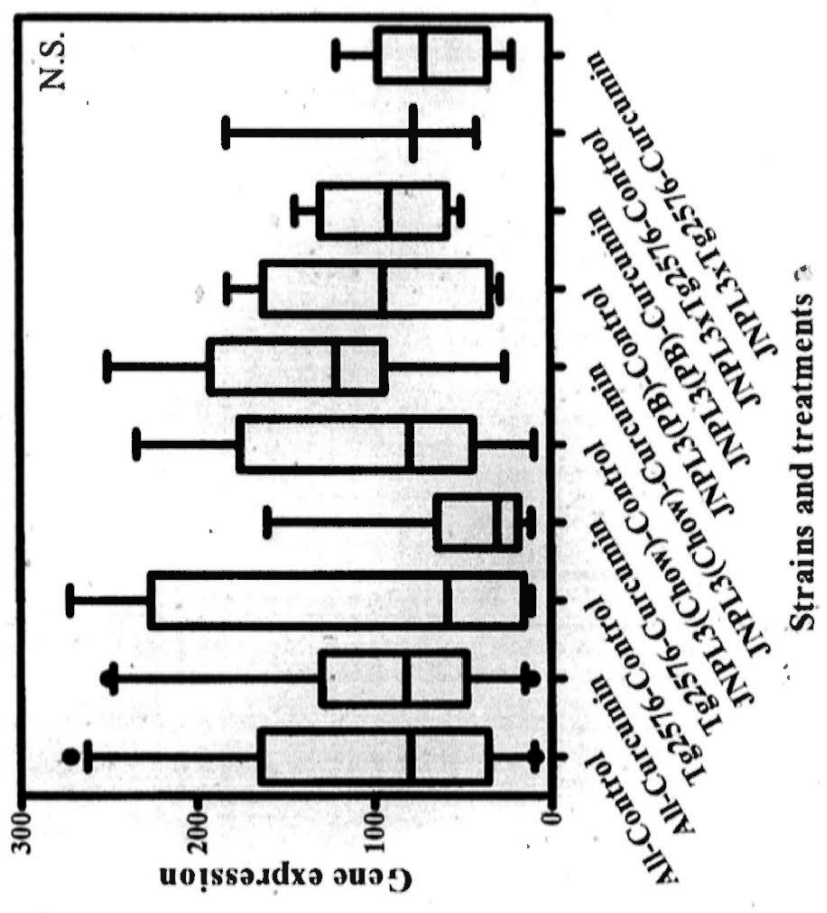
(c) Ide



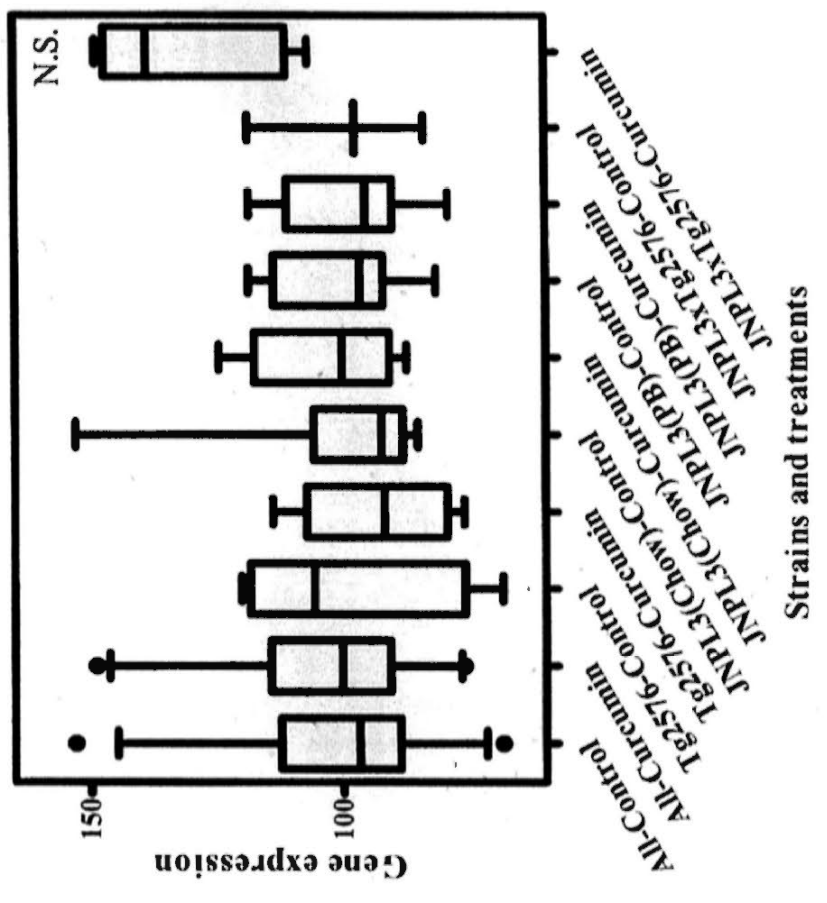
(d) Mmp2



(e) Mmp3



(f) Mmp9



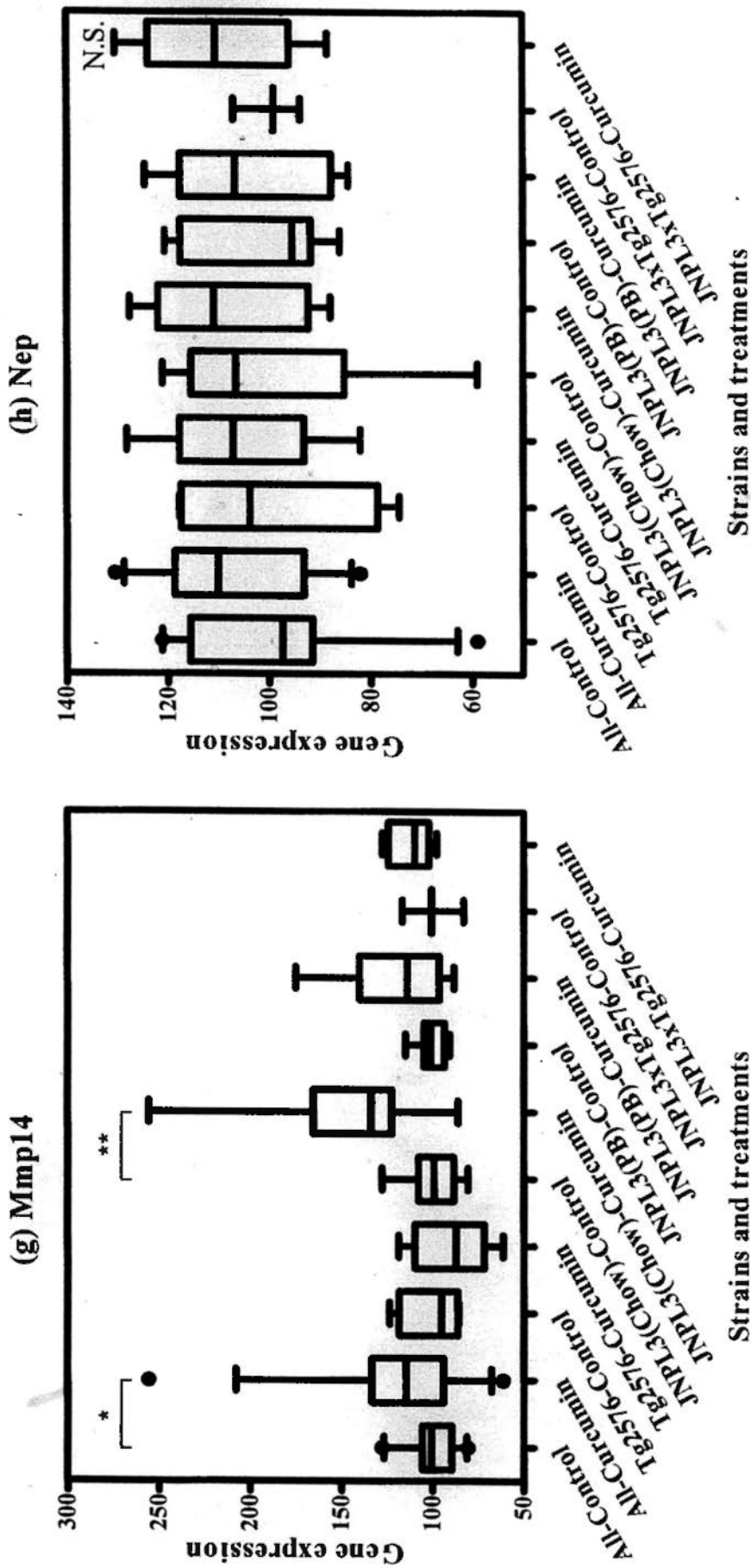


Figure 3.4.2.1 Comparison of mRNA expressions of (a) Ace, (b) Bsg, (c) Ide, (d) Mmp2, (e) Mmp3, (f) Mmp9, (g) Mmp14 and (h) Nep in hippocampus of different mice strains between curcumin treatment and control groups. The boxes indicate median, 25 and 75 percentile; whisker caps indicate 5 and 95 percentile; filled circles indicate outliers. Significant difference between treatment groups of different strains were determined by Mann-Whitney U test using SPSS, and data were plotted using GraphPad Prism. *, $p < 0.05$; **, $p < 0.005$; N.S., no significant difference between treatment and control groups amongst all and between individual strains.

3.5 Effects of curcumin on A β removal

3.5.1 Cell culture study

3.5.1.1 MTT assay of tested compounds

Before determining the effect of phenolic compounds on ApoE secretion from BV-2 microglial cells, MTT cell viability assays were performed to test the toxicity of curcumin, ferulic acid and tannic acid. Measurement of toxicity is necessary because the level of ApoE and all other proteins secreted to the medium could be affected by toxicity which reduces the total cell number.

Figure 3.5.1.1.1 (A) illustrates the viability of BV-2 cells after eight hours incubation in serum-free medium with these three compounds at a range of concentrations. Since the stock solution of curcumin was prepared in DMSO and those of the others were in water, the experiment of each compound was run with its own solvent control. After incubating with the cells, the compound-containing conditioned medium was replaced by fresh serum-free medium with dissolved MTT. The purple formazan crystals that formed inside the living cells were dissolved and quantified by spectrophotometry.

Data showed that curcumin and ferulic acid were not toxic in the range of concentrations tested. Surprisingly, both of them significantly increased cell viability at the highest concentration tested, which may be due to increased metabolic rate or cell numbers. Tannic acid was shown to have very mild but significant toxicity at the lowest two concentrations tested. The toxicity was increased dramatically at the two highest concentrations. Tannic acid at 6.25 and 15.625 μ M extremely significantly reduced cell viability, by 34 and 50 percent, respectively.

MTT assay of BV-2 cell under different compounds treatment for 8 hours

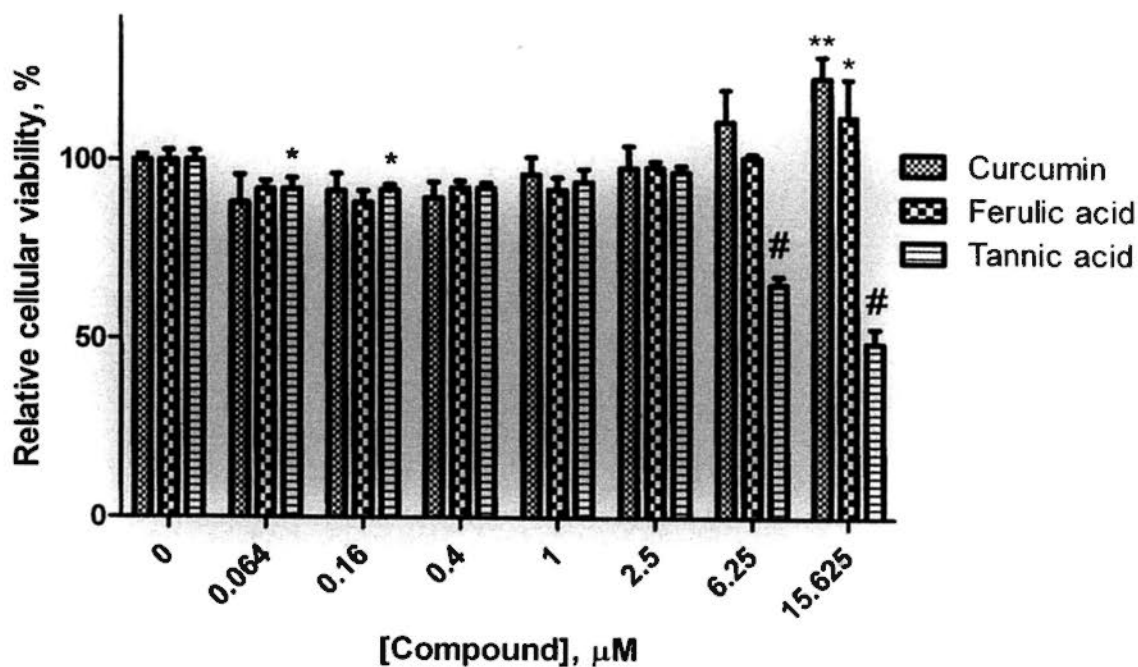


Figure 3.5.1.1.1 (A) MTT cell viability assay of BV2 microglial cells after 8 hours of treatment with various concentrations of curcumin, ferulic acid or tannic acid. Results are expressed as mean \pm SD from triplicate measurements. Statistical difference between control and various concentrations of compounds was determined by one-way ANOVA for multiple comparison and Tukey HSD test as a *post hoc* test. *, $p < 0.05$; **, $p < 0.01$; #, $p < 0.001$.

3.5.1.2 ApoE secretion from BV2 microglial cells treated with phenolic compounds

To determine the effect of compounds on ApoE secretion from microglia, the BV-2 microglial cell line was used. Since ApoE and albumin are highly abundant in serum, which may interfere with ApoE metabolism and quantification, the medium has to be serum-free. As the level of secreted ApoE at eight hours is under the limit of detection by western blotting, a more sensitive method, dot blotting, was used to quantify ApoE. Conditioned medium was harvested and centrifuged to get rid of floating cells. Medium was transferred to the nitrocellulose membrane and passed through it by applying a vacuum to the dot blot apparatus. ApoE protein in the medium bound to the membrane when the solution passed through it. Another common protein binding membrane, PVDF, was not used due to the loss of binding capacity when it is dried under vacuum suction.

An image from one of at least three experiments is shown in **Figure 3.5.1.2.1 (A)**. Each concentration was run in triplicate in each experiment. Results were quantified and compared as illustrated in **Figure 3.5.1.2.1 (B)**. Curcumin, even at the lowest concentration tested, increased the level of ApoE secretion significantly, and such an effect was maintained up to 1 μM . Further increasing the concentration of curcumin beyond that level reduced its capacity to enhance ApoE secretion. At 15.6 μM , there was no significant difference in the ApoE secretion level between curcumin and control.

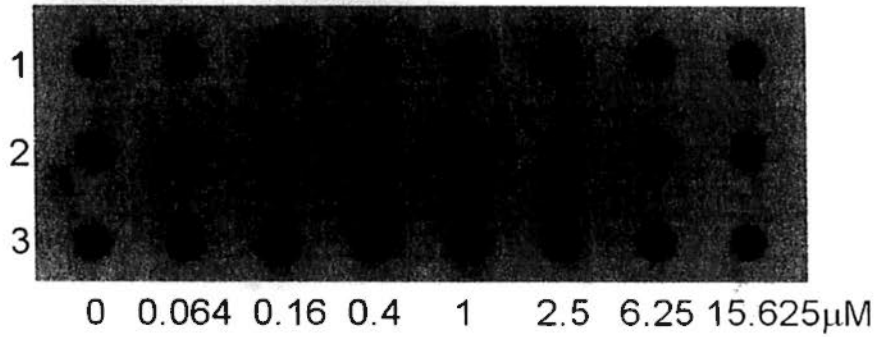
The reliability of dot blotting quantification was further confirmed by running a western blot of conditioned medium which was concentrated 50 times before loading on the gel (see **Figure 3.5.1.2.1 (C)**). Even without quantification, it is easily

observable from the blot that nanomolar concentrations of curcumin increased ApoE secretion to the conditioned medium.

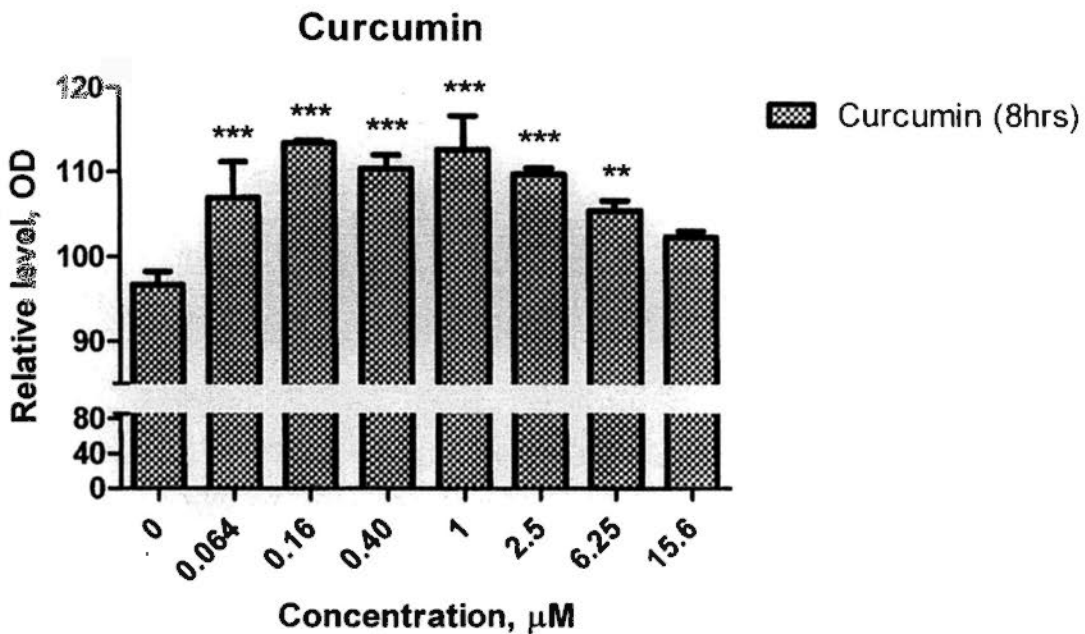
A dot blot showing the effect of ferulic acid on ApoE secretion can be seen in **Figure 3.5.1.2.2 (A)**. Quantification of the blot is illustrated in **Figure 3.5.1.2.2 (B)**. Result showed that ferulic acid significantly increased ApoE secretion from BV-2 cell at the concentration over 0.4 μM . However, the effect of ferulic acid did not go up further or down significantly beyond this concentration since the level of secreted ApoE at 0.4 μM has no significant difference between it and higher concentrations tested.

Figure 3.5.1.2.3 (A) illustrates the dot blotting result of the effect of tannic acid on ApoE secretion from BV-2 cells after eight hours incubation. Data in **Figure 3.5.1.2.3 (B)** showed that tannic acid increased ApoE secretion with significant effect at concentration of at least 1 μM . The effect went up as the concentration of tannic acid increased. However, the effect dramatically disappeared at concentration of 15.6 μM . Furthermore, tannic acid was significantly shown to reduce ApoE secretion at concentration of 50 μM by about 15 percent.

A. Curcumin



B.

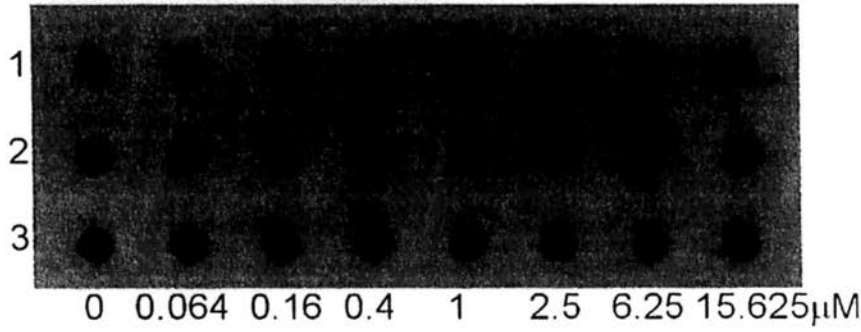


C.



Figure 3.5.1.2.1 (A) Dot blotting analysis of the level of ApoE secreted from curcumin-treated BV2 microglial cells for 8 hours. Curcumin concentration is labeled on the bottom of the blot, and replicate number is shown on the left of the blot. (B) Quantification of the dot blot. Results are expressed as mean \pm SD from triplicate measurements. Statistical difference between control and various concentrations of curcumin was determined by one-way ANOVA for multiple comparison and Tukey HSD test as *post hoc* test. **, $p < 0.01$; ***, $p < 0.001$. The specificity of the antibody and reliability of the dot blotting experiment were confirmed by (C) western blotting with conditioned medium that was concentrated 50x.

A. Ferulic acid



B.

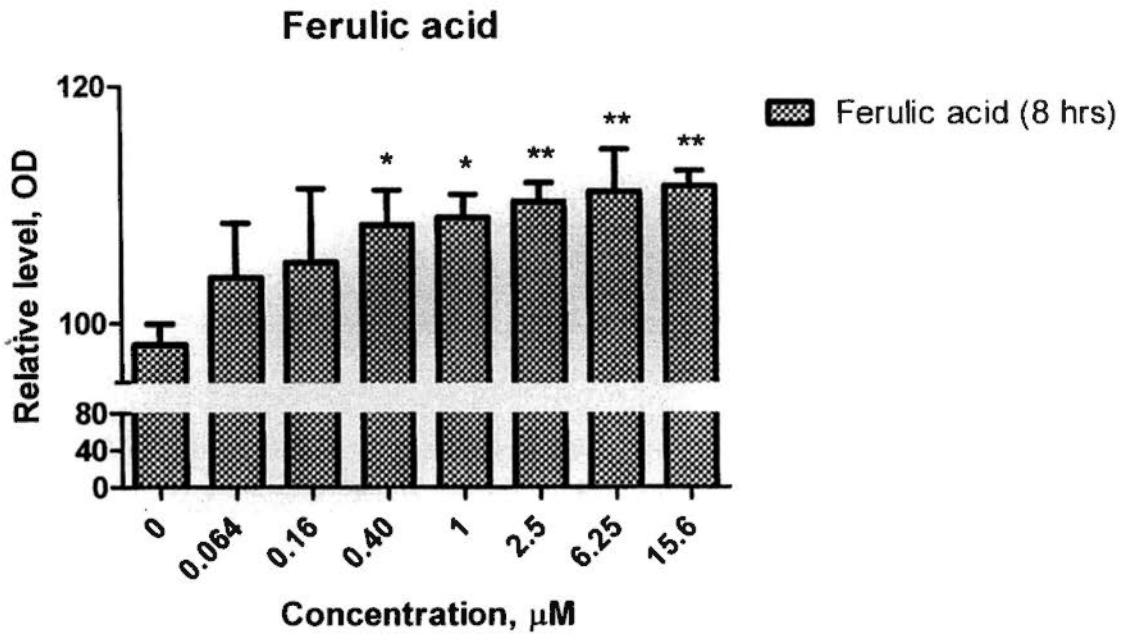
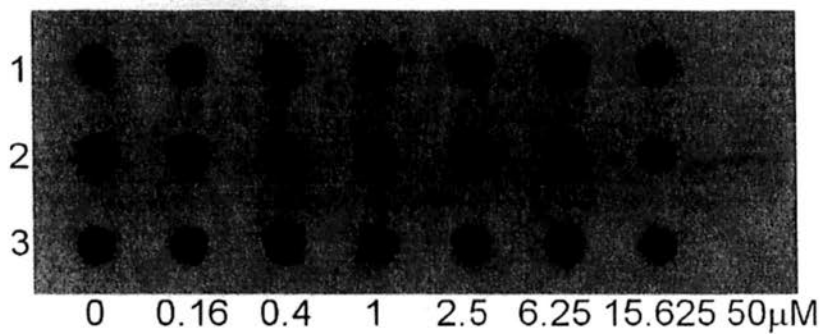


Figure 3.5.1.2.2 (A) Dot blotting analysis of the level of ApoE secreted from ferulic acid-treated BV2 microglial cells for 8 hours. (B) Quantification of the dot blot. Results are expressed as mean \pm SD from triplicate measurements. Statistical difference between control and various concentrations of ferulic acid was determined by one-way ANOVA for multiple comparison and Tukey HSD as *post hoc* test. *, $p < 0.05$; **, $p < 0.01$.

A. Tannic acid



B.

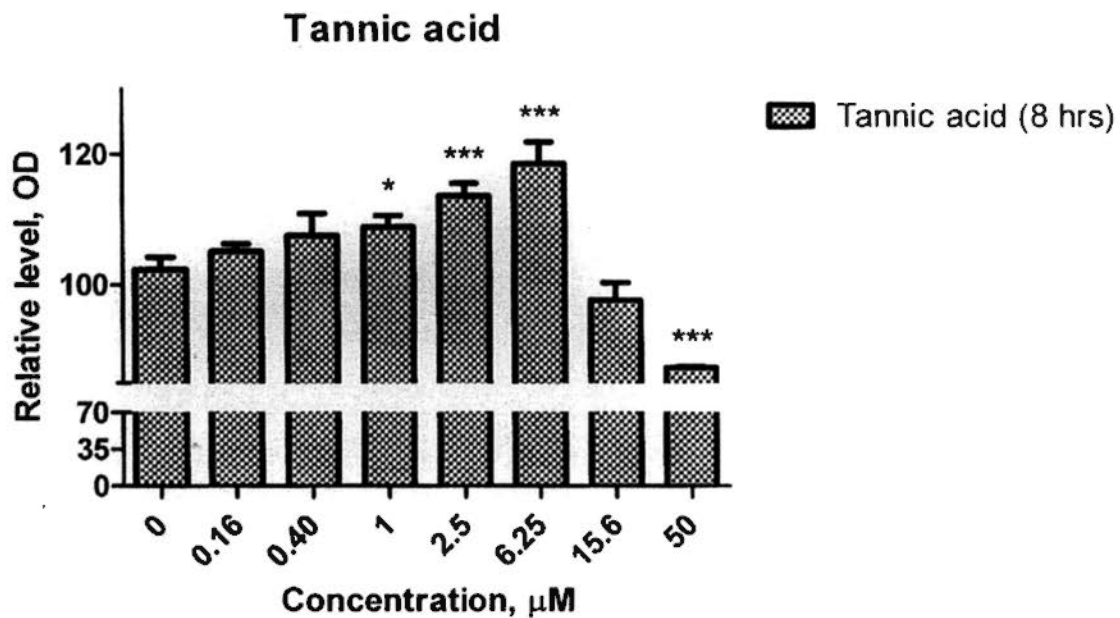


Figure 3.5.1.2.3 (A) Dot blotting analysis of the level of ApoE secreted from tannic acid-treated BV2 microglial cells for 8 hours. **(B)** Quantification of the dot blot. Results are expressed as mean \pm SD from triplicate measurements. Statistical difference between control and various concentrations of tannic acid was determined by one-way ANOVA for multiple comparison and Tukey HSD as *post hoc* test. *, $p < 0.05$; ***, $p < 0.001$.

3.5.2 Microarray of A β transporter and receptor genes

3.5.2.1 A β transporters

The genes known to transport and remove A β peptides are shown in **Table 3.5.2.1.1.**, which lists the fold change of expression, measured by microarray, for each gene and pair of groups of mice due to curcumin compared to control treatment. Curcumin reduced the expression of ApoA1 over two fold in JNPL3 (peanut butter) mice. Ltf was upregulated in JNPL3 (peanut butter) but downregulated in JNPL3 (chow) over two fold. Ttr was upregulated over two fold in JNPL3 (chow and peanut butter) and JNPL3xTg2576 strains. Ttr expression in JNPL3 (peanut butter) was upregulated 30 fold.

3.5.2.2 A β receptors

The genes known to act as receptors involved in direct or indirect uptake of A β peptides are shown in **Table 3.5.2.2.1.** Amongst them, microarray results showed that expression of Ager and Msr1 were increased by over two fold by curcumin treatment in the JNPL3 (peanut butter) and JNPL3xTg2576 groups, respectively. Curcumin downregulated Cd36 by almost three folds in JNPL3 (peanut butter) mice.

Table 3.5.2.1.1 Fold change of RNA levels of genes involved in A β peptide interaction and transport in the hippocampus region of selected mice in pooled RNA samples.

Genes	JNPL3 (Chow)	JNPL3 (PB)	Tg2576	JNPL3 x Tg2576
A2M	1.49	1.16	1.02	1.30
ApoA1	1.02	<u>-2.22</u>	1.07	-1.06
ApoE	1.03	-1.07	1.03	1.00
ApoJ/Clusterin (Clu)	1.06	1.17	-1.07	1.07
Ltf	<u>-3.00</u>	<u>2.57</u>	-1.39	1.67
Ttr	<u>2.26</u>	<u>29.77</u>	-1.08	<u>2.08</u>

Samples with fold change over two are underlined for easy reference.

Table 3.5.2.2.1 Fold change of RNA levels of genes involved in A β peptide uptake in the hippocampus region of selected mice in pooled RNA samples.

Genes	JNPL3 (Chow)	JNPL3 (PB)	Tg2576	JNPL3 x Tg2576
Ager	1.19	<u>2.54</u>	-1.16	-1.26
Cd36	-1.39	<u>-2.94</u>	1.55	1.19
Colec12	-1.07	1.75	-1.12	1.30
Ldlr	-1.53	1.13	1.17	-1.12
Lrp1	1.10	-1.01	1.04	-1.07
Lrp2 (Megalin)	1.31	-1.15	1.09	1.56
Lrp8 (Apoer2)	1.01	1.11	-1.05	1.05
Msr1	1.10	1.54	1.23	<u>2.11</u>
Sort1	-1.18	-1.08	1.07	-1.07

Samples with fold change over two are underlined for easy reference. 3.5.3

3.5.3 Real-time PCR of A β transporter and receptor genes

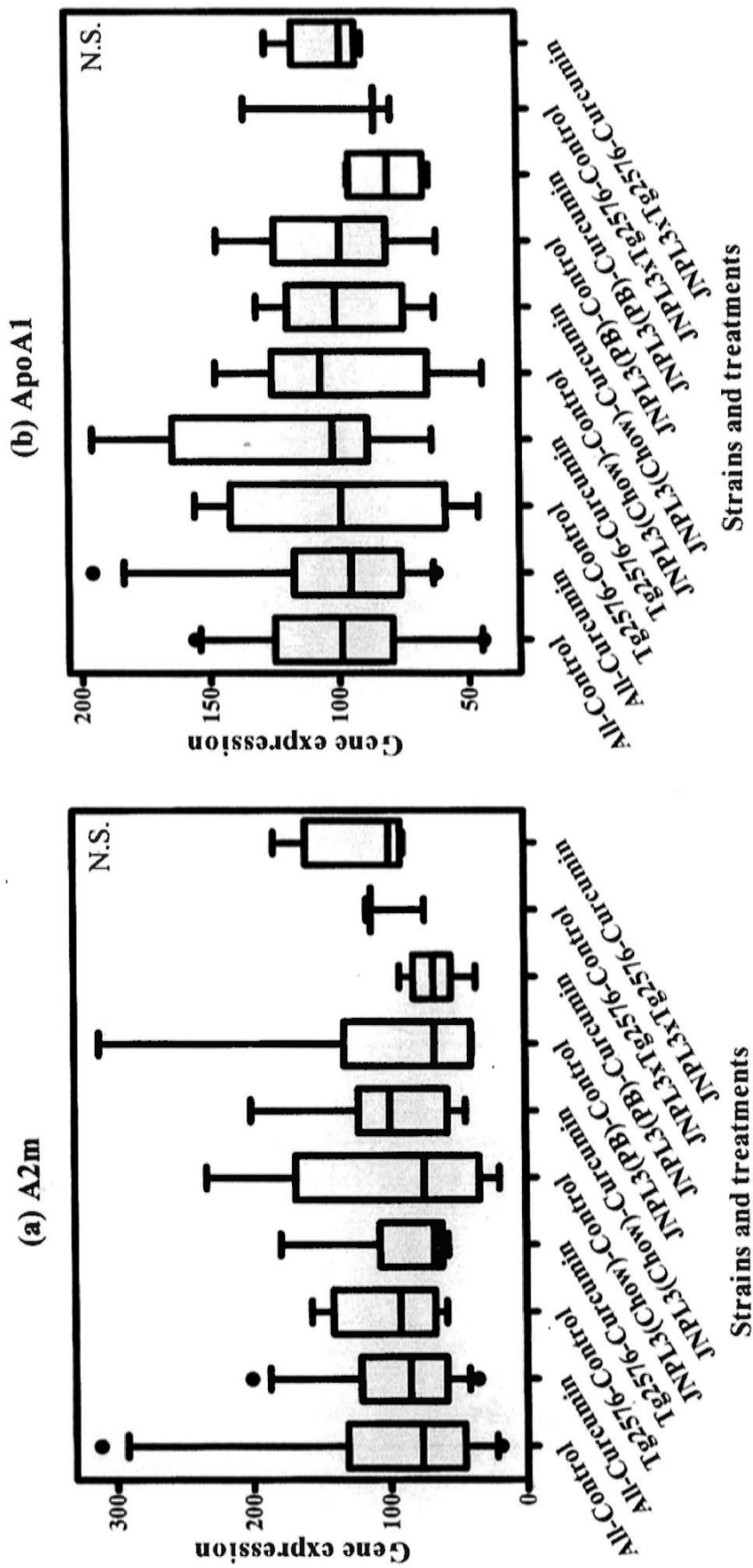
3.5.3.1 Gene expression of A β transporters

Of genes known as transporters of A β peptides, A2M, ApoA1, ApoE, ApoJ, L1f and Ttr were selected for real-time PCR confirmation. None of the A β transporter candidate genes revealed a significant difference in their expression levels between curcumin and control treated groups.

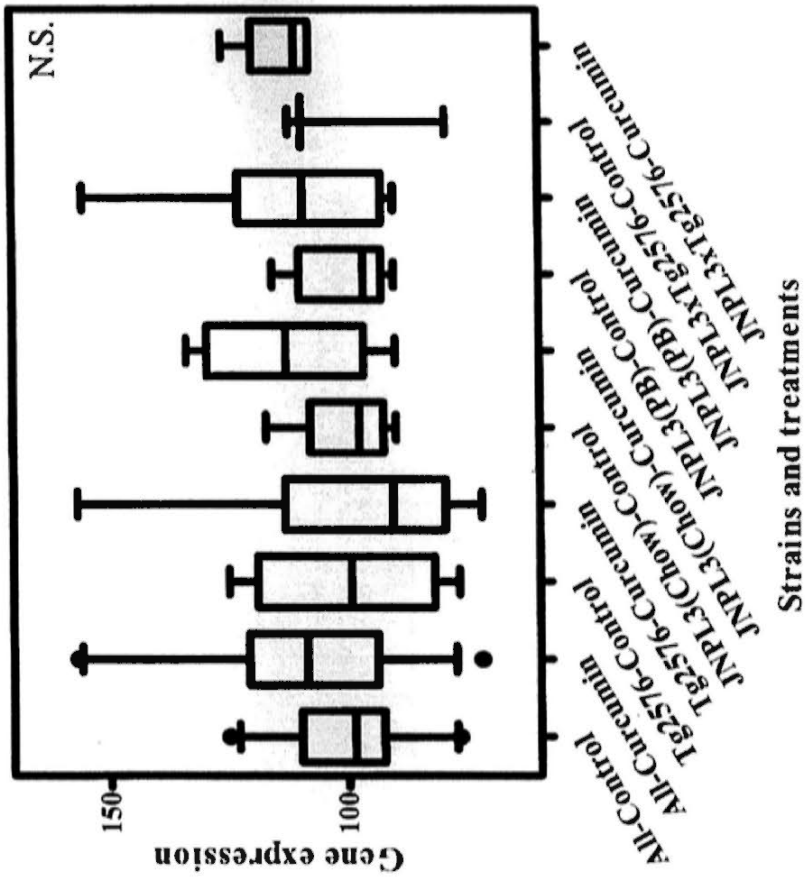
3.5.3.2 Gene expression of A β receptors

Ager, ApoeR2, Cd36, Colec12, Ldlr, Lrp1, Lrp2, Msr1 and Sort1 are known receptors for A β peptides. By examining their expression using real-time PCR, Lrp2 was found to be significantly upregulated, by 12 percent, in all curcumin treated mice versus controls. However, curcumin did not significantly upregulate Lrp2 in any particular groups. ApoeR2, Lrp1 and Msr1 were confirmed to be significantly upregulated by curcumin treatment in JNPL3 (chow) mice, by 37, 30 and 46 percent, respectively.

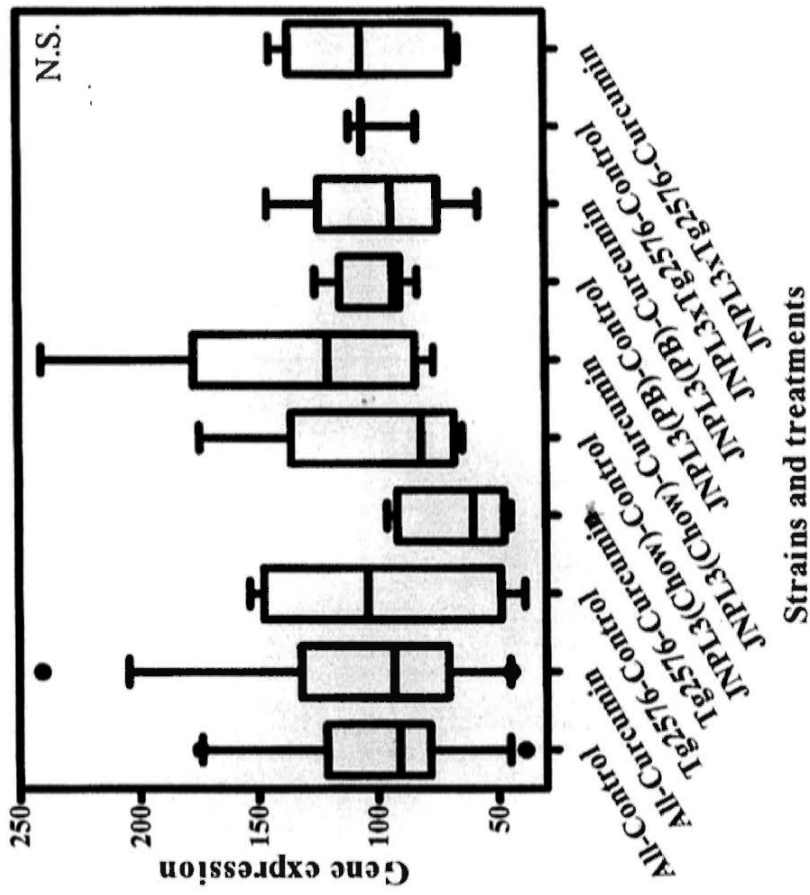
3.5.3.1 Gene expression of A β transporters



(d) ApoJ



(c) ApoE



65

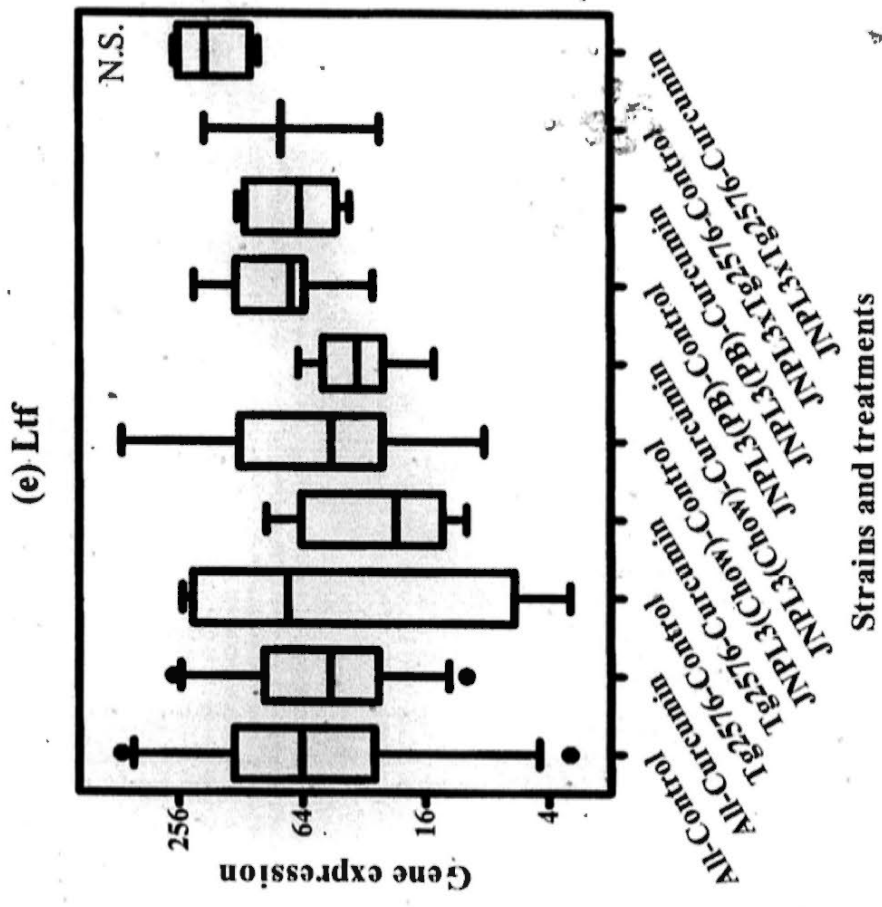
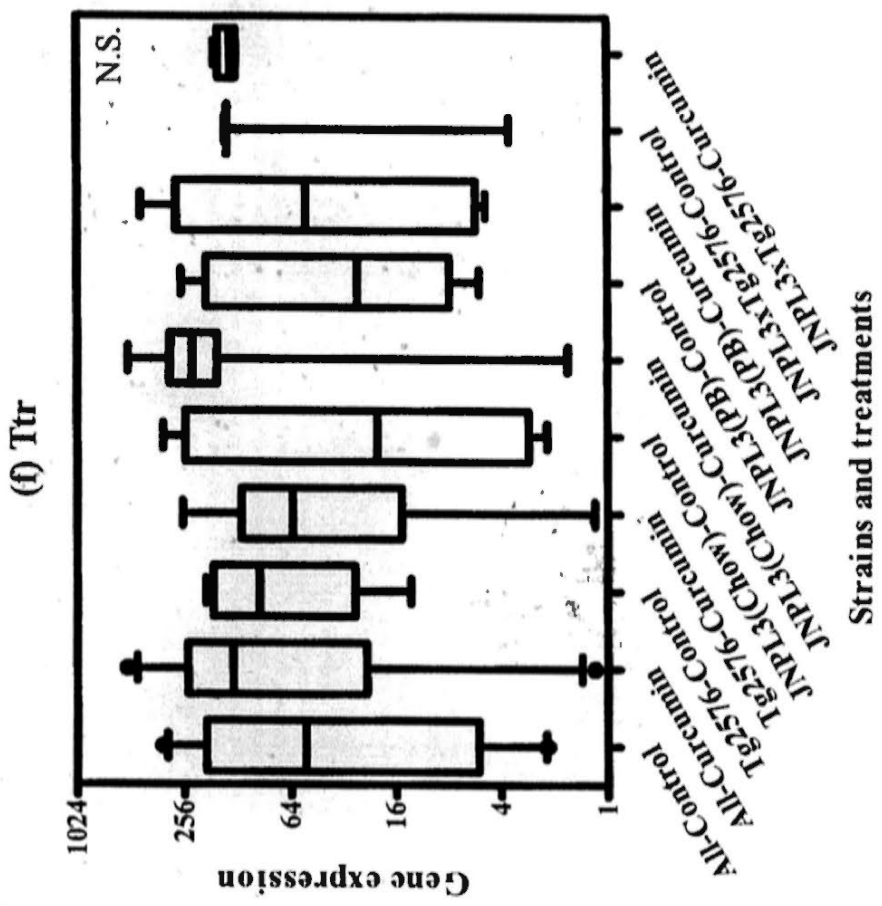
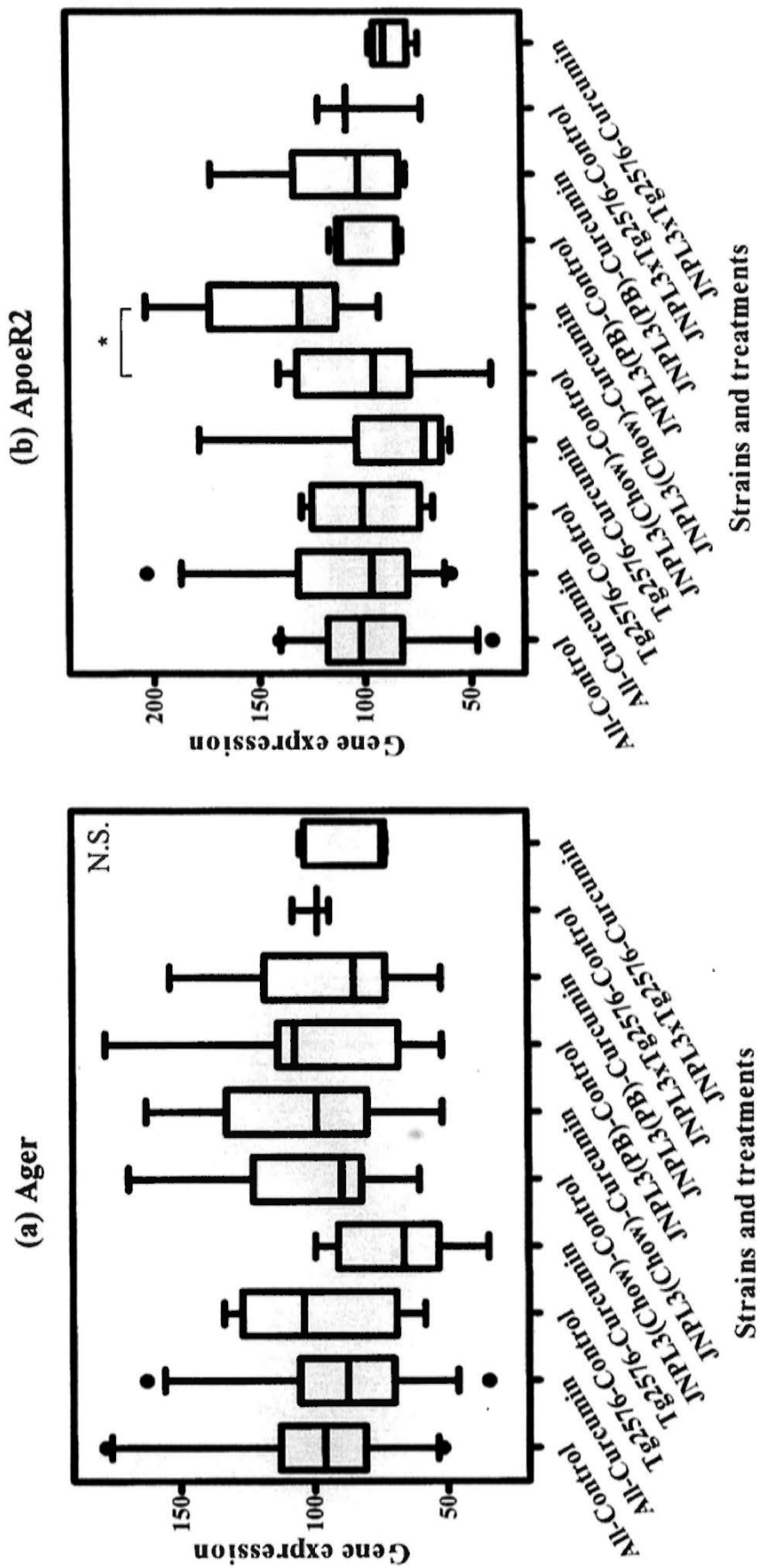
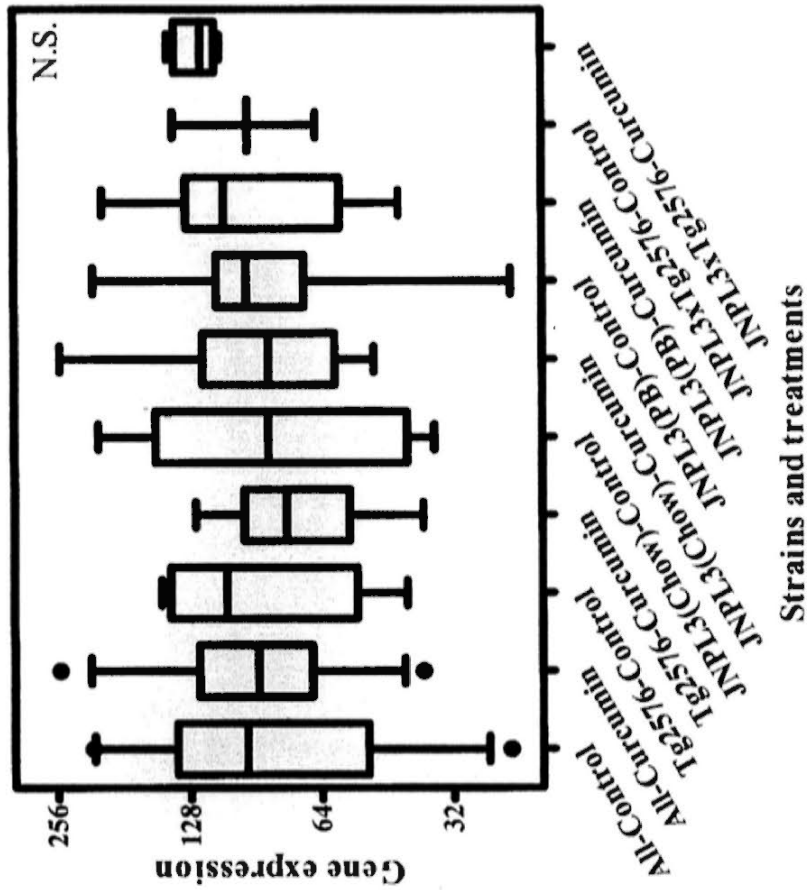


Figure 3.5.3.1.1 Comparison of mRNA expression of (a) A2m, (b) ApoA1, (c) ApoE, (d) ApoJ, (e) Ltf and (f) Ttr in hippocampus of different mice strains between curcumin treatment and control groups. The boxes indicate median, 25 and 75 percentile; whisker caps indicate 5 and 95 percentile; filled circles indicate outliers. Significant difference between treatment groups of different strains was determined by Mann-Whitney U test using SPSS, and data were plotted using GraphPad Prism. N.S., no significant difference between treatment and control groups amongst all strains and amongst individual strains.

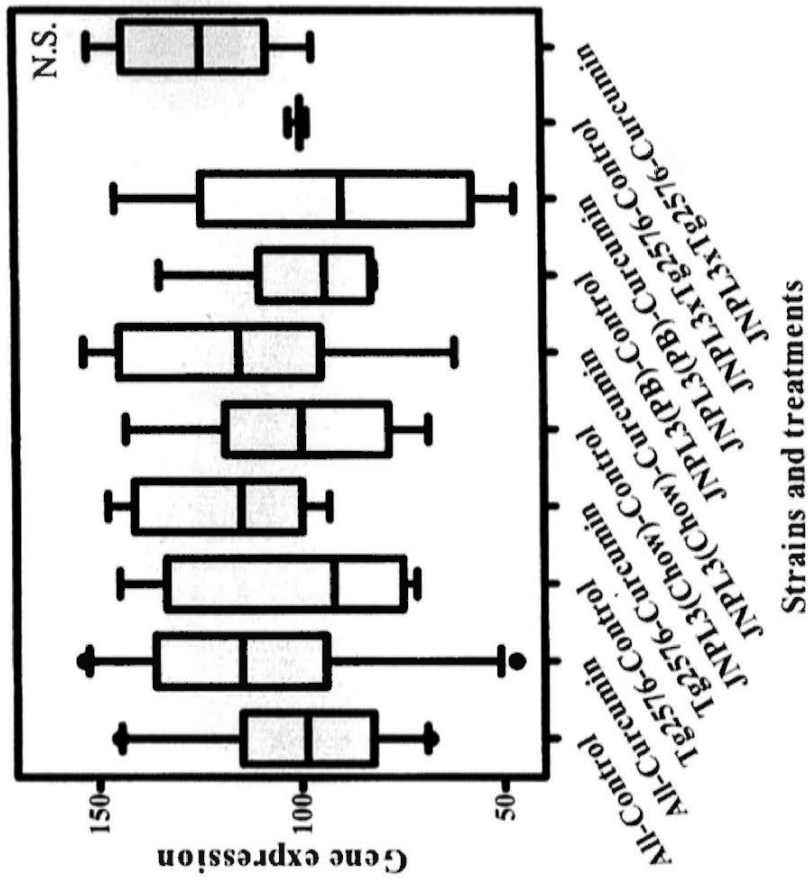
3.5.3.2 Gene expression of A β receptors



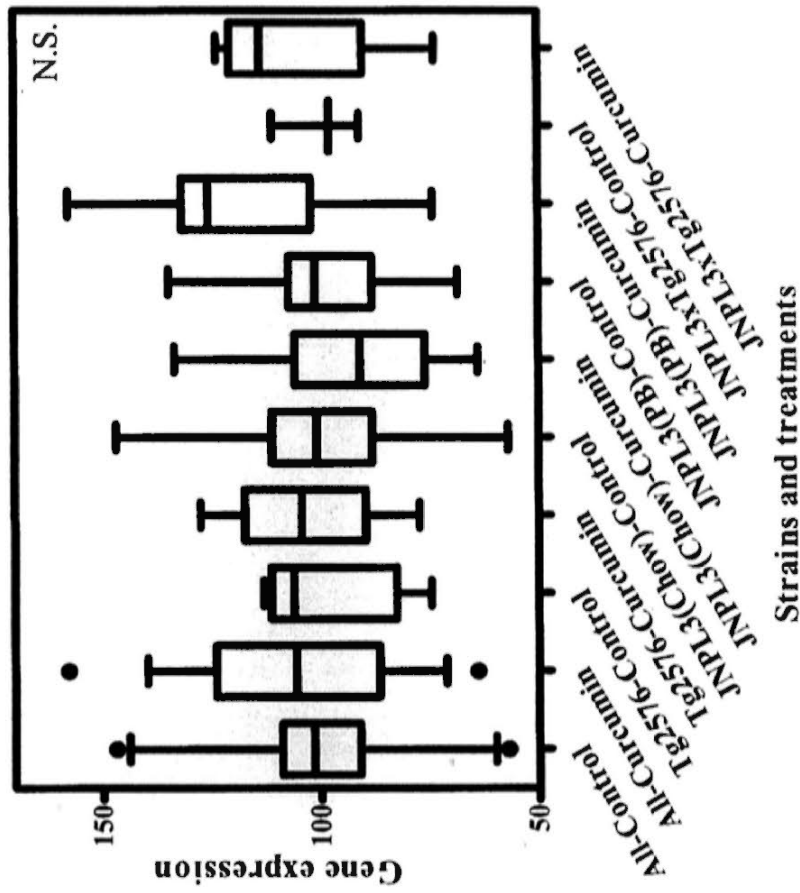
(c) Cd36



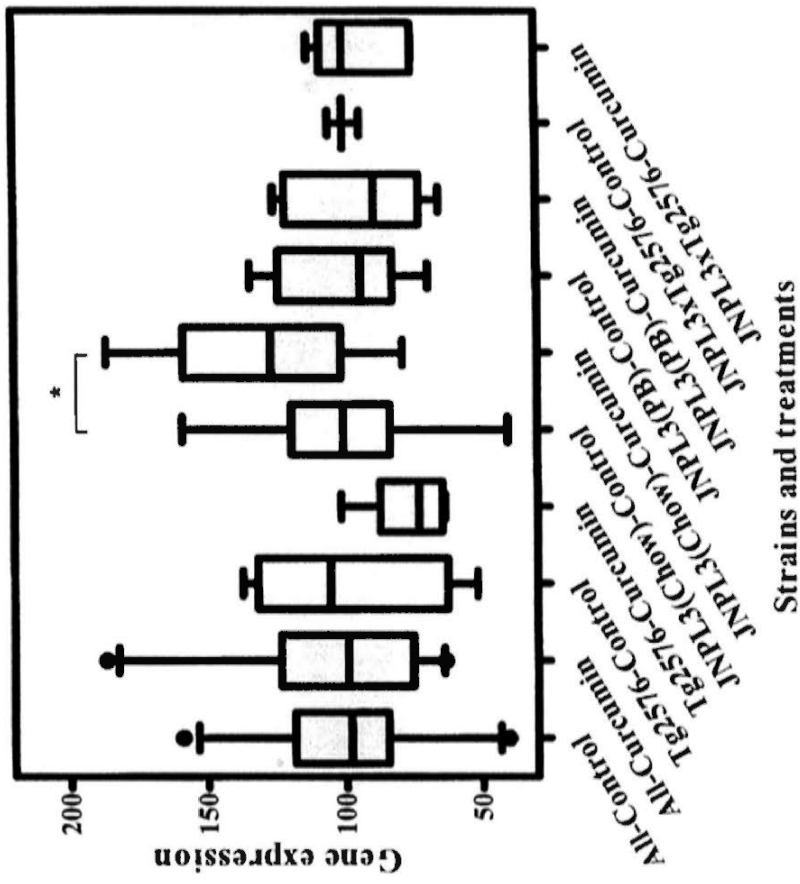
(d) Colec12



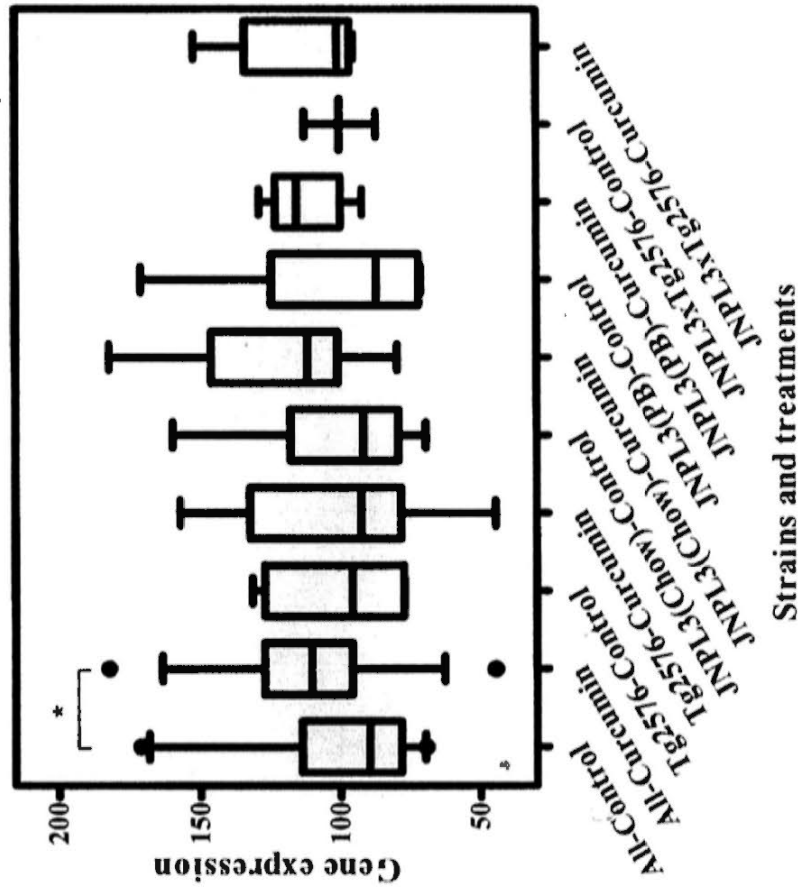
(e) Ldlr



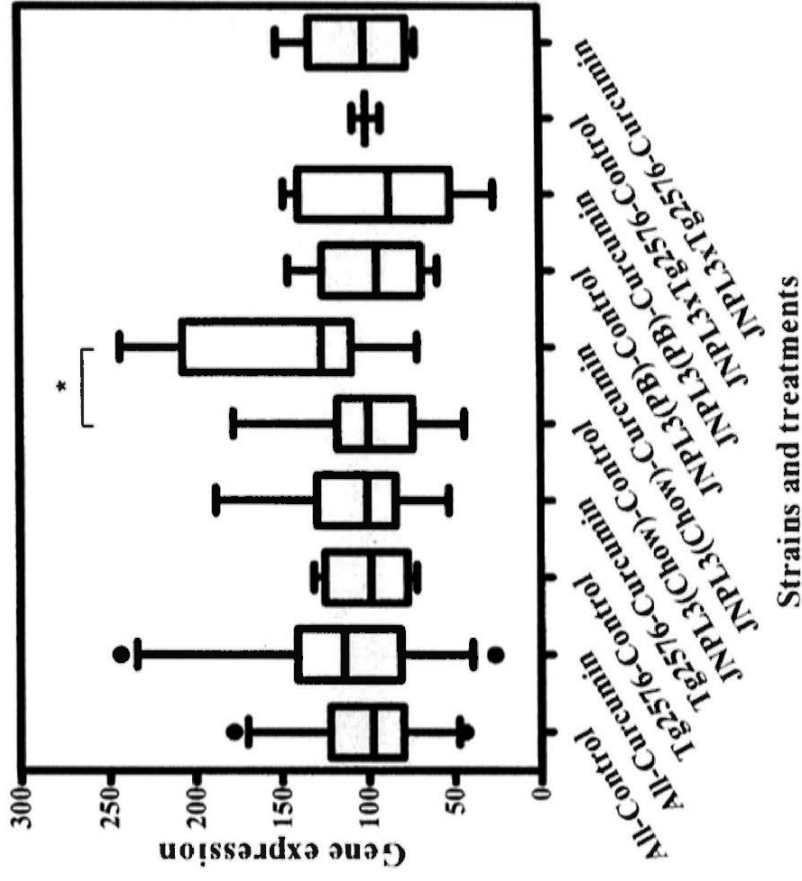
(f) Lrp1



(g) Lrp2



(h) Msr1



(i) Sort1

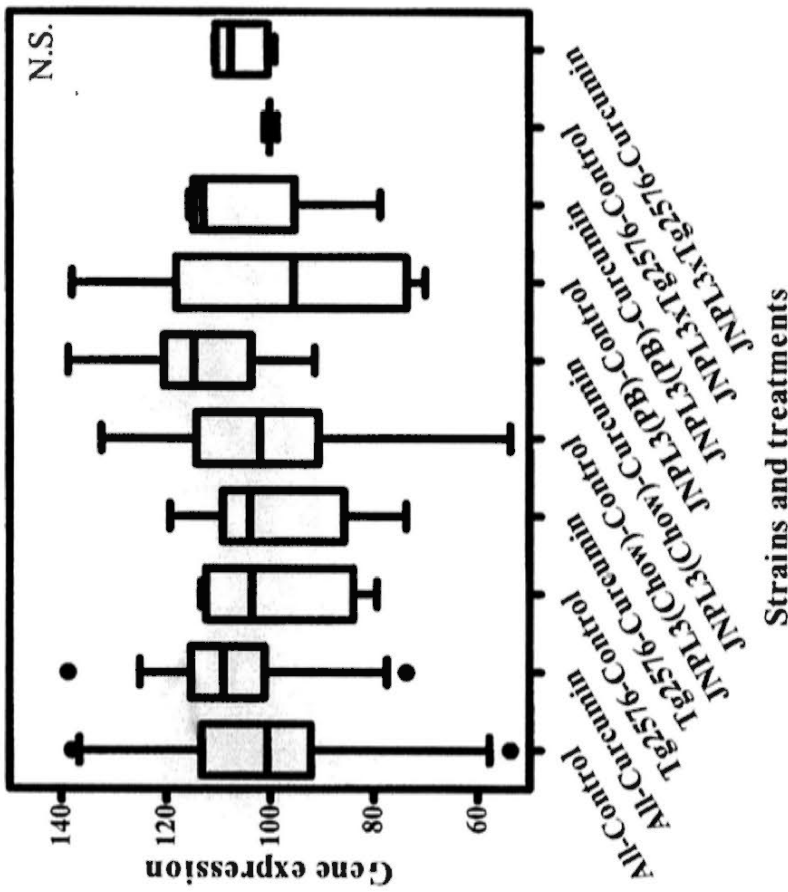


Figure 3.5.3.2.1 Comparison of mRNA expression of (a) Ager, (b) ApoeR2, (c) Cd36, (d) Colec12, (e) Ldlr, (f) Lrp1, (g) Lrp2, (h) Msr1 and (i) Sort1 in hippocampus of different mice strains between curcumin treatment and control groups. The boxes indicate median, 25 and 75 percentile; whisker caps indicate 5 and 95 percentile; filled circles indicate outliers. Significant difference between treatment groups of different strains was determined by Mann-Whitney U test using SPSS, and data were plotted using GraphPad Prism. *, $p < 0.05$; N.S., no significant difference between treatment and control groups amongst all strains and amongst individual strains.

3.6 Effects of curcumin on cholinergic function

3.6.1 Microarray of cholinergic genes

Nicotinic and muscarinic acetylcholine receptors and glutamate receptors are known to be involved in controlling cholinergic function of neurons. The change of expression of these genes upon curcumin treatment was detected using microarrays (**Table 3.6.1.1**).

Microarray differential expression data for genes that have been relatively well documented as being involved in regulating acetylcholine homeostasis in neurons are listed in **Table 3.6.1.2**. Microarray data showed that ChAT gene expression was 16-fold reduced after curcumin treatment of JNPL3 (peanut butter) mice. Curcumin increased choline transporter Cht1 gene expression in JNPL3 (peanut butter) and JNPL3xTg2576 by over two and 500 fold, respectively. Gene expression of Vacht was found to be 2-fold increased in JNPL3 (chow) but decreased in Tg2576 by curcumin treatment.

3.6.2 Real-time PCR data on expression of genes regulating acetylcholine homeostasis

To confirm the microarray data showing changes in the expression of Ache, ChAT, Cht1 and Vacht, real-time PCR was performed. Amongst these genes, none of them was significantly different by curcumin in any group.

Table 3.6.1.1 Fold change of RNA level of genes involved in cholinergic function in the hippocampus region of selected mice in pooled RNA samples.

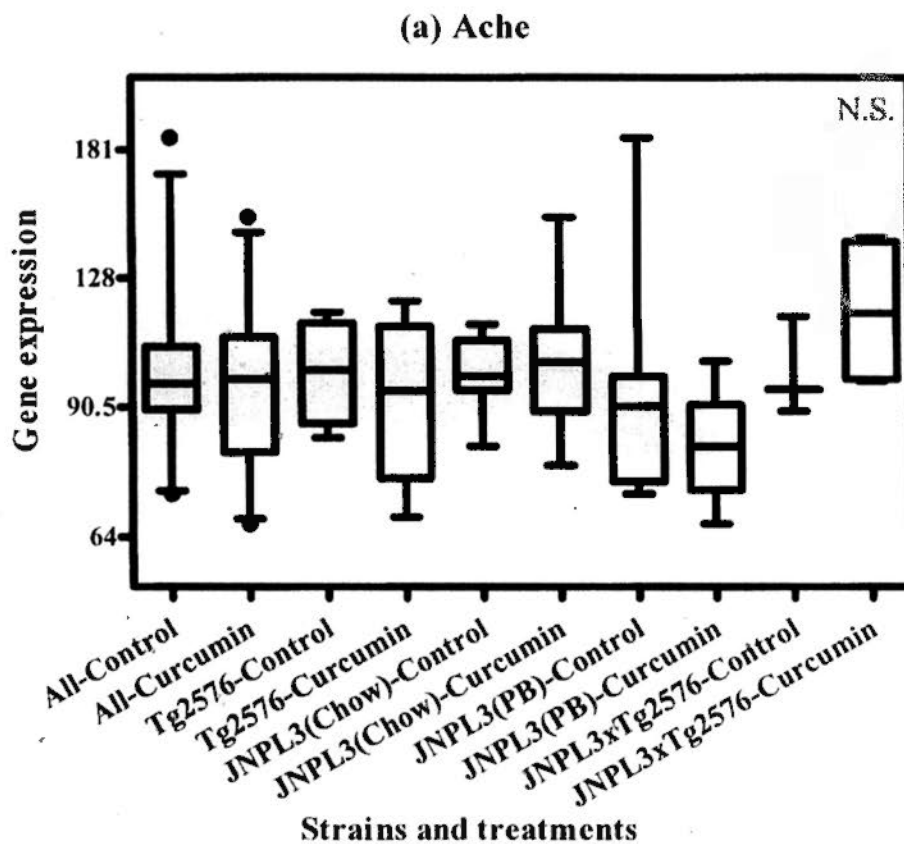
Genes	JNPL3 (Chow)	JNPL3 (PB)	Tg2576	JNPL3 x Tg2576
<u>Nicotinic acetylcholine receptors (nAChRs)</u>				
Chrna1	-1.28	-1.05	-1.23	-1.15
Chrna2	-1.10	<u>-2.03</u>	1.22	<u>-4.76</u>
Chrna3	1.19	-1.77	1.32	-1.03
Chrna4	1.37	-1.02	-1.17	1.07
Chrna5	1.28	-1.06	-1.09	1.04
Chrna6	-1.56	<u>-2.19</u>	1.26	-1.02
Chrna7	-1.25	-1.01	-1.17	-1.19
Chrna9	-1.22	-1.79	-1.21	1.04
Chrna10	1.00	1.21	-1.18	<u>-3.28</u>
Chrnb1	-1.63	1.62	-1.16	1.41
Chrnb2	1.02	-1.01	1.00	-1.16
Chrnb3	-1.46	-1.77	-1.05	-1.07
Chrnb4	-1.09	<u>-2.01</u>	1.25	1.53
Chrnd	-1.08	<u>-2.25</u>	<u>2.10</u>	1.03
Chrne	1.13	1.12	1.35	1.58
Chrng	1.49	<u>-2.13</u>	-1.11	-1.25
<u>Muscarinic acetylcholine receptors (mAChR)</u>				
Chrm1	-1.14	1.25	-1.20	-1.23
Chrm2	<u>3.65</u>	-1.06	-1.14	-1.57
Chrm3	-1.25	1.19	1.12	-1.12
Chrm4	<u>2.96</u>	-1.11	1.20	-1.25
Chrm5	1.81	-1.04	-1.12	1.67
<u>Glutamate receptors (NMDA)</u>				
Grin1	1.28	1.01	-1.25	1.02
Grin2a	-1.01	-1.05	-1.35	-1.15
Grin2b	-1.05	-1.07	-1.18	-1.08
Grin2c	-1.09	-1.09	1.11	-1.05
Grin2d	1.06	-1.17	1.46	-1.06
Grin3a	-1.05	<u>-2.10</u>	1.32	-1.05
Grin3b	-1.19	1.24	-1.33	-1.13
Grina	1.07	-1.07	1.06	1.73

Samples with fold change over two are underlined for easy reference.

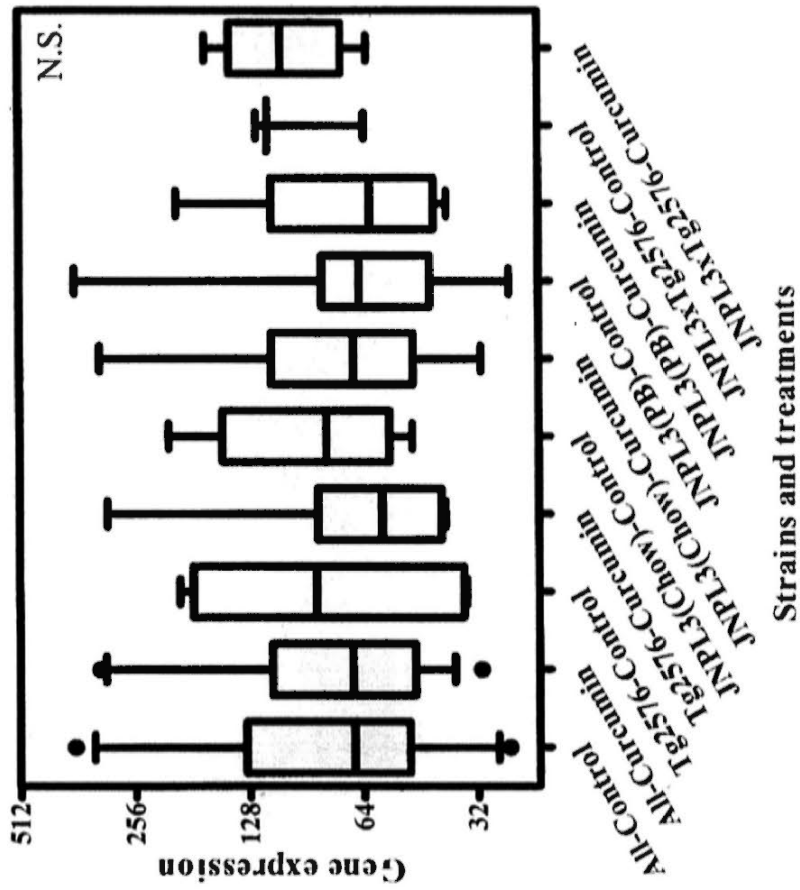
Table 3.6.1.2 Fold change of RNA level of genes involved in acetylcholine homeostasis in the hippocampal region of selected mice in pooled RNA samples.

Genes	JNPL3 (Chow)	JNPL3 (PB)	Tg2576	JNPL3 x Tg2576
Ache	1.29	-1.06	-1.33	-1.14
ChAT	-1.82	<u>-16.76</u>	1.04	1.46
Cht1 (Slc5a7)	1.32	<u>2.38</u>	1.10	<u>501.92</u>
Vacht (Slc18a3)	<u>2.38</u>	1.14	<u>-2.50</u>	1.37

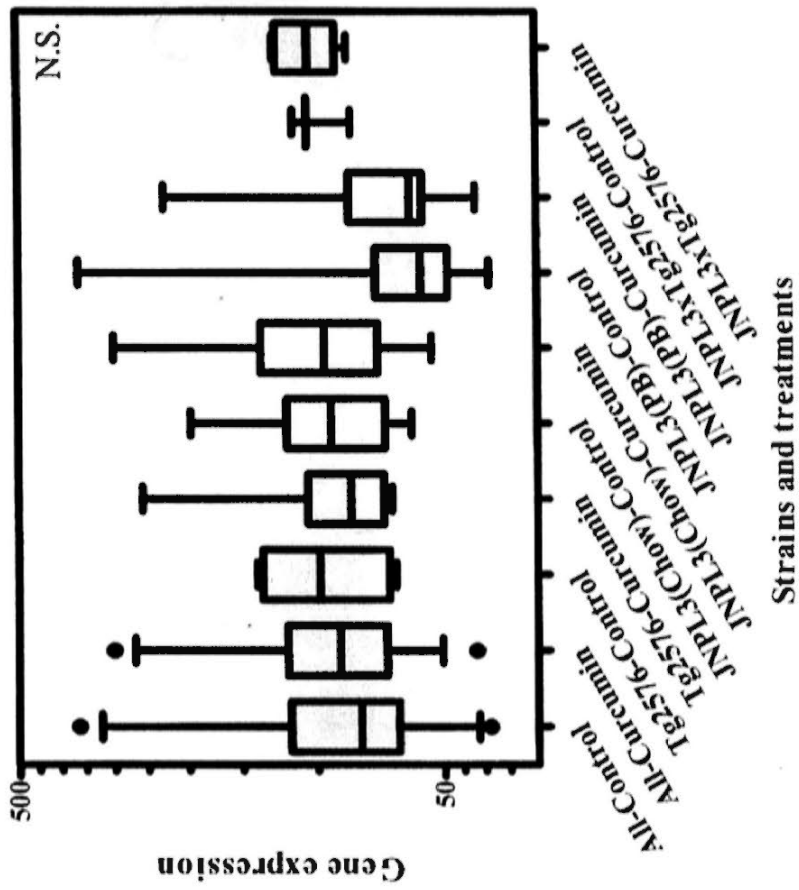
Samples with fold change over two are underlined for easy reference.



(b) ChAT



(c) Cht1



(d) Vacht

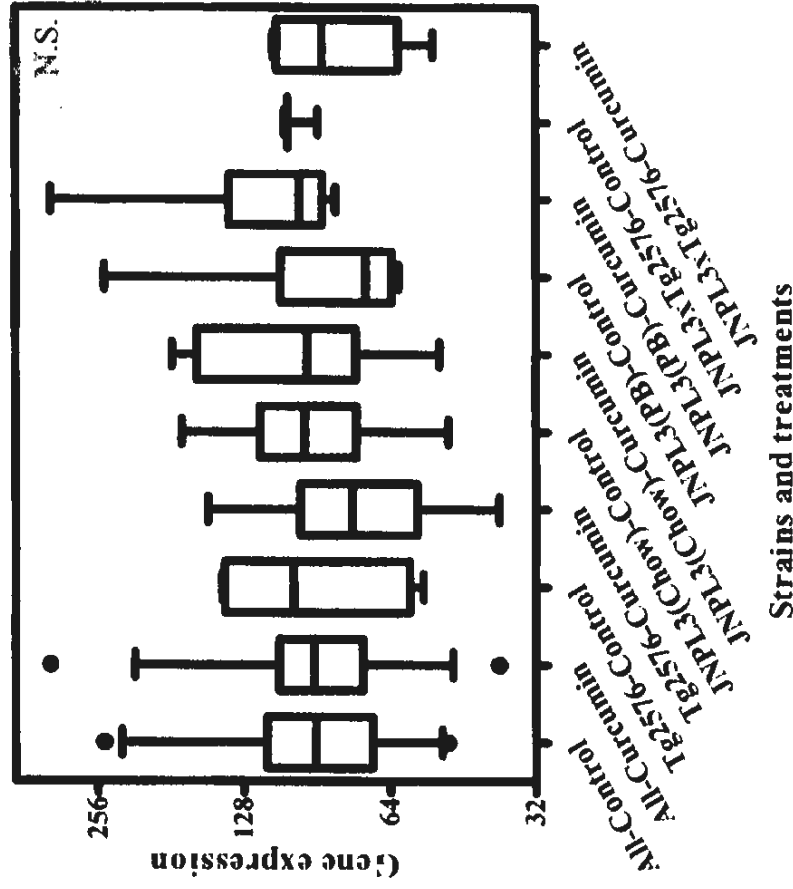


Figure 3.6.2.1 Comparison of mRNA expression of (a) Ache, (b) ChAT, (c) Cht1 and (d) Vacht in hippocampus of different mice strains between curcumin treatment and control groups. The boxes indicate median, 25 and 75 percentile; whisker caps indicate 5 and 95 percentile; filled circles indicate outliers. Significant difference between treatment groups of different strains was determined by Mann-Whitney U test using SPSS, and data were plotted using GraphPad Prism. N.S., no significant difference between treatment and control groups amongst all strains and amongst individual strains.

3.7 Other neuroprotective and harmful effects of curcumin

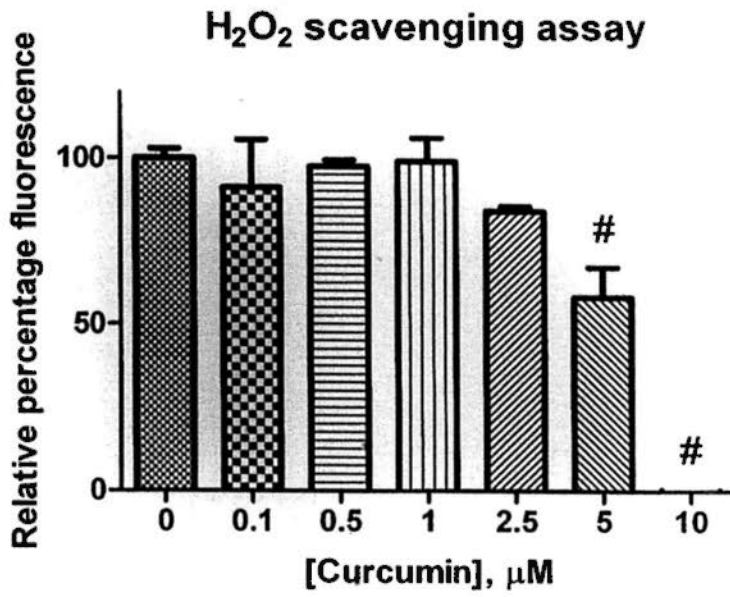
3.7.1 Cell free assay

3.7.1.1 Hydrogen peroxide scavenging assay

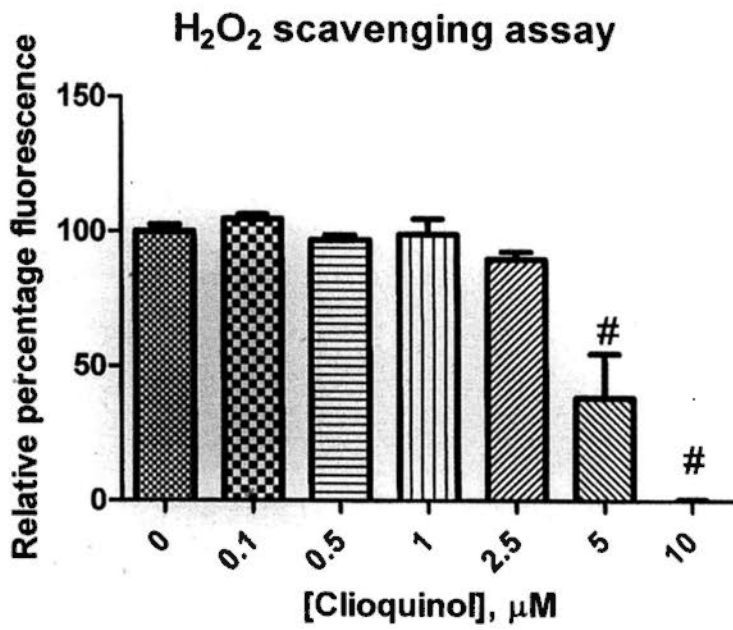
To determine the antioxidative properties of curcumin, an assay specifically designed to mimic the hydrogen peroxide (H_2O_2) generation process in brain using A β 1-42 peptide and Cu(II) ion was adopted. A metal chelator, clioquinol, was used as the positive control for this assay. Clioquinol can chelate and decrease the ability of redox active metal ions, such as Cu(II), to generate H_2O_2 from A β 1-42 peptide. With the presence of DCF in the mixture, the level of fluorescent signal generated is proportional to the amount of H_2O_2 and can be detected by excitation at 485 nm and emission at 535 nm.

Figure 3.7.1.1.1 (A & B) show that curcumin and clioquinol significantly reduced the amount of H_2O_2 in the reaction mixture, by about 40 and 60 percent at 5 μ M, respectively. The inhibition due to either compound reached 100 percent at 10 μ M. Dose vs. response curves in **Figure 3.7.1.1.1 (C)** show that the IC_{50} of H_2O_2 inhibition for curcumin and clioquinol is about 5.2 μ M and 4.4 μ M, respectively. The R^2 of the goodness of fit of the curves is about 0.94 and 0.97 for curcumin and clioquinol, respectively.

A.



B.



C.

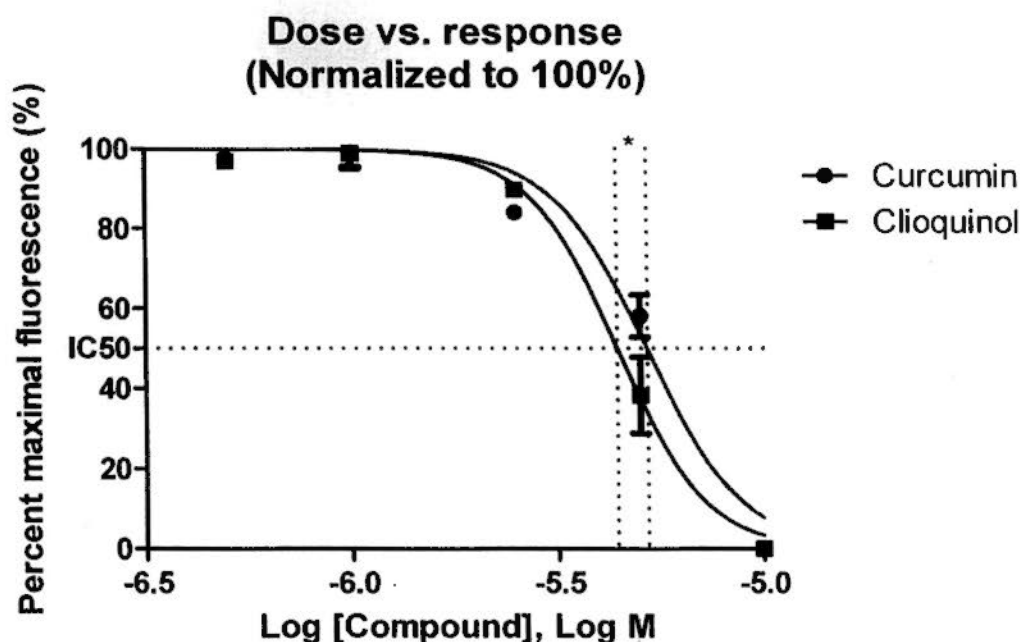


Figure 3.7.1.1.1 H_2O_2 scavenging assay of (A) curcumin and (B) clioquinol. H_2O_2 generated by $A\beta_{1-42}$ peptide in the presence of $Cu(II)$ ions was monitored by the fluorescent signal of DCF. (C) Comparison of dose-response curves of curcumin and clioquinol on inhibition of $A\beta_{1-42}:Cu$ -induced H_2O_2 generation. Significant differences of the effect of increasing concentration of curcumin and clioquinol in (A) and (B) were determined by one-way ANOVA for multiple comparison with Tukey HSD as *post hoc* test. Normalized data were fitted, relative IC_{50} were determined and the significance of differences was determined by nonlinear regression using GraphPad Prism. *, $p < 0.05$; #, $p < 0.0001$.

3.7.2 Microarray of neuroprotective and neurotoxic genes

To examine the neuroprotective and harmful effects of curcumin *in vivo*, RNA was extracted from the hippocampus region of each mouse for global differential gene expression analysis by microarray experiment. Microarray results for genes of interest were examined.

Differential expression data of *Alox15*, *Cd74*, *Gpr3*, *Myocd* and *Ngfr*, which are known to be involved in reducing the level of A β plaques *in vivo* by mechanisms not directly involving APP generation, APP cleavage, A β transport, or A β degradation, are listed in **Table 3.7.2.1**. From the table, it can be seen that curcumin affected expression of most of these genes only in JNPL3 (PB) mice. In these mice, the expression of *Alox15*, *Gpr3* and *Myocd* were reduced by over two fold by curcumin treatment, while the expression of *Cd74* was increased by over three fold.

We then studied the differential expression of genes which have no known effect on A β metabolism but exert protection against A β toxicity. Amongst the numerous genes that have this function, *Fas*, *Igf2*, *Irs1*, *Pla2g4a*, *Rho* and *Tnf* were selected for further examination because curcumin changed their expression about two fold or more in the microarray data. The fold changes of the expression of these genes are listed in **Table 3.7.2.2**. Curcumin suppressed the expression of *Fas*, *Pla2g4a*, *Rho* and *Tnf* by around or over two fold in JNPL3 (PB) mice. On the other hand, curcumin increased the expression of *Igf2* in all mice overexpressing tau: JNPL3 (Chow), JNPL3 (PB), and JNPL3xTg276. Curcumin also increased *Irs1* expression, but only in JNPL3 (PB) mice.

Since the antioxidative properties of curcumin have been studied extensively in many cell-free assays and in vitro studies, we are interested in studying the effect of curcumin on the expression of oxidative stress related genes in vivo. Six genes with a fold change of expression of or over two were selected and are listed in **Table 3.7.2.4**. Amongst them, Duox1, Nos2, Nox1 and Nox3 were downregulated and Bmp6 and Sod3 were upregulated by curcumin in JNPL3 (PB) mice.

Table 3.7.2.1 Fold change of RNA levels of genes involved in decreasing the level of A β plaques in the hippocampus region of selected mice in pooled RNA samples.

Genes	JNPL3 (Chow)	JNPL3 (PB)	Tg2576	JNPL3 x Tg2576
Alox15	-1.09	<u>-2.12</u>	-1.30	-1.03
Cd74	1.22	<u>3.12</u>	-1.17	1.43
Gpr3	-1.09	<u>-2.03</u>	1.25	-1.02
Myocd	1.10	<u>-2.13</u>	-1.20	1.40
Ngfr (p75NTR)	1.13	1.69	1.10	1.47

Samples with fold change over two are underlined for easy reference.

Table 3.7.2.2 Fold change of RNA levels of genes involved in protection against A β toxicity in the hippocampus region of selected mice in pooled RNA samples.

Genes	JNPL3 (Chow)	JNPL3 (PB)	Tg2576	JNPL3 x Tg2576
Fas	-1.35	<u>-2.07</u>	-1.14	1.04
Igf2	<u>2.10</u>	<u>3.66</u>	-1.00	1.82
Irs1	1.03	<u>2.08</u>	1.24	-1.05
Pla2g4a	-1.03	<u>-2.11</u>	-1.21	-1.05
Rho	-1.02	<u>-2.11</u>	-1.08	1.02
Tnf	1.07	-1.97	-1.31	-1.06

Samples with fold change over two are underlined for easy reference.

Table 3.7.2.3 Fold change of RNA levels of genes involved in oxidative stress in the hippocampus region of selected mice in pooled RNA samples.

Genes	JNPL3 (Chow)	JNPL3 (PB)	Tg2576	JNPL3 x Tg2576
Bmp6	1.84	<u>2.75</u>	1.03	1.44
Duox1	-1.07	<u>-2.12</u>	-1.06	1.07
Nos2	-1.02	<u>-2.10</u>	1.21	1.01
Nox1	-1.07	<u>-1.99</u>	1.29	-1.05
Nox3	-1.05	<u>-2.25</u>	1.22	-1.00
Sod3	1.81	<u>3.86</u>	-1.50	1.01

Samples with fold change over two are underlined for easy reference.

3.7.3 Real-time PCR of neuroprotective and neurotoxic genes

To confirm the differential gene expression observed from the microarray experiment, real-time PCR was used. Amongst the genes which are involved in regulating the level of A β production or accumulation, Alox15, Cd74, Gpr3 and Ngfr were further studied. Data are illustrated in **Figure 3.7.3.1.1**. Curcumin treatment of JNPL3xTg2576 mice significantly upregulated Cd74, by over 50 percent, as shown in **Figure 3.7.3.1.1(b)**. Expression of Gpr3 was very significantly higher in all mice treated with curcumin, as shown in **Figure 3.7.3.1.1(c)**.

Regarding the genes involved in providing protection against A β toxicity, Igf2, Irs1, Fas, Pla2g4a, Rho and Tnf were further examined by real-time PCR. Data are presented in **Figure 3.7.3.2.1**. Amongst them, only Igf2 (**Figure 3.7.3.2.1(a)**) and Irs1 (**Figure 3.7.3.2.1(b)**) were very significantly overexpressed in curcumin treated JNPL3 (Chow) mice compared to controls. The mean expression levels of Igf2 and Irs1 were about 130 and 30 percent increased, respectively.

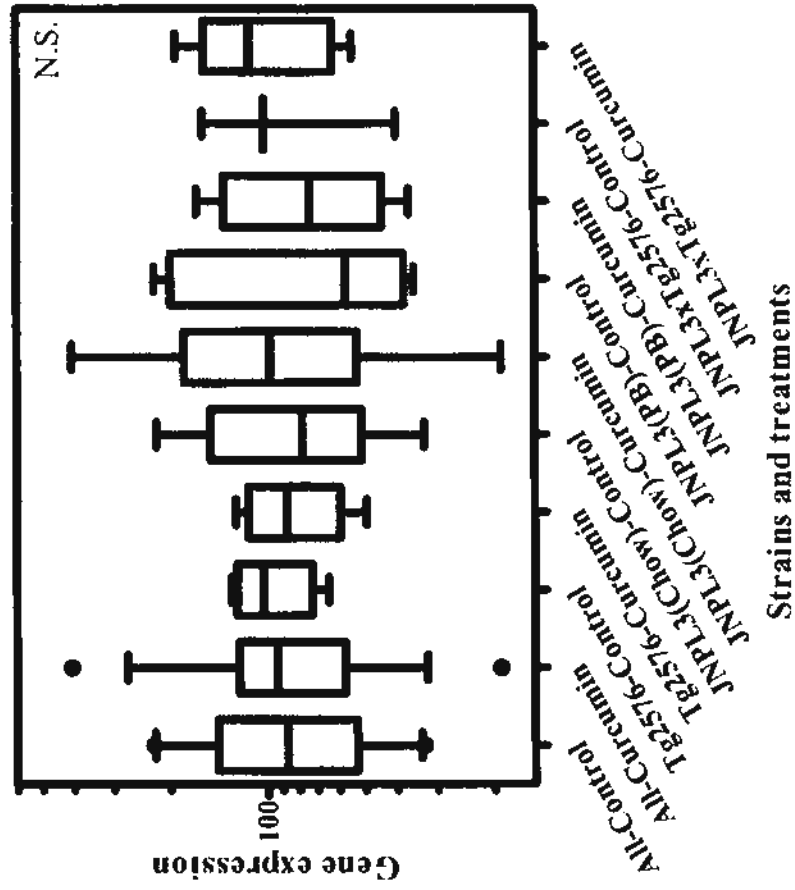
To understand the physiological function of curcumin as an antioxidant in vivo, expression of relevant genes that were reported from the microarray experiment, Duox1, Nos2, Nox1, Nox3, Sod3 and Bmp6, were quantified by real-time PCR. **Figure 3.7.3.3.1** shows their differential expression. Amongst them, curcumin increased expression of several genes. Nos2 was shown to be significantly upregulated, by about 18 percent, in all mice treated with curcumin compared to control treatment (**Figure 3.7.3.3.1(b)**). Analysis by individual groups showed that it was about 25 percent higher in curcumin treated JNPL3 (Chow) mice than controls. Expression of Sod3 was significantly higher, by about 60 percent, in JNPL3 (Chow) mice (**Figure 3.7.3.3.1(e)**). In all mice treated with curcumin, mean expression of

Bmp6 was found to be significantly increased, by 26 percent, compared to mice in control groups (**Figure 3.7.3.3.1(f)**). The difference was even more significant in JNPL3 (Chow) groups, with an increase of 46 percent.

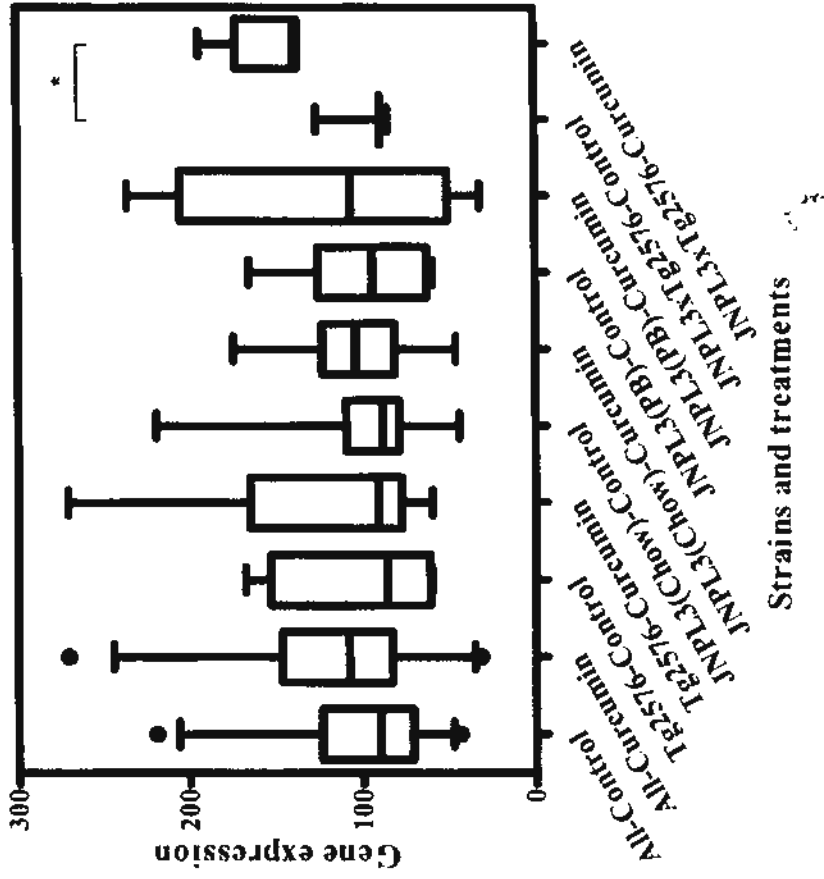
On the contrary, curcumin decreased expression of other genes. The mean expression level of Nox1 was shown to be very significantly reduced, by 30 percent, in all mice (**Figure 3.7.3.3.1(c)**). Individual strain analysis showed that the downregulation of Nox1 was significant only in JNPL3 (Chow) mice, with a 43 percent decrease. Gene expression of Nox3 was also significantly but only very slightly lowered by 6 percent in the Tg2576 strain only (**Figure 3.7.3.3.1(d)**).

3.7.3.1 Gene expression of proteins regulating A β level

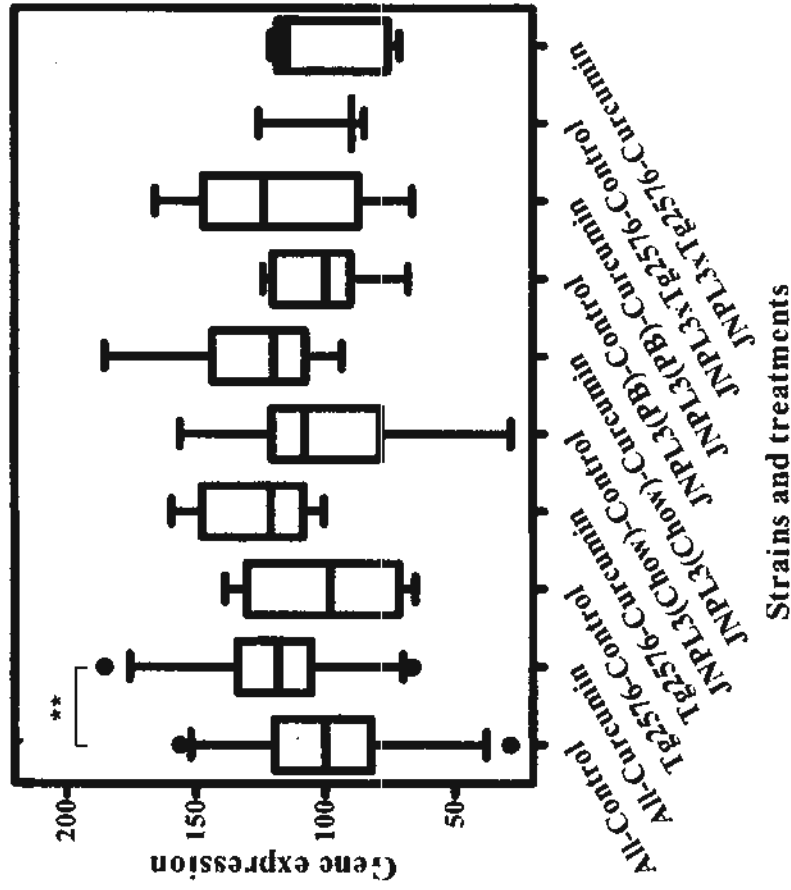
(a) Alox15



(b) Cd74



(c) Gpr3



(d) Ngfr

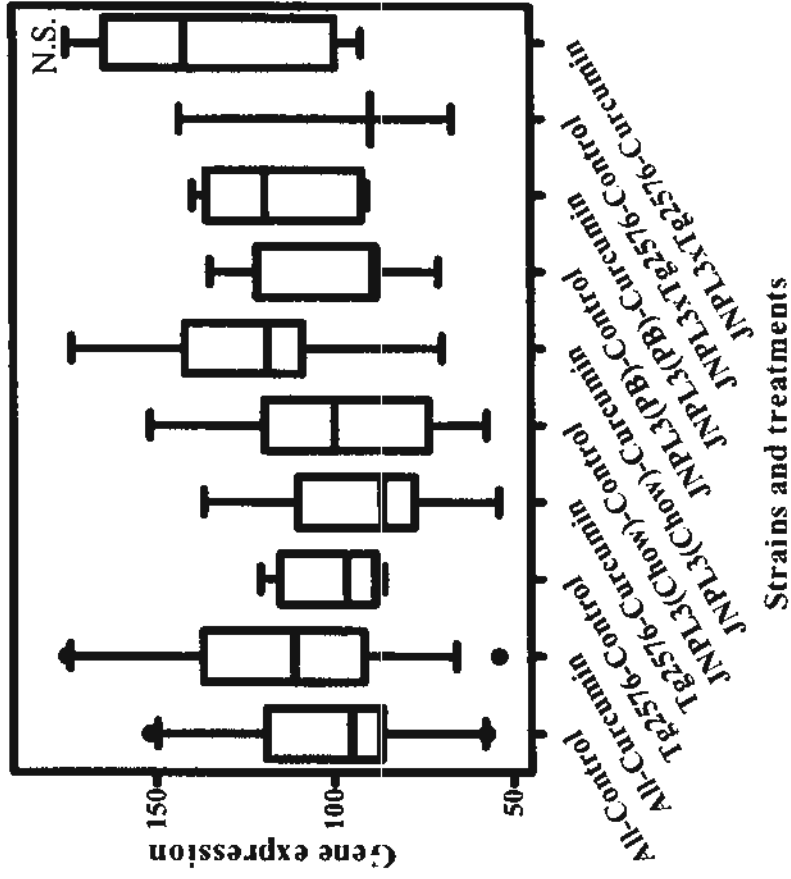
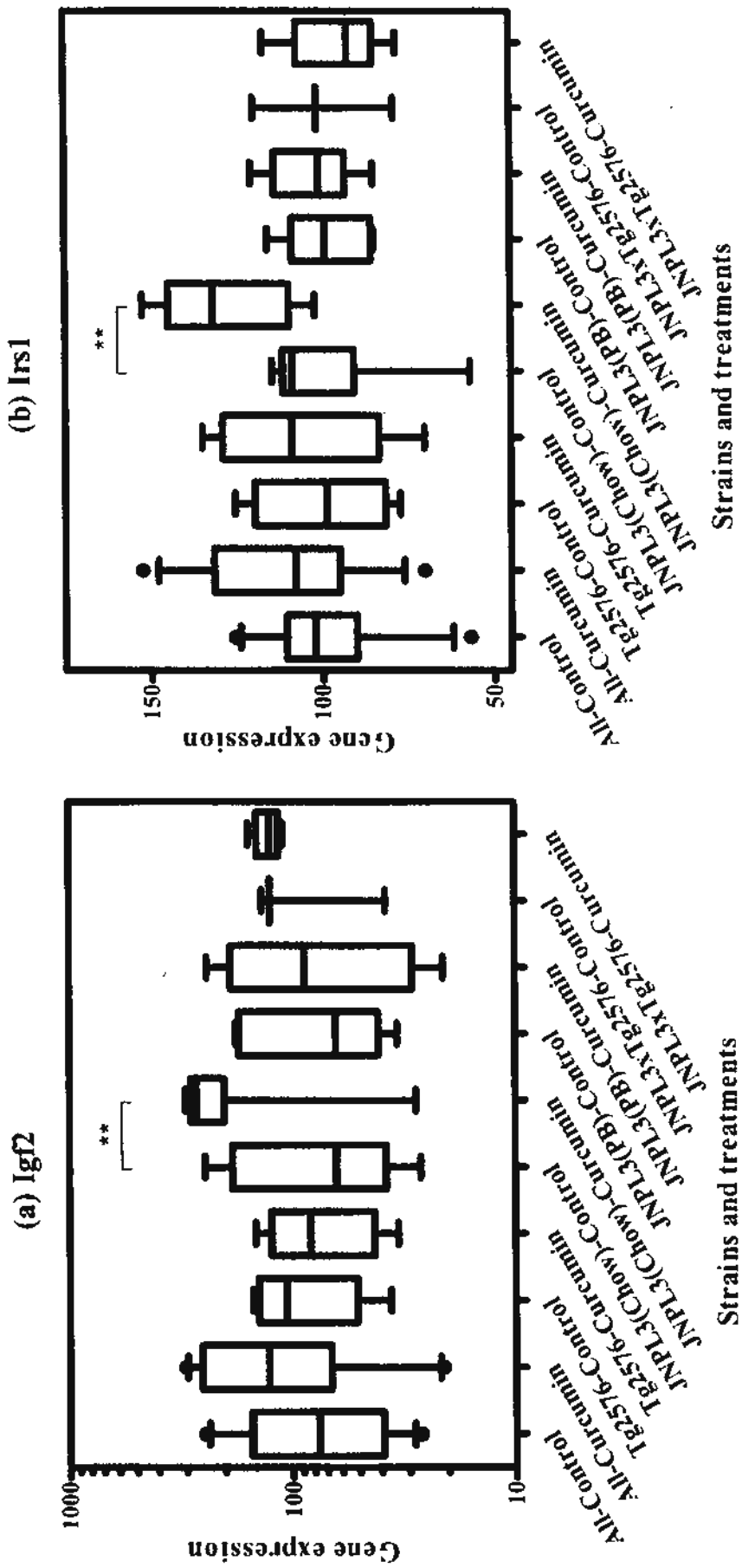
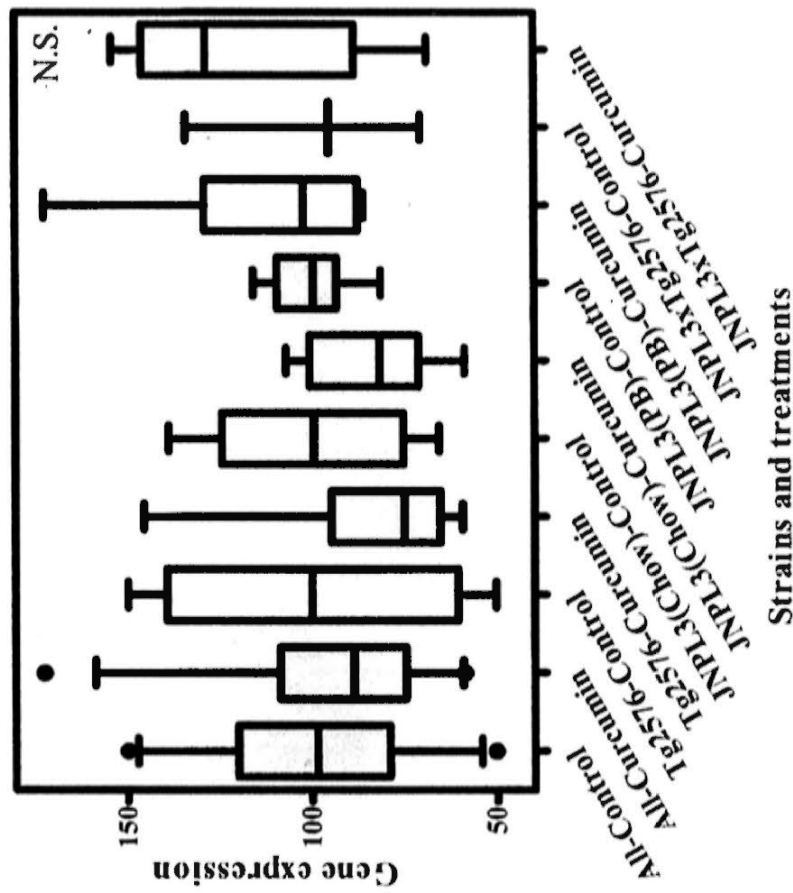


Figure 3.7.3.1.1 Comparison of mRNA expression of (a) Alox15, (b) Cd74, (c) Gpr3 and (d) Ngfr in hippocampus of different mice strains between curcumin treatment and control groups. The boxes indicate median, 25 and 75 percentile; whisker caps indicate 5 and 95 percentile; filled circles indicate outliers. Significant difference between treatment groups of different strains was determined by Mann-Whitney U test using SPSS, and data were plotted using GraphPad Prism. *, $p < 0.05$; **, $p < 0.01$; N.S., no significant difference between treatment and control groups amongst all groups and amongst individual groups.

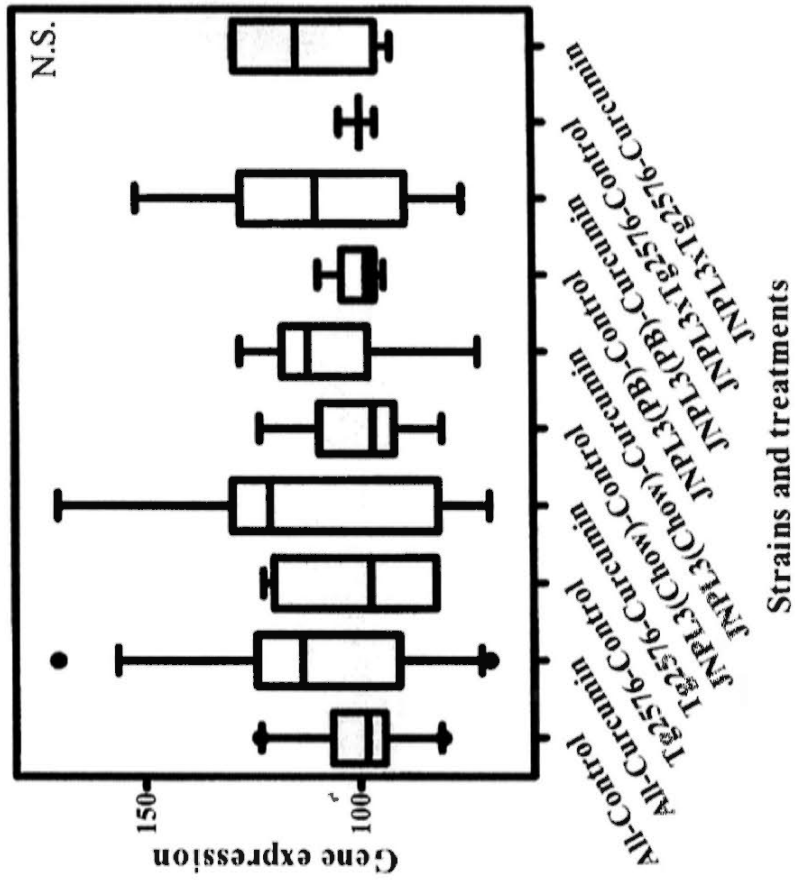
3.7.3.2 Gene expression of proteins reducing A β toxicity



(c) Fas



(d) Pla2g4a



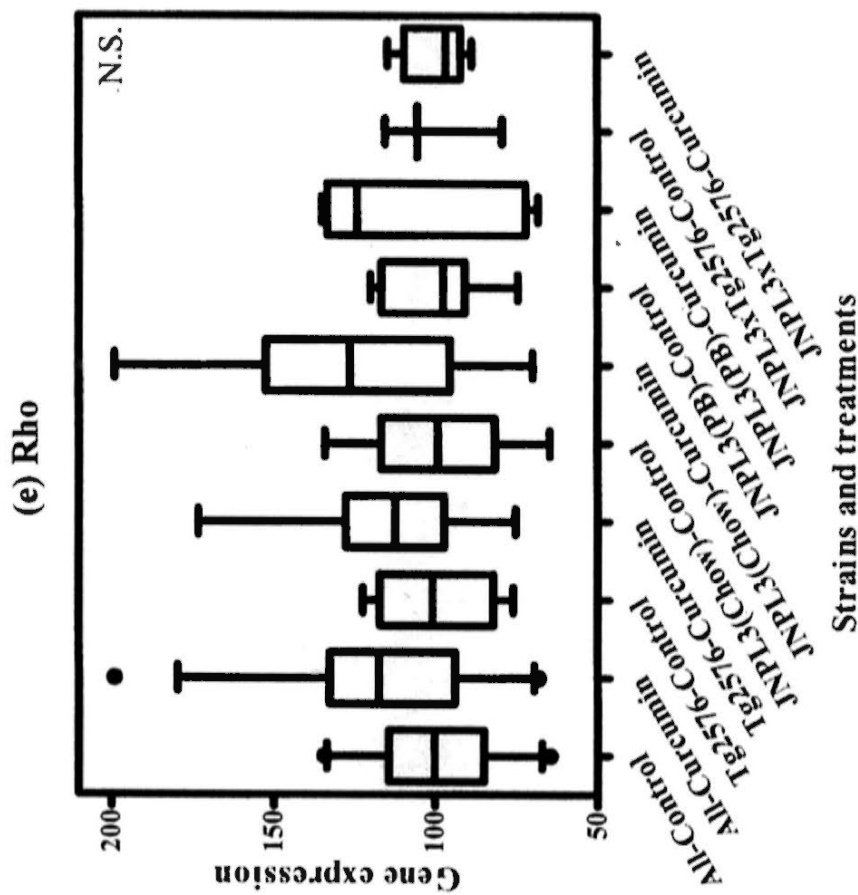
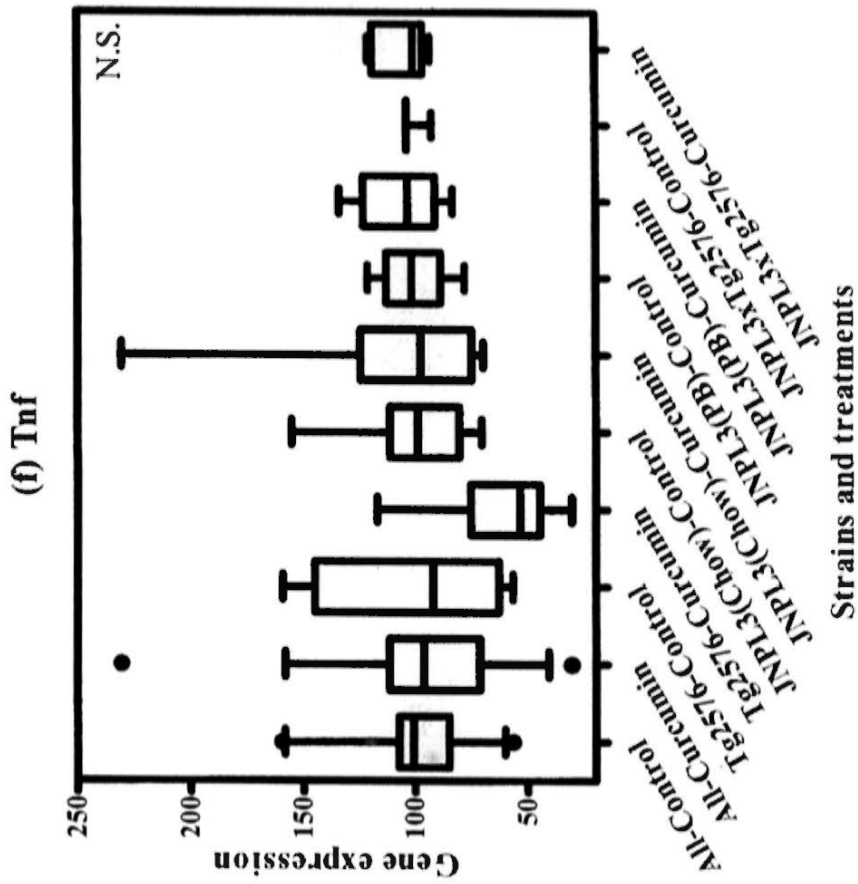
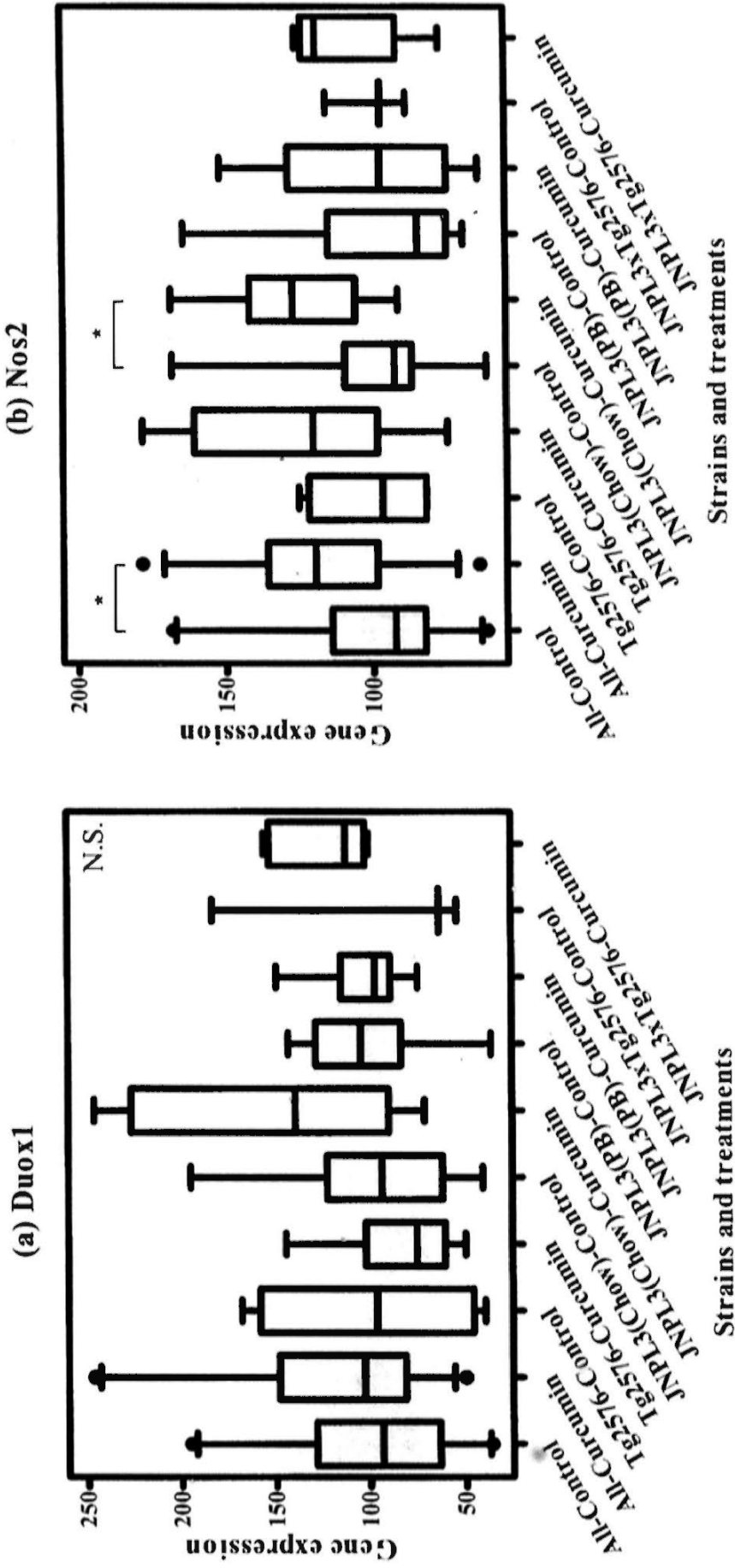
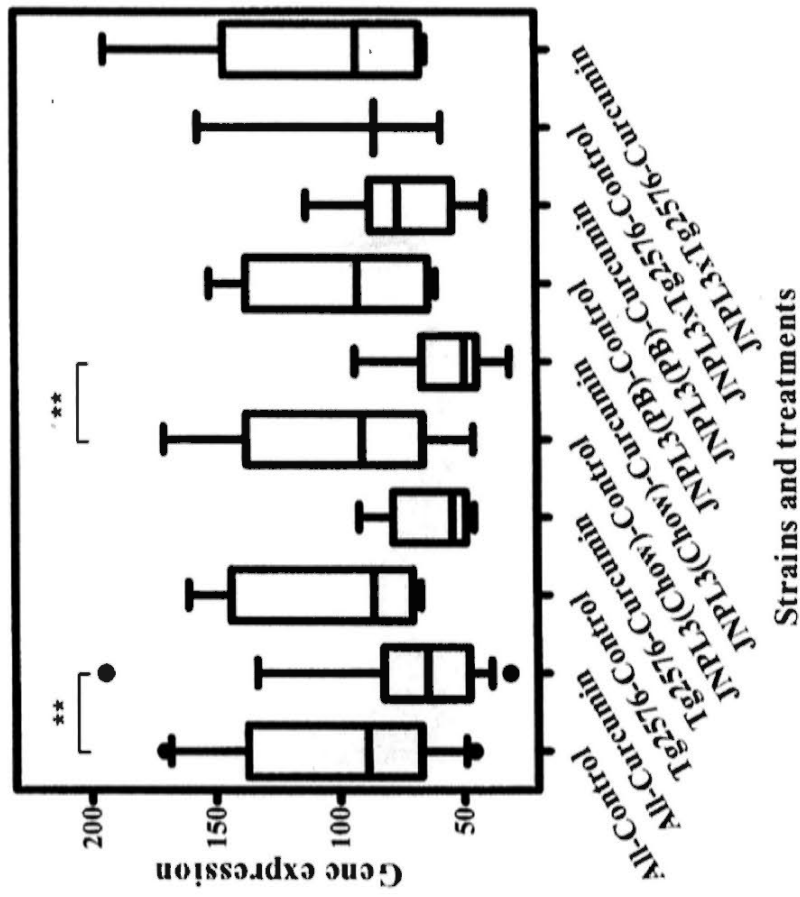


Figure 3.7.3.2.1 Comparison of mRNA expression of (a) Igf2, (b) Irs1, (c) Fas, (d) Pla2g4a, (e) Rho and (f) Tnf in hippocampus of different mice strains between curcumin treatment and control groups. The boxes indicate median, 25 and 75 percentile; whisker caps indicate 5 and 95 percentile; filled circles indicate outliers. Significant difference between treatment groups of different strains was determined by Mann-Whitney U test using SPSS, and data were plotted using GraphPad Prism. *, $p < 0.05$; **, $p < 0.01$.

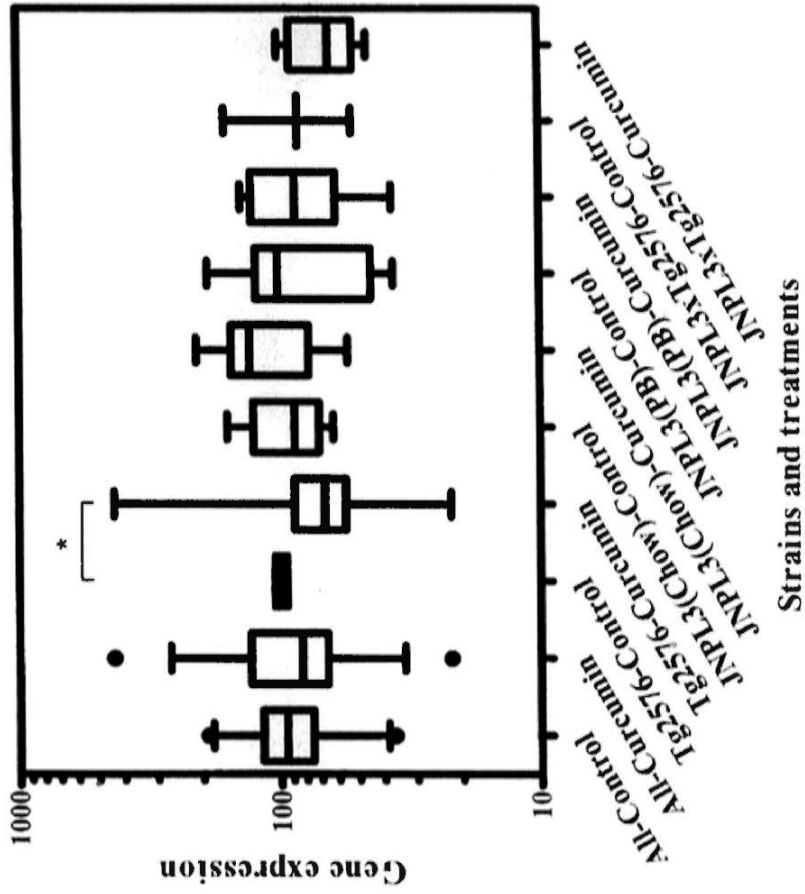
3.7.3.3 Gene expression of proteins involving oxidative stress



(c) Nox1



(d) Nox3



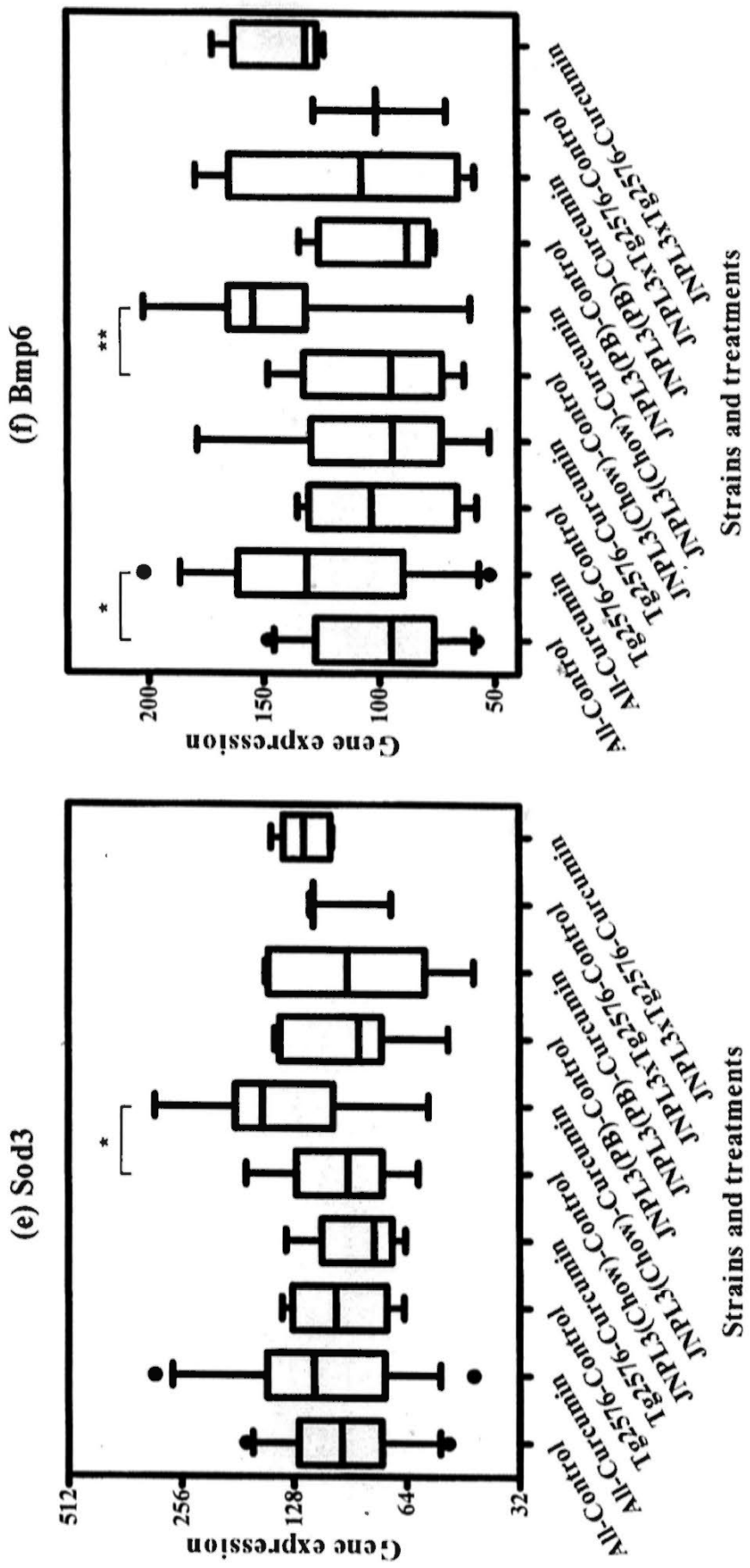


Figure 3.7.3.3.1 Comparison of mRNA expressions of (a) Duox1, (b) Nos2, (c) Nox1, (d) Nox3, (e) Sod3 and (f) Bmp6 in hippocampus of different mice strains between curcumin treatment and control groups. The boxes indicate median, 25 and 75 percentile; whisker caps indicate 5 and 95 percentile; filled circles indicate outliers. Significant difference between treatment groups of different strains was determined by Mann-Whitney U test using SPSS, and data were plotted using GraphPad Prism. *, $p < 0.05$; **, $p < 0.01$; N.S., no significant difference between treatment and control groups amongst all groups and amongst individual groups.

3.8 Effects of Curcumin on Tauopathy

To investigate the effects of curcumin on tauopathy *in vivo*, a transgenic mouse model, JNPL3, was used. JNPL3 mice overexpress human mutant P301L tau protein from the *Mapt* gene. Due to the presence of this mutant transgene, the mice develop intracellular neurofibrillary tangles (NFT) as they grow old. NFT appear extensively in some brain regions, such as spinal cord, medulla, pons, hypothalamus and thalamus, and to a lesser extent in amygdala and entorhinal cortex. Therefore, the effect of curcumin on tauopathy can be studied by monitoring the level of NFT in these regions after the course of treatment.

Before studying the final effect on NFT development, we are interested to determine whether curcumin has any effect on the expression of the endogenous *Mapt* gene, especially in the hippocampus region since NFT are particularly abundant in the human AD hippocampus, so that we would know whether the final level of NFT is due partly to a change in the endogenous tau expression level. From the microarray data shown in **Table 3.8.1.1.1**, curcumin did not alter the expression of *mapt* in the hippocampus in any group of mice. This negative result was then confirmed by real-time PCR, and the data are shown in **Figure 3.8.1.2.1**.

Next, we are interested to know if curcumin has any effect on the protein expression level of mutant tau in the brain. Cortical regions were used for western blotting, and the total level of human mutant tau was detected by antibody HT7, which is specific for human tau protein. One representative western blot image of each sex is shown in **Figure 3.8.2.1.1**. Parts (A) and (B) of the figure show male and female JNPL3 mice, respectively, treated with or without curcumin in chow as vehicle for six months. Results were analysed and illustrated in **Figure 3.8.2.1.1(C)**. They

show that there was no significant difference of human mutant tau protein level between the mice in curcumin and control groups. However, inspecting the western blot image of females revealed that the mutant tau protein level varied widely. Some female JNPL3 mice did not have mutant tau protein at a detectable level.

Then, we determined the change of the level of NFT in male and female JNPL3 mice treated with or without curcumin for six months in chow as vehicle. We examined the pons since this brain region was reported to have high numbers of NFTs in JNPL3 mice. A very traditional technique, namely Bielschowsky's silver staining, was used to detect NFTs, which appeared as deep brown to black intracellular structures in the pons. Images of the staining of the pons region of male JNPL3 mice are shown in **Figure 3.8.3.1.1**. The number of tangles was recorded and compared, which revealed that curcumin tended to reduce the number of tangles in male mice, but the effect was not statistically significant. **Figure 3.8.3.1.2** compares the number of tangles in male and female JNPL3 mice treated with or without curcumin for six months. Due to the wide variation of the expression of mutant tau and the numbers of tangles, female mice were excluded from further analysis of tauopathy.

Bielschowsky's staining suffers from a high background signal. To reduce the background staining, we performed immunohistochemical staining using antibody AT8, which specifically detects phosphorylated tau protein and thus labels NFTs. The staining was done on the entorhinal cortex/amygdala and medulla. Images of AT8 immunostaining of male JNPL3 mice treated with or without curcumin in chow as vehicle for six months are shown for medulla (**Figure 3.8.3.2.1**) and entorhinal cortex/amygdala (**Figure 3.8.3.2.2**). Comparisons of the percentage area covered by AT8-positive staining of medulla and entorhinal cortex/amygdala are shown in **Figure 3.8.3.2.3 (A) and (B)**, respectively. There were no significant differences

between curcumin-treated and untreated brains in the AT8-positive area in either medulla and entorhinal cortex/amygdala.

Since the Bielschowsky's silver staining and the immunostaining revealed that the numbers of NFTs are very low. We suspected that the mice had not developed enough NFT pathology for comparison. Therefore, we added another group of male JNPL3 mice at an older age: 16 months before treatment. The mice were administered peanut butter with or without curcumin for 10 weeks. The medulla and entorhinal cortex/amygdala regions were stained with AT8, and the images are shown in **Figure 3.8.3.2.4** and **Figure 3.8.3.2.5**, respectively. Comparisons of the AT8-positive area in medulla and entorhinal cortex of mice treated with or without curcumin are shown in **Figure 3.8.3.2.6 (A)** and **Figure 3.8.3.2.6 (B)**, respectively. Interestingly, curcumin significantly reduced the AT8-positive area in the medulla region (by 75 percent) but not in the entorhinal cortex/amygdala regions.

The main component of NFT is paired helical filaments (PHF). To further investigate whether there was any effect of curcumin on tauopathy in the younger JNPL3 mice (age 8 months before treatment) treated with or without curcumin for six months, we isolated PHF and compared their levels in the cortex. After isolating the sarkosyl insoluble fraction, which is supposed to contain most of the PHF, the levels of PHF were compared by western blotting. Blots of male and female mice are shown in **Figure 3.8.4.1 (A)** and **Figure 3.8.4.1 (B)**, respectively. Comparisons of the levels of PHF are shown in **Figure 3.8.4.2**. The data showed that curcumin did not reduce the level of PHF in male or female JNPL3 mice.

3.8.1 Gene expression of endogenous Mapt

3.8.1.1 Microarray of Mapt

Table 3.8.1.1.1 Fold change of RNA level of Mapt in the hippocampus region of selected mice in pooled RNA samples.

Genes	JNPL3 (Chow)	JNPL3 (PB)	Tg2576	JNPL3 x Tg2576
Mapt	-1.13	1.02	1.11	-1.03

3.8.1.2 Gene expression of endogenous Mapt by real-time PCR

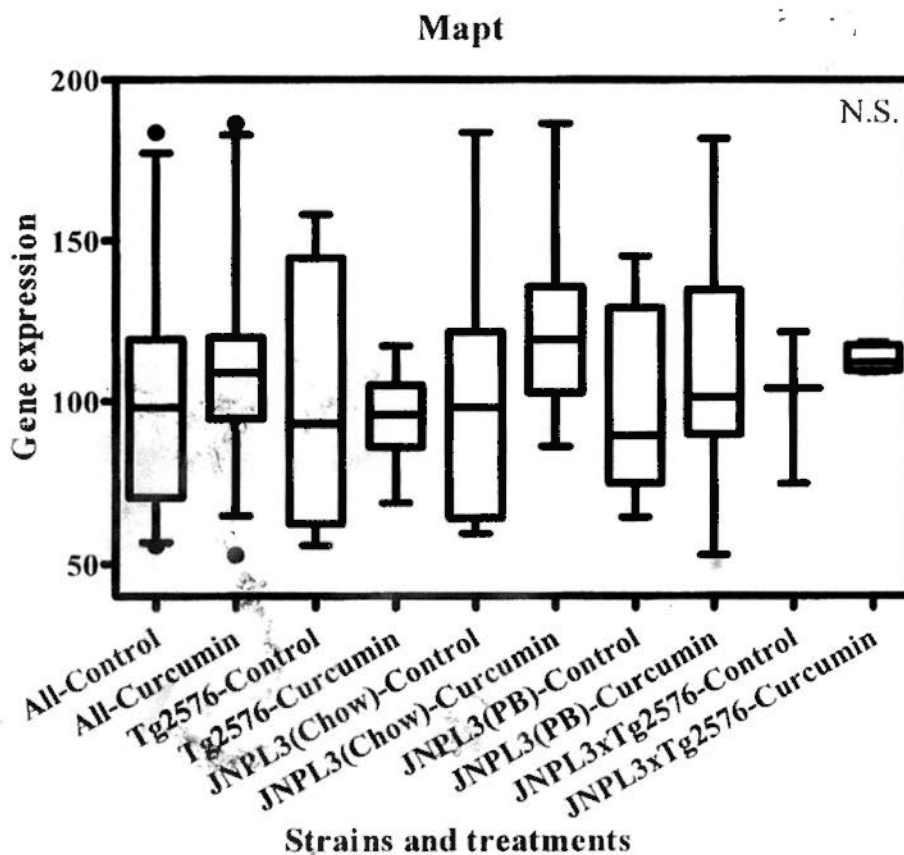


Figure 3.8.1.2.1 Comparison of mRNA expression of Mapt in hippocampus of different mice strains between curcumin treatment and control groups. The boxes indicate median, 25 and 75 percentile; whisker caps indicate 5 and 95 percentile; filled circles indicate outliers. Data were analyzed by Mann-Whitney U test using SPSS, and were plotted using GraphPad Prism. No significant differences (N.S.) due to curcumin were found in any group or amongst all groups.

3.8.2 Protein expression of transgenic mutant tau

3.8.2.1 Total human mutant tau expression

A. Male JNPL3



B. Female JNPL3



C.

Total human mutant tau protein level of JNPL3

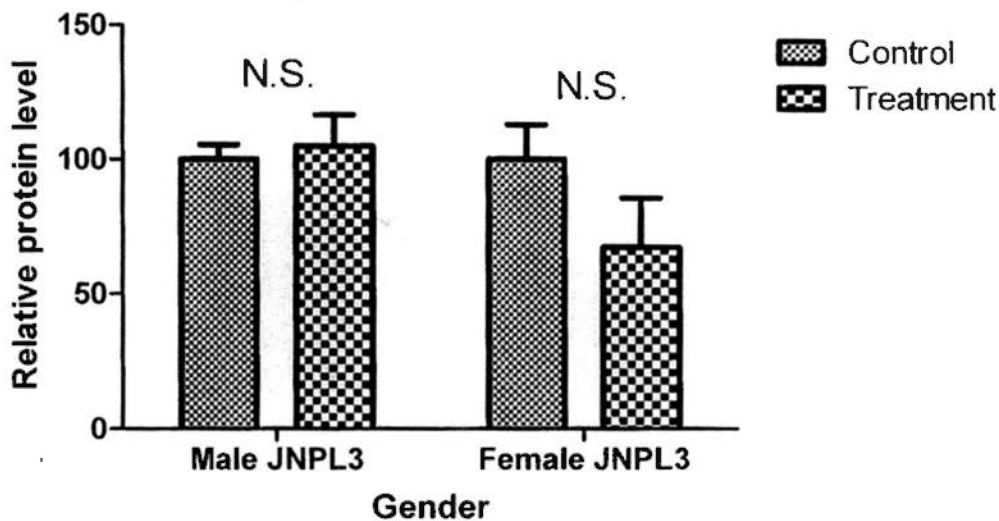


Figure 3.8.2.1.1 Western blotting analysis comparing the total human mutant tau protein expression level in the cortex of JNPL3 mice treated with or without curcumin in chow as vehicle for six months. (A) Selected blot of male JNPL3 mice. (B) Selected blot of female mice. T, curcumin treatment; C, control treatment. (C) Quantification of the protein level of treatment and control samples. Data from the blots were quantified using ImageJ software. Results are expressed as mean \pm SEM. Statistical differences between control and curcumin groups were determined by Student's t-test using SPSS, and were plotted using GraphPad Prism. N.S., no significant difference.

3.8.3 Neurofibrillary tangles

3.8.3.1 Bielschowsky's silver staining

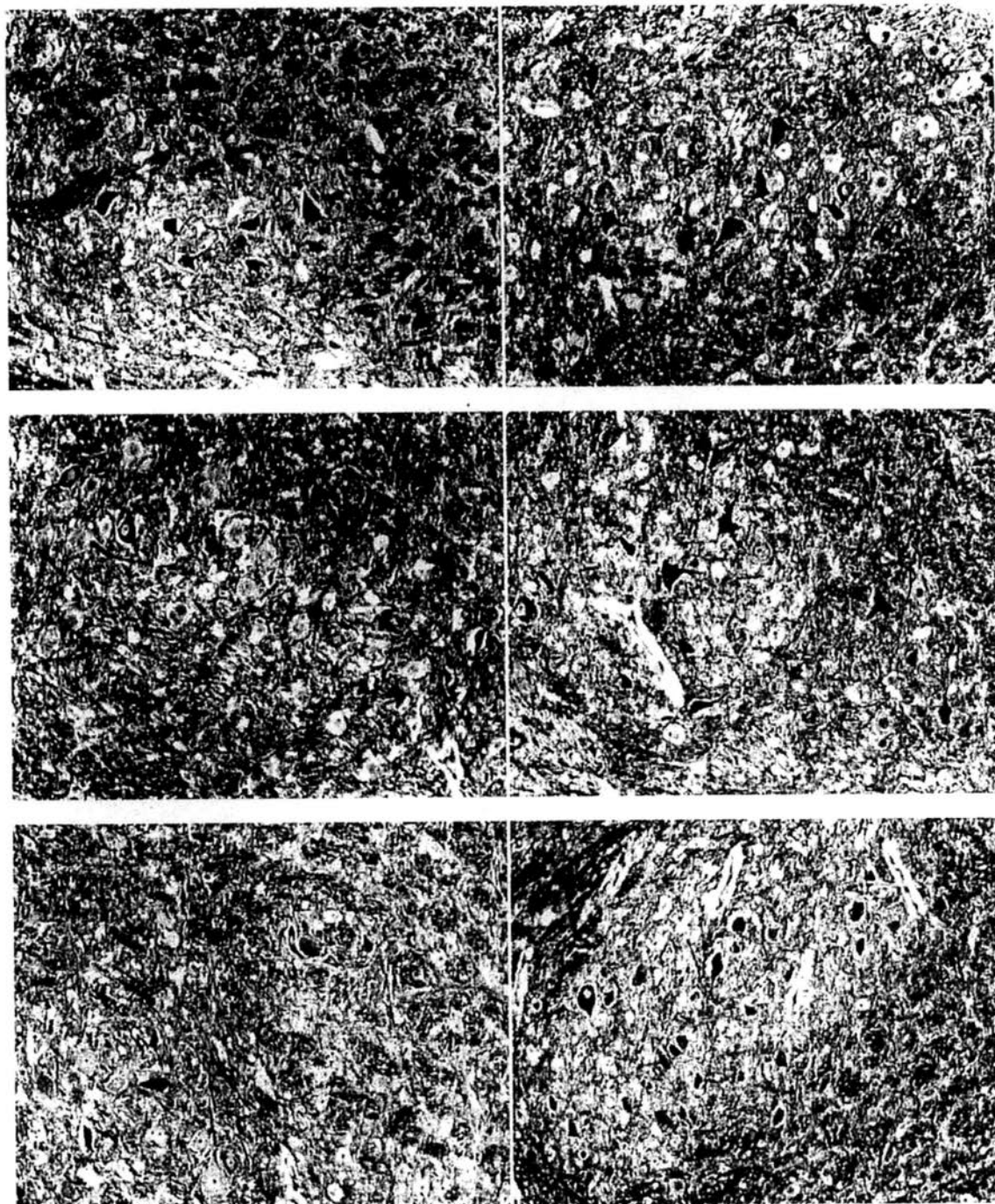


Figure 3.8.3.1.1 Bielschowsky's silver staining of pons sections of male JNPL3 mice treated with (left) or without (right) curcumin in chow as vehicle.

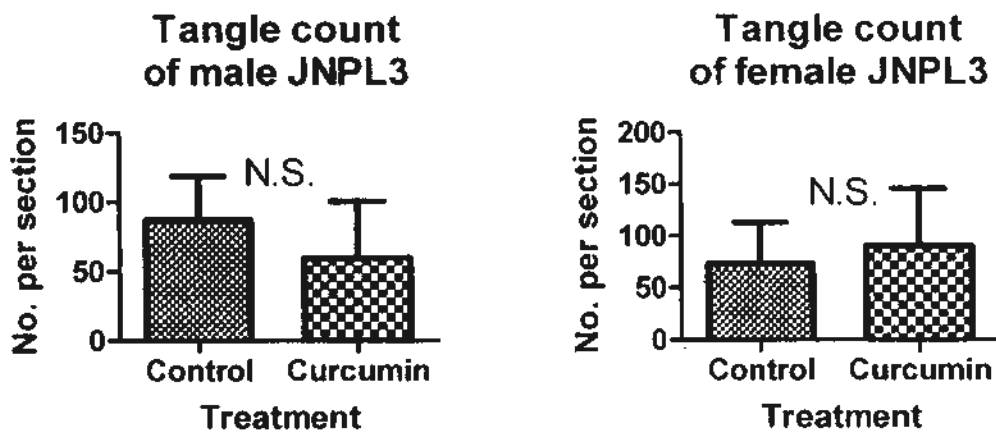


Figure 3.8.3.1.2 Quantification of the number of tangles in pons sections of JNPL3 male and female mice treated with or without curcumin in chow as vehicle. Results are expressed as mean \pm SD. Statistical difference between control and curcumin groups was determined by Student's t-test using SPSS, and was plotted using GraphPad Prism. N.S., no significant difference.

3.8.3.2 Immunohistochemical staining of AT8-immunopositive tangle



Figure 3.8.3.2.1 Immunohistochemical staining of neurofibrillary tangles of the medulla of male JNPL3 mice treated with (left) or without (right) curcumin in chow as vehicle. Antibody AT8, which is specific for phosphorylated tau, was used. Images were captured at 40x magnification.

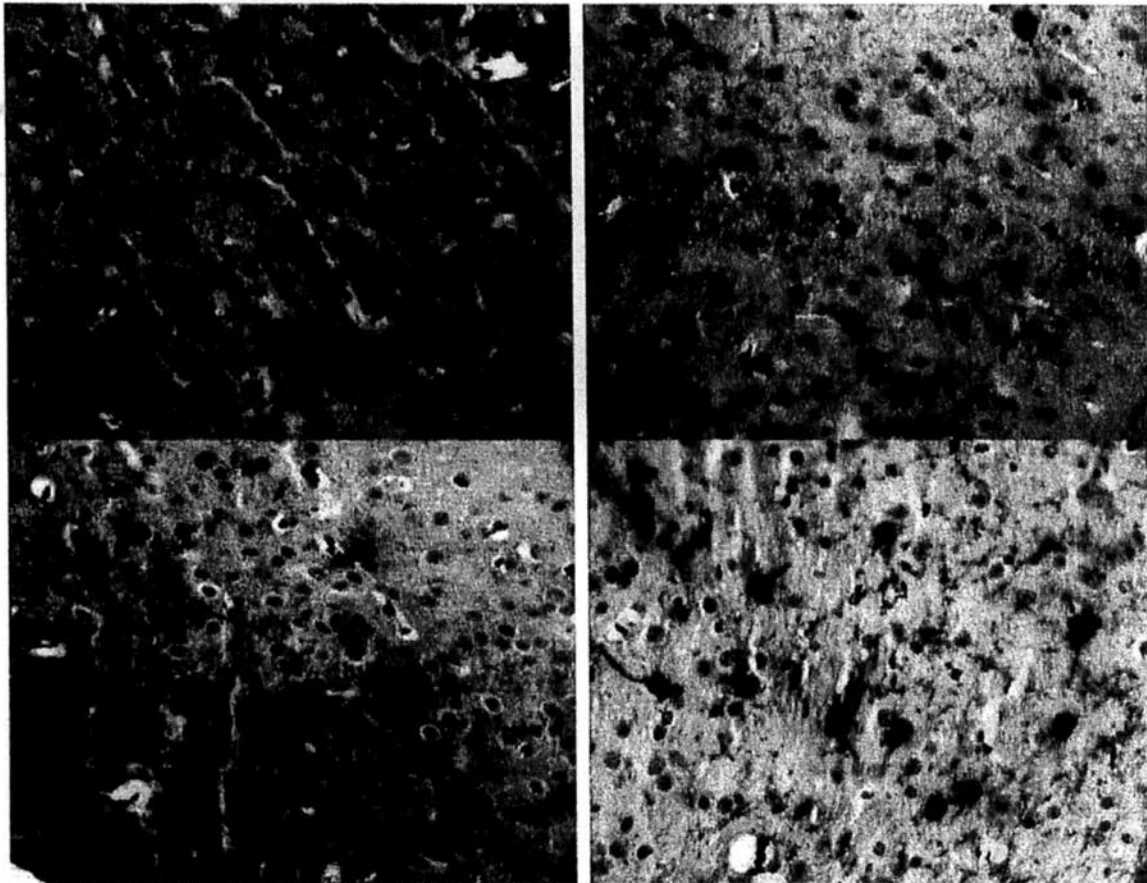


Figure 3.8.3.2.2 Immunohistochemical staining of neurofibrillary tangles of the entorhinal cortex and amygdala regions of male JNPL3 mice treated with (left) or without (right) curcumin in chow as vehicle. Antibody AT8 was used. Images were captured at 40x magnification.

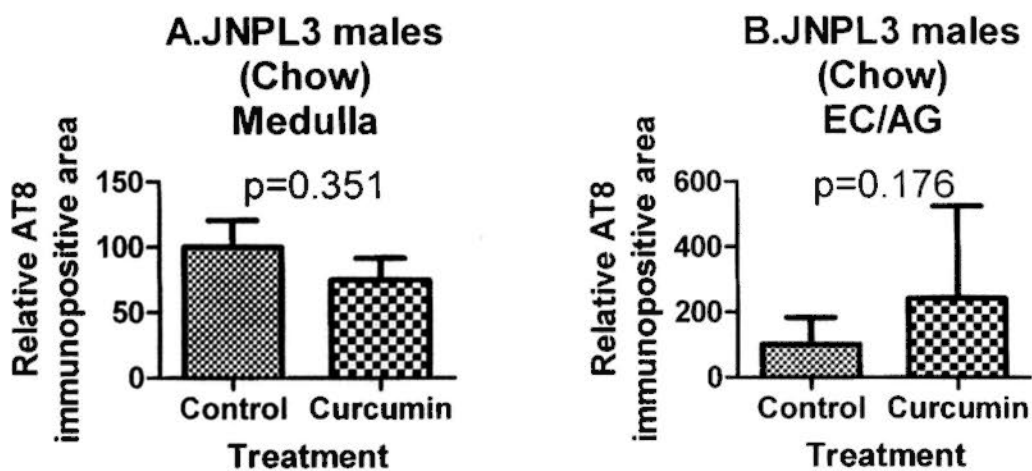


Figure 3.8.3.2.3 Quantification of percentage tangle (AT8-immunopositive) area in (A) medulla and (B) EC/AG sections of JNPL3 male mice treated with or without curcumin in chow as vehicle. Data are normalized to 100 for the control group. Results are expressed as mean \pm SEM. Statistical differences between control and curcumin groups were determined by Student's t-test using SPSS, and were plotted using GraphPad Prism. N.S., no significant difference. EC/AG, entorhinal cortex and amygdala.

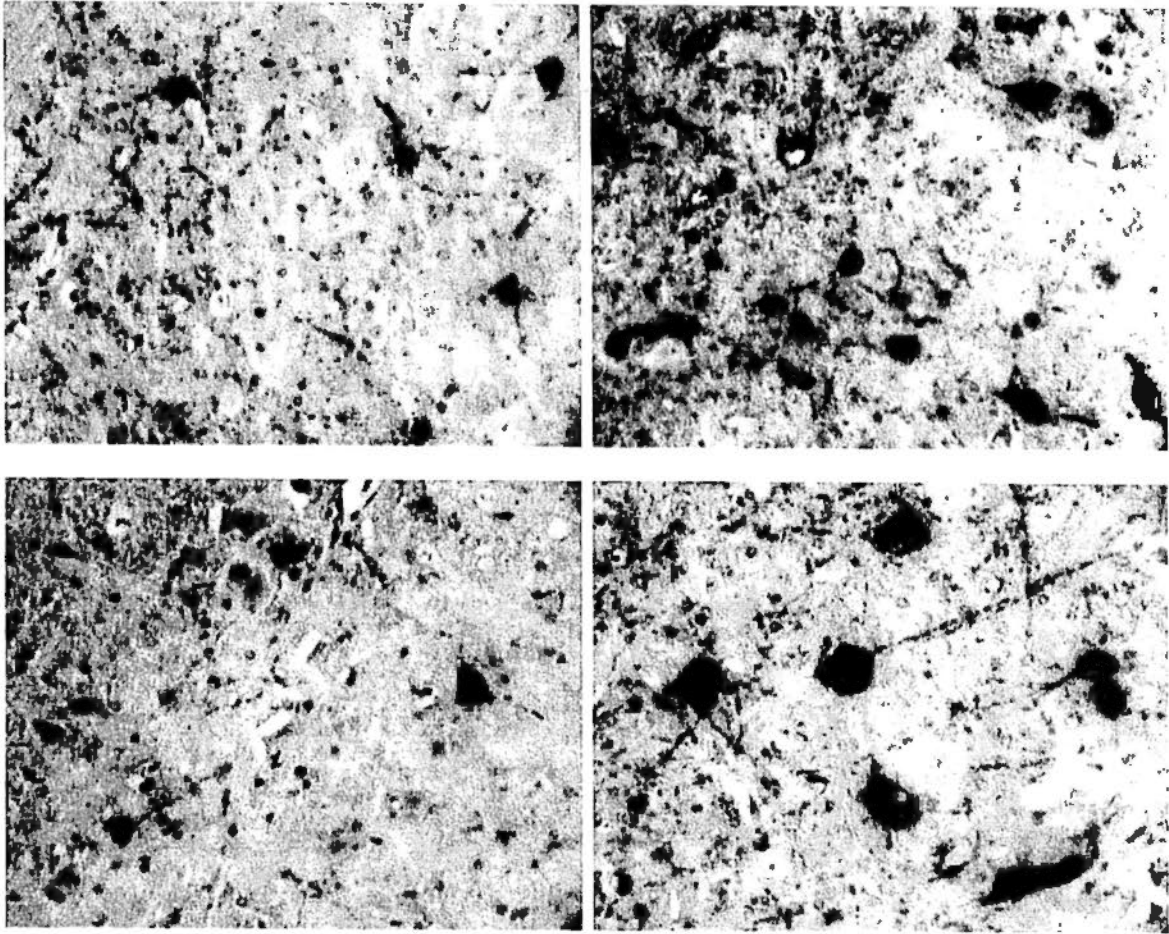


Figure 3.8.3.2.4 Immunohistochemical staining of neurofibrillary tangles of the medulla of male JNPL3 mice treated with (left) or without (right) curcumin in peanut butter as vehicle. Antibody AT8 was used. Images were captured at 40x magnification.

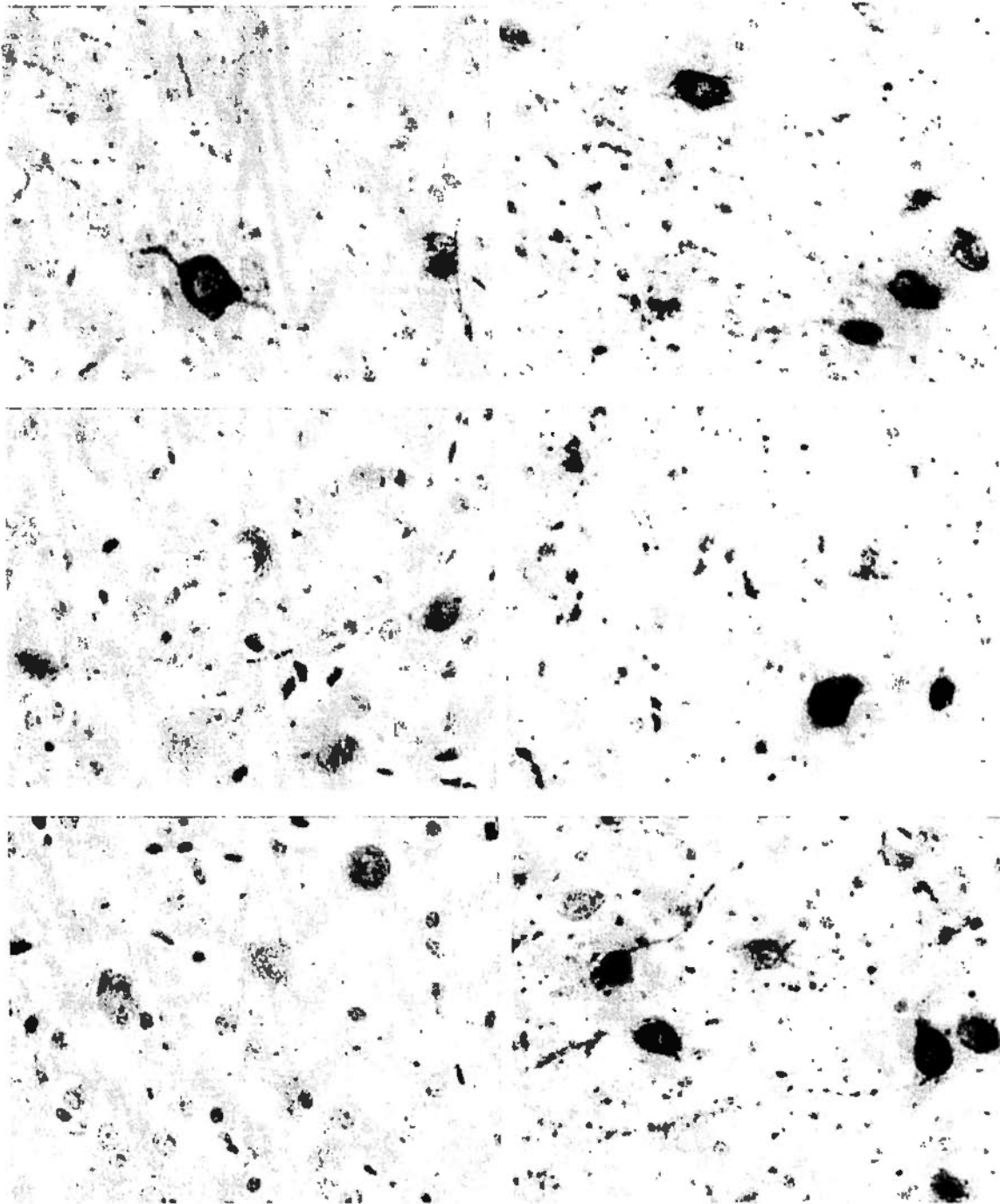


Figure 3.8.3.2.5 Immunohistochemical staining of neurofibrillary tangles of the entorhinal cortex and amygdala regions of male JNPL3 mice treated with (left) or without (right) curcumin in peanut butter as vehicle. Antibody AT8 was used. Images were captured at 40x magnification.

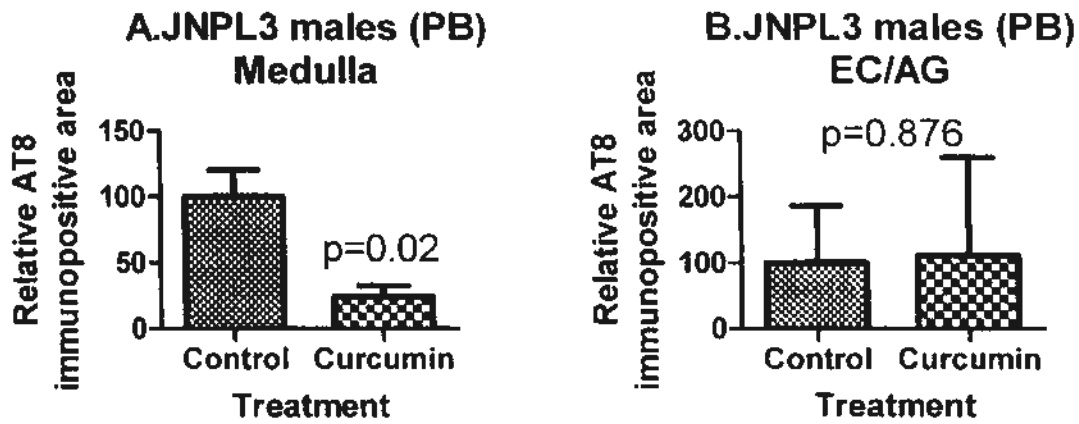
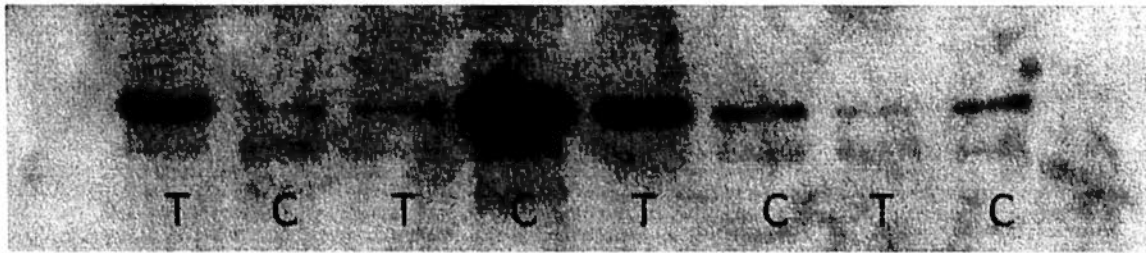


Figure 3.8.3.2.6 Quantification of percentage tangle (AT8-immunopositive) area in (A) medulla and (B) EC/AG sections of JNPL3 male mice treated with or without curcumin in peanut butter as vehicle. Data are normalized to 100 for the control group. Results are expressed as mean \pm SEM. Statistical differences between control and curcumin groups were compared by Student's t-test using SPSS, and were plotted using GraphPad Prism. *, $p < 0.05$; N.S., no significant difference. EC/AG, entorhinal cortex and amygdala.

3.8.4 PHF level

A. Male



B. Female

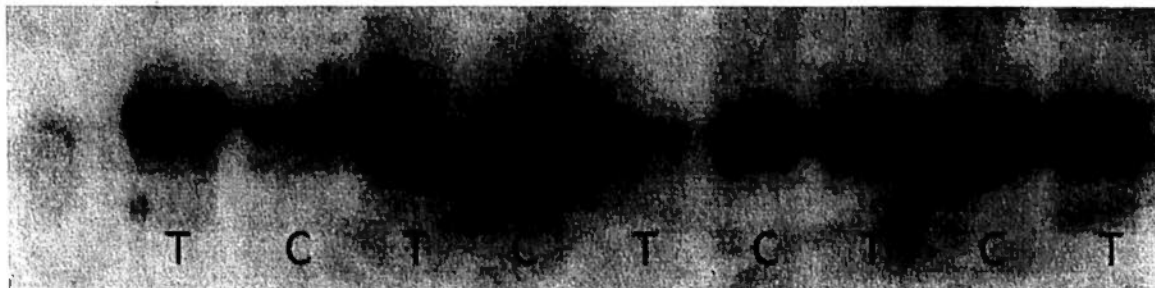


Figure 3.8.4.1 Representative Western blots of sarkosyl-insoluble tau (PHF) extracted from the cortex of JNPL3 mice treated with or without curcumin in chow. (A) male and (B) female mice. T, curcumin treatment; C, control.

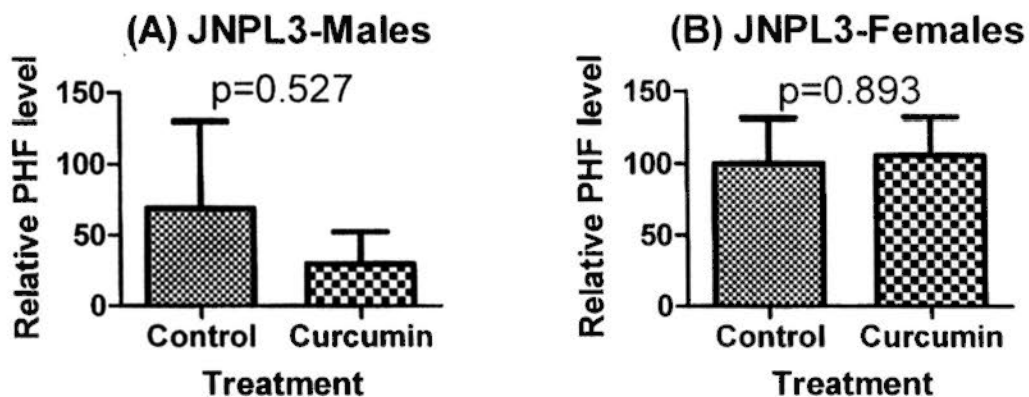


Figure 3.8.4.2 Quantification of PHF from JNPL3 male and female mice treated with or without curcumin in chow as vehicle. Data from blots were quantified using ImageJ software. Results are expressed as mean \pm SEM. Statistical differences between control and curcumin groups were compared by Student's t-test using SPSS and were plotted using GraphPad Prism. N.S., no significant difference.

CHAPTER FOUR: DISCUSSION

4.1 Effects of curcumin on phenotypic changes

As a preliminary study using animals at the most elementary level, the health of the subjects was monitored for any possible side effects that could not be identified in cell culture studies. Body weight change is easily observable. Mortality is especially important in assessing the safe use of a medicine for long term treatment. In addition, for a particular disease model, specific behavioural assessment which characterizes the beneficial use of the medicine in curing the disease is of the ultimate importance.

4.1.1 Effect of curcumin treatment on body weight

Our finding suggests that long term use of curcumin has a significant effect on slowing the loss of body weight. This effect is consistent in most strains of both sexes and particularly statistically significant in males of the JNPL3xTg2576 strain, females of the JNPL3 strain, and the combination of both sexes and all strains. This finding is our first evidence which suggests that prolonged use of curcumin is not harmful and, at the same time, may delay or slow the aging progress. The transgenic mouse models of AD we use in this study develop symptoms and histopathological features only at old ages. The body weight generally decreases along with physical activities, which suggests that the aging progress and the disease have already begun. In fact there is a study showing that the onset of disease in JNPL3 mice is followed by weight loss (Bolmont et al., 2007). In aging, Tg2576 mice become less aggressive, JNPL3 mice begin to have paralysed hind legs, and JNPL3xTg2576 mice (which are the offspring

of female JNPL3 and male Tg2576 mice) show both features even earlier than either parent strain.

Therefore, by slowing the loss of body weight, it is possible that curcumin may delay the onset or slow the rate of aging and, to some extent, AD. Body weight could be affected by many factors, such as physical exercise, metabolic rate and the amount of food intake. It has been suggested that aging is inversely associated with insulin sensitivity and protein level of glucose transporter 4 (Glut4) (Houmard et al., 1995). Another study showed that curcumin increases glucose uptake into the skeletal muscles in vitro by upregulation of membrane Glut4 expression in a muscarinic M-1 cholinceptor and phosphoinositide 3-kinase dependent manner (Cheng et al., 2009). Taken together, this evidence suggests that curcumin may slow the loss of body weight during aging by increasing glucose uptake into skeletal muscle.

Moreover, some studies suggest an association between body weight loss and AD (Cronin-Stubbs et al., 1997; Wolf-Klein and Silverstone, 1994), or the use of accelerated weight loss as a preclinical indicator of AD (Johnson et al., 2006). Therefore, our observations suggest that curcumin may slow the progression of AD. Nevertheless, there is a lack of studies suggesting whether there is any relationship between glucose uptake into skeletal muscle and AD, and the mechanism connecting accelerated weight loss with AD is still unknown (Wolf-Klein and Silverstone, 1994). Although the mechanism by which curcumin slows body weight loss is outside the scope of this study, it is worth further investigation, as is the connection between body weight loss and AD.

4.1.2 Mortality upon curcumin treatment

Further investigation into the toxicity of long term use of curcumin suggests that it significantly reduced the mortality of all mice treated with curcumin in this study. The effect was significant in male but not female mice, which suggests that the protection has a gender-dependent effect. Performing analyses of individual strains found that curcumin significantly reduced the mortality of only one strain, male JNPL3xTg2576 mice, which suggest that it has a strain-dependent effect. However, all strains and treatments of male mice exhibited a tendency toward protection by curcumin, thus it is possible that experiments using larger numbers of mice would demonstrate significant mortality reduction of all groups of male mice. Although there is one report that curcumin extends life span in *Drosophila melanogaster* (Lee et al., 2010), our study is the first to show that long term use of curcumin reduces mortality in mammalian AD models.

Loss of statistical significance in females often occurs in animal studies due to physiological variations of the reproductive system. Therefore, by excluding all female mice, the analysis showed that the reduced mortality was much more statistically significant.

It has already been shown that transgenic mice which overexpress the human Swedish mutant APP transgene have high premature lethality (Hsiao et al., 1995). Another report mentioned that mice of the Tg2576 strain had increased mortality, especially during the ages of six to 12 months, compared to a non-transgenic background strain (King and Arendash, 2002). There is no report on whether the survival rate is affected in JNPL3 mice, which overexpress mutant Mapt. The offspring produced by crossing JNPL3 and Tg2576 have earlier and more severe and

extensive development of neurofibrillary tangles but not of plaques, which suggests that the interaction of mutant APP and Mapt enhanced the toxicity of tauopathy (Lewis et al., 2001). Thus, it is possible that the exaggerated toxicity induced by the overexpression of both mutant APP and Mapt increases mortality in JNPL3xTg2576. In our study, we noticed that JNPL3xTg2576 mice died earlier than their parent strains. Therefore, we had shifted our design to use younger mice of this strain for long term curcumin treatment.

After the course of treatment, we noticed the reduced mortality with curcumin treatment of JNPL3 and more obviously of Tg2576, though the reduction did not reach statistical significance. Curcumin reduced the mortality of JNPL3xTg2576 to a greater degree than either of its parents, suggesting that the toxicities from overexpressing mutant APP or Mapt are enhanced in this strain. Therefore, curcumin may target these toxicities by multiple pathways.

Here, we must emphasize that most human AD patients, unlike our transgenic mice, have neither APP nor Mapt mutations and have late-onset disease without a drastic decrease in longevity. The search for possible mechanisms by which curcumin reduces mortality are not in the scope of this study. Our result does not suggest that long term curcumin treatment can extend the life span of other animal models of AD or of human patients. Rather, it suggests that curcumin may ameliorate the adverse effects exerted by overexpression of mutant APP and Mapt, and thereby delay the death that occurs at an unusually early age.

4.1.3 Rotarod performance upon curcumin treatment

The most obvious phenotypic impairment of JNPL3 mice is their deteriorating motor function performance (Lewis et al., 2000). In our study, assessment of male JNPL3 strains found no statistically significant change of motor function between mice with or without curcumin treatment, although there was a trend toward increasing the difference of the mean performance between treatment and control groups.

The lack of significance may be due to the large variation of the time of onset of motor function impairment of this strain, with a range of about four months (Bolmont et al., 2007). In our study, we did not observe deterioration of the rotarod performance of male JNPL3 mice at the age of 14 months after six months of curcumin treatment. Therefore, we excluded the mice of this age from motor performance assessment for the effect of curcumin treatment. Female mice were excluded, too, since they generally have large physiological variations. Before starting treatment, it is not possible to predict which individual mice will develop a phenotype of early onset of motor function impairment. However, we can screen out those which have developed hind leg paralysis. In order to narrow the variation of phenotype, we used mice at an older age, 16 months old, with no observable motor function impairment. The vehicle for curcumin administration was changed to peanut butter for easier control of dosage.

As we expected, deterioration of motor function occurred during the course of treatment. There was great variation among individual mice, with some mice displaying very severe impairment which caused complete inability to perform the rotarod test, and other mice performing very well on the test. Therefore, we had to shorten the treatment period to 10 weeks. Since the starting and ending number of

mice was too small to discern moderate effects in the face of large interindividual variation, we were not able to conclude whether or not curcumin has a beneficial effect on motor function impairment caused by overexpression of mutant human Mapt.

Since AD is a form of dementia, the appearance of a memory deficit is the most important phenotypic change of Tg2576 mice for modeling AD in human patients (Hsiao et al., 1996). However, we encountered several problems in assessing memory loss. Memory studies of Tg2576 mice are often performed using the Morris water maze. However, we found in our preliminary experiment that most of our mice at the age of 13 months either only stayed in the water without swimming or died by drowning. Moreover, there is a report showing that the cognitive performance of this strain was greatly affected by the genetic background, and the decline of memory did not differ from that of a non-transgenic control strain with the same genetic background (King and Arendash, 2002). Furthermore, we ended up with very few mice surviving to finish the treatment regime. Therefore, the use of this strain for memory assessment was aborted.

For JNPL3xTg2576 mice, in principle, the effect of long term curcumin treatment on phenotypic changes could be monitored by both the rotarod test and the Morris water maze. However, for the same reasons as mentioned for the individual parent strains, and since the mortality of this strain is so high, we estimated that behavioural assessment would not have enough statistical power to reach meaningful conclusions. Therefore, this strain was excluded from behavioural studies.

Taking all the data together, phenotypic assessment does not suggest the benefit of long term use of curcumin. The most important reason is the small sample size of each strain in this study in the context of high genetic variability, which may

seriously affect the consistency of the results. Nevertheless, with the observation of a tendency toward better rotarod performance with curcumin treatment of male JNPL3 mice, further study using larger numbers of phenotype-screened JNPL3 mice is highly recommended. Further experiments using Tg2576 mice should consider choosing a suitable inbred strain, backcrossing in order to inbreed mice for enough generations to reduce the genetic variability, screening out the mice which cannot swim and using control strains with the same genetic composition.

4.2 Effects of curcumin on A β generation

One logical approach to study the effect of drugs on treating AD is to track down the effect of the drugs on mechanisms of the development of AD neuropathologies. Since curcumin has been shown to reduce A β cytotoxicity in vitro (Qin et al., 2009; Qin et al., 2010) and decrease amyloid plaque formation in vivo (Lim et al., 2001), we are interested to know whether curcumin treatment has any effect on the initial prerequisite stage of plaque development – A β peptide generation.

4.2.1 Microarray of APP cleavage enzyme and competitive substrate genes

Microarray is the fastest method to simultaneously observe the differential expression of the complete set of over 30,000 genes. We used it as a preliminary screening to identify genes whose expression is influenced by curcumin treatment. Since the reliability of microarray experiments could be affected by many factors, such as the integrity of RNA across samples and the quality of printed spots for individual genes across chips, the confirmation of microarray results is necessary, and can be accomplished by methods such as real-time PCR.

Our microarray results suggest that expression of secretases involved in α -, β - and γ - cleavage of APP protein for the generation of A β peptide was not obviously affected by curcumin treatment. On the other hand, the data also reveal that the expression of many substrates of these secretases was upregulated or downregulated over two fold, with Btc, Cd46, Ereg, Fc ϵ r2a, Muc1 and Sell being downregulated, and

Hs6st3 and Kl upregulated. However, it is very important to note that the changes we observed in gene expression usually are not consistent among different strains.

The microarray data of our study are unreliable, which makes the analysis very difficult. Besides the technical issues that cannot be overcome, the pooling of RNA samples introduced another element of variability which made the data less representative of each group of mice. In order to reduce the cost, we prepared pools of RNA from the mice of the same strain, treatment and administration mode by mixing equal amounts of RNA samples that met RNA integrity standards. Therefore, we had four pairs of treatment and control groups: JNPL3 with peanut butter as vehicle, JNPL3 with chow as vehicle, Tg2576 with chow as vehicle and JNPL3xTg2576 with chow as vehicle.

For the groups with curcumin administered in chow, the dosage of curcumin intake and time of final dose were hard to control. Therefore, they were dissected after overnight fasting in order to show the long term effect of curcumin treatment. For curcumin administered in peanut butter, the mice were fed with curcumin by the dosage that is equivalent to the daily consumption of mice in groups administered in chow, assuming that the daily chow consumption is about 20% of body weight. The mice were dissected about one to 1.5 hour after the final administration, which could be used to study the acute effect of curcumin on regulation of gene expression.

Besides the differences of treatment modes, the small sample sizes of mice for pooling in each group reduced the representativeness of each pool. Another problem is that each pair of groups is actually of different strains or ages. As a whole, the microarray results could be analysed by the consistency of fold change observed

across groups and could serve as a guideline for candidate gene selection for studies of different pathways.

4.2.2 Real-time PCR of APP cleavage enzyme and competitive substrate genes

Our results from real-time PCR experiments confirm that curcumin has no long term or acute effect on the expression levels of α -secretases (Adam9, Adam10 and Adam17) or of the β -secretase (Bace1) in vivo. α -secretases can cleave APP at the α -site. Bace1 is the only known physiological β -secretase, which cleaves APP at the β -site. It has been shown that Bace1 expression was increased in response to oxidative stress (Tamagno et al., 2003), which can be generated by A β 1-42 peptide (Butterfield, 2002), and by the presence of redox-active metal ions, such as Cu(II) (Huang et al., 1999a; Huang et al., 1999b). Protein expression and activity of Bace1 were shown to be increased in the brain of sporadic AD patients (Marks and Berg, 2008). Recent study has shown that curcumin can suppress A β 1-42 peptide-induced upregulation of Bace1 expression (Shimmyo et al., 2008). Another study has shown that only redox active metal ions increase Bace1 expression in vitro (Lin et al., 2008), which can be inhibited by curcumin.

However, these studies only showed the direct effect of pure A β 1-42 peptide and pure metal ions in vitro. The effect of curcumin on inhibiting Bace1 expression in these studies may be a result of direct neutralization of the toxicity by preventing A β from forming toxic species and chelating redox active metal ions. Moreover, applying curcumin to cultured cells cannot show the effect of metabolized curcumin, which can

only exist naturally in the brain. Furthermore, a study using Tg2576 mice showed that Bace1 activities increased with aging, but the protein and mRNA levels are not changed (Apelt et al., 2004). Thus, even though ROS increased in response to increasing A β level, it is not enough to increase Bace1 expression. Therefore, the results from these studies may only show that curcumin can reduce the toxicity of A β 1-42 peptide and metal ions in vitro at physiological irrelevant conditions.

We did not artificially elevate Bace1 expression in our mice. This means that the expression occurred under physiological conditions. Also, curcumin was taken orally, which means it was metabolized before entering the brain. Therefore, our result shows a reliable in vivo study on the effect of naturally existing and metabolized curcumin on the natural expression of Bace1 in the hippocampus region. Our data from four different groups of mice suggest that curcumin treatment has no significant effect on Bace1 expression.

Although the expressions of genes for α - and β -secretases were not affected by curcumin, the rate of APP cleavage may be influenced by the level of other proteins which are the substrates of secretases competing with APP. Our real-time PCR data show that the levels of Btc, Kl and Sell were increased by curcumin treatment. Since the changes were only in JNPL3 (chow) mice but not JNPL3 (PB) mice, we suggest that they were not caused by acute effect of curcumin treatment and that a single high-dose treatment per day is not enough to produce this response.

Btc (betacellulin) is an epidermal growth factor-like growth factor. It is expressed in precursor form as a transmembrane protein. It can be proteolytically processed by Adam10, Adam17 and γ -secretase (Hinkle et al., 2004; Sanderson et al., 2005; Stoeck et al., 2010). Its function in the brain is not clear. However, α - and γ -

secretase cleavage of pro-Btc can be enhanced by H_2O_2 stimulation (Sanderson et al., 2006).

K1 (klotho) is a type-I transmembrane protein highly expressed in brain. It is proteolytic processed by Adam10, 17, Bace1 and γ -secretase (Bloch et al., 2009). Data showed that overexpression of K1 extends life span of mice (Kurosu et al., 2005), a very interesting finding since this effect is consistent with our data that mortality was reduced in our mice treated with curcumin. It is also a protective protein against oxidative stress (Yamamoto et al., 2005). K1 mutant mice develop cognitive impairment at the age of seven weeks (Nagai et al., 2003), suggesting that loss of function of K1 has deleterious effects in the brain. Therefore, upregulation of K1 not only protects the brain against ROS toxicity, but also extends the healthy life of the brain and reduces the mortality of subjects, and K1 upregulation has been targeted as a potential treatment for AD (Wolfe, 2010).

Sell (selectin I) is a member of the family of adhesion receptors (Bevilacqua et al., 1991). It is a substrate of Adam17. The expression and function in the brain is not known. Although its expression in the curcumin treated group of JNPL3xTg2576 mice was statistically significantly different from the control group, the result is not very reliable since the sample size of this strain is very small in both the curcumin and control group (5 vs 3).

Taken together, our data show that expression of α - and β -secretases was not affected by curcumin at a transcriptional level. Interestingly, we found that K1 was increased upon long term curcumin treatment. This finding and our finding of reduced mortality are consistent with a study showing that overexpression of K1 increases life span (Kurosu et al., 2005). Further investigation on how curcumin increases K1

expression, on whether increasing K1 expression has any effect on APP or A β metabolism, on tauopathy, on maintenance of cholinergic functions and on neurodegeneration are very interesting follow-up project directions.

4.2.3 Secretase function assays

It is important to remember that the expression of α and β -secretases may not clearly represent the functional activities of these secretases. Activity assays for each of them must be performed.

Our data show that curcumin significantly suppresses the α -secretase activity in female JNPL3xTg2576 mice. However, it has no effect on males or other strains. This result should be taken with caution since this strain has high interindividual variation (because it was bred on a mixed genetic background), and the sample size of females in both treatment and control groups was extremely small (5 vs 3).

For β - and γ -secretase activity assays, our data suggest that curcumin has no significant effect.

Taken together, we did not find any reliable and significant effect of curcumin on α -, β - and γ -secretase activities. Therefore, we conclude that mechanism by which curcumin may treat AD is not through A β production pathways.

4.3 Effects of curcumin on A β aggregate formation

Since we found that secretase activity is not affected by curcumin treatment *in vivo*, the toxicity of A β peptides should not be diminished by curcumin through suppressing A β generation. Therefore, the next question we would like to know is whether curcumin has any effect on reducing the toxicity of A β peptides by inhibiting the formation of toxic A β aggregates.

4.3.1 A β aggregation Thioflavin T assay

A β aggregates induced by metal ions were used for testing the effectiveness of curcumin in reversing A β aggregation. Our data suggest that curcumin disaggregates the preformed A β aggregates. Thioflavin-T, which binds to β -sheet structure specifically, is used as a detector to quantify the level of β -sheet structure of A β aggregates. Therefore, the results also suggest that curcumin converts the β -sheet structure which is adopted by amyloid and insoluble A β fibrils to soluble forms. This effect of curcumin is useful because conversion to β -sheet structure is a prerequisite step in the formation of insoluble plaque. The concentration of curcumin which inhibits half of A β aggregate formation is between 0.3 and 0.9 μ M, which is in agreement with previous reports that used A β fibrils that were not induced by metal ions and found an IC₅₀ of curcumin between 0.1 and 1 μ M (Ono et al., 2004).

To mimic the formation of A β aggregates more physiologically, we used aggregates which are induced by the metal ions Cu(II) and Zn(II) (Bush, 2003). Although curcumin has very different binding affinity to Cu(II) and Zn(II) ions

(Baum and Ng, 2004), we did not observe a big difference of the IC_{50} between aggregates induced by Cu(II) and Zn(II) and between ours and the studies by (Ono et al., 2004). Moreover, a study showed that curcumin binds to amyloid plaques in vivo (Yang et al., 2005). Therefore, we suggest that the mechanism by which curcumin disaggregates A β is not metal chelation. Curcumin may bind to insoluble A β plaques or fibrils and turn them back to a soluble form.

Curcumin is very insoluble in aqueous solution, which makes it very poorly absorbed through oral administration. The reported concentration of free curcumin administrated by oral feeding is around 1.4 μ M in the brain (Begum et al., 2008), but it is below the detection limit in plasma. Glucuronidated curcumin is the predominant form in plasma. However, glucuronidated curcumin may not help to treat AD since it does not pass through the blood brain barrier (Begum et al., 2008). Based on the fact that the IC_{50} of curcumin for the formation of A β aggregates is within the physiologically relevant concentration of free curcumin in the brain, we suggest that curcumin disaggregating amyloid plaques and preventing their formation from A β peptides are physiologically possible.

4.3.2 Western blotting of monomeric A β from anti-A β aggregation assay

Although curcumin can disaggregate A β aggregates, it is not clear whether the solubilized A β would form other multimeric forms which may be toxic. We used western blotting to check the change of the level of monomeric A β peptide upon curcumin disaggregation. Our data show that the level of monomeric A β peptide is

significantly increased with increasing concentration of curcumin. It is important to know that curcumin, even within its physiological concentration range, still significantly disaggregates $A\beta$ and returns it to monomeric form, which is more readily removed or degraded. Therefore, the data further strengthen the protective effect of curcumin on inhibiting amyloid plaques and facilitating their clearance in a physiological relevant manner.

4.3.3 Immunohistochemical staining of 4G8-immunopositive plaques

In order to reproduce the effect of curcumin on reducing amyloid plaques *in vivo*, we repeated other studies on treating APP^{swc} overexpressing mice, Tg2576, with curcumin (Hamaguchi et al., 2009; Lim et al., 2001; Yang et al., 2005). However, our data do not confirm the effect of curcumin on amyloid plaque reduction. We believe that this is due to two major reasons.

First of all, the mortality of this strain during the treatment period was high: only nine curcumin-treated and four control male mice completed the treatment. It is possible that all mice with more severe amyloid pathology died, which would be consistent with the observation that the mice which completed the treatment showed relatively few plaques.

Secondly, this strain was bred on a mixed background of two different strains. This makes the genetic composition vary greatly among individual mice (Lassalle et al., 2008). This genetic diversity would likely correspond with variation in the onset and severity of amyloid pathology. The way to overcome the genetic variation is by backcrossing to an inbred strain for enough generations until a consistently narrow

range of amyloid pathology is confirmed by histology. However, repeated backcrossing to an inbred strain for many generations may lead to eventual loss of the transgene. Therefore, problems of the genetic background cannot be solved quickly. Nevertheless, it is still possible to use this strain for treatment studies, provided that the number of mice is large enough to cover different durations of treatment strategies.

Our data suggest that curcumin can disaggregate amyloid plaques and prevent the formation of aggregates from soluble A β . Disassembling aggregates into monomeric A β may allow easier clearance by other pathways in a physiological relevant manner.

4.4 Effects of curcumin on A β degradation

As curcumin can reverse the formation of toxic A β species, it would eventually lead to an increased level of soluble, non-toxic A β . Once the concentration of curcumin returns to an ineffective level, more toxic A β species can be readily formed. Therefore, reducing A β toxicity by reversing the formation of A β aggregates may not entirely explain the effect of curcumin treatment on reduced plaque burden. Since we showed that curcumin has no effect on reducing A β production in vivo, and a report showed that curcumin can reduce the amyloid plaque formed from intracerebroventricular infusion of A β (Frautschy et al., 2001), we are interested to know whether curcumin has a direct effect on the catabolism of A β peptides in vivo.

4.4.1 Microarray of A β degrading enzyme genes

In the microarray study of male mice, our data suggest that *Ace*, *Bsg* and *Mmp2* were selectively upregulated by over two fold in some groups treated with curcumin. However, *Mmp3* was upregulated over two fold in JNPL3 (PB) and JNPL3xTg2576 but downregulated by a similar magnitude in Tg2576. However, after selection of samples by RNA integrity, the sample size of Tg2576 and JNPL3xTg2576 involved in the pool were just 8 vs 4 (for curcumin vs control) and 5 vs 2, respectively. Another problem was that the mice were bred on a mixed genetic background. Thus, we did not try to draw a conclusion based on this result. Nonetheless, we chose genes for real-time PCR based on the current literature on the candidates for involvement in A β degradation and the results from JNPL3 (PB) mice, which were screened by the pathological change and had well-controlled feeding amount and dissection time.

4.4.2 Real-time PCR on gene expression of A β degrading enzymes

After confirmation of gene expression by real-time PCR, our findings suggest that long term use of curcumin significantly upregulates Ide, Mmp2 and Mmp14 expression. Since we only see the effect on JNPL3 (chow) but not JNPL3 (PB), we suggest that the upregulation of Ide, Mmp2 and Mmp14 is not due to an acute effect of curcumin, and a single high dose administration per day is obviously ineffective.

Ide (insulin-degrading enzyme) is a 110 kDa zinc-binding protease which was identified by insulin degradation ability (Affholter et al., 1988). The purified Ide from rat brain can degrade A β peptide (Kurochkin and Goto, 1994). It can exist as a cytosolic form, a secreted form from microglia and a membrane associated form in differentiated neurons (Vekrellis et al., 2000). It can be found in cerebrospinal fluid as a functional form which can degrade extracellular A β (Qiu et al., 1998). Since Ide has higher affinity to insulin than to A β peptide, insulin can inhibit the degradation of A β peptide by Ide (Kurochkin and Goto, 1994). It has been shown that Ide can degrade A β in vivo—deletion of Ide in mice increased the cerebral concentration of endogenous A β and decreased A β degradation by the membrane fraction of brain tissue by half (Farris et al., 2003)—which suggests that Ide is not the only protease for A β degradation. Genetic linkage analysis showed that the chromosome 10q23-24 region containing the Ide gene is associated with AD (Bertram et al., 2000). Functional analysis of the polymorphism showed that the catalytic activity of Ide was decreased without a change in the mRNA level (Kim et al., 2007). These reports suggest that reducing the activity of Ide would increase A β accumulation and the

chance of developing AD. Furthermore, overexpression of I α 2 reduced plaque and A β levels by increasing A β degradation, which also reduced premature lethality of APP overexpressing mice (Leissring et al., 2003). Taken together, these studies support the beneficial effects of upregulation of I α 2 in reducing A β and treating AD.

Mmp2 (matrix metalloproteinase 2) is a 72 kDa type IV collagenase (Devarajan et al., 1992). It is expressed as the pro-Mmp2 form, which requires Mmp14 for activation (Strongin et al., 1995). It can cleave A β at Lys16-Leu17, Leu34-Met35 and Met35-Val36 in vitro (Roher et al., 1994). It is expressed and secreted by astrocytes (Yin et al., 2006). Expression of Mmp2 is increased in A β -stimulated human cerebrovascular smooth muscle cells (Jung et al., 2003), astrocytes and mixed hippocampal cells in vitro (Deb and Gottschall, 1996) and plaque-surrounding astrocytes (Yin et al., 2006). In vitro study showed that conditioned medium from astrocytes can cause A β peptide fragmentation (Deb et al., 2003) which is inhibited by Mmp2 inhibitors (Yin et al., 2006). In vivo study showed that A β concentration is increased in Mmp2 knockout mice (Yin et al., 2006). This evidence suggests that Mmp2 is required at least by astrocytes for degradation of extracellular A β , and that Mmp2 is upregulated in response to increased A β level in the brain, which supports the beneficial use of curcumin to enhance Mmp2 expression for A β clearance in treating AD.

Mmp14, membrane type-1 (MT1)-matrix metalloproteinase, is a 66 kDa integral membrane protein (Sato et al., 1994). It is expressed by microglia and astrocytes in the brain (Liao and Van Nostrand, 2010; Yamada et al., 1995). Expression in human astrocytoma cells and cerebrovascular smooth muscle cells can be increased by A β in vitro, which enhances Mmp2 activity (Deb et al., 2003; Jung et

al., 2003). Cos-1 cells expressing transfected Mmp14 alone, without Mmp2, can degrade exogenous A β peptides in vitro (Liao and Van Nostrand, 2010). Truncated Mmp14, without the transmembrane domain, still possesses the ability to cleave A β peptides, and it can also degrade synthetic fibrillar A β 1-42 and amyloid plaques from Tg2576 mice (Liao and Van Nostrand, 2010). As with Mmp2, an in vivo study showed that Mmp14 expression is also increased in the reactive astrocytes surrounding microvascular amyloid deposits (Liao and Van Nostrand, 2010), which suggests its expression is induced in response to A β in order to clear A β from the brain. Therefore, the upregulation of Mmp14 not only increases A β peptide and fibril degradation, but also activates Mmp2 for A β clearance, which suggests multiple advantages of curcumin to enhance Mmp14 expression for A β degradation.

Another interesting result we noted by comparing the effects in different groups is that the upregulation of Ide, Mmp2 and Mmp14 only happened in JNPL3 (chow) but not in JNPL3 (PB). One explanation could be different dosages of curcumin. The amount of curcumin fed to JNPL3 (PB) mice was calculated by the daily consumption that we assumed the mice in JNPL3 (chow) would take from the chow. That means JNPL3 (PB) took a single dose which was eaten by JNPL3 (chow) mice over a whole day. We believe this is the adverse effect of high dose curcumin treatment since another group also found that high dose curcumin treatment of Tg2576 did not reduce amyloid plaques, insoluble and soluble A β and the astrocytic marker GFAP compared to low dose curcumin treatment (Lim et al., 2001). They observed that a high dose of curcumin suppressed clearance of A β by glia. Interestingly, Ide, Mmp2, and Mmp14 are all produced by glia.

There are some limitations of this study. First of all, the activities of these proteases have not been confirmed. For example, Mmp2 function requires activation by Mmp14, thus the degrading activity of a protease may not be proportional to its mRNA level. Secondly, this result was only confirmed in JNPL3 (chow) mice but not in Tg2576 mice, perhaps due to an insufficient number of mice in the latter strain. It would be interesting to know if there is any inter-strain variations, if the basal expression levels of these proteases are higher in Tg2576 than JNPL3 mice in response to the presence of higher overall levels of soluble A β and amyloid plaques in the brain, and if curcumin can still produce the same effect in Tg2576 if the basal expression of these proteases was already upregulated. Future investigation should also study whether curcumin can increase their expression in different neural cell types, how curcumin upregulates their expression, what dosage and duration of treatment are important for such an effect, whether curcumin still has an effect on A β reduction when these genes are knocked out, and to identify other possible degrading enzymes upregulated by curcumin. However, due to the limitation of time and resource, the above suggested studies are not covered in this project.

In summary, our result is the first and the only in vivo study to report that curcumin increases the expression of several of the known A β degrading enzymes, Ide, Mmp2 and Mmp14. This upregulation may be related to the reduction of amyloid plaques and soluble A β peptides.

4.5 Effects of curcumin on A β removal

Degradation is not the sole pathway by which A β level can be reduced. There are transporters and receptors responsible for transferring and taking up A β to cells for turning over or transporting to the circulatory system. Therefore, the next issue we would like to address is whether curcumin treatment can affect the levels of these transporters and receptors in vitro and in vivo.

4.5.1 Cell culture study

Our data suggest that phenolic compounds, curcumin, ferulic acid and tannic acid, have significant effects on increasing the secretion of ApoE protein from microglial cells. In the MTT cell viability assay, we noted significant changes of cell viability at relatively high concentrations of phenolic compounds. Curcumin at concentrations over 15 μ M increased cell viability and reduced ApoE secretion. However, curcumin cannot reach this concentration in vivo. Tannic acid at over 6 μ M dramatically reduced cell viability and sharply reduced ApoE secretion. Therefore, although we observed a decrease of ApoE secretion corresponding to decreased cell viability, the increase of ApoE secretion at low curcumin concentrations was not likely to be affected by the cell viability, which did not change at a reasonably low and non-toxic level of curcumin.

ApoE is a 34 kDa protein responsible for cholesterol transport and metabolism of lipoproteins in plasma (Weisgraber and Mahley, 1996). It is expressed and secreted by astrocytes and microglia in the brain tissue. It has been shown that ApoE can interact with A β and facilitate its uptake through ApoE receptors. Different ApoE

isoforms show different A β clearance rates, in the order of ApoE2 > ApoE3 > ApoE4 (Castellano et al., 2011). Carriers of the ApoE4 allele have increased risk of developing LOAD (Corder et al., 1993). A clinical study showed that the levels of ApoE inversely correlated with A β levels in the brain (Lambert et al., 2005). Recent in vitro and in vivo studies showed that ApoE isoforms affect ApoE protein levels in conditioned medium of astrocyte cultures and in the brains, CSF and plasma of mice selectively expressing one of these isoforms in the order of E2/E2 > E3/E3 > E4/E4 (Riddell et al., 2008). This evidence suggests that loss-of-function of ApoE increases the risk of developing LOAD, probably due to a reduced level of ApoE. Therefore, we believe that increased extracellular ApoE could facilitate A β removal.

Nevertheless, although we saw an increased level of ApoE in the microglia conditioned medium, it is possible that this was due to reduced degradation of ApoE by microglia. Moreover, we did not try to show that increased ApoE level could increase the uptake of A β peptide in our cultured cells. Due to the limitation of time and resources, these experiments may be conducted in the future.

In summary, based on the literature and our data, we suggest that curcumin may reduce amyloid plaque formation by increasing A β removal through increasing the level of extracellular ApoE secreted from microglial cells.

4.5.2 Microarray of A β transporter and receptor genes

4.5.2.1 A β transporters

In examining transporters of A β , our microarray data suggest that levels of ApoA1, Ttr and Ltf may be affected by curcumin treatment. ApoA1 may be suppressed. Ttr may be increased since it was consistently upregulated over 2 fold, except in the Tg2576 group, with a 27 fold rise in the JNPL3 (PB) group, which may suggest an acute effect of curcumin on upregulation of Ttr. Ltf was upregulated in JNPL3 (chow) but downregulated in JNPL3 (PB) which may suggest that the long term and acute effects of curcumin are opposite.

4.5.2.2 A β receptors

Examination of A β receptor genes in our microarray data showed that Ager, Cd36 and Msr1 expression were affected. Ager and Cd36 were only affected in JNPL3 (PB), suggesting that the changes were in response to acute curcumin treatment. Since Msr1 was only upregulated in JNPL3xTg2576, but not other groups, we believe it may not be a reliable result.

4.5.3 Real-time PCR of A β transporter and receptor genes

4.5.3.1 Gene expression of A β transporters

Our results for the confirmation of A β transporter levels suggest that no known A β transporters were significantly up or down regulated by long term or acute curcumin

treatment. For ApoE expression, the data are important as comparison to the microglial cell culture result. Based on the cell culture and animal studies on protein and mRNA levels, respectively, we suggest that curcumin can increase the extracellular ApoE protein level but that the increase is not caused by higher ApoE expression.

4.5.3.2 Gene expression of A β receptors

Our data of real-time PCR for the gene expression of A β receptors confirm that curcumin significantly upregulates ApoeR2, Lrp1 and Msr1. The fact that the significant changes occur only in JNPL3 (chow) mice, but not JNPL3 (PB) mice, suggest that they were not caused by an acute effect of curcumin treatment and that a single high dose treatment per day is not enough to produce this response. Our data also show that Lrp2 was significantly affected by curcumin treatment. Since there was no significant difference within individual strains, we believe the data of this gene are not reliable, and it will not be discussed further.

ApoeR2 (Apolipoprotein E receptor 2, also called low density lipoprotein receptor-related protein 8, or Lrp8), is a membrane protein with multiple domains. It can act as a receptor for low density lipoprotein (LDL) and very low density lipoprotein (VLDL) (Kim et al., 1996). It is widely expressed in brain, especially, in granule cells, pyramidal neurons and Purkinje cells of hippocampus and cerebellum regions (Clatworthy et al., 1999). It is found that ApoeR2 colocalizes with and increases cell surface and lipid raft associated APP level, and its expression associated with increased A β production in vitro (Fuentecalba et al., 2007). However, severe

neurological dysfunction was observed upon double knockout of this gene, which may be due to the loss of binding function to selenoprotein P, which maintains the selenium level in the brain (Burk et al., 2007). A recent report did not show an association between ApocR2 polymorphism and dementia (Helbecque et al., 2009). But a case-control study showed that the R952Q variant of ApoE2 has an additive effect to ApoE isoforms in affecting the ApoE level in plasma (Martinelli et al., 2009), which suggests an association between the ApoE level and ApoE2. Nevertheless, the relationship amongst ApoE2, A β and AD is still unknown. Therefore, it is still not known whether ApoE2 upregulation has any protective or adverse effect to the development of AD. Further study is needed to confirm whether ApoE2 level would affect the metabolism of A β .

Lrp1 (low density lipoprotein receptor-related protein 1), which is a well known receptor for ApoE (Myklebost et al., 1989) and alpha-2-macroglobulin (Chappell et al., 1992), is a membrane protein which is expressed as a 600 kDa precursor form and is then cleaved into two non-covalently linked protein subunits: an extracellular 515 kDa heavy chain and an 85 kDa transmembrane light chain. Genetic association studies suggested that Lrp1 polymorphisms associated with LOAD (Baum et al., 1998; Kamboh et al., 1998; Kang et al., 1997; Wavrant-DeVricze et al., 1999). An *in vitro* study showed that overexpression of functional Lrp1 minireceptor increased, but deletion of Lrp1 reduced, A β 1-42 uptake (Fuentelba et al., 2010), which suggest that Lrp1 is involved in A β 1-42 uptake. A recent study showed that the internalization of A β into an endothelial cell line derived from blood-brain barrier is mediated by Lrp1 (Yamada et al., 2008). Another study demonstrated that Lrp1 uptake of A β 1-42 is mediated by ApoE (Zerbinatti et al., 2006). Decline of the protein level of Lrp1 at the blood-brain barrier was shown to be age-dependent (Silverberg et

al., 2010). The expression of Lrp1 was shown to be reduced with AD associated Lrp1 polymorphic genotypes, which was also shown to cause increased soluble A β and amyloid plaques (Kang et al., 2000). These findings suggest that Lrp1 is involved in A β internalization via ApoE. As we found that the protein level of secreted ApoE is increased by curcumin, we suggest that the Lrp1 upregulation we observed in response to long term curcumin treatment can enhance the removal of A β .

Msr1 (macrophage scavenger receptor 1) is a trimeric integral membrane glycoprotein which takes up acetyl-low density lipoproteins (Ac-LDLs), oxidized LDLs and A β peptide. Msr1 mediates attachment of microglia to amyloid fibrils (El Khoury et al., 1996). Histological study demonstrated that Msr1 is expressed in microglia but not astrocytes or neurons, and the expression is upregulated in microglia associated with senile plaques in the brain (Christie et al., 1996). It has been demonstrated that Msr1 is required by microglial cells for internalization of A β in either soluble or microaggregate forms (Paresce et al., 1996). Co-expressing Msr1 and human APPSwe showed that A β in the conditioned medium was reduced by 40 percent (Malherbe et al., 1999). The above evidence suggests that Msr1 can assist the internalization of soluble and fibrillar A β by microglia. Therefore, we suggest that curcumin, based on its upregulation of Msr1 in our study, may enhance removal of soluble A β and amyloid plaques by microglial internalization.

Our data on A β receptors suggest that curcumin can enhance the removal of soluble and aggregated A β by increasing ApoE secretion, by increasing clearance through Msr1 made by microglia, and by increasing Lrp1 expression and thus internalization of A β through endothelial cells of the blood brain barrier. These pathways provide a beneficial effect of curcumin in treating AD.

4.6 Effects of curcumin on cholinergic functions

In studies of cognitive function, other groups showed that curcumin can improve the memory performance of a cognitively impaired rat model induced by intracerebroventricular (ICV) infusion of A β (Frautschy et al., 2001) or intraperitoneal injection of scopolamine (Ahmed and Gilani, 2009). Some studies also showed that curcumin reverses the activation of acetylcholinesterase induced by aluminium (Sharma et al., 2009) and increases the activity of choline acetyltransferase in a cognitive impaired rat model induced by ICV infusion of streptozotocin (Ishrat et al., 2009). Therefore, we are interested to know whether there is any effect of curcumin, at the transcriptional level, on the cholinergic functions regulated by acetylcholine homeostasis.

4.6.1 Microarray of cholinergic genes

By focusing on the genes which are involved in regulating the homeostasis of acetylcholine through formation, degradation and reuptake, our microarray data suggest that the expression of ChAT, Cht1 and Vacht were affected by curcumin. There may be an acute effect of curcumin on suppressing ChAT and enhancing Cht1 expression. On the other hand, upregulation of Vacht may be a long term effect of curcumin.

4.6.2 Real-time PCR on expression of genes regulating acetylcholine homeostasis

Since the cholinergic neurons in AD brain are degenerating, the amount of acetylcholine (ACh) that can be synthesized and secreted by the presynaptic terminal is decreasing and is insufficient to fully stimulate the ACh receptors on the postsynaptic membrane. Therefore, acetylcholinesterase inhibitors were developed to maintain the level of ACh (Davis et al., 1992).

Our data on mRNA levels of genes regulating the availability of acetylcholine show that curcumin has no significant effect on the differential expression of these genes. These results are relevant in that they help us determine whether curcumin treatment has any effect on the balance of acetylcholine, which affects cognitive performance in AD. Since their activity levels are not entirely reflected by their mRNA expression, functional assays of AChE and ChAT should be performed to assess the effect of curcumin treatment.

Curcumin can inhibit AChE activity in scopolamine or aluminium administered models in vivo (Ahmed and Gilani, 2009; Sharma et al., 2009). However, the effect of curcumin on inhibiting AChE activity in an ex-vivo model with enhanced AChE activity is not detectable (Ahmed and Gilani, 2009). It may be suggested that curcumin has no effect on inhibiting AChE enzymatic activity directly; instead, it might interrupt the toxic pathways leading to AChE activation. A similar explanation might be applied to another streptozotocin-induced model, in which ChAT activity is decreased and partly restored by curcumin (Ishrat et al., 2009; Sharma and Gupta, 2001). The loss of ChAT activity in this model is caused by the oxidative stress generated by streptozotocin directly damaging membrane integrity. Curcumin may

restore ChAT activity by reducing the oxidative stress before the activity of ChAT is impaired, rather than by restoring the activity of ChAT. These evidences suggest that curcumin may not affect the enzymatic function of ChAT and AChE. Instead, curcumin may only suppress the toxicities of the agents used to generate the models.

On the other hand, it has been demonstrated that an APP^{swc} overexpressing model, Tg2576, has no impairment in ChAT or enhancement in AChE activities (Gau et al., 2002), which suggests that A β toxicity may not lead to the development of cholinergic degeneration. Therefore, the cause of cholinergic degeneration in AD needs to be confirmed. In addition, the use of chemical agents to induce AChE activation and ChAT inhibition may not be physiologically relevant to the cause of cholinergic abnormality in AD. Taken together, these evidences suggest that these models may not be suitable for studying the change in cholinergic function of AD.

Nevertheless, since our data show that curcumin has no effect on regulating the expression of genes related to acetylcholine homeostasis, the evidence does not support further investigation of the effect of curcumin on cholinergic function.

4.7 Other neuroprotective and harmful effects of curcumin

The multipotent nature of curcumin has been described for many years. For a macroscopic view on the physiological functions of curcumin, we would like to study whether curcumin can provide any other protective functions *in vivo* at the transcriptional level.

4.7.1 Cell free assay

4.7.1.1 Hydrogen peroxide (H₂O₂) scavenging assay

A reactive oxygen species generation assay was developed by combining A β 1-42 and redox active metal ions, which has been proposed to be one of the causes of neurotoxicity to the brain (Huang et al., 1999a; Huang et al., 1999b). We used this assay to determine if physiological concentrations of curcumin possess enough antioxidative ability to potentially protect against AD.

Our results suggest that curcumin has significantly inhibits H₂O₂ generation. However, we do not suggest that the function is physiologically relevant because the lowest effective dosage of curcumin in this assay is at least 5 μ M, which is much higher than the concentration of 1.4 μ M achieved in the brain (Begum et al., 2008). Although there are studies that showed that curcumin treatment in AD rodent models reduces oxidative stress and damage (Frautschy et al., 2001; Lim et al., 2001), we believe that the oxidative stress is indeed alleviated through inhibiting the toxicity of A β by disaggregating it and increasing its removal by degradation and internalization, as shown in our data in previous sections.

4.7.2 Microarray of neuroprotective and neurotoxic genes

To further explore the microarray results, we searched for the effect of curcumin on groups of genes which can reduce amyloid plaque levels, provide protection against A β toxicity and affect oxidative stress. Since microarray data indicated that there were many genes affected by curcumin, but the number of real-time PCR results confirming the microarray data was very low, we will discuss only the confirmatory results.

4.7.3 Real-time PCR of neuroprotective and neurotoxic genes

Genes known to regulate A β plaque level, other than the genes already examined, were semi-quantitatively confirmed. However, we do not suggest that curcumin treatment has any effect on the expression of these genes. Although there are statistically significant changes of Cd74 and Gpr3, Cd74 was only shown to be changed in JNPL3xTg2576 mice, of which only 5 were treated by curcumin and 3 were controls. Gpr3 was not changed in any individual group. Therefore, we do not think the results are representative enough.

Some genes have been shown to provide protection against A β toxicity. Our data suggest that upon curcumin treatment Igf2 and Irs1 were upregulated. Only long term and continuous low dosage treatment but not short term treatment produced the upregulation since we only observe such changes in JNPL3 (chow) but not JNPL3 (PB) groups.

Igf2 (insulin-like growth factor II) is a short polypeptide belonging to the insulin family of polypeptide growth factors. It is involved in promoting growth and development of the brain. Autoradiographic study showed that it is highly concentrated in the hippocampus (Kar et al., 1993). Gene expression study showed that Igf2 is downregulated in aged brain, including hippocampus (Kitraki et al., 1993). A study using primary neurons from embryonic rat insulted by $A\beta$ peptide followed by treating with Igf2 showed that Igf2 caused a significant recovery from $A\beta$ -induced toxicity (Jarvis et al., 2007). In an animal study, Igf2 was found to be upregulated in hippocampus upon inhibitory avoidance learning (Chen et al., 2011). Recombinant Igf2 can significantly improve memory consolidation by injecting into the hippocampus of rats after training and can enhance continued long-term potentiation in hippocampal slices (Chen et al., 2011). Based on these results, we suggest that Igf2 upregulation by curcumin treatment may provide beneficial effects for AD treatment by protecting the brain against $A\beta$ toxicity and enhancing memory consolidation.

Irs1 (insulin receptor substrate 1) is coupled to insulin receptors (White, 2002) and relays the signal from insulin to activate downstream signaling (Virkamaki et al., 1999). It was shown that the Irs1 level in AD neurons was decreased, while there was an increase in the levels of phospho(Ser312) Irs1 and phospho(Ser616) Irs1, which are inactivated forms (Moloney et al., 2010) that are correlated to insulin-resistance. In a hippocampal cell culture study, $A\beta$ oligomer was demonstrated to increase the phosphorylated forms of Irs1, and this effect could be reduced by treating with curcumin (Ma et al., 2009). An animal study showed that curcumin increases the Irs1 level in a transgenic mouse model of AD (Ma et al., 2009). It was suggested that the reduced level of phosphorylated Irs1 and increased level of total Irs1 after curcumin treatment may be due to inhibition of JNK activation (Ma et al., 2009). In our study,

we confirm that *Irs1* expression was increased upon curcumin treatment. Therefore, increased protein level of unphosphorylated *Irs1* after curcumin treatment may be due to increased *Irs1* gene expression, rather than decreased phosphorylation of *Irs1* protein. As a whole, based on our finding, we suggest that curcumin can increase *Irs1* expression and therefore restore the insulin-signaling function which was impaired by toxic A β species and, thereby, provide an extra beneficial effect to the treatment of AD.

Oxidative stress is frequently mentioned as a cause of the toxicity in AD brains. Our data suggest that curcumin significantly upregulates *Nos2*, *Sod3* and *Bmp6*, and downregulates *Nox1*, all genes involved in oxidative stress.

Nos2, encodes a protein called inducible nitric oxide synthase (iNOS) (Geller et al., 1993). Nitric oxide (NO) is generated by iNOS using L-arginine and oxygen; it is a signaling molecule which can be produced by endothelial cells in the brain as a vasorelaxant or by neurons as a neurotransmitter (Malinski, 2007). It is commonly believed that increased expression of *Nos2* and production of NO is cytotoxic (Moncada and Higgs, 1991). Its adverse effects were described by many studies (Guix et al., 2005). Genetic association studies did not suggest that *Nos2* polymorphisms were associated with increased risk of AD (Singleton et al., 2001; Xu et al., 2000). A *Nos2* double knockout mouse model was generated to test the effect of removing iNOS and NO in mice overexpressing mutant APP (Swedish K760N/M671L, Dutch E693Q and Iowa D694N). Surprisingly, the result did not show that brain damage was lessened. Rather, the mice displayed greater impairment of cognitive function, with severe tauopathy and neuronal loss in the hippocampus (Wilcock et al., 2008), which better recapitulates human AD neuropathology.

Based on the above evidence, we suggest that Nos2 expression in response to A β toxicity may be a mechanism to neutralize toxic species and prevent further damage of neurons, such as by formation of neurofibrillary tangles. However, in contradiction to our result, another study showed that curcumin suppresses NO production and iNOS mRNA and protein expression in lipopolysaccharides (LPS) or interferon- γ insulted RAW 264.7 cells due to the inhibition of c-JUN/AP-1 activity (Brouet and Ohshima, 1995). Moreover, another study confirmed the iNOS expression inhibition effect by curcumin in mouse peritoneal macrophages and livers (Chan et al., 1998).

When comparing these data to our result, one must be very careful to consider the dosage and preparation of curcumin, the types of cells and the target organs. The first study showed that the IC₅₀ of curcumin on iNOS suppression was 6 μ M, which is too high to achieve in vivo, and this study used a macrophage cell line, which may be irrelevant to the nervous system. Although the second study showed that as little as 1 μ M curcumin inhibited iNOS expression, the study used peritoneal macrophages, which may not be informative with regard to effects on the brain. For treating animals, curcumin was prepared by firstly dissolving in NaOH, which quickly degrades curcumin, and since the bioavailability of curcumin was not measured in the study, we do not know what concentrations of curcumin and its metabolites entered the body. Moreover, the target of studying the level of iNOS was liver, which is the main organ for metabolizing curcumin. Furthermore, for all models in this study, the iNOS level was increased by LPS stimulation. Other potential problems were that the liver may not have received the same amount of curcumin as the brain; there were different preparation and administration methods; and the liver may have had a different response than the brain. Therefore, we believe that our data are more physiologically

reliable for showing that curcumin-induced Nos2 expression provides a beneficial effect in slowing the progression of AD by preventing tangle formation and neuronal loss.

Sod3 (extracellular superoxide dismutase [EC-SOD]), is an antioxidant enzyme which is secreted into extracellular regions. It provides protection to the brain by converting superoxide radicals to H₂O₂ and oxygen (Zelko et al., 2002). So far, there is no study connecting the function of Sod3 and AD. We may speculate on its function based on other studies. A study using transgenic mice demonstrated that Sod3 overexpression leads to reduced levels of superoxide, protein carbonyl, p38 and extracellular signal-related kinase 2 phosphorylation, with improved hippocampal LTP, motor learning and spatial learning ability (Hu et al., 2006). This study may suggest that Sod3 can suppress oxidative stress and improve synaptic plasticity and memory. Therefore, our result, demonstrating that curcumin increased Sod3 expression, may suggest beneficial effects to treating AD by reducing oxidative stress and improving synaptic plasticity and memory.

Bmp6 (bone morphogenic protein 6) is a member of the TGF β superfamily and is a secreted signaling molecule. Previously, it was demonstrated that adding Bmp6 either before or after H₂O₂ insult diminished primary cortical cell death (Du et al., 2007). Another study showed that Bmp6 expression was upregulated upon A β 1-42 treatment in vitro (Crews et al., 2010). This group also confirmed the upregulation of Bmp6 mRNA and protein levels in the hippocampus of AD patients and a mouse model of AD. Histological study further confirmed the presence of high levels of Bmp6 surrounding the plaques in the brains of AD patients and in a mouse model (Crews et al., 2010). However, the author believes that upregulation of Bmp6 has

adverse effects in the hippocampus because another experiment by this group showed that recombinant Bmp6 inhibited neurogenesis. Nevertheless, the above studies still cannot draw a final conclusion on the effect of upregulation of Bmp6 in response to nearby amyloid plaques because it is not clear whether the upregulated Bmp6 provides more protection or harmful effect to the nearby cells. Stopping neurogenesis of the cells surrounding the plaque could be a protective mechanism if the effect is temporary, but could be deleterious if it persists long enough. Therefore, we do not conclude whether Bmp6 upregulation by curcumin has any protective or harmful effect in AD treatment. Further projects are required to confirm the effect of Bmp6 change.

Nox1 (NADPH oxidase 1) is an enzyme homolog of the catalytic domain of superoxide-generating NADPH oxidase (Suh et al., 1999), which generates reactive oxygen species, superoxide and H₂O₂ when upregulated in fibroblast cells. Not much is known about its function in AD. A cell culture study demonstrated that inhibiting NADPH oxidase suppressed apoptotic cell death (Coyoy et al., 2008). Another study showed that suppressing Nox1 expression abrogated intracellular ROS generation-induced cell death (Kim et al., 2011). An animal study found that Nox1 knockout in mice reduced by 55 percent the size of ischemic lesions caused by middle cerebral artery occlusion (Kahles et al., 2010). Taken together, the above evidence suggests that suppressing Nox1 protects against apoptotic death. Since there is not enough evidence to prove that Nox1 suppression helps protect against AD, we do not conclude that curcumin-induced Nox1 reduction is beneficial in AD treatment. Further investigation is necessary to show the connection between AD neuropathology and Nox1 expression, localization and toxicity.

In summary, our data suggest that curcumin provides beneficial effects in the treatment of AD by protecting the brain against $A\beta$ toxicity and enhancing memory consolidation through Igf2 upregulation, restoring insulin-signaling pathways through Irs1 upregulation, slowing the progression of AD and preventing tangle formation and neuronal cell loss by enhancing Nos2 expression, and reducing oxidative stress and improving synaptic plasticity and memory by increasing Sod3 expression.

4.8 Effects of Curcumin on Tauopathy

Tau hyperphosphorylation is one of the main foci of tauopathy research. Many kinases have been shown to be able to phosphorylate tau, such as GSK3 β (Doble and Woodgett, 2003), JNK and Cdk5 (Patrick et al., 1999). Tau acetylation was recently found to prevent phosphorylated tau from degradation, and histone acetyltransferase p300 can acetylate tau (Min et al., 2010). Curcumin has been found to possess JNK (Somasundaram et al., 2002) and p300 (Marcu et al., 2006) inhibiting properties. Therefore, in this study, we would like to know whether long term curcumin treatment can be beneficial to tauopathy by reducing the level of intracellular neurofibrillary tangles (NFT). JNPL3 transgenic mice which overexpress human mutant P301L tau develop NFT in some brain regions at an old age, therefore JNPL3 mice were used as in vivo model of tauopathy. To investigate whether long term curcumin treatment has any effect on the development of tauopathy, brains of mice were harvested for gene expression and protein expression study, followed by confirmation of the disease progression by histological and proteomic studies.

4.8.1 Gene expression of endogenous Mapt

Microarray and real-time PCR experiments suggest that long term treatment with curcumin has no significant effect on the expression level of the endogenous Mapt gene in the hippocampus. In this study, we had two groups of JNPL3 mice: one treated with curcumin in chow from age eight months for duration of six months, and the other treated with curcumin in peanut butter from age 16 months for duration of 10 weeks. The daily consumption of curcumin per mouse in these two groups was

equivalent. To compare whether there is long term or acute effect of curcumin on endogenous Mapt expression, the mice treated with curcumin in chow were dissected after overnight fasting, while the mice treated with curcumin in peanut butter were dissected at one to two hours after the final dose of curcumin. The lack of a statistically significant effect of curcumin on endogenous Mapt expression in either group of mice indicates that there is no acute or long term effect of curcumin on endogenous Mapt expression. It is important to note that the endogenous gene expression of Mapt is not affected by curcumin treatment because suppression of endogenous Mapt expression increases the level of NFT formation from the human tau protein (Andorfer et al., 2003). If there was any effect on mouse Mapt expression, it would complicate the interpretation of the effect on NFT formation.

4.8.2 Protein expression of transgenic mutant tau

Western blotting analysis on the protein level of human mutant tau suggests that long term use of curcumin had no significant effect on the expression and stability of total human tau. We compared male and female JNPL3 mice with the same administration method and duration. Results are similar, but female mice have a large variation in the protein level of human mutant tau. It is also important to know the level of human mutant tau because the level has an impact on tauopathy severity and on the age of onset of the pathologies (Lewis et al., 2000).

4.8.3 Neurofibrillary tangles

In the first histological study, our results suggest that long term use of curcumin has no statistically significant effect on the level of NFT in the pons region of male and female mice, though there is a trend toward reduction of the number of NFT in male JNPL3. Bielschowsky's silver staining was employed as a cheap and preliminary check of the amount of NFT. JNPL3 does not develop NFT in the hippocampus, but extensive NFT normally appear in the spinal cord, pons, medulla, hypothalamus (Lewis et al., 2000), thus we selected pons for this experiment. Since Bielschowsky's silver staining was used to analyze human AD brain for the presence of both NFT and amyloid plaques in the early history of AD research, we suspected that it may not be specific enough to distinguish NFT from other pathology. Therefore, this study was followed by immunostaining, for which we used an antibody, AT8, that specifically binds to phosphorylated tau, which is highly enriched in NFT.

The results from the immunostaining of different brain sections from the same treatment groups of male JNPL3 show that long term use of curcumin has no significant impact on the level of AT8-positive NFT. To broaden the analysis, the medulla, entorhinal cortex, and amygdala regions were used. Interestingly, we observed large variation in the number of tangles in Bielschowsky's stained sections and in the percentage area covered by AT8-positive staining. Moreover, both staining methods show that the level of NFT was indeed very low in the treatment and non-treatment groups. The histopathological results seem consistent with the motor function performance test in that the variation is large and the pathologies are too mild to be seen, which is in agreement with the findings from another study (Bolmont et al., 2007). The above evidence suggests that the mice we used might have just begun to

develop the pathologies at the time of their dissection. Therefore, it would be necessary to increase the sample size and extend the treatment period, or to reduce the variation within groups and start the treatment at the time that the pathologies are about to develop, in order to give sufficient statistical power.

In dealing with the above issue, we chose another group of mice from a few litters lacking mice that died or developed pathologies of hindlimb paralysis. The mice looked healthy and did not show hindlimb paralysis at the age of around 16 months. During the first five weeks of treatment, a consistent drop in body weight was observable amongst most mice, which suggested the onset of pathologies. After another five weeks of treatment, many mice had already developed severe hindlimb dysfunction.

Immunostaining of different brain sections of the older JNPL3 mice administered with peanut butter as the vehicle shows that 10 weeks of curcumin treatment significantly reduces the level of AT8-positive NFT in the medulla. However, such an effect was not observed in entorhinal cortex/amygdala regions. These results suggest that curcumin may have site-specific effects.

NFT require tau hyperphosphorylation by kinases, such as JNK (Goedert et al., 1997). Curcumin was shown to be able to inhibit JNK activation in vitro (Chen and Tan, 1998) and in vivo (Ma et al., 2009). Our finding on the effect of curcumin on reducing AT8-positive NFT is in agreement with a recent finding that curcumin reduced JNK and tau phosphorylation (Ma et al., 2009). These pieces of evidence, together with our finding, suggest that long term use of curcumin has a prolonged effect of reducing NFT, at least partly by suppressing JNK activation.

It is important to note that our result on the effect of curcumin on NFT reduction is the first study using a model that can form NFT, which is different from another study, that used a model which cannot develop NFT and that only has phosphorylated tau, which was reduced by curcumin (Ma et al., 2009). Since formation of NFT is affected not only by tau phosphorylation, suppression of tau phosphorylation by curcumin may not completely explain the cause of NFT reduction in our result.

Recently, a report suggested that tau acetylation is enhanced in tauopathy patients and that such acetylation prevents phosphorylated tau from degradation (Min et al., 2010). Acetylation can be balanced by histone acetyltransferases and deacetylases. One of the histone acetyltransferases, p300, can acetylate tau (Min et al., 2010). Curcumin was found to be a selective inhibitor of p300 (Marcu et al., 2006). Therefore, it may be possible that curcumin can reduce the NFT level by inhibiting p300, which, in turn, limits the acetylation of tau. It would be interesting to study whether phosphorylation, acetylation or other pathways are affected by curcumin to reduce NFT formation. Due to the limitations of time and resources, the study of the molecular pathways of tauopathy which are affected by curcumin will not be covered by this thesis but will be followed by later projects.

4.8.4 PHF level

Using another approach to evaluate the effectiveness of curcumin on tauopathy, western blotting was employed to characterize the level of paired helical filaments (PHF), which are the main component of NFT. Our results show that long term curcumin treatment has no statistically significant effect on the level of PHF.

Consistent with the general findings from others, PHF is more abundant in female than male JNPL3 mice of the same age (Bolmont et al., 2007; Lewis et al., 2000), which suggests that the development of NFT was still in the initial phase. The level of PHF of male JNPL3 mice was consistent with the Bielschowsky's silver staining and immunostaining results in that they all showed reduced mean levels upon long term curcumin treatment, consistent with the observed trend toward preservation of motor function performance. However, none of the results were statistically significant. As suggested before, this lack of significance could be largely due to genetic variation, which caused large variation in the time of onset of the disease pathology. Therefore, a larger sample size of this strain and an older age may improve follow up experiments. Another approach could be to extend the treatment duration until there are considerable numbers of mice developing motor function impairment.

In summary, the results in this section suggest that long term curcumin treatment has beneficial effects on reducing the amount of NFT of mice which have developed severe tauopathy. It is not conclusive whether curcumin can delay the onset of NFT development in mice. Nevertheless, based on these results, a study using a large cohort of transgenic animals is highly recommended to confirm this enticing possibility.

CHAPTER FIVE: CONCLUSIONS AND FUTURE PERSPECTIVE

5.1 Conclusions

Although there are many studies suggesting the functions or mechanisms of curcumin in treating AD, most of this research was performed *in vitro* using physiologically irrelevant concentrations of curcumin. Examination of the protective functions of curcumin needs to be associated with the pathways of AD development *in vivo*. In this project, we have demonstrated the activities of curcumin on regulating the function and expression of the key players which had been concluded to have significant modulating effects on the development of or protection against AD.

To address the problem of physiological relevance in studying the functions of curcumin in cell-free systems, we used two hypothetical cell-free models which mimic the initial toxic pathways of AD development. For modeling A β aggregation, metal ions were used to simulate the oligomer or plaque formation of AD brain. We have shown that curcumin at concentrations attainable *in vivo* can effectively disaggregate pre-formed A β aggregates. We used a ROS generation model which simulates the toxicity of A β 1-42 peptide enhanced by redox-active naturally existing metal ions. However, we showed that curcumin has no observable effect on inhibiting H₂O₂ generation, which suggests that curcumin may not be as antioxidative as most people had shown, and it may not act as an antioxidant by itself *in vivo*.

Problems that may not be addressed *in vivo* require cell culture models to solve. We showed that curcumin at physiologically attainable concentrations can raise the ApoE protein level in the conditioned medium of BV-2 mouse microglial cells, which may assist the turnover of A β in the brain. We also showed that the

transcriptional level of ApoE was not affected by curcumin treatment *in vivo*. No matter whether ApoE secretion is increased or turnover is reduced, increased available ApoE may provide extra capability to remove A β from the extracellular space.

Nevertheless, the only way to translate hypotheses to medical treatment necessarily requires animal models to provide an appropriate physiological environment. We used three transgenic mouse models which resemble different clinical manifestations of AD. We also determined the acute and long term effect of curcumin treatment. Although Tg2576 and JNPL3xTg2576 were eventually ignored due to small sample sizes and large genetic variation, two groups of inbred JNPL3 mice provided reliable comparison of the effects of curcumin treatment *in vivo*.

We found that the loss of body weight and mortality which occurred with aging were reduced upon curcumin treatment. Although these effects were not shown to be related specifically to AD development, they demonstrate the general beneficial use of curcumin.

Our results revealed a number of protective pathways of curcumin against the progression of AD. First, on A β generation, our results suggested that curcumin may reduce APP metabolism which leads to A β production by increasing the competitive substrates of secretases, such as Btc, Kl and Sell. Amongst them, Kl was shown by other groups to extend life span and protect against oxidative stress. Second, on A β degradation, our results demonstrated that curcumin may increase A β catabolism by increasing the expression of some of the known A β degrading enzymes: Ide, Mmp2 and Mmp14. Third, on A β removal, our results suggested that curcumin may increase the internalization of A β from extracellular space through upregulation of two A β receptors, Lrp1 and Msr1. Last but not least, on pathways not associated with A β

metabolism, our data suggested that curcumin may provide protection against $A\beta$ toxicity and oxidative stress, and improve memory consolidation and synaptic plasticity, by increasing Igf2 and Sod3 expression; restore insulin-signaling pathways by upregulating Irs1 expression; and prevent tangle formation and neuronal loss by increasing Nos2 expression. Reduced stress on the brain by increased Igf2, Sod3 (van Deel et al., 2008) and Irs1 (Standen et al., 2009) may have an inhibitory effect on JNK activation. These effects, together with that of Nos2, might explain why the level of NFT was reduced in JNPL3 mice in our study.

5.2 Future Perspective

As several studies showed protective effects of curcumin on AD treatment in vivo (Frautschy et al., 2001; Lim et al., 2001; Yang et al., 2005), people may believe that it may be an effective medicine to cure AD. However, those studies did not show by what mechanisms curcumin can reduce AD pathology.

Through our results, we demonstrated a number of pathways by which curcumin might slow AD progression. Our gene expression results were from only one transgenic mouse model, and future projects should be repeated with larger sample sizes and in different transgenic and non-transgenic models.

Short term, high dosage treatment and long term, low dosage treatment gave somewhat different results. Therefore, future studies should include different treatment dosages and administrative methods in order to reveal the direct targets, maximize the protective effects and minimize the adverse effects of the use of curcumin.

In addition, genetic and physiological variations were shown to have large impacts on the consistency and reliability of results in our study. Therefore, in the future, we can minimize the variations by backcrossing to inbred strains for generations. We can also try to compare the effect of different inbred strains in order to choose the appropriate one. At the same time, the phenotype can be screened to prevent the loss of expression of the transgenes. In addition, different transgenic models should be tried.

Furthermore, functional studies should be performed on the effects of changed expression of the genes identified in our data. These may include labeling A β and

injecting it into the brain to trace it in neurons and epithelial cells on the blood-brain barrier for receptor-dependent A β internalization studies, and to trace labeled fragments for A β degrading enzyme studies. Specific genes may be suppressed to observe the effects on plaque and tangle pathology. In order to obtain physiologically relevant results, future studies should use animals to answer as many questions as possible.

REFERENCES

- Adlard, P.A., Cherny, R.A., Finkelstein, D.I., Gautier, E., Robb, E., Cortes, M., Volitakis, I., Liu, X., Smith, J.P., Perez, K., *et al.* (2008). Rapid restoration of cognition in Alzheimer's transgenic mice with 8-hydroxy quinoline analogs is associated with decreased interstitial Abeta. *Neuron* 59, 43-55.
- Affholter, J.A., Fried, V.A., and Roth, R.A. (1988). Human insulin-degrading enzyme shares structural and functional homologies with *E. coli* protease III. *Science* 242, 1415-1418.
- Aggarwal, B.B., Sundaram, C., Malani, N., and Ichikawa, H. (2007). Curcumin: the Indian solid gold. *Adv Exp Med Biol* 595, 1-75.
- Agrawal, R., Mishra, B., Tyagi, E., Nath, C., and Shukla, R. (2010). Effect of curcumin on brain insulin receptors and memory functions in STZ (ICV) induced dementia model of rat. *Pharmacol Res* 61, 247-252.
- Ahmed, T., and Gilani, A.H. (2009). Inhibitory effect of curcuminoids on acetylcholinesterase activity and attenuation of scopolamine-induced amnesia may explain medicinal use of turmeric in Alzheimer's disease. *Pharmacol Biochem Behav* 91, 554-559.
- Akiyama, H., Shii, K., Yokono, K., Yonezawa, K., Sato, S., Watanabe, K., and Baba, S. (1988). Cellular localization of insulin-degrading enzyme in rat liver using monoclonal antibodies specific for this enzyme. *Biochem Biophys Res Commun* 155, 914-922.
- Alvarez, A., Munoz, J.P., and Maccioni, R.B. (2001). A Cdk5-p35 stable complex is involved in the beta-amyloid-induced deregulation of Cdk5 activity in hippocampal neurons. *Exp Cell Res* 264, 266-274.
- Anders, A., Gilbert, S., Garten, W., Postina, R., and Fahrenholz, F. (2001). Regulation of the alpha-secretase ADAM10 by its prodomain and proprotein convertases. *FASEB J* 15, 1837-1839.
- Andorfer, C., Kress, Y., Espinoza, M., de Silva, R., Tucker, K.L., Barde, Y.A., Duff, K., and Davies, P. (2003). Hyperphosphorylation and aggregation of tau in mice expressing normal human tau isoforms. *J Neurochem* 86, 582-590.

Apelt, J., Ach, K., and Schliebs, R. (2003). Aging-related down-regulation of neprilysin, a putative beta-amyloid-degrading enzyme, in transgenic Tg2576 Alzheimer-like mouse brain is accompanied by an astroglial upregulation in the vicinity of beta-amyloid plaques. *Neurosci Lett* 339, 183-186.

Apelt, J., Bigl, M., Wunderlich, P., and Schliebs, R. (2004). Aging-related increase in oxidative stress correlates with developmental pattern of beta-secretase activity and beta-amyloid plaque formation in transgenic Tg2576 mice with Alzheimer-like pathology. *Int J Dev Neurosci* 22, 475-484.

Arendt, T. (2001). Alzheimer's disease as a disorder of mechanisms underlying structural brain self-organization. *Neuroscience* 102, 723-765.

Bachurin, S.O., Shevtsova, E.P., Kireeva, E.G., Oxenkrug, G.F., and Sablin, S.O. (2003). Mitochondria as a target for neurotoxins and neuroprotective agents. *Ann N Y Acad Sci* 993, 334-344; discussion 345-339.

Backstrom, J.R., Lim, G.P., Cullen, M.J., and Tokes, Z.A. (1996). Matrix metalloproteinase-9 (MMP-9) is synthesized in neurons of the human hippocampus and is capable of degrading the amyloid-beta peptide (1-40). *J Neurosci* 16, 7910-7919.

Backstrom, J.R., Miller, C.A., and Tokes, Z.A. (1992). Characterization of neutral proteinases from Alzheimer-affected and control brain specimens: identification of calcium-dependent metalloproteinases from the hippocampus. *J Neurochem* 58, 983-992.

Baig, S., Joseph, S.A., Tayler, H., Abraham, R., Owen, M.J., Williams, J., Kehoe, P.G., and Love, S. (2010). Distribution and expression of picalm in Alzheimer disease. *J Neuropathol Exp Neurol* 69, 1071-1077.

Balasubramanyam, K., Varier, R.A., Altaf, M., Swaminathan, V., Siddappa, N.B., Ranga, U., and Kundu, T.K. (2004). Curcumin, a novel p300/CREB-binding protein-specific inhibitor of acetyltransferase, represses the acetylation of histone/nonhistone proteins and histone acetyltransferase-dependent chromatin transcription. *J Biol Chem* 279, 51163-51171.

Bales, K.R., Liu, F., Wu, S., Lin, S., Koger, D., DeLong, C., Hansen, J.C., Sullivan, P.M., and Paul, S.M. (2009). Human APOE isoform-dependent effects on brain beta-amyloid levels in PDAPP transgenic mice. *J Neurosci* 29, 6771-6779.

Bales, K.R., Verina, T., Cummins, D.J., Du, Y., Dodel, R.C., Saura, J., Fishman, C.E., DeLong, C.A., Piccardo, P., Petegnief, V., *et al.* (1999). Apolipoprotein E is essential for amyloid deposition in the APP(V717F) transgenic mouse model of Alzheimer's disease. *Proc Natl Acad Sci U S A* 96, 15233-15238.

Ballatore, C., Lee, V.M., and Trojanowski, J.Q. (2007). Tau-mediated neurodegeneration in Alzheimer's disease and related disorders. *Nat Rev Neurosci* 8, 663-672.

Barnes, K., Turner, A.J., and Kenny, A.J. (1992). Membrane localization of endopeptidase-24.11 and peptidyl dipeptidase A (angiotensin converting enzyme) in the pig brain: a study using subcellular fractionation and electron microscopic immunocytochemistry. *J Neurochem* 58, 2088-2096.

Bassett, C.N., and Montine, T.J. (2003). Lipoproteins and lipid peroxidation in Alzheimer's disease. *J Nutr Health Aging* 7, 24-29.

Bateman, R.J., Simers, E.R., Mawuenyega, K.G., Wen, G., Browning, K.R., Sigurdson, W.C., Yarasheski, K.E., Friedrich, S.W., Demattos, R.B., May, P.C., *et al.* (2009). A gamma-secretase inhibitor decreases amyloid-beta production in the central nervous system. *Ann Neurol* 66, 48-54.

Baum, L., Chen, L., Ng, H.K., Chan, Y.S., Mak, Y.T., Woo, J., Chiu, H.F., and Pang, C.P. (1998). Low density lipoprotein receptor related protein gene exon 3 polymorphism association with Alzheimer's disease in Chinese. *Neurosci Lett* 247, 33-36.

Baum, L., Lam, C.W., Cheung, S.K., Kwok, T., Lui, V., Tsoh, J., Lam, L., Leung, V., Hui, E., Ng, C., *et al.* (2008). Six-month randomized, placebo-controlled, double-blind, pilot clinical trial of curcumin in patients with Alzheimer disease. *J Clin Psychopharmacol* 28, 110-113.

Baum, L., and Ng, A. (2004). Curcumin interaction with copper and iron suggests one possible mechanism of action in Alzheimer's disease animal models. *J Alzheimers Dis* 6, 367-377; discussion 443-369.

- Beal, M.F. (2000). Oxidative metabolism. *Ann N Y Acad Sci* 924, 164-169.
- Bear, M.F., Connors, B.W., and Paradiso, M.A. (2001). *Neuroscience: Exploring the brain*, 2nd edn.
- Begum, A.N., Jones, M.R., Lim, G.P., Morihara, T., Kim, P., Heath, D.D., Rock, C.J., Pruitt, M.A., Yang, F., Hudspeth, B., *et al.* (2008). Curcumin structure-function, bioavailability, and efficacy in models of neuroinflammation and Alzheimer's disease. *J Pharmacol Exp Ther* 326, 196-208.
- Benjannet, S., Elagöz, A., Wickham, L., Mamarbachi, M., Munzer, J.S., Basak, A., Lazure, C., Cromlish, J.A., Sisodia, S., Checler, F., *et al.* (2001). Post-translational processing of beta-secretase (beta-amyloid-converting enzyme) and its ectodomain shedding. The pro- and transmembrane/cytosolic domains affect its cellular activity and amyloid-beta production. *J Biol Chem* 276, 10879-10887.
- Bentley, P., Driver, J., and Dolan, R.J. (2009). Modulation of fusiform cortex activity by cholinesterase inhibition predicts effects on subsequent memory. *Brain* 132, 2356-2371.
- Bernstein, H.G., Ansorge, S., Riederer, P., Reiser, M., Frolich, L., and Bogerts, B. (1999). Insulin-degrading enzyme in the Alzheimer's disease brain: prominent localization in neurons and senile plaques. *Neurosci Lett* 263, 161-164.
- Bertram, L., Blacker, D., Mullin, K., Keency, D., Jones, J., Basu, S., Yhu, S., McInnis, M.G., Go, R.C., Vekrellis, K., *et al.* (2000). Evidence for genetic linkage of Alzheimer's disease to chromosome 10q. *Science* 290, 2302-2303.
- Bertrand, P., Poirier, J., Oda, T., Finch, C.E., and Pasinetti, G.M. (1995). Association of apolipoprotein E genotype with brain levels of apolipoprotein E and apolipoprotein J (clusterin) in Alzheimer disease. *Brain Res Mol Brain Res* 33, 174-178.
- Bevilacqua, M., Butcher, E., Furie, B., Gallatin, M., Gimbrone, M., Harlan, J., Kishimoto, K., Lasky, L., McEver, R., and *et al.* (1991). Selectins: a family of adhesion receptors. *Cell* 67, 233.
- Bierer, L.M., Hof, P.R., Purohit, D.P., Carlin, L., Schmeidler, J., Davis, K.L., and Perl, D.P. (1995). Neocortical neurofibrillary tangles correlate with dementia severity in Alzheimer's disease. *Arch Neurol* 52, 81-88.

Bishop, G.M., and Robinson, S.R. (2003). Human Abeta1-42 reduces iron-induced toxicity in rat cerebral cortex. *J Neurosci Res* 73, 316-323.

Bishop, G.M., and Robinson, S.R. (2004). The amyloid paradox: amyloid-beta-metal complexes can be neurotoxic and neuroprotective. *Brain Pathol* 14, 448-452.

Black, R.A., Rauch, C.T., Kozlosky, C.J., Peschon, J.J., Slack, J.L., Wolfson, M.F., Castner, B.J., Stocking, K.L., Reddy, P., Srinivasan, S., *et al.* (1997). A metalloproteinase disintegrin that releases tumour-necrosis factor-alpha from cells. *Nature* 385, 729-733.

Blinkov, S.M., and Glezer, I.I. (1968). The human brain in figures and tables: A quantitative handbook. (New York, Plenum Press).

Bloch, L., Sineshchekova, O., Reichenbach, D., Reiss, K., Saftig, P., Kuro-o, M., and Kaether, C. (2009). Klotho is a substrate for alpha-, beta- and gamma-secretase. *FEBS Lett* 583, 3221-3224.

Bolmont, T., Clavaguera, F., Meyer-Luchmann, M., Herzog, M.C., Radde, R., Staufenbiel, M., Lewis, J., Hutton, M., Tolnay, M., and Jucker, M. (2007). Induction of tau pathology by intracerebral infusion of amyloid-beta -containing brain extract and by amyloid-beta deposition in APP x Tau transgenic mice. *Am J Pathol* 171, 2012-2020.

Braak, H., and Braak, E. (1995). Staging of Alzheimer's disease-related neurofibrillary changes. *Neurobiol Aging* 16, 271-278; discussion 278-284.

Brou, C., Logeat, F., Gupta, N., Bessia, C., LeBail, O., Doedens, J.R., Cumano, A., Roux, P., Black, R.A., and Israel, A. (2000). A novel proteolytic cleavage involved in Notch signaling: the role of the disintegrin-metalloprotease TACE. *Mol Cell* 5, 207-216.

Brouet, I., and Ohshima, H. (1995). Curcumin, an anti-tumour promoter and anti-inflammatory agent, inhibits induction of nitric oxide synthase in activated macrophages. *Biochem Biophys Res Commun* 206, 533-540.

Burk, R.F., Hill, K.E., Olson, G.E., Weeber, E.J., Motley, A.K., Winfrey, V.P., and Austin, L.M. (2007). Deletion of apolipoprotein E receptor-2 in mice lowers brain selenium and causes severe neurological dysfunction and death when a low-selenium diet is fed. *J Neurosci* 27, 6207-6211.

- Bush, A.I. (2003). The metallobiology of Alzheimer's disease. *Trends Neurosci* 26, 207-214.
- Butterfield, D.A. (2002). Amyloid beta-peptide (1-42)-induced oxidative stress and neurotoxicity: implications for neurodegeneration in Alzheimer's disease brain. A review. *Free Radic Res* 36, 1307-1313.
- Buxbaum, J.D., Koo, E.H., and Greengard, P. (1993). Protein phosphorylation inhibits production of Alzheimer amyloid beta/A4 peptide. *Proc Natl Acad Sci U S A* 90, 9195-9198.
- Buxbaum, J.D., Liu, K.N., Luo, Y., Slack, J.L., Stocking, K.L., Peschon, J.J., Johnson, R.S., Castner, B.J., Cerretti, D.P., and Black, R.A. (1998). Evidence that tumor necrosis factor alpha converting enzyme is involved in regulated alpha-secretase cleavage of the Alzheimer amyloid protein precursor. *J Biol Chem* 273, 27765-27767.
- Calvo, A.C., Moreno-Igoa, M., Manzano, R., Ordovas, I., Yague, G., Olivan, S., Munoz, M.J., Zaragoza, P., and Osta, R. (2008). Determination of protein and RNA expression levels of common housekeeping genes in a mouse model of neurodegeneration. *Proteomics* 8, 4338-4343.
- Caporaso, G.L., Takei, K., Gandy, S.E., Matteoli, M., Mundigl, O., Greengard, P., and De Camilli, P. (1994). Morphologic and biochemical analysis of the intracellular trafficking of the Alzheimer beta/A4 amyloid precursor protein. *J Neurosci* 14, 3122-3138.
- Carpentier, M., Robitaille, Y., DesGroseillers, L., Boileau, G., and Marcinkiewicz, M. (2002). Declining expression of neprilysin in Alzheimer disease vasculature: possible involvement in cerebral amyloid angiopathy. *J Neuropathol Exp Neurol* 61, 849-856.
- Castellano, J.M., Kim, J., Stewart, F.R., Jiang, H., Demattos, R.B., Patterson, B.W., Fagan, A.M., Morris, J.C., Mawucnyega, K.G., Cruchaga, C., *et al.* (2011). Human apoE Isoforms Differentially Regulate Brain Amyloid- β Peptide Clearance. *Sci Transl Med* 3, 89ra57.
- Chan, M.M., Huang, H.I., Fenton, M.R., and Fong, D. (1998). In vivo inhibition of nitric oxide synthase gene expression by curcumin, a cancer preventive natural product with anti-inflammatory properties. *Biochem Pharmacol* 55, 1955-1962.

- Chang, W.P., Downs, D., Huang, X.P., Da, H., Fung, K.M., and Tang, J. (2007). Amyloid-beta reduction by memapsin 2 (beta-secretase) immunization. *FASEB J* 21, 3184-3196.
- Chappell, D.A., Fry, G.L., Waknitz, M.A., Iverius, P.H., Williams, S.E., and Strickland, D.K. (1992). The low density lipoprotein receptor-related protein/alpha 2-macroglobulin receptor binds and mediates catabolism of bovine milk lipoprotein lipase. *J Biol Chem* 267, 25764-25767.
- Chen, D.Y., Stern, S.A., Garcia-Osta, A., Saunier-Rebori, B., Pollonini, G., Bambah-Mukku, D., Blitzer, R.D., and Alberini, C.M. (2011). A critical role for IGF-II in memory consolidation and enhancement. *Nature* 469, 491-497.
- Chen, Y.R., and Tan, T.H. (1998). Inhibition of the c-Jun N-terminal kinase (JNK) signaling pathway by curcumin. *Oncogene* 17, 173-178.
- Cheng, T.C., Lin, C.S., Hsu, C.C., Chen, L.J., Cheng, K.C., and Cheng, J.T. (2009). Activation of muscarinic M-1 cholinceptors by curcumin to increase glucose uptake into skeletal muscle isolated from Wistar rats. *Neurosci Lett* 465, 238-241.
- Christie, R.H., Freeman, M., and Hyman, B.T. (1996). Expression of the macrophage scavenger receptor, a multifunctional lipoprotein receptor, in microglia associated with senile plaques in Alzheimer's disease. *Am J Pathol* 148, 399-403.
- Clatworthy, A.F., Stockinger, W., Christie, R.H., Schneider, W.J., Nimpf, J., Hyman, B.T., and Rebeck, G.W. (1999). Expression and alternate splicing of apolipoprotein E receptor 2 in brain. *Neuroscience* 90, 903-911.
- Cleary, J.P., Walsh, D.M., Hofmeister, J.J., Shankar, G.M., Kuskowski, M.A., Selkoe, D.J., and Ashe, K.H. (2005). Natural oligomers of the amyloid-beta protein specifically disrupt cognitive function. *Nat Neurosci* 8, 79-84.
- Cole, G.M., Teter, B., and Frautschy, S.A. (2007). Neuroprotective effects of curcumin. *Adv Exp Med Biol* 595, 197-212.
- Corder, E.H., Saunders, A.M., Risch, N.J., Strittmatter, W.J., Schmechel, D.E., Gaskell, P.C., Jr., Rimmler, J.B., Locke, P.A., Conneally, P.M., Schmechel, K.E., *et al.* (1994). Protective effect of apolipoprotein E type 2 allele for late onset Alzheimer disease. *Nat Genet* 7, 180-184.

- Corder, E.H., Saunders, A.M., Strittmatter, W.J., Schmechel, D.E., Gaskell, P.C., Small, G.W., Roses, A.D., Haines, J.L., and Pericak-Vance, M.A. (1993). Gene dose of apolipoprotein E type 4 allele and the risk of Alzheimer's disease in late onset families. *Science* 261, 921-923.
- Coulson, D.T., Beyer, N., Quinn, J.G., Brockbank, S., Hellemans, J., Irvine, G.B., Ravid, R., and Johnston, J.A. (2010). BACE1 mRNA expression in Alzheimer's disease postmortem brain tissue. *J Alzheimers Dis* 22, 1111-1122.
- Coyoy, A., Valencia, A., Guemez-Gamboa, A., and Moran, J. (2008). Role of NADPH oxidase in the apoptotic death of cultured cerebellar granule neurons. *Free Radic Biol Med* 45, 1056-1064.
- Crews, L., Adame, A., Patrick, C., Delaney, A., Pham, E., Rockenstein, E., Hansen, L., and Masliah, E. (2010). Increased BMP6 levels in the brains of Alzheimer's disease patients and APP transgenic mice are accompanied by impaired neurogenesis. *J Neurosci* 30, 12252-12262.
- Cronin-Stubbs, D., Beckett, L.A., Scherr, P.A., Field, T.S., Chown, M.J., Pilgrim, D.M., Bennett, D.A., and Evans, D.A. (1997). Weight loss in people with Alzheimer's disease: a prospective population based analysis. *BMJ* 314, 178-179.
- Cruts, M. (2011). Alzheimer Disease Mutation Database. In *Alzheimer Disease & Frontotemporal Dementia Mutation Database* [online].
- Cruts, M., Backhovens, H., Wang, S.Y., Van Gassen, G., Theuns, J., De Jonghe, C.D., Wehnert, A., De Vocht, J., De Winter, G., Cras, P., *et al.* (1995). Molecular genetic analysis of familial early-onset Alzheimer's disease linked to chromosome 14q24.3. *Hum Mol Genet* 4, 2363-2371.
- Davis, K.L., Thal, L.J., Gamzu, E.R., Davis, C.S., Woolson, R.F., Gracon, S.I., Drachman, D.A., Schneider, L.S., Whitehouse, P.J., Hoover, T.M., *et al.* (1992). A double-blind, placebo-controlled multicenter study of tacrine for Alzheimer's disease. The Tacrine Collaborative Study Group. *N Engl J Med* 327, 1253-1259.
- Dawson, G.R., Scabrook, G.R., Zheng, H., Smith, D.W., Graham, S., O'Dowd, G., Bowery, B.J., Boyce, S., Trumbauer, M.E., Chen, H.Y., *et al.* (1999). Age-related cognitive deficits, impaired long-term potentiation and reduction in synaptic marker density in mice lacking the beta-amyloid precursor protein. *Neuroscience* 90, 1-13.

- De Strooper, B. (2003). Aph-1, Pen-2, and Nicastrin with Presenilin generate an active gamma-Secretase complex. *Neuron* 38, 9-12.
- De Strooper, B., and Annaert, W. (2000). Proteolytic processing and cell biological functions of the amyloid precursor protein. *J Cell Sci* 113 (Pt 11), 1857-1870.
- De Strooper, B., Annaert, W., Cupers, P., Saftig, P., Craessaerts, K., Mumm, J.S., Schroeter, E.H., Schrijvers, V., Wolfe, M.S., Ray, W.J., *et al.* (1999). A presenilin-1-dependent gamma-secretase-like protease mediates release of Notch intracellular domain. *Nature* 398, 518-522.
- De Strooper, B., Saftig, P., Craessaerts, K., Vanderstichele, H., Guhde, G., Annaert, W., Von Figura, K., and Van Leuven, F. (1998). Deficiency of presenilin-1 inhibits the normal cleavage of amyloid precursor protein. *Nature* 391, 387-390.
- Deane, R., Wu, Z., Sagare, A., Davis, J., Du Yan, S., Hamm, K., Xu, F., Parisi, M., LaRue, B., Hu, H.W., *et al.* (2004). LRP/amyloid beta-peptide interaction mediates differential brain efflux of Abeta isoforms. *Neuron* 43, 333-344.
- Deb, S., and Gottschall, P.E. (1996). Increased production of matrix metalloproteinases in enriched astrocyte and mixed hippocampal cultures treated with beta-amyloid peptides. *J Neurochem* 66, 1641-1647.
- Deb, S., Wenjun Zhang, J., and Gottschall, P.E. (2003). Beta-amyloid induces the production of active, matrix-degrading proteases in cultured rat astrocytes. *Brain Res* 970, 205-213.
- Devarajan, P., Johnston, J.J., Ginsberg, S.S., Van Wart, H.E., and Berliner, N. (1992). Structure and expression of neutrophil gelatinase cDNA. Identity with type IV collagenase from HT1080 cells. *J Biol Chem* 267, 25228-25232.
- Dewachter, I., Reverse, D., Caluwaerts, N., Ris, L., Kuiperi, C., Van den Haute, C., Spittaels, K., Umans, L., Serneels, L., Thiry, E., *et al.* (2002). Neuronal deficiency of presenilin 1 inhibits amyloid plaque formation and corrects hippocampal long-term potentiation but not a cognitive defect of amyloid precursor protein [V717I] transgenic mice. *J Neurosci* 22, 3445-3453.
- Doble, B.W., and Woodgett, J.R. (2003). GSK-3: tricks of the trade for a multi-tasking kinase. *J Cell Sci* 116, 1175-1186.

- Dodel, R.C., Du, Y., Depboylu, C., Hampel, H., Frolich, L., Haag, A., Hemmeter, U., Paulsen, S., Teipel, S.J., Brettschneider, S. *et al.* (2004). Intravenous immunoglobulins containing antibodies against beta-amyloid for the treatment of Alzheimer's disease. *J Neurol Neurosurg Psychiatry* 75, 1472-1474.
- Doody, R.S., Gavrilova, S.I., Sano, M., Thomas, R.G., Aisen, P.S., Bachurin, S.O., Secly, L., and Hung, D. (2008). Effect of dimebon on cognition, activities of daily living, behaviour, and global function in patients with mild-to-moderate Alzheimer's disease: a randomised, double-blind, placebo-controlled study. *Lancet* 372, 207-215.
- Du, J., Zhu, Y., Chen, X., Fei, Z., Yang, S., Yuan, W., Zhang, J., and Zhu, T. (2007). Protective effect of bone morphogenetic protein-6 on neurons from H₂O₂ injury. *Brain Res* 1163, 10-20.
- Dumont, M., Wille, E., Stack, C., Calingasan, N.Y., Beal, M.F., and Lin, M.T. (2009). Reduction of oxidative stress, amyloid deposition, and memory deficit by manganese superoxide dismutase overexpression in a transgenic mouse model of Alzheimer's disease. *FASEB J* 23, 2459-2466.
- Eckman, C.B., Mehta, N.D., Crook, R., Perez-tur, J., Prihar, G., Pfeiffer, E., Graff-Radford, N., Hinder, P., Yager, D., Zenk, B., *et al.* (1997). A new pathogenic mutation in the APP gene (I716V) increases the relative proportion of A beta 42(43). *Hum Mol Genet* 6, 2087-2089.
- Edbauer, D., Winkler, E., Haass, C., and Steiner, H. (2002). Presenilin and nicastrin regulate each other and determine amyloid beta-peptide production via complex formation. *Proc Natl Acad Sci U S A* 99, 8666-8671.
- Eikelenboom, P., and Veerhuis, R. (1996). The role of complement and activated microglia in the pathogenesis of Alzheimer's disease. *Neurobiol Aging* 17, 673-680.
- El Khoury, J., Hickman, S.E., Thomas, C.A., Cao, L., Silverstein, S.C., and Loike, J.D. (1996). Scavenger receptor-mediated adhesion of microglia to beta-amyloid fibrils. *Nature* 382, 716-719.
- Erickson, J.D., and Varoqui, H. (2000). Molecular analysis of vesicular amine transporter function and targeting to secretory organelles. *FASEB J* 14, 2450-2458.
- Etcheberrigaray, R., Tan, M., Dewachter, I., Kuiperi, C., Van der Auwera, I., Wera, S., Qiao, L., Bank, B., Nelson, T.J., Kozikowski, A.P., *et al.* (2004). Therapeutic effects

of PKC activators in Alzheimer's disease transgenic mice. *Proc Natl Acad Sci U S A* *101*, 11141-11146.

Farris, W., Mansourian, S., Chang, Y., Lindsley, L., Eckman, E.A., Frosch, M.P., Eckman, C.B., Tanzi, R.E., Selkoe, D.J., and Guenette, S. (2003). Insulin-degrading enzyme regulates the levels of insulin, amyloid beta-protein, and the beta-amyloid precursor protein intracellular domain in vivo. *Proc Natl Acad Sci U S A* *100*, 4162-4167.

Ferri, C.P., Prince, M., Brayne, C., Brodaty, H., Fratiglioni, L., Ganguli, M., Hall, K., Hasegawa, K., Hendric, H., Huang, Y., *et al.* (2005). Global prevalence of dementia: a Delphi consensus study. *Lancet* *366*, 2112-2117.

Fischer, P.M. (2008). Turning down tau phosphorylation. *Nat Chem Biol* *4*, 448-449.

Franberg, J., Karlstrom, H., Winblad, B., Tjernberg, L.O., and Frykman, S. (2010). gamma-Secretase dependent production of intracellular domains is reduced in adult compared to embryonic rat brain membranes. *PLoS One* *5*, e9772.

Francis, R., McGrath, G., Zhang, J., Ruddy, D.A., Sym, M., Apfeld, J., Nicoll, M., Maxwell, M., Hai, B., Ellis, M.C., *et al.* (2002). *aph-1* and *pen-2* are required for Notch pathway signaling, gamma-secretase cleavage of betaAPP, and presenilin protein accumulation. *Dev Cell* *3*, 85-97.

Frautschy, S.A., Hu, W., Kim, P., Miller, S.A., Chu, T., Harris-White, M.E., and Cole, G.M. (2001). Phenolic anti-inflammatory antioxidant reversal of Abeta-induced cognitive deficits and neuropathology. *Neurobiol Aging* *22*, 993-1005.

Fuentealba, R.A., Barria, M.I., Lee, J., Cam, J., Araya, C., Escudero, C.A., Inestrosa, N.C., Bronfman, F.C., Bu, G., and Marzolo, M.P. (2007). ApoER2 expression increases Abeta production while decreasing Amyloid Precursor Protein (APP) endocytosis: Possible role in the partitioning of APP into lipid rafts and in the regulation of gamma-secretase activity. *Mol Neurodegener* *2*, 14.

Fuentealba, R.A., Liu, Q., Zhang, J., Kanekiyo, T., Hu, X., Lee, J.M., LaDu, M.J., and Bu, G. (2010). Low-density lipoprotein receptor-related protein 1 (LRP1) mediates neuronal Abeta42 uptake and lysosomal trafficking. *PLoS One* *5*, e11884.

- Fukumoto, H., Cheung, B.S., Hyman, B.T., and Irizarry, M.C. (2002). Beta-secretase protein and activity are increased in the neocortex in Alzheimer disease. *Arch Neurol* 59, 1381-1389.
- Gandy, S., Simon, A.J., Steele, J.W., Lublin, A.L., Lah, J.J., Walker, L.C., Levey, A.I., Krafft, G.A., Levy, F., Checler, F., *et al.* (2010). Days to criterion as an indicator of toxicity associated with human Alzheimer amyloid-beta oligomers. *Ann Neurol* 68, 220-230.
- Gau, J.T., Steinhilb, M.L., Kao, T.C., D'Amato, C.J., Gaut, J.R., Frey, K.A., and Turner, R.S. (2002). Stable beta-secretase activity and presynaptic cholinergic markers during progressive central nervous system amyloidogenesis in Tg2576 mice. *Am J Pathol* 160, 731-738.
- Geller, D.A., Lowenstein, C.J., Shapiro, R.A., Nussler, A.K., Di Silvio, M., Wang, S.C., Nakayama, D.K., Simmons, R.L., Snyder, S.H., and Billiar, T.R. (1993). Molecular cloning and expression of inducible nitric oxide synthase from human hepatocytes. *Proc Natl Acad Sci U S A* 90, 3491-3495.
- Gilman, S., Koller, M., Black, R.S., Jenkins, L., Griffith, S.G., Fox, N.C., Fisner, L., Kirby, L., Rovira, M.B., Forette, F., *et al.* (2005). Clinical effects of Abeta immunization (AN1792) in patients with AD in an interrupted trial. *Neurology* 64, 1553-1562.
- Glennner, G.G., and Wong, C.W. (1984). Alzheimer's disease: initial report of the purification and characterization of a novel cerebrovascular amyloid protein. *Biochem Biophys Res Commun* 120, 885-890.
- Goedert, M., Hasegawa, M., Jakes, R., Lawler, S., Cuenda, A., and Cohen, P. (1997). Phosphorylation of microtubule-associated protein tau by stress-activated protein kinases. *FEBS Lett* 409, 57-62.
- Goedert, M., Spillantini, M.G., Jakes, R., Rutherford, D., and Crowther, R.A. (1989). Multiple isoforms of human microtubule-associated protein tau: sequences and localization in neurofibrillary tangles of Alzheimer's disease. *Neuron* 3, 519-526.
- Goedert, M., Wischik, C.M., Crowther, R.A., Walker, J.E., and Klug, A. (1988). Cloning and sequencing of the cDNA encoding a core protein of the paired helical

filament of Alzheimer disease: identification as the microtubule-associated protein tau. *Proc Natl Acad Sci U S A* 85, 4051-4055.

Gong, C.X., Liu, F., Grundke-Iqbal, I., and Iqbal, K. (2005). Post-translational modifications of tau protein in Alzheimer's disease. *J Neural Transm* 112, 813-838.

Goodman, Y., and Mattson, M.P. (1994). Secreted forms of beta-amyloid precursor protein protect hippocampal neurons against amyloid beta-peptide-induced oxidative injury. *Exp Neurol* 128, 1-12.

Goutte, C., Tsunozaki, M., Hale, V.A., and Priess, J.R. (2002). APH-1 is a multipass membrane protein essential for the Notch signaling pathway in *Caenorhabditis elegans* embryos. *Proc Natl Acad Sci U S A* 99, 775-779.

Griffin, W.S., Stanley, L.C., Ling, C., White, L., MacLeod, V., Perrot, L.J., White, C.L., 3rd, and Araoz, C. (1989). Brain interleukin 1 and S-100 immunoreactivity are elevated in Down syndrome and Alzheimer disease. *Proc Natl Acad Sci U S A* 86, 7611-7615.

Guibal, F.C., Alberich-Jorda, M., Hirai, H., Ebralidze, A., Levantini, E., Di Ruscio, A., Zhang, P., Santana-Lemos, B.A., Neuberg, D., Wagers, A.J., *et al.* (2009). Identification of a myeloid committed progenitor as the cancer-initiating cell in acute promyelocytic leukemia. *Blood* 114, 5415-5425.

Guix, F.X., Uribealago, I., Coma, M., and Munoz, F.J. (2005). The physiology and pathophysiology of nitric oxide in the brain. *Prog Neurobiol* 76, 126-152.

Gura, T. (2008). Hope in Alzheimer's fight emerges from unexpected places. *Nat Med* 14, 894.

Haass, C., Schlossmacher, M.G., Hung, A.Y., Vigo-Pelfrey, C., Mellon, A., Ostaszewski, B.L., Lieberburg, I., Koo, E.H., Schenk, D., Teplow, D.B., *et al.* (1992). Amyloid beta-peptide is produced by cultured cells during normal metabolism. *Nature* 359, 322-325.

Haass, C., and Selkoe, D.J. (1993). Cellular processing of beta-amyloid precursor protein and the genesis of amyloid beta-peptide. *Cell* 75, 1039-1042.

Hamaguchi, T., Ono, K., Murase, A., and Yamada, M. (2009). Phenolic compounds prevent Alzheimer's pathology through different effects on the amyloid-beta aggregation pathway. *Am J Pathol* 175, 2557-2565.

Hampel, H., Ewers, M., Burger, K., Annas, P., Mortberg, A., Bogstedt, A., Frolich, L., Schroder, J., Schonknecht, P., Riepe, M.W., *et al.* (2009). Lithium trial in Alzheimer's disease: a randomized, single-blind, placebo-controlled, multicenter 10-week study. *J Clin Psychiatry* *70*, 922-931.

Harold, D., Abraham, R., Hollingworth, P., Sims, R., Gerrish, A., Hamshere, M.L., Pahwa, J.S., Moskvina, V., Dowzell, K., Williams, A., *et al.* (2009). Genome-wide association study identifies variants at CLU and PICALM associated with Alzheimer's disease. *Nat Genet* *41*, 1088-1093.

Hartmann, D., de Strooper, B., Serneels, L., Craessaerts, K., Herreman, A., Annaert, W., Umans, L., Lubke, T., Lena Illert, A., von Figura, K., *et al.* (2002). The disintegrin/metalloprotease ADAM 10 is essential for Notch signalling but not for alpha-secretase activity in fibroblasts. *Hum Mol Genet* *11*, 2615-2624.

Hatcher, H., Planalp, R., Cho, J., Torti, F.M., and Torti, S.V. (2008). Curcumin: from ancient medicine to current clinical trials. *Cell Mol Life Sci* *65*, 1631-1652.

Helbecque, N., Cottel, D., and Amouyel, P. (2009). Low-density lipoprotein receptor-related protein 8 gene polymorphisms and dementia. *Neurobiol Aging* *30*, 266-271.

Henley, D.B., May, P.C., Dean, R.A., and Siemers, E.R. (2009). Development of semagacestat (LY450139), a functional gamma-secretase inhibitor, for the treatment of Alzheimer's disease. *Expert Opin Pharmacother* *10*, 1657-1664.

Hensley, K., Carney, J.M., Mattson, M.P., Aksenova, M., Harris, M., Wu, J.F., Floyd, R.A., and Butterfield, D.A. (1994). A model for beta-amyloid aggregation and neurotoxicity based on free radical generation by the peptide: relevance to Alzheimer disease. *Proc Natl Acad Sci U S A* *91*, 3270-3274.

Hensley, K., Hall, N., Subramaniam, R., Cole, P., Harris, M., Aksenov, M., Aksenova, M., Gabbita, S.P., Wu, J.F., Carney, J.M., *et al.* (1995). Brain regional correspondence between Alzheimer's disease histopathology and biomarkers of protein oxidation. *J Neurochem* *65*, 2146-2156.

Herz, J. (2003). I.RP: a bright beacon at the blood-brain barrier. *J Clin Invest* *112*, 1483-1485.

Hinkle, C.L., Sunnarborg, S.W., Loiselle, D., Parker, C.E., Stevenson, M., Russell, W.E., and Lee, D.C. (2004). Selective roles for tumor necrosis factor alpha-converting

enzyme/ADAM17 in the shedding of the epidermal growth factor receptor ligand family: the juxtamembrane stalk determines cleavage efficiency. *J Biol Chem* 279, 24179-24188.

Hotoda, N., Koike, H., Sasagawa, N., and Ishiura, S. (2002). A secreted form of human ADAM9 has an alpha-secretase activity for APP. *Biochem Biophys Res Commun* 293, 800-805.

Houmard, J.A., Weidner, M.D., Dolan, P.L., Leggett-Frazier, N., Gavigan, K.E., Hickey, M.S., Tyndall, G.L., Zheng, D., Alshami, A., and Dohm, G.L. (1995). Skeletal muscle GLUT4 protein concentration and aging in humans. *Diabetes* 44, 555-560.

Hsiao, K., Borchelt, D.R., Olson, K., Johannsdottir, R., Kitt, C., Yunis, W., Xu, S., Eckman, C., Younkin, S., Price, D., *et al.* (1995). Age-related CNS disorder and early death in transgenic FVB/N mice overexpressing Alzheimer amyloid precursor proteins. *Neuron* 15, 1203-1218.

Hsiao, K., Chapman, P., Nilsen, S., Eckman, C., Harigaya, Y., Younkin, S., Yang, F., and Cole, G. (1996). Correlative memory deficits, Abeta elevation, and amyloid plaques in transgenic mice. *Science* 274, 99-102.

Hu, D., Serrano, F., Oury, T.D., and Klann, E. (2006). Aging-dependent alterations in synaptic plasticity and memory in mice that overexpress extracellular superoxide dismutase. *J Neurosci* 26, 3933-3941.

Hu, L., Wong, T.P., Cote, S.L., Bell, K.F., and Cuellar, A.C. (2003). The impact of Abeta-plaques on cortical cholinergic and non-cholinergic presynaptic boutons in Alzheimer's disease-like transgenic mice. *Neuroscience* 121, 421-432.

Huang, X., Atwood, C.S., Hartshorn, M.A., Multhaup, G., Goldstein, L.E., Scarpa, R.C., Cuajungco, M.P., Gray, D.N., Lim, J., Moir, R.D., *et al.* (1999a). The A beta peptide of Alzheimer's disease directly produces hydrogen peroxide through metal ion reduction. *Biochemistry* 38, 7609-7616.

Huang, X., Cuajungco, M.P., Atwood, C.S., Hartshorn, M.A., Tyndall, J.D., Hanson, G.R., Stokes, K.C., Leopold, M., Multhaup, G., Goldstein, L.E., *et al.* (1999b). Cu(II) potentiation of Alzheimer abeta neurotoxicity. Correlation with cell-free hydrogen peroxide production and metal reduction. *J Biol Chem* 274, 37111-37116.

- Huse, J.T., Pijak, D.S., Leslie, G.J., Lee, V.M., and Doms, R.W. (2000). Maturation and endosomal targeting of beta-site amyloid precursor protein-cleaving enzyme. The Alzheimer's disease beta-secretase. *J Biol Chem* 275, 33729-33737.
- Hussain, I., Hawkins, J., Harrison, D., Hille, C., Wayne, G., Cutler, L., Buck, T., Walter, D., Demont, E., Howes, C., *et al.* (2007). Oral administration of a potent and selective non-peptidic BACE-1 inhibitor decreases beta-cleavage of amyloid precursor protein and amyloid-beta production in vivo. *J Neurochem* 100, 802-809.
- Hussain, I., Powell, D., Howlett, D.R., Tew, D.G., Meek, T.D., Chapman, C., Gloger, I.S., Murphy, K.E., Southan, C.D., Ryan, D.M., *et al.* (1999). Identification of a novel aspartic protease (Asp 2) as beta-secretase. *Mol Cell Neurosci* 14, 419-427.
- Hutton, M., Busfield, F., Wragg, M., Crook, R., Perez-Tur, J., Clark, R.F., Prihar, G., Talbot, C., Phillips, H., Wright, K., *et al.* (1996). Complete analysis of the presenilin 1 gene in early onset Alzheimer's disease. *Neuroreport* 7, 801-805.
- Ida, N., Hartmann, T., Pantel, J., Schroder, J., Zerfass, R., Forstl, H., Sandbrink, R., Masters, C.L., and Beyreuther, K. (1996). Analysis of heterogeneous A4 peptides in human cerebrospinal fluid and blood by a newly developed sensitive Western blot assay. *J Biol Chem* 271, 22908-22914.
- Irizarry, M.C., McNamara, M., Fedorchak, K., Hsiao, K., and Hyman, B.T. (1997). APPSw transgenic mice develop age-related A beta deposits and neuropil abnormalities, but no neuronal loss in CA1. *J Neuropathol Exp Neurol* 56, 965-973.
- Ishrat, T., Hoda, M.N., Khan, M.B., Yousuf, S., Ahmad, M., Khan, M.M., Ahmad, A., and Islam, F. (2009). Amelioration of cognitive deficits and neurodegeneration by curcumin in rat model of sporadic dementia of Alzheimer's type (SDAT). *Eur Neuropsychopharmacol* 19, 636-647.
- Iwatsubo, T., Odaka, A., Suzuki, N., Mizusawa, H., Nukina, N., and Ihara, Y. (1994). Visualization of A beta 42(43) and A beta 40 in senile plaques with end-specific A beta monoclonals: evidence that an initially deposited species is A beta 42(43). *Neuron* 13, 45-53.
- Jarrett, J.T., Berger, E.P., and Lansbury, P.T., Jr. (1993). The carboxy terminus of the beta amyloid protein is critical for the seeding of amyloid formation: implications for the pathogenesis of Alzheimer's disease. *Biochemistry* 32, 4693-4697.

- Jarvis, K., Assis-Nascimento, P., Mudd, L.M., and Montague, J.R. (2007). Beta-amyloid toxicity and reversal in embryonic rat septal neurons. *Neurosci Lett* 423, 184-188.
- Johnson, D.K., Wilkins, C.H., and Morris, J.C. (2006). Accelerated weight loss may precede diagnosis in Alzheimer disease. *Arch Neurol* 63, 1312-1317.
- Jung, S.S., Zhang, W., and Van Nostrand, W.E. (2003). Pathogenic A beta induces the expression and activation of matrix metalloproteinase-2 in human cerebrovascular smooth muscle cells. *J Neurochem* 85, 1208-1215.
- Kahles, T., Kohlen, A., Heumueller, S., Rappert, A., Bechmann, I., Liebner, S., Wittko, I.M., Neumann-Haefelin, T., Steinmetz, H., Schroeder, K., *et al.* (2010). NADPH oxidase Nox1 contributes to ischemic injury in experimental stroke in mice. *Neurobiol Dis* 40, 185-192.
- Kamboh, M.I., Ferrell, R.E., and DeKosky, S.T. (1998). Genetic association studies between Alzheimer's disease and two polymorphisms in the low density lipoprotein receptor-related protein gene. *Neurosci Lett* 244, 65-68.
- Kang, D.E., Pietrzik, C.U., Baum, L., Chevallier, N., Merriam, D.E., Kounnas, M.Z., Wagner, S.L., Troncoso, J.C., Kawas, C.H., Katzman, R., *et al.* (2000). Modulation of amyloid beta-protein clearance and Alzheimer's disease susceptibility by the LDL receptor-related protein pathway. *J Clin Invest* 106, 1159-1166.
- Kang, D.E., Saitoh, T., Chen, X., Xia, Y., Masliah, E., Hansen, L.A., Thomas, R.G., Thal, L.J., and Katzman, R. (1997). Genetic association of the low-density lipoprotein receptor-related protein gene (LRP), an apolipoprotein E receptor, with late-onset Alzheimer's disease. *Neurology* 49, 56-61.
- Kang, J., Lemaire, H.G., Unterbeck, A., Salbaum, J.M., Masters, C.L., Grzeschik, K.H., Multhaup, G., Beyreuther, K., and Muller-Hill, B. (1987). The precursor of Alzheimer's disease amyloid A4 protein resembles a cell-surface receptor. *Nature* 325, 733-736.
- Kar, S., Chabot, J.G., and Quirion, R. (1993). Quantitative autoradiographic localization of [125I]insulin-like growth factor I, [125I]insulin-like growth factor II, and [125I]insulin receptor binding sites in developing and adult rat brain. *J Comp Neurol* 333, 375-397.

- Kendzierski, C., Irizarry, R.A., Chen, K.S., Haag, J.D., and Gould, M.N. (2005). On the utility of pooling biological samples in microarray experiments. *Proc Natl Acad Sci U S A* 102, 4252-4257.
- Kim, D.H., Iijima, H., Goto, K., Sakai, J., Ishii, H., Kim, H.J., Suzuki, H., Kondo, H., Saeki, S., and Yamamoto, T. (1996). Human apolipoprotein E receptor 2. A novel lipoprotein receptor of the low density lipoprotein receptor family predominantly expressed in brain. *J Biol Chem* 271, 8373-8380.
- Kim, K.A., Kim, J.Y., Lee, Y.A., Song, K.J., Min, D., and Shin, M.H. (2011). NOX1 participates in ROS-dependent cell death of colon epithelial Caco2 cells induced by *Entamoeba histolytica*. *Microbes Infect.*
- Kim, M., Hersh, L.B., Leissring, M.A., Ingelsson, M., Matsui, T., Farris, W., Lu, A., Hyman, B.T., Selkoe, D.J., Bertram, L., *et al.* (2007). Decreased catalytic activity of the insulin-degrading enzyme in chromosome 10-linked Alzheimer disease families. *J Biol Chem* 282, 7825-7832.
- Kimberly, W.T., LaVoie, M.J., Ostaszewski, B.L., Ye, W., Wolfe, M.S., and Selkoe, D.J. (2003). Gamma-secretase is a membrane protein complex comprised of presenilin, nicastrin, Aph-1, and Pen-2. *Proc Natl Acad Sci U S A* 100, 6382-6387.
- King, D.L., and Arendash, G.W. (2002). Behavioral characterization of the Tg2576 transgenic model of Alzheimer's disease through 19 months. *Physiol Behav* 75, 627-642.
- Kitaguchi, N., Takahashi, Y., Tokushima, Y., Shiojiri, S., and Ito, H. (1988). Novel precursor of Alzheimer's disease amyloid protein shows protease inhibitory activity. *Nature* 331, 530-532.
- Kitraki, E., Bozas, E., Philippidis, H., and Stylianopoulou, F. (1993). Aging-related changes in IGF-II and c-fos gene expression in the rat brain. *Int J Dev Neurosci* 11, 1-9.
- Klimov, D.K., and Thirumalai, D. (2003). Dissecting the assembly of Abeta16-22 amyloid peptides into antiparallel beta sheets. *Structure* 11, 295-307.
- Klyubin, I., Walsh, D.M., Lemere, C.A., Cullen, W.K., Shankar, G.M., Betts, V., Spooner, E.T., Jiang, L., Anwyl, R., Selkoe, D.J., *et al.* (2005). Amyloid beta protein

immunotherapy neutralizes Abeta oligomers that disrupt synaptic plasticity in vivo. *Nat Med* 11, 556-561.

Kontush, A., Berndt, C., Weber, W., Akopyan, V., Arlt, S., Schippling, S., and Beisiegel, U. (2001). Amyloid-beta is an antioxidant for lipoproteins in cerebrospinal fluid and plasma. *Free Radic Biol Med* 30, 119-128.

Koo, E.H., and Squazzo, S.L. (1994). Evidence that production and release of amyloid beta-protein involves the endocytic pathway. *J Biol Chem* 269, 17386-17389.

Kuo, W.L., Montag, A.G., and Rosner, M.R. (1993). Insulin-degrading enzyme is differentially expressed and developmentally regulated in various rat tissues. *Endocrinology* 132, 604-611.

Kurochkin, I.V., and Goto, S. (1994). Alzheimer's beta-amyloid peptide specifically interacts with and is degraded by insulin degrading enzyme. *FEBS Lett* 345, 33-37.

Kurosu, H., Yamamoto, M., Clark, J.D., Pastor, J.V., Nandi, A., Gurnani, P., McGuinness, O.P., Chikuda, H., Yamaguchi, M., Kawaguchi, H., *et al.* (2005). Suppression of aging in mice by the hormone Klotho. *Science* 309, 1829-1833.

Kurz, A., Altland, K., Lautenschlager, N., Zimmer, R., Busch, R., Gerundt, I., Lauter, H., and Muller, U. (1996). Apolipoprotein E type 4 allele and Alzheimer's disease: effect on age at onset and relative risk in different age groups. *J Neurol* 243, 452-456.

Lam, L.C., Tam, C.W., Lui, V.W., Chan, W.C., Chan, S.S., Wong, S., Wong, A., Tham, M.K., Ho, K.S., Chan, W.M., *et al.* (2008). Prevalence of very mild and mild dementia in community-dwelling older Chinese people in Hong Kong. *Int Psychogeriatr* 20, 135-148.

Lambert, J.C., Heath, S., Even, G., Champion, D., Sleegers, K., Hiltunen, M., Combarros, O., Zelenika, D., Bullido, M.J., Tavernier, B., *et al.* (2009). Genome-wide association study identifies variants at CLU and CR1 associated with Alzheimer's disease. *Nat Genet* 41, 1094-1099.

Lambert, J.C., Mann, D., Richard, F., Tian, J., Shi, J., Thaker, U., Merrot, S., Harris, J., Frigard, B., Iwatsubo, T., *et al.* (2005). Is there a relation between APOE expression and brain amyloid load in Alzheimer's disease? *J Neurol Neurosurg Psychiatry* 76, 928-933.

Lambert, M.P., Barlow, A.K., Chromy, B.A., Edwards, C., Freed, R., Liosatos, M., Morgan, T.E., Rozovsky, I., Trommer, B., Viola, K.L., *et al.* (1998). Diffusible, nonfibrillar ligands derived from Abeta1-42 are potent central nervous system neurotoxins. *Proc Natl Acad Sci U S A* 95, 6448-6453.

Lammich, S., Kojro, E., Postina, R., Gilbert, S., Pfeiffer, R., Jasionowski, M., Haass, C., and Fahrenholz, F. (1999). Constitutive and regulated alpha-secretase cleavage of Alzheimer's amyloid precursor protein by a disintegrin metalloprotease. *Proc Natl Acad Sci U S A* 96, 3922-3927.

Lannfelt, L., Blennow, K., Zetterberg, H., Batsman, S., Ames, D., Harrison, J., Masters, C.L., Targum, S., Bush, A.I., Murdoch, R., *et al.* (2008). Safety, efficacy, and biomarker findings of PBT2 in targeting Abeta as a modifying therapy for Alzheimer's disease: a phase IIa, double-blind, randomised, placebo-controlled trial. *Lancet Neurol* 7, 779-786.

Lassalle, J.M., Halley, H., Daumas, S., Verret, L., and Frances, B. (2008). Effects of the genetic background on cognitive performances of TG2576 mice. *Behav Brain Res* 191, 104-110.

Leal, M.C., Dorfman, V.B., Gamba, A.F., Frangione, B., Wisniewski, T., Castano, E.M., Sigurdsson, E.M., and Morelli, L. (2006). Plaque-associated overexpression of insulin-degrading enzyme in the cerebral cortex of aged transgenic tg2576 mice with Alzheimer pathology. *J Neuropathol Exp Neurol* 65, 976-987.

Lee, K.S., Lee, B.S., Semnani, S., Avanesian, A., Um, C.Y., Jeon, H.J., Seong, K.M., Yu, K., Min, K.J., and Jafari, M. (2010). Curcumin extends life span, improves health span, and modulates the expression of age-associated aging genes in *Drosophila melanogaster*. *Rejuvenation Res* 13, 561-570.

Lee, S.F., Shah, S., Li, H., Yu, C., Han, W., and Yu, G. (2002). Mammalian APH-1 interacts with presenilin and nicastrin and is required for intramembrane proteolysis of amyloid-beta precursor protein and Notch. *J Biol Chem* 277, 45013-45019.

Lee, V.M., Wang, J., and Trojanowski, J.Q. (1999). Purification of paired helical filament tau and normal tau from human brain tissue. *Methods Enzymol* 309, 81-89.

Leissring, M.A., Farris, W., Chang, A.Y., Walsh, D.M., Wu, X., Sun, X., Frosch, M.P., and Selkoe, D.J. (2003). Enhanced proteolysis of beta-amyloid in APP

transgenic mice prevents plaque formation, secondary pathology, and premature death. *Neuron* 40, 1087-1093.

Lesne, S., Koh, M.T., Kotilinek, L., Kaye, R., Glabe, C.G., Yang, A., Gallagher, M., and Ashe, K.H. (2006). A specific amyloid-beta protein assembly in the brain impairs memory. *Nature* 440, 352-357.

LeVine, H., 3rd (1999). Quantification of beta-sheet amyloid fibril structures with thioflavin T. *Methods Enzymol* 309, 274-284.

Levy-Lahad, E., Wasco, W., Poorkaj, P., Romano, D.M., Oshima, J., Pettingell, W.H., Yu, C.E., Jondro, P.D., Schmidt, S.D., Wang, K., *et al.* (1995). Candidate gene for the chromosome 1 familial Alzheimer's disease locus. *Science* 269, 973-977.

Levy, E., Carman, M.D., Fernandez-Madrid, I.J., Power, M.D., Lieberburg, I., van Duinen, S.G., Bots, G.T., Luyendijk, W., and Frangione, B. (1990). Mutation of the Alzheimer's disease amyloid gene in hereditary cerebral hemorrhage, Dutch type. *Science* 248, 1124-1126.

Lewis, J., Dickson, D.W., Lin, W.L., Chisholm, L., Corral, A., Jones, G., Yen, S.H., Sahara, N., Skipper, L., Yager, D., *et al.* (2001). Enhanced neurofibrillary degeneration in transgenic mice expressing mutant tau and APP. *Science* 293, 1487-1491.

Lewis, J., McGowan, E., Rockwood, J., Melrose, H., Nacharaju, P., Van Slegtenhorst, M., Gwinn-Hardy, K., Paul Murphy, M., Baker, M., Yu, X., *et al.* (2000). Neurofibrillary tangles, amyotrophy and progressive motor disturbance in mice expressing mutant (P301L) tau protein. *Nat Genet* 25, 402-405.

Li, Y.M., Lai, M.T., Xu, M., Huang, Q., DiMuzio-Mower, J., Sardana, M.K., Shi, X.P., Yin, K.C., Shafer, J.A., and Gardell, S.J. (2000). Presenilin 1 is linked with gamma-secretase activity in the detergent solubilized state. *Proc Natl Acad Sci U S A* 97, 6138-6143.

Liao, M.C., and Van Nostrand, W.E. (2010). Degradation of soluble and fibrillar amyloid beta-protein by matrix metalloproteinase (MT1-MMP) in vitro. *Biochemistry* 49, 1127-1136.

- Lim, G.P., Chu, T., Yang, F., Beech, W., Frautschy, S.A., and Cole, G.M. (2001). The curry spice curcumin reduces oxidative damage and amyloid pathology in an Alzheimer transgenic mouse. *J Neurosci* *21*, 8370-8377.
- Lin, R., Chen, X., Li, W., Han, Y., Liu, P., and Pi, R. (2008). Exposure to metal ions regulates mRNA levels of APP and BACE1 in PC12 cells: blockage by curcumin. *Neurosci Lett* *440*, 344-347.
- Liu, F., Iqbal, K., Grundke-Iqbal, I., Hart, G.W., and Gong, C.X. (2004). O-GlcNAcylation regulates phosphorylation of tau: a mechanism involved in Alzheimer's disease. *Proc Natl Acad Sci U S A* *101*, 10804-10809.
- Liu, H., Li, Z., Qiu, D., Gu, Q., Lei, Q., and Mao, L. (2010). The inhibitory effects of different curcuminoids on beta-amyloid protein, beta-amyloid precursor protein and beta-site amyloid precursor protein cleaving enzyme 1 in swAPP HEK293 cells. *Neurosci Lett* *485*, 83-88.
- Lorenzo, A., and Yankner, B.A. (1994). Beta-amyloid neurotoxicity requires fibril formation and is inhibited by congo red. *Proc Natl Acad Sci U S A* *91*, 12243-12247.
- Lue, L.F., Kuo, Y.M., Roher, A.E., Brachova, L., Shen, Y., Sue, L., Beach, T., Kurth, J.H., Rydel, R.E., and Rogers, J. (1999). Soluble amyloid beta peptide concentration as a predictor of synaptic change in Alzheimer's disease. *Am J Pathol* *155*, 853-862.
- Luo, Y., Bolon, B., Kahn, S., Bennett, B.D., Babu-Khan, S., Denis, P., Fan, W., Kha, H., Zhang, J., Gong, Y., *et al.* (2001). Mice deficient in BACE1, the Alzheimer's beta-secretase, have normal phenotype and abolished beta-amyloid generation. *Nat Neurosci* *4*, 231-232.
- Ma, Q.L., Yang, F., Rosario, E.R., Ubeda, O.J., Beech, W., Gant, D.J., Chen, P.P., Hudspeth, B., Chen, C., Zhao, Y., *et al.* (2009). Beta-amyloid oligomers induce phosphorylation of tau and inactivation of insulin receptor substrate via c-Jun N-terminal kinase signaling: suppression by omega-3 fatty acids and curcumin. *J Neurosci* *29*, 9078-9089.
- Maccioni, R.B., and Cambiazo, V. (1995). Role of microtubule-associated proteins in the control of microtubule assembly. *Physiol Rev* *75*, 835-864.
- Maccioni, R.B., Farias, G., Morales, I., and Navarrete, L. (2010). The revitalized tau hypothesis on Alzheimer's disease. *Arch Med Res* *41*, 226-231.

- Mahley, R.W. (1988). Apolipoprotein E: cholesterol transport protein with expanding role in cell biology. *Science* 240, 622-630.
- Malherbe, P., Richards, J.G., Gaillard, H., Thompson, A., Diener, C., Schuler, A., and Huber, G. (1999). cDNA cloning of a novel secreted isoform of the human receptor for advanced glycation end products and characterization of cells co-expressing cell-surface scavenger receptors and Swedish mutant amyloid precursor protein. *Brain Res Mol Brain Res* 71, 159-170.
- Malinski, T. (2007). Nitric oxide and nitroxidative stress in Alzheimer's disease. *J Alzheimers Dis* 11, 207-218.
- Mandybur, T.I., and Chuirazzi, C.C. (1990). Astrocytes and the plaques of Alzheimer's disease. *Neurology* 40, 635-639.
- Mangialasche, F., Solomon, A., Winblad, B., Mecocci, P., and Kivipelto, M. (2010). Alzheimer's disease: clinical trials and drug development. *Lancet Neurol* 9, 702-716.
- Marcade, M., Bourdin, J., Loiseau, N., Peillon, H., Rayer, A., Drouin, D., Schweighoffer, F., and Desire, L. (2008). Etazolate, a neuroprotective drug linking GABA(A) receptor pharmacology to amyloid precursor protein processing. *J Neurochem* 106, 392-404.
- Marcu, M.G., Jung, Y.J., Lee, S., Chung, E.J., Lee, M.J., Trepel, J., and Neckers, L. (2006). Curcumin is an inhibitor of p300 histone acetyltransferase. *Med Chem* 2, 169-174.
- Marcus, D.L., Thomas, C., Rodriguez, C., Simberkoff, K., Tsai, J.S., Strafaci, J.A., and Freedman, M.L. (1998). Increased peroxidation and reduced antioxidant enzyme activity in Alzheimer's disease. *Exp Neurol* 150, 40-44.
- Marks, N., and Berg, M.J. (2008). Neurosecretases provide strategies to treat sporadic and familial Alzheimer disorders. *Neurochem Int* 52, 184-215.
- Martin, L., Latypova, X., and Terro, F. (2011). Post-translational modifications of tau protein: implications for Alzheimer's disease. *Neurochem Int* 58, 458-471.
- Martinelli, N., Olivieri, O., Shen, G.Q., Trabetti, E., Pizzolo, F., Busti, F., Friso, S., Bassi, A., Li, L., Hu, Y., *et al.* (2009). Additive effect of LRP8/APOER2 R952Q variant to APOE epsilon2/epsilon3/epsilon4 genotype in modulating apolipoprotein E

concentration and the risk of myocardial infarction: a case-control study. *BMC Med Genet* 10, 41.

Massaad, C.A., Washington, T.M., Pautler, R.G., and Klann, E. (2009). Overexpression of SOD-2 reduces hippocampal superoxide and prevents memory deficits in a mouse model of Alzheimer's disease. *Proc Natl Acad Sci U S A* 106, 13576-13581.

Mazanetz, M.P., and Fischer, P.M. (2007). Untangling tau hyperphosphorylation in drug design for neurodegenerative diseases. *Nat Rev Drug Discov* 6, 464-479.

Mecocci, P., MacGarvey, U., and Beal, M.F. (1994). Oxidative damage to mitochondrial DNA is increased in Alzheimer's disease. *Ann Neurol* 36, 747-751.

Min, S.W., Cho, S.H., Zhou, Y., Schroeder, S., Haroutunian, V., Sceley, W.W., Huang, E.J., Shen, Y., Masliah, E., Mukherjee, C., *et al.* (2010). Acetylation of tau inhibits its degradation and contributes to tauopathy. *Neuron* 67, 953-966.

Miners, J.S., Baig, S., Palmer, J., Palmer, L.E., Kehoe, P.G., and Love, S. (2008). Abeta-degrading enzymes in Alzheimer's disease. *Brain Pathol* 18, 240-252.

Miners, J.S., Van Helmond, Z., Chalmers, K., Wilcock, G., Love, S., and Kehoe, P.G. (2006). Decreased expression and activity of neprilysin in Alzheimer disease are associated with cerebral amyloid angiopathy. *J Neuropathol Exp Neurol* 65, 1012-1021.

Moloney, A.M., Griffin, R.J., Timmons, S., O'Connor, R., Ravid, R., and O'Neill, C. (2010). Defects in IGF-1 receptor, insulin receptor and IRS-1/2 in Alzheimer's disease indicate possible resistance to IGF-1 and insulin signalling. *Neurobiol Aging* 31, 224-243.

Moncada, S., and Higgs, E.A. (1991). Endogenous nitric oxide: physiology, pathology and clinical relevance. *Eur J Clin Invest* 21, 361-374.

Moreira, P.I., Santos, M.S., Moreno, A., and Oliveira, C. (2001). Amyloid beta-peptide promotes permeability transition pore in brain mitochondria. *Biosci Rep* 21, 789-800.

Morton, R.A., Kuenzi, F.M., Fitzjohn, S.M., Rosahl, T.W., Smith, D., Zheng, H., Shearman, M., Collingridge, G.L., and Seabrook, G.R. (2002). Impairment in

hippocampal long-term potentiation in mice under-expressing the Alzheimer's disease related gene presenilin-1. *Neurosci Lett* 319, 37-40.

Moss, M.L., Jin, S.L., Milla, M.E., Bickett, D.M., Burkhart, W., Carter, H.L., Chen, W.J., Clay, W.C., Didsbury, J.R., Hassler, D. *et al.* (1997). Cloning of a disintegrin metalloproteinase that processes precursor tumour-necrosis factor-alpha. *Nature* 385, 733-736.

Moss, M.L., and Rasmussen, F.H. (2007). Fluorescent substrates for the proteinases ADAM17, ADAM10, ADAM8, and ADAM12 useful for high-throughput inhibitor screening. *Anal Biochem* 366, 144-148.

Mount, C., and Downton, C. (2006). Alzheimer disease: progress or profit? *Nat Med* 12, 780-784.

Mueller, E.A., Moore, M.M., Kerr, D.C., Sexton, G., Camicioli, R.M., Howieson, D.B., Quinn, J.F., and Kaye, J.A. (1998). Brain volume preserved in healthy elderly through the eleventh decade. *Neurology* 51, 1555-1562.

Muhs, A., Hickman, D.T., Pihlgren, M., Chuard, N., Giriens, V., Meerschman, C., van der Auwera, I., van Leuven, F., Sugawara, M., Weingertner, M.C., *et al.* (2007). Liposomal vaccines with conformation-specific amyloid peptide antigens define immune response and efficacy in APP transgenic mice. *Proc Natl Acad Sci U S A* 104, 9810-9815.

Myklebost, O., Arheden, K., Rogne, S., Geurts van Kessel, A., Mandahl, N., Herz, J., Stanley, K., Heim, S., and Mitelman, F. (1989). The gene for the human putative apoE receptor is on chromosome 12 in the segment q13-14. *Genomics* 5, 65-69.

Nagai, T., Yamada, K., Kim, H.C., Kim, Y.S., Noda, Y., Imura, A., Nabeshima, Y., and Nabeshima, T. (2003). Cognition impairment in the genetic model of aging klotho gene mutant mice: a role of oxidative stress. *FASEB J* 17, 50-52.

Ng, S., and Chan, W. (2009). Dementia in Hong Kong. In *Public health and epidemiology Bulletin*, pp. 52.

Noble, W., Planel, E., Zehr, C., Olm, V., Meyerson, J., Suleman, F., Gaynor, K., Wang, L., LaFrancois, J., Feinstein, B., *et al.* (2005). Inhibition of glycogen synthase kinase-3 by lithium correlates with reduced tauopathy and degeneration in vivo. *Proc Natl Acad Sci U S A* 102, 6990-6995.

- Okuda, T., Haga, T., Kanai, Y., Endou, H., Ishihara, T., and Katsura, J. (2000). Identification and characterization of the high-affinity choline transporter. *Nat Neurosci* 3, 120-125.
- Ono, K., Hasegawa, K., Naiki, H., and Yamada, M. (2004). Curcumin has potent anti-amyloidogenic effects for Alzheimer's beta-amyloid fibrils in vitro. *J Neurosci Res* 75, 742-750.
- Orellana, D.I., Quintanilla, R.A., and Maccioni, R.B. (2007). Neuroprotective effect of TNFalpha against the beta-amyloid neurotoxicity mediated by CDK5 kinase. *Biochim Biophys Acta* 1773, 254-263.
- Padurariu, M., Ciobica, A., Hritcu, L., Stoica, B., Bild, W., and Stefanescu, C. (2010). Changes of some oxidative stress markers in the serum of patients with mild cognitive impairment and Alzheimer's disease. *Neurosci Lett* 469, 6-10.
- Palacios, G., Palacios, J.M., Mengod, G., and Frey, P. (1992). Beta-amyloid precursor protein localization in the Golgi apparatus in neurons and oligodendrocytes. An immunocytochemical structural and ultrastructural study in normal and axotomized neurons. *Brain Res Mol Brain Res* 15, 195-206.
- Paresce, D.M., Ghosh, R.N., and Maxfield, F.R. (1996). Microglial cells internalize aggregates of the Alzheimer's disease amyloid beta-protein via a scavenger receptor. *Neuron* 17, 553-565.
- Park, S.Y., Kim, H.S., Cho, E.K., Kwon, B.Y., Phark, S., Hwang, K.W., and Sul, D. (2008). Curcumin protected PC12 cells against beta-amyloid-induced toxicity through the inhibition of oxidative damage and tau hyperphosphorylation. *Food Chem Toxicol* 46, 2881-2887.
- Patrick, G.N., Zukerberg, L., Nikolic, M., de la Monte, S., Dikkes, P., and Tsai, L.H. (1999). Conversion of p35 to p25 deregulates Cdk5 activity and promotes neurodegeneration. *Nature* 402, 615-622.
- Paxinos, G., and Franklin, J. (2001). *The mouse brain in stereotaxic coordinates*. Second edn.
- Plant, L.D., Boyle, J.P., Smith, I.F., Peers, C., and Pearson, H.A. (2003). The production of amyloid beta peptide is a critical requirement for the viability of central neurons. *J Neurosci* 23, 5531-5535.

Pratico, D., Uryu, K., Leight, S., Trojanowski, J.Q., and Lee, V.M. (2001). Increased lipid peroxidation precedes amyloid plaque formation in an animal model of Alzheimer amyloidosis. *J Neurosci* 21, 4183-4187.

Puzzo, D., Privitera, L., Fa, M., Staniszewski, A., Hashimoto, G., Aziz, F., Sakurai, M., Ribe, E.M., Troy, C.M., Mercken, M., *et al.* (2011). Endogenous amyloid-beta is necessary for hippocampal synaptic plasticity and memory. *Ann Neurol* 69, 819-830.

Qin, X.Y., Cheng, Y., Cui, J., Zhang, Y., and Yu, L.C. (2009). Potential protection of curcumin against amyloid beta-induced toxicity on cultured rat prefrontal cortical neurons. *Neurosci Lett* 463, 158-161.

Qin, X.Y., Cheng, Y., and Yu, L.C. (2010). Potential protection of curcumin against intracellular amyloid beta-induced toxicity in cultured rat prefrontal cortical neurons. *Neurosci Lett* 480, 21-24.

Qiu, W.Q., Walsh, D.M., Ye, Z., Vekrellis, K., Zhang, J., Podlisny, M.B., Rosner, M.R., Safavi, A., Hersh, L.B., and Selkoe, D.J. (1998). Insulin-degrading enzyme regulates extracellular levels of amyloid beta-protein by degradation. *J Biol Chem* 273, 32730-32738.

Quintanilla, R.A., Orellana, D.I., Gonzalez-Billault, C., and Maccioni, R.B. (2004). Interleukin-6 induces Alzheimer-type phosphorylation of tau protein by deregulating the cdk5/p35 pathway. *Exp Cell Res* 295, 245-257.

Rakover, I., Arbel, M., and Solomon, B. (2007). Immunotherapy against APP beta-secretase cleavage site improves cognitive function and reduces neuroinflammation in Tg2576 mice without a significant effect on brain abeta levels. *Neurodegener Dis* 4, 392-402.

Reddy, P.H., and Beal, M.F. (2008). Amyloid beta, mitochondrial dysfunction and synaptic damage: implications for cognitive decline in aging and Alzheimer's disease. *Trends Mol Med* 14, 45-53.

Relkin, N.R., Szabo, P., Adamiak, B., Burgut, T., Monthe, C., Lent, R.W., Younkin, S., Younkin, L., Schiff, R., and Weksler, M.E. (2009). 18-Month study of intravenous immunoglobulin for treatment of mild Alzheimer disease. *Neurobiol Aging* 30, 1728-1736.

- Riddell, D.R., Zhou, H., Atchison, K., Warwick, H.K., Atkinson, P.J., Jefferson, J., Xu, L., Aschmies, S., Kirksey, Y., Hu, Y., *et al.* (2008). Impact of apolipoprotein E (ApoE) polymorphism on brain ApoE levels. *J Neurosci* 28, 11445-11453.
- Roberds, S.L., Anderson, J., Basi, G., Bienkowski, M.J., Branstetter, D.G., Chen, K.S., Freedman, S.B., Frigon, N.L., Games, D., Hu, K., *et al.* (2001). BACE knockout mice are healthy despite lacking the primary beta-secretase activity in brain: implications for Alzheimer's disease therapeutics. *Hum Mol Genet* 10, 1317-1324.
- Robinson, D.M., and Plosker, G.L. (2006). Galantamine extended release in Alzheimer's disease: profile report. *Drugs Aging* 23, 839-842.
- Rogaeva, E., Meng, Y., Lee, J.H., Gu, Y., Kawarai, T., Zou, F., Katayama, T., Baldwin, C.T., Cheng, R., Hasegawa, H., *et al.* (2007). The neuronal sortilin-related receptor SORL1 is genetically associated with Alzheimer disease. *Nat Genet* 39, 168-177.
- Roher, A.E., Baudry, J., Chaney, M.O., Kuo, Y.M., Stine, W.B., and Emmerling, M.R. (2000). Oligomerization and fibril assembly of the amyloid-beta protein. *Biochim Biophys Acta* 1502, 31-43.
- Roher, A.F., Kasunic, T.C., Woods, A.S., Cotter, R.J., Ball, M.J., and Fridman, R. (1994). Proteolysis of A beta peptide from Alzheimer disease brain by gelatinase A. *Biochem Biophys Res Commun* 205, 1755-1761.
- Ropcer, A.H., and Samuels, M.A. (2009). "Chapter 21. Dementia and the Amnesic (Korsakoff) Syndrome with Comments on the Neurology of Intelligence and Memory" (Chapter). In *Adams and Victor's Principles of Neurology*, 9c: <http://www.accessmedicine.com/content.aspx?aID=3633470>.
- Roy, S., Zhang, B., Lee, V.M., and Trojanowski, J.Q. (2005). Axonal transport defects: a common theme in neurodegenerative diseases. *Acta Neuropathol* 109, 5-13.
- Rozas, G., Guerra, M.J., and Labandeira-Garcia, J.L. (1997). An automated rotarod method for quantitative drug-free evaluation of overall motor deficits in rat models of parkinsonism. *Brain Res Brain Res Protoc* 2, 75-84.
- Rusinek, H., De Santi, S., Frid, D., Tsui, W.H., Tarshish, C.Y., Convit, A., and de Leon, M.J. (2003). Regional brain atrophy rate predicts future cognitive decline: 6-year longitudinal MR imaging study of normal aging. *Radiology* 229, 691-696.

Sadock, B.J., Sadock, V.A., and Ruiz, P. (2009). Chapter 10.3. Dementia. In Kaplan and Sadock's Comprehensive Textbook of Psychiatry.

Sambrook, J., and Russell, D. (2001). Molecular Cloning: A Laboratory Manual, Third edn.

Sanderson, M.P., Abbott, C.A., Tada, H., Seno, M., Dempsey, P.J., and Dunbar, A.J. (2006). Hydrogen peroxide and endothelin-1 are novel activators of betacellulin ectodomain shedding. *J Cell Biochem* 99, 609-623.

Sanderson, M.P., Erickson, S.N., Gough, P.J., Garton, K.J., Wille, P.T., Raines, E.W., Dunbar, A.J., and Dempsey, P.J. (2005). ADAM10 mediates ectodomain shedding of the betacellulin precursor activated by p-aminophenylmercuric acetate and extracellular calcium influx. *J Biol Chem* 280, 1826-1837.

Sato, H., Takino, T., Okada, Y., Cao, J., Shinagawa, A., Yamamoto, E., and Seiki, M. (1994). A matrix metalloproteinase expressed on the surface of invasive tumour cells. *Nature* 370, 61-65.

Schagger, H. (2006). Tricine-SDS-PAGE. *Nat Protoc* 1, 16-22.

Scheuner, D., Eckman, C., Jensen, M., Song, X., Citron, M., Suzuki, N., Bird, T.D., Hardy, J., Hutton, M., Kukull, W., *et al.* (1996). Secreted amyloid beta-protein similar to that in the senile plaques of Alzheimer's disease is increased in vivo by the presenilin 1 and 2 and APP mutations linked to familial Alzheimer's disease. *Nat Med* 2, 864-870.

Schlondorff, J., Becherer, J.D., and Blobel, C.P. (2000). Intracellular maturation and localization of the tumour necrosis factor alpha convertase (TACE). *Biochem J* 347 Pt 1, 131-138.

Schneider, L.S., Dagerman, K.S., Higgins, J.P., and McShane, R. (2011). Lack of Evidence for the Efficacy of Memantine in Mild Alzheimer Disease. *Arch Neurol*.

Schraufstatter, E., and Bernt, H. (1949). Antibacterial action of curcumin and related compounds. *Nature* 164, 456.

Seabrook, G.R., Smith, D.W., Bowery, B.J., Easter, A., Reynolds, T., Fitzjohn, S.M., Morton, R.A., Zheng, H., Dawson, G.R., Sirinathsinghji, D.J., *et al.* (1999). Mechanisms contributing to the deficits in hippocampal synaptic plasticity in mice lacking amyloid precursor protein. *Neuropharmacology* 38, 349-359.

- Seidah, N.G., and Chretien, M. (1999). Proprotein and prohormone convertases: a family of subtilases generating diverse bioactive polypeptides. *Brain Res* 848, 45-62.
- Selkoe, D.J. (1991). The molecular pathology of Alzheimer's disease. *Neuron* 6, 487-498.
- Selkoe, D.J., and Wolfe, M.S. (2007). Presenilin: running with scissors in the membrane. *Cell* 131, 215-221.
- Seltzer, B. (2007). Donepezil: an update. *Expert Opin Pharmacother* 8, 1011-1023.
- Shankar, G.M., Li, S., Mehta, T.H., Garcia-Munoz, A., Shepardson, N.E., Smith, I., Brett, F.M., Farrell, M.A., Rowan, M.J., Lemere, C.A., *et al.* (2008). Amyloid-beta protein dimers isolated directly from Alzheimer's brains impair synaptic plasticity and memory. *Nat Med* 14, 837-842.
- Sharma, D., Sethi, P., Hussain, E., and Singh, R. (2009). Curcumin counteracts the aluminium-induced ageing-related alterations in oxidative stress, Na⁺, K⁺ ATPase and protein kinase C in adult and old rat brain regions. *Biogerontology* 10, 489-502.
- Sharma, M., and Gupta, Y.K. (2001). Intracerebroventricular injection of streptozotocin in rats produces both oxidative stress in the brain and cognitive impairment. *Life Sci* 68, 1021-1029.
- Shen, J., Bronson, R.T., Chen, D.F., Xia, W., Selkoe, D.J., and Tonggawa, S. (1997). Skeletal and CNS defects in Presenilin-1-deficient mice. *Cell* 89, 629-639.
- Sherrington, R., Rogacov, E.I., Liang, Y., Rogacva, E.A., Levesque, G., Ikeda, M., Chi, H., Lin, C., Li, G., Holman, K., *et al.* (1995). Cloning of a gene bearing missense mutations in early-onset familial Alzheimer's disease. *Nature* 375, 754-760.
- Shibata, M., Yamada, S., Kumar, S.R., Calero, M., Bading, J., Frangione, B., Holtzman, D.M., Miller, C.A., Strickland, D.K., Ghiso, J., *et al.* (2000). Clearance of Alzheimer's amyloid-ss(1-40) peptide from brain by LDL receptor-related protein-1 at the blood-brain barrier. *J Clin Invest* 106, 1489-1499.
- Shimmyo, Y., Kihara, T., Akaike, A., Niidome, T., and Sugimoto, H. (2008). Epigallocatechin-3-gallate and curcumin suppress amyloid beta-induced beta-site APP cleaving enzyme-1 upregulation. *Neuroreport* 19, 1329-1333.

- Siemers, E.R., Friedrich, S., Dean, R.A., Gonzales, C.R., Farlow, M.R., Paul, S.M., and Demattos, R.B. (2010). Safety and changes in plasma and cerebrospinal fluid amyloid beta after a single administration of an amyloid beta monoclonal antibody in subjects with Alzheimer disease. *Clin Neuropharmacol* *33*, 67-73.
- Silverberg, G.D., Messier, A.A., Miller, M.C., Machan, J.T., Majumdar, S.S., Stopa, E.G., Donahue, J.E., and Johanson, C.E. (2010). Amyloid efflux transporter expression at the blood-brain barrier declines in normal aging. *J Neuropathol Exp Neurol* *69*, 1034-1043.
- Singleton, A.B., Gibson, A.M., McKeith, I.G., Ballard, C.G., Edwardson, J.A., and Morris, C.M. (2001). Nitric oxide synthase gene polymorphisms in Alzheimer's disease and dementia with Lewy bodies. *Neurosci Lett* *303*, 33-36.
- Sinha, S., Anderson, J.P., Barbour, R., Basi, G.S., Caccavello, R., Davis, D., Doan, M., Dovey, H.F., Frigon, N., Hong, J., *et al.* (1999). Purification and cloning of amyloid precursor protein beta-secretase from human brain. *Nature* *402*, 537-540.
- Smesny, S., Stein, S., Willhardt, I., Lasch, J., and Sauer, H. (2008). Decreased phospholipase A2 activity in cerebrospinal fluid of patients with dementia. *J Neural Transm* *115*, 1173-1179.
- Snyder, S.W., Lador, U.S., Wade, W.S., Wang, G.T., Barrett, L.W., Matayoshi, E.D., Huffaker, H.J., Krafft, G.A., and Holzman, T.F. (1994). Amyloid-beta aggregation: selective inhibition of aggregation in mixtures of amyloid with different chain lengths. *Biophys J* *67*, 1216-1228.
- Somasundaram, S., Edmund, N.A., Moore, D.T., Small, G.W., Shi, Y.Y., and Orłowski, R.Z. (2002). Dietary curcumin inhibits chemotherapy-induced apoptosis in models of human breast cancer. *Cancer Res* *62*, 3868-3875.
- Standen, C.L., Kennedy, N.J., Flavell, R.A., and Davis, R.J. (2009). Signal transduction cross talk mediated by Jun N-terminal kinase-interacting protein and insulin receptor substrate scaffold protein complexes. *Mol Cell Biol* *29*, 4831-4840.
- Stoeck, A., Shang, L., and Dempsey, P.J. (2010). Sequential and gamma-secretase-dependent processing of the betacellulin precursor generates a palmitoylated intracellular-domain fragment that inhibits cell growth. *J Cell Sci* *123*, 2319-2331.

- Strimpakos, A.S., and Sharma, R.A. (2008). Curcumin: preventive and therapeutic properties in laboratory studies and clinical trials. *Antioxid Redox Signal* 10, 511-545.
- Strongin, A.Y., Collier, I., Bannikov, G., Marmer, B.L., Grant, G.A., and Goldberg, G.I. (1995). Mechanism of cell surface activation of 72-kDa type IV collagenase. Isolation of the activated form of the membrane metalloprotease. *J Biol Chem* 270, 5331-5338.
- Sucher, N.J., Awobuluyi, M., Choi, Y.B., and Lipton, S.A. (1996). NMDA receptors: from genes to channels. *Trends Pharmacol Sci* 17, 348-355.
- Suh, Y.A., Arnold, R.S., Lassegue, B., Shi, J., Xu, X., Sorescu, D., Chung, A.B., Griendling, K.K., and Lambeth, J.D. (1999). Cell transformation by the superoxide-generating oxidase Mox1. *Nature* 401, 79-82.
- Suzuki, N., Cheung, T.T., Cai, X.D., Ohtsuka, A., Otvos, L., Jr., Eckman, C., Golde, T.E., and Younkin, S.G. (1994). An increased percentage of long amyloid beta protein secreted by familial amyloid beta protein precursor (beta APP717) mutants. *Science* 264, 1336-1340.
- Tagliavini, F., Giaccone, G., Frangione, B., and Bugiani, O. (1988). Precursor amyloid deposits in the cerebral cortex of patients with Alzheimer's disease and nondemented individuals. *Neurosci Lett* 93, 191-196.
- Takahashi, T., and Mihara, H. (2008). Peptide and protein mimetics inhibiting amyloid beta-peptide aggregation. *Acc Chem Res* 41, 1309-1318.
- Takasugi, N., Tomita, T., Hayashi, I., Tsuruoka, M., Niimura, M., Takahashi, Y., Thinakaran, G., and Iwatsubo, T. (2003). The role of presenilin cofactors in the gamma-secretase complex. *Nature* 422, 438-441.
- Tamagno, E., Guglielmotto, M., Bardini, P., Santoro, G., Davit, A., Di Simone, D., Danni, O., and Tabaton, M. (2003). Dehydroepiandrosterone reduces expression and activity of BACE in NT2 neurons exposed to oxidative stress. *Neurobiol Dis* 14, 291-301.
- Tamaoka, A., Sawamura, N., Fukushima, T., Shoji, S., Matsubara, E., Shoji, M., Hirai, S., Furiya, Y., Endoh, R., and Mori, H. (1997). Amyloid beta protein 42(43) in cerebrospinal fluid of patients with Alzheimer's disease. *J Neurol Sci* 148, 41-45.

- Tanaka, S., Shiojiri, S., Takahashi, Y., Kitaguchi, N., Ito, H., Kameyama, M., Kimura, J., Nakamura, S., and Ueda, K. (1989). Tissue-specific expression of three types of beta-protein precursor mRNA: enhancement of protease inhibitor-harboring types in Alzheimer's disease brain. *Biochem Biophys Res Commun* 165, 1406-1414.
- Thinakaran, G., Borchelt, D.R., Lee, M.K., Slunt, H.H., Spitzer, L., Kim, G., Ratovitsky, T., Davenport, F., Nordstedt, C., Seeger, M., *et al.* (1996). Endoproteolysis of presenilin 1 and accumulation of processed derivatives in vivo. *Neuron* 17, 181-190.
- Tomic, J.L., Pensalfini, A., Head, E., and Glabe, C.G. (2009). Soluble fibrillar oligomer levels are elevated in Alzheimer's disease brain and correlate with cognitive dysfunction. *Neurobiol Dis* 35, 352-358.
- Tomimoto, H., Akiguchi, I., Wakita, H., Nakamura, S., and Kimura, J. (1995). Ultrastructural localization of amyloid protein precursor in the normal and postischemic gerbil brain. *Brain Res* 672, 187-195.
- Tomita, T. (2009). Secretase inhibitors and modulators for Alzheimer's disease treatment. *Expert Rev Neurother* 9, 661-679.
- Tomlinson, B.E., Blessed, G., and Roth, M. (1968). Observations on the brains of non-demented old people. *J Neurol Sci* 7, 331-356.
- Tomlinson, B.E., Blessed, G., and Roth, M. (1970). Observations on the brains of demented old people. *J Neurol Sci* 11, 205-242.
- Turkington, C., and Mitchell, D. (2011). The encyclopedia of Alzheimer's disease. In *The encyclopedia of Alzheimer's disease*, pp. 12.
- Turner, A.J., Brown, C.D., Carson, J.A., and Barnes, K. (2000). The neprilysin family in health and disease. *Adv Exp Med Biol* 477, 229-240.
- van Belle, G., Gibson, K., Nochlin, D., Sumi, M., and Larson, E.B. (1997). Counting plaques and tangles in Alzheimer's disease: concordance of technicians and pathologists. *J Neurol Sci* 145, 141-146.
- van Deel, E.D., Lu, Z., Xu, X., Zhu, G., Hu, X., Oury, T.D., Bache, R.J., Duncker, D.J., and Chen, Y. (2008). Extracellular superoxide dismutase protects the heart against oxidative stress and hypertrophy after myocardial infarction. *Free Radic Biol Med* 44, 1305-1313.

- Vassar, R., Bennett, B.D., Babu-Khan, S., Kahn, S., Mendiaz, E.A., Denis, P., Teplow, D.B., Ross, S., Amarante, P., Loeloff, R., *et al.* (1999). Beta-secretase cleavage of Alzheimer's amyloid precursor protein by the transmembrane aspartic protease BACE. *Science* 286, 735-741.
- Vekrellis, K., Ye, Z., Qiu, W.Q., Walsh, D., Hartley, D., Chesneau, V., Rosner, M.R., and Selkoe, D.J. (2000). Neurons regulate extracellular levels of amyloid beta-protein via proteolysis by insulin-degrading enzyme. *J Neurosci* 20, 1657-1665.
- Virkamaki, A., Ueki, K., and Kahn, C.R. (1999). Protein-protein interaction in insulin signaling and the molecular mechanisms of insulin resistance. *J Clin Invest* 103, 931-943.
- von Bergen, M., Barghorn, S., Li, L., Marx, A., Biernat, J., Mandelkow, E.M., and Mandelkow, E. (2001). Mutations of tau protein in frontotemporal dementia promote aggregation of paired helical filaments by enhancing local beta-structure. *J Biol Chem* 276, 48165-48174.
- Walsh, D.M., Klyubin, I., Fadeeva, J.V., Cullen, W.K., Anwyl, R., Wolfe, M.S., Rowan, M.J., and Selkoe, D.J. (2002). Naturally secreted oligomers of amyloid beta protein potently inhibit hippocampal long-term potentiation in vivo. *Nature* 416, 535-539.
- Wang, C., Wurtman, R.J., and Lee, R.K. (2000). Amyloid precursor protein and membrane phospholipids in primary cortical neurons increase with development, or after exposure to nerve growth factor or Abeta(1-40). *Brain Res* 865, 157-167.
- Wang, C.Y., Finstad, C.L., Walfield, A.M., Sia, C., Sokoll, K.K., Chang, T.Y., Fang, X.D., Hung, C.H., Hutter-Paier, B., and Windisch, M. (2007). Site-specific UB1Th amyloid-beta vaccine for immunotherapy of Alzheimer's disease. *Vaccine* 25, 3041-3052.
- Wang, J., Xiong, S., Xie, C., Markesbery, W.R., and Lovell, M.A. (2005). Increased oxidative damage in nuclear and mitochondrial DNA in Alzheimer's disease. *J Neurochem* 93, 953-962.
- Wavrant-DeVrieze, F., Lambert, J.C., Stas, L., Crook, R., Cotel, D., Pasquier, F., Frigard, B., Lambrechts, M., Thiry, E., Amouyel, P., *et al.* (1999). Association

between coding variability in the LRP gene and the risk of late-onset Alzheimer's disease. *Hum Genet* 104, 432-434.

Wegiel, J., and Wisniewski, H.M. (1990). The complex of microglial cells and amyloid star in three-dimensional reconstruction. *Acta Neuropathol* 81, 116-124.

Weidemann, A., König, G., Bunke, D., Fischer, P., Salbaum, J.M., Masters, C.L., and Beyreuther, K. (1989). Identification, biogenesis, and localization of precursors of Alzheimer's disease A4 amyloid protein. *Cell* 57, 115-126.

Weisgraber, K.H., and Mahley, R.W. (1996). Human apolipoprotein E: the Alzheimer's disease connection. *FASEB J* 10, 1485-1494.

White, M.F. (2002). IRS proteins and the common path to diabetes. *Am J Physiol Endocrinol Metab* 283, E413-422.

Whitehouse, P.J., Price, D.L., Struble, R.G., Clark, A.W., Coyle, J.T., and Delon, M.R. (1982). Alzheimer's disease and senile dementia: loss of neurons in the basal forebrain. *Science* 215, 1237-1239.

Wiessner, C., Wiederhold, K.H., Tissot, A.C., Frey, P., Danner, S., Jacobson, L.H., Jennings, G.T., Luond, R., Ortmann, R., Reichwald, J., *et al.* (2011). The second-generation active Abeta immunotherapy CAD106 reduces amyloid accumulation in APP transgenic mice while minimizing potential side effects. *J Neurosci* 31, 9323-9331.

Wilcock, D.M., Lewis, M.R., Van Nostrand, W.E., Davis, J., Previti, M.L., Gharkholonarche, N., Vitek, M.P., and Colton, C.A. (2008). Progression of amyloid pathology to Alzheimer's disease pathology in an amyloid precursor protein transgenic mouse model by removal of nitric oxide synthase 2. *J Neurosci* 28, 1537-1545.

Winblad, B., Grossberg, G., Frolich, L., Farlow, M., Zechner, S., Nagel, J., and Lane, R. (2007). IDEAL: a 6-month, double-blind, placebo-controlled study of the first skin patch for Alzheimer disease. *Neurology* 69, S14-22.

Wolf-Klein, G.P., and Silverstone, F.A. (1994). Weight loss in Alzheimer's disease: an international review of the literature. *Int Psychogeriatr* 6, 135-142.

- Wolfe, M.S. (2010). Alzheimer's Disease Drug Discovery--11th International Conference--Promising New Therapeutic Approaches. 27-28 September 2010, Jersey City, NJ, USA. *IDrugs 13*, 825-827.
- Wolfe, M.S., Xia, W., Ostaszewski, B.L., Dichl, T.S., Kimberly, W.T., and Selkoe, D.J. (1999). Two transmembrane aspartates in presenilin-1 required for presenilin endoproteolysis and gamma-secretase activity. *Nature 398*, 513-517.
- Wong, C.W., Quaranta, V., and Glenner, G.G. (1985). Neuritic plaques and cerebrovascular amyloid in Alzheimer disease are antigenically related. *Proc Natl Acad Sci U S A 82*, 8729-8732.
- Wyss-Coray, T., Yan, F., Lin, A.H., Lambris, J.D., Alexander, J.J., Quigg, R.J., and Masliah, E. (2002). Prominent neurodegeneration and increased plaque formation in complement-inhibited Alzheimer's mice. *Proc Natl Acad Sci U S A 99*, 10837-10842.
- Xu, W., Liu, L., Emson, P., Harrington, C.R., McKeith, I.G., Perry, R.H., Morris, C.M., and Charles, I.G. (2000). The CCTTT polymorphism in the NOS2A gene is associated with dementia with Lewy bodies. *Neuroreport 11*, 297-299.
- Yamada, K., Hashimoto, T., Yabuki, C., Nagae, Y., Tachikawa, M., Strickland, D.K., Liu, Q., Bu, G., Basak, J.M., Holtzman, D.M., *et al.* (2008). The low density lipoprotein receptor-related protein 1 mediates uptake of amyloid beta peptides in an in vitro model of the blood-brain barrier cells. *J Biol Chem 283*, 34554-34562.
- Yamada, T., Yoshiyama, Y., Sato, H., Sciki, M., Shinagawa, A., and Takahashi, M. (1995). White matter microglia produce membrane-type matrix metalloprotease, an activator of gelatinase A, in human brain tissues. *Acta Neuropathol 90*, 421-424.
- Yamamoto, M., Clark, J.D., Pastor, J.V., Gurnani, P., Nandi, A., Kurosu, H., Miyoshi, M., Ogawa, Y., Castrillon, D.H., Rosenblatt, K.P., *et al.* (2005). Regulation of oxidative stress by the anti-aging hormone klotho. *J Biol Chem 280*, 38029-38034.
- Yan, R., Bienkowski, M.J., Shuck, M.E., Miao, H., Tory, M.C., Pauley, A.M., Brashier, J.R., Stratman, N.C., Mathews, W.R., Buhl, A.E., *et al.* (1999). Membrane-anchored aspartyl protease with Alzheimer's disease beta-secretase activity. *Nature 402*, 533-537.
- Yang, F., Lim, G.P., Begum, A.N., Ubeda, O.J., Simmons, M.R., Ambegaokar, S.S., Chen, P.P., Kaye, R., Glabe, C.G., Frautschi, S.A., *et al.* (2005). Curcumin inhibits

formation of amyloid beta oligomers and fibrils, binds plaques, and reduces amyloid in vivo. *J Biol Chem* 280, 5892-5901.

Yin, K.J., Cirrito, J.R., Yan, P., Hu, X., Xiao, Q., Pan, X., Bateman, R., Song, H., Hsu, F.F., Turk, J., *et al.* (2006). Matrix metalloproteinases expressed by astrocytes mediate extracellular amyloid-beta peptide catabolism. *J Neurosci* 26, 10939-10948.

Yu, G., Nishimura, M., Arawaka, S., Levitan, D., Zhang, L., Tandon, A., Song, Y.Q., Rogacva, E., Chen, F., Kawarai, T., *et al.* (2000). Nicastrin modulates presenilin-mediated notch/glp-1 signal transduction and betaAPP processing. *Nature* 407, 48-54.

Yuzwa, S.A., Macauley, M.S., Heinonen, J.F., Shan, X., Dennis, R.J., He, Y., Whitworth, G.E., Stubbs, K.A., McEachern, E.J., Davies, G.J., *et al.* (2008). A potent mechanism-inspired O-GlcNAcase inhibitor that blocks phosphorylation of tau in vivo. *Nat Chem Biol* 4, 483-490.

Zehr, C., Lewis, J., McGowan, E., Crook, J., Lin, W.L., Godwin, K., Knight, J., Dickson, D.W., and Hutton, M. (2004). Apoptosis in oligodendrocytes is associated with axonal degeneration in P301L tau mice. *Neurobiol Dis* 15, 553-562.

Zelko, I.N., Mariani, T.J., and Folz, R.J. (2002). Superoxide dismutase multigene family: a comparison of the Cu/Zn-SOD (SOD1), Mn-SOD (SOD2), and EC-SOD (SOD3) gene structures, evolution, and expression. *Free Radic Biol Med* 33, 337-349.

Zerbinatti, C.V., Wahrle, S.E., Kim, H., Cam, J.A., Bales, K., Paul, S.M., Holtzman, D.M., and Bu, G. (2006). Apolipoprotein E and low density lipoprotein receptor-related protein facilitate intraneuronal Abeta42 accumulation in amyloid model mice. *J Biol Chem* 281, 36180-36186.

Zhang, C., Browne, A., Child, D., and Tanzi, R.E. (2010a). Curcumin decreases amyloid-beta peptide levels by attenuating the maturation of amyloid-beta precursor protein. *J Biol Chem* 285, 28472-28480.

Zhang, L., Fiala, M., Cashman, J., Sayre, J., Espinosa, A., Mahanian, M., Zaghi, J., Badmaev, V., Graves, M.C., Bernard, G., *et al.* (2006). Curcuminoids enhance amyloid-beta uptake by macrophages of Alzheimer's disease patients. *J Alzheimers Dis* 10, 1-7.

Zhang, S., Hedskog, L., Petersen, C.A., Winblad, B., and Ankarcrona, M. (2010b). Dimebon (latrepirdine) enhances mitochondrial function and protects neuronal cells from death. *J Alzheimers Dis* 21, 389-402.

Zhao, S., and Fernald, R.D. (2005). Comprehensive algorithm for quantitative real-time polymerase chain reaction. *J Comput Biol* 12, 1047-1064.

Zheng, H., and Koo, E.H. (2006). The amyloid precursor protein: beyond amyloid. *Mol Neurodegener* 1, 5.

APPENDICES

PUBLICATIONS

Papers

1. Baum L, Cheung SKK, Mok V, Lam L, Leung V, Hui E, Ng C, Chow M, Ho PC, Lam S, Woo J, Chiu H, Goggins W, Zee B, Wong A, Mok H, Cheng W, Fong C, Lee JSW, Chan MH, Szeto S, Lui V, Tsoh J, Kwok T, Chan I, Lam C. Curcumin effects on blood lipid profile in a six-month human study. *Pharmacological Research* 2007;56:509-14.
2. Baum L, Lam CWK, Cheung SKK, Kwok T, Lui V, Tsoh J, Lam L, Leung V, Hui E, Ng C, Woo J, Chiu HFK, Goggins WB, Zee BCY, Cheng KF, Fong CYS, Wong A, Mok H, Chow MSS, Ho PC, Ip SP, Ho CS, Yu XW, Lai CYL, Chan MH, Szeto S, Chan IHS, Mok V. Six month randomized, placebo-controlled, double-blind, pilot clinical trial of curcumin in Alzheimer's disease patients. *Journal of Clinical Psychopharmacology* 2008;28:110-3.
3. Baum L, Chan I, Cheung SKK, Goggins WB, Mok V, Lam L, Leung V, Hui E, Ng C, Woo J, Chiu H, Zee B, Cheng W, Chan MH, Szeto S, Lui V, Tsoh J, Bush A, Lam C, Kwok T. Serum zinc is decreased in Alzheimer's disease and serum arsenic correlates positively with cognitive ability. *Biometals* 2010;23:173-9.

Conference abstracts

1. Cheung SKK, Baum L. 2006. Poster: Curcumin reverses metal-induced A β aggregation independent of metal chelation. Society for Neuroscience 36th Annual Meeting, Atlanta, USA, 14-18 October.
2. Baum L, Cheung SKK. 2006. Poster: Pilot clinical trial of curcumin for treating Alzheimer's disease. Society for Neuroscience 36th Annual Meeting, Atlanta, USA, 14-18 October.
3. Cheung SKK, Baum L. 2006. Poster: Curcumin reverses metal-induced A β aggregation independent of metal chelation. The 4th Congress of Federation of Asian-Oceanian Neuroscience Societies (FAONS) & Annual Meeting of the

Hong Kong Society of Neurosciences, Hong Kong, 30 November – 2 December.

4. Cheung SKK, Lee J, Baum L. 2007. Poster: Polyphenolic compounds curcumin, ferrulic acid and tannic acid enhance Apolipoprotein E secretion. Society for Neuroscience 37th Annual Meeting, San Diego, USA, 3-7 November.
5. Baum L, Chan HHS, Cheung SKK, Goggins WB, Mok V, Lam L, Leung V, Hui E, Ng C, Woo J, Chiu HFK, Zee BCY, Cheng W, Chan MH, Szeto S, Lui V, Tsoh J, Bush AI, Lam CWK, Kwok T. 2007. Poster: Serum zinc is decreased in Alzheimer's disease and serum arsenic correlates positively with cognitive ability. Society for Neuroscience 37th Annual Meeting, San Diego, USA, 3-7 November.
6. Baum L, Cheung SKK. 2010. Talk: Curcumin for treating Alzheimer's disease. Alzheimer's Disease Conference: From Public Health to Therapeutic Insights, Hong Kong, 28 May.
7. Cheung SKK, Ho A, Baum L. 2010. Poster: Curcumin reduces the level of neurofibrillary tangles in tau P301L transgenic mice. Alzheimer's Association International Conference on Alzheimer's Disease, Honolulu, Hawaii, USA, 10-15 July.
8. Baum L, Ho A, Goggins W, Cheung SKK. 2010. Poster: Treatment of tau P301L transgenic mice by 17-AAG. Alzheimer's Association International Conference on Alzheimer's Disease, Honolulu, Hawaii, USA, 10-15 July.